Publishing House ASV

begell house, inc. publishers

PAACH

Scientific coordination is carried out by the Russian Academy of Architecture and Construction Sciences (RAACS)

Volume 18 • Issue 1 • 2022

ISSN 2588-0195 (Online)
ISSN 2587-9618 (Print) Continues ISSN 1524-5845

International Journal for

Computational Civil and Structural Engineering

Международный журнал по расчету гражданских и строительных конструкций

http://raasn.ru/public.php
http://ijccse.iasv.ru/index.php/IJCCSE

DOI: 10.22337/2587-9618
GICID: 71.0000.1500.2830

PUBLISHER

ASV Publishing House
(ООО «Издательство АСВ»)
19/1,12, Yaroslavskoe Shosse, 120338, Moscow, Russia
Tel. +7(925)084-74-24; E-mail: iasv@iasv.ru; Интернет-сайт: http://iasv.ru/

ADVISORY EDITORIAL BOARD

TECHNICAL EDITOR

EDITORIAL TEAM

INVITED REVIEWERS

AIMS AND SCOPE

The aim of the Journal is to advance the research and practice in structural engineering through the application of computational methods. The Journal will publish original papers and educational articles of general value to the field that will bridge the gap between high-performance construction materials, large-scale engineering systems and advanced methods of analysis.

The scope of the Journal includes papers on computer methods in the areas of structural engineering, civil engineering materials and problems concerned with multiple physical processes interacting at multiple spatial and temporal scales. The Journal is intended to be of interest and use to researches and practitioners in academic, governmental and industrial communities.

ОБЩАЯ ИНФОРМАЦИЯ О ЖУРНАЛЕ

International Journal for Computational Civil and Structural Engineering

(Международный журнал по расчету гражданских и строительных конструкций)

Международный научный журнал "International Journal for Computational Civil and Structural Engineering (Международный журнал по расчету гражданских и строительных конструкций)" (IJCCSE) является ведущим научным периодическим изданием по направлению «Инженерные и технические науки», издаваемым, начиная с 1999 года (ISSN 2588-0195 (Online); ISSN 2587-9618 (Print) Continues ISSN 1524-5845). В журнале на высоком научно-техническом уровне рассматриваются проблемы численного и компьютерного моделирования в строительстве, актуальные вопросы разработки, исследования, развития, верификации, апробации и приложений численных, численно-аналитических методов, программно-алгоритмического обеспечения и выполнения автоматизированного проектирования, мониторинга и комплексного наукоемкого расчетно-теоретического и экспериментального обоснования напряженно-деформированного (и иного) состояния, прочности, устойчивости, надежности и безопасности ответственных объектов гражданского и промышленного строительства, энергетики, машиностроения, транспорта, биотехнологий и других высокотехнологичных отраслей.

В редакционный совет журнала входят известные российские и зарубежные деятели науки и техники (в том числе академики, члены-корреспонденты, иностранные члены, почетные члены и советники Российской академии архитектуры и строительных наук). Основной критерий отбора статей для публикации в журнале − их высокий научный уровень, соответствие которому определяется в ходе высококвалифицированного рецензирования и объективной экспертизы, поступающих в редакцию материалов.

Журнал входит в Перечень ВАК РФ ведущих рецензируемых научных изданий, в которых должны быть опубликованы основные научные результаты диссертаций на соискание ученой степени кандидата наук, на соискание ученой степени доктора наук по научным специальностям и соответствующим им отраслям науки:

- 01.02.04 – Механика деформируемого твердого тела (технические науки),
- 05.13.18 – Математическое моделирование численные методы и комплексы программ (технические науки),
- 05.23.01 – Строительные конструкции, здания и сооружения (технические науки),
- 05.23.02 – Основания и фундаменты, подземные сооружения (технические науки),
- 05.23.05 – Строительные материалы и изделия (технические науки),
- 05.23.07 – Гидротехническое строительство (технические науки),
- 05.23.17 – Строительная механика (технические науки).

В Российской Федерации журнал индексируется Российским индексом научного цитирования (РИНЦ).

Журнал входит в базу данных Russian Science Citation Index (RSCI), полностью интегрированную с платформой Web of Science. Журнал имеет международный статус и высылается в ведущие библиотеки и научные организации мира.

Издатели журнала – *Издательство Ассоциации строительных высших учебных заведений /АСВ/* (Россия, г. Москва) и до 2017 года *Издательский дом Begell House Inc*. (США, г. Нью-Йорк). Официальными партнерами издания является *Российская академия архитектуры и строительных наук* (РААСН), осуществляющая научное курирование издания, и *Научно-исследовательский центр СтаДиО* (ЗАО НИЦ СтаДиО).

Цели журнала – демонстрировать в публикациях российскому и международному профессиональному сообществу новейшие достижения науки в области вычислительных методов

решения фундаментальных и прикладных технических задач, прежде всего в области строительства.

Задачи журнала:

• предоставление российским и зарубежным ученым и специалистам возможности публиковать результаты своих исследований;

• привлечение внимания к наиболее актуальным, перспективным, прорывным и интересным направлениям развития и приложений численных и численно-аналитических методов решения фундаментальных и прикладных технических задач, совершенствования технологий математического, компьютерного моделирования, разработки и верификации реализующего программно-алгоритмического обеспечения;

• обеспечение обмена мнениями между исследователями из разных регионов и государств.

Тематика журнала. К рассмотрению и публикации в журнале принимаются аналитические материалы, научные статьи, обзоры, рецензии и отзывы на научные публикации по фундаментальным и прикладным вопросам технических наук, прежде всего в области строительства. В журнале также публикуются информационные материалы, освещающие научные мероприятия и передовые достижения Российской академии архитектуры и строительных наук, научно-образовательных и проектно-конструкторских организаций.

Тематика статей, принимаемых к публикации в журнале, соответствует его названию и охватывает направления научных исследований в области разработки, исследования и приложений численных и численно-аналитических методов, программного обеспечения, технологий компьютерного моделирования в решении прикладных задач в области строительства, а также соответствующие профильные специальности, представленные в диссертационных советах профильных образовательных организациях высшего образования.

Редакционная политика. Политика редакционной коллегии журнала базируется на современных юридических требованиях в отношении авторского права, законности, плагиата и клеветы, изложенных в законодательстве Российской Федерации, и этических принципах, поддерживаемых сообществом ведущих издателей научной периодики.

За публикацию статей плата с авторов не взымается. Публикация статей в журнале бесплатная. На платной основе в журнале могут быть опубликованы материалы рекламного характера, имеющие прямое отношение к тематике журнала.

Журнал предоставляет непосредственный открытый доступ к своему контенту, исходя из следующего принципа: свободный открытый доступ к результатам исследований способствует увеличению глобального обмена знаниями.

Индексирование. Публикации в журнале входят в системы расчетов индексов цитирования авторов и журналов. «Индекс цитирования» – числовой показатель, характеризующий значимость данной статьи и вычисляющийся на основе последующих публикаций, ссылающихся на данную работу.

Авторам. Прежде чем направить статью в редакцию журнала, авторам следует ознакомиться со всеми материалами, размещенными в разделах сайта журнала (интернет-сайт Российской академии архитектуры и строительных наук (http://raasn.ru); подраздел «Издания РААСН» или интернет-сайт Издательства АСВ (http://iasv.ru); подраздел «Журнал IJCCSE»): с основной информацией о журнале, его целями и задачами, составом редакционной коллегии и редакционного совета, редакционной политикой, порядком рецензирования направляемых в журнал статей, сведениями о соблюдении редакционной этики, о политике авторского права и лицензирования, о представлении журнала в информационных системах (индексировании), информацией о подписке на журнал, контактными данными и пр. Журнал работает по лицензии Creative Commons типа cc by-nc-sa (Attribution Non-Commercial Share Alike) – Лицензия «С указанием авторства – Некоммерческая – Копилефт».

Рецензирование. Все научные статьи, поступившие в редакцию журнала, проходят обязательное двойное слепое рецензирование (рецензент не знает авторов рукописи, авторы рукописи не знаю рецензентов).

Заимствования и плагиат. Редакционная коллегия журнала при рассмотрении статьи проводит проверку материала с помощью системы «Антиплагиат». В случае обнаружения многочисленных заимствований редакция действует в соответствии с правилами COPE.

Подписка. Журнал зарегистрирован в Федеральном агентстве по средствам массовой информации и охраны культурного наследия Российской Федерации. Индекс в общероссийском каталоге РОСПЕЧАТЬ − 18076.

По вопросам подписки на международный научный журнал “International Journal for Computational Civil and Structural Engineering (Международный журнал по расчету гражданских и строительных конструкций)” обращайтесь в Агентство «Роспечать» (Официальный сайт в сети Интернет: http://www.rosp.ru/) или в издательство Ассоциации строительных вузов (АСВ) в соответствии со следующими контактными данными:

ООО «Издательство АСВ»

Юридический адрес: 129337, Россия, г. Москва, Ярославское ш., д. 26, офис 705;

Фактический адрес: 129337, Россия, г. Москва, Ярославское ш., д. 19, корп. 1, 5 этаж, офис 12 (ТЦ Соле Молл);

Телефоны: +7 (925) 084-74-24, +7 (926) 010-91-33;

Интернет-сайт: www.iasv.ru. Адрес электронной почты: iasv@iasv.ru.

Контактная информация. По всем вопросам работы редакции, рецензирования, согласования правки текстов и публикации статей следует обращаться к главному редактору журнала члену-корреспонденту РААСН *Сидорову Владимиру Николаевичу* (адреса электронной почты: sidorov.vladimir@gmail.com, sidorov@iasv.ru, iasv@iasv.ru, sidorov@raasn.ru) или к техническому редактору журнала советнику РААСН *Кайтукову Таймуразу Батразовичу* (адреса электронной почты: tkaytukov@gmail.com; kaytukov@raasn.ru). Кроме того, по указанным вопросам, а также по вопросам размещения в журнале рекламных материалов можно обращаться к генеральному директору ООО «Издательство АСВ» *Никитиной Надежде Сергеевне* (адреса электронной почты: iasv@iasv.ru, nsnikitina@mail.ru, ijccse@iasv.ru).

Журнал становится технологичнее. Издательство АСВ с сентября 2016 года является членом Международной ассоциации издателей научной литературы (Publishers International Linking Association (PILA)), осуществляющей свою деятельность на платформе CrossRef. Оригинальным статьям, публикуемым в журнале, будут присваиваться уникальные номера (индексы DOI – Digital Object Identifier), что значительно облегчит поиск метаданных и местонахождение полнотекстового произведения. DOI – это система определения научного контента в сети Интернет.

С октября 2016 года стал возможен прием статей на рассмотрение и рецензирование через онлайн систему приема статей Open Journal Systems на сайте журнала (электронная редакция): http://ijccse.iasv.ru/index.php/IJCCSE.

Автор имеет возможность следить за продвижением статьи в редакции журнала в личном кабинете Open Journal Systems и получать соответствующие уведомления по электронной почте.

В феврале 2018 года журнал был зарегистрирован в Directory of open access journals (DOAJ) (это один из самых известных поисковых сервисов в мире, который предоставляет открытый доступ к материалам и индексирует не только заголовки журналов, но и научные статьи), в сентябре 2018 года включен в продукты EBSCO Publishing.

В ноябре 2020 года журнал начал индексироваться в международной базе Scopus.

International Journal for
Computational Civil and Structural Engineering
(Международный журнал по расчету гражданских и строительных конструкций)
Volume 18, Issue 1 ***2022***

Scientific coordination is carried out by the Russian Academy of Architecture and Construction Sciences (RAACS)

CONTENTS

Application of the Theory of the Multicomponent Dry Friction in Some of Control Robot Systems **14**
Alexey A. Kireenkov, Grigory V. Fedotenkov, Anton V. Shiriaev, Sergey I. Zhavoronok

Control of Heavy Concrete Characteristics Affecting Structural Stiffness **24**
Semen S. Kaprielov, Andrey V. Sheinfeld, Nikita M. Selyutin

The Effect of Draw-Off on Filtration Regime of Earth-Fil Dam **40**
Nikolay A. Aniskin, Stanislav S. Sergeev

Forecasting and Determining of Cost Performance Index of Tunnels Projects Using Artificial Neural Networks **51**
Oday Hammoody, Jumaa A. AL-Somaydaii, Faiq M. S. Al-Zwainy, Gasim Hayder

Numerical Modeling of Cyclotron Flow Acceleration Modes in Aerodynamic Modules of Solar Aerobaric Power Plants **61**
Alexander A. Soloviev, Dmitry A. Soloviev, Liubov A. Shilova

The Loop Resultant Method for Static Structural Analysis **72**
Vladimir V. Lalin, Huu H. Ngo

Assessment of the Influence of the Rotational Components of Seismic Action on the Sss of a Multistorey Reinforced Concrete Building **82**
Andrej A. Reshetov, Ekaterina M. Lokhova

Calculations of 3D Anisotropic Membrane Structures Under Various Conditions of Fixing **92**
Anatoly I. Bedov, Ruslan F. Vagapov, Azat I. Gabitov, Alexander S. Salov

Analysis of the Moisture Content Effect on the Specific Index and Damage Accumulation Kinetics in the Structure of Polymeric Materials During Natural Climatic Aging **99**
Vladimir P. Selyaev, Tatyana A. Nizina, Dmitry R. Nizin, Nadezhda S. Kanaeva

On the Loss of Stability and Postcritical Equilibrium of Compressed Thin-Walled Angle Bars 109
Gaik A. Manuylov, Sergey B. Kosytsyn, Maxim M. Begichev

Numerical Assessment of Carrying Capacity and Analysis of Pilot Barett Behavior in Geological Conditions of Vietnam 119
Rashid A. Mangushev, Nadezhda S. Nikitina, Le Van Chong, Ivan Yu. Tereshchenko

Filtration Problem with Nonlinear Filtration and Concentration Functions 129
Galina L. Safina

Forecast of the Soil Deformations and Decrease of the Bearing Capacity of Pile Foundations Operating in the Cryolithozone 141
Nadezhda S. Nikiforova, Artem V. Konnov

About the National Software System for Structural Analysis
Pavel A. Akimov, Alexander M. Belostotsky, Oleg V. Kabantsev, 151
Vladimir N. Sidorov, Alexander R. Tusnin

International Journal for
Computational Civil and Structural Engineering
(Международный журнал по расчету гражданских и строительных конструкций)
Volume 18, Issue 1 ***2022***

Scientific coordination is carried out by the Russian Academy of Architecture and Construction Sciences (RAACS)

СОДЕРЖАНИЕ

Применение теории многокомпонентного сухого трения в некоторых системах управления робототехникой **14**
А.А. Киреенков, Г.В. Федотенков, А.В. Ширяев, С.И. Жаворонок

Управление характеристиками тяжёлого бетона, влияющими на жёсткость конструкций **24**
С.С. Каприелов, А.В. Шейнфельд, Н.М. Селютин

Влияние сработки водохранилища на фильтрационный режим грунтовой плотины **40**
Н.А. Анискин, С.А. Сергеев

Прогнозирование и определение показателей экономической эффективности проектов тоннелей с использованием искусственных нейронных сетей **51**
Одай Хаммуди, Джумаа А. Аль-Сомайдаии, Фаик М.С. Аль-Звайни, Гасим Хайдер

Численное моделирование режимов циклотронного ускорения потока в аэродинамических модулях гелиоаэробарических электростанций **61**
А. А. Соловьев, Д. А. Соловьев, Л. А. Шилова

Метод контурных усилий в статике стержневых систем **72**
В. В. Лалин, Х. Х. Нго

Оценка влияния ротационных компонент сейсмического воздействия на ндс многоэтажного железобетонного здания **82**
А.А. Решетов, Е.М. Лохова

Расчеты пространственных анизотропных мембранных конструкций при различных условиях закрепления **92**
А.И. Бедов, Р.Ф. Вагапов, А.И. Габитов, А.С. Салов

Анализ влияния влагосодержания на удельный показатель и кинетику накопления повреждений в структуре полимерных материалов в процессе натурного климатического старения **99**
В.П. Селяев, Т.А. Низина, Д.Р. Низин, Н.С. Канаева

О потере устойчивости и закритическом равновесии сжатых тонкостенных стержней уголкового профиля **109**
Г.А. Мануйлов, С.Б. Косицын, М.М. Бегичев

Численная оценка и анализ работы несущей способности свай-баретт в инженерно-геологических условиях Вьетнама **119**
Р.А. Мангушев, Н.С. Никитина, Ле Ван Чонг, И.Ю. Терещенко

Задача фильтрации с нелинейными функциями фильтрации и концентрации **129**
Г.Л. Сафина

Прогноз деформаций основания и снижения несущей способности свайных фундаментов в криолитозоне **141**
Н.С. Никифорова, А.В. Коннов

О национальном вычислительном комплексе для строительной отрасли
П.А. Акимов, А.М. Белостоцкий, О.В. Кабанцев, **151**
В.Н. Сидоров, А.Р. Туснин

DOI:10.22337/2587-9618-2022-18-1-14-23

APPLICATION OF THE THEORY OF THE MULTICOMPONENT DRY FRICTION IN SOME OF CONTROL ROBOT SYSTEMS

Alexey A. Kireenkov [1,2], Grigory V. Fedotenkov [3,4], Anton V. Shiriaev [5], Sergey I. Zhavoronok [6,7]

[1] A.Yu. Ishlinskiy Institute for Problems in Mechanics of the Russian Academy of Sciences, Moscow, RUSSIA
[2] Moscow Institute of Physics and Technology (National Investigation University), Dolgoprudny, Moscow Region, RUSSIA
[3] Research Institute of Mechanics Lomonosov Moscow State University, Moscow, RUSSIA,
[4] Moscow Aviation Institute (National Research University), Moscow, RUSSIA
[5] Department of Engineering Cybernetics, Norwegian University of Science and Technology (NTNU), Trondheim, NORWAY
[6] Institute of Applied Mechanics of Russian Academy of Sciences, Moscow, RUSSIA
[7] National Research University MGSU, Moscow, RUSSIA

Abstract: The implementations of the theory of multicomponent dry friction [1-19] for analyze the dynamics of some robotic systems, such as a butterfly robot [16-18, 20] or a humanoid robot is proposed. Since the main controlled element of these systems is a spherical, elastic composite shell, it is required to calculate the distribution of normal contact stresses inside the contact spot. The contact pressure distribution for such elements is constructed using the S. A. Ambartsumyan's equation for a transversally isotropic spherical shell. This equation is modified by introducing the averaged contact pressure and normal displacements for the shell. The construction of the resolving integral equation for the contact pressure is based on the principle of superposition and the method of Green's functions. For this, the corresponding Green's function is constructed, which is the normal displacement of the shell as a solution to the problem of the effect of concentrated pressure. Green's function as well as the contact pressure, it is sought in the form of series expansions in Legendre polynomials, taking into account additional relations for the reduced contact pressure and normal displacements. Using the Green's function, an integral equation solving the problem is constructed. As a result, the problem is reduced to determining the expansion coefficients in a series of the reduced contact pressure. Restricting ourselves to a finite number of terms in the series of expansions, using the discretization of the contact area and the properties of Legendre polynomials, the problem is reduced to solving a system of algebraic equations for the expansion coefficients for the reduced pressure. After that, from the additional relation, the coefficients of the required expansion of the contact pressure in a series in Legendre polynomials are determined. To describe the conditions of shell contact with the surface, the theory of multicomponent anisotropic dry friction is used, taking into account the combined kinematics of shell motion (simultaneous sliding, rotation and rolling). The coefficients of the dry friction model can be calculated using simple explicit formulas [1-19] based on numerical experiments.

Keywords: spherical composite shell; contact problem; theory of the multicomponent anisotropic dry friction.

ПРИМЕНЕНИЕ ТЕОРИИ МНОГОКОМПОНЕНТНОГО СУХОГО ТРЕНИЯ В НЕКОТОРЫХ УПРАВЛЯЕМЫХ РОБОТОТЕХНИЧЕСКИХ СИСТЕМАХ

А.А. Киреенков [1,2], Г.В. Федотенков [3,4], А.В. Ширяев [5], С.И. Жаворонок [6,7]

[1] Институт проблем механики РАН им. А.Ю. Ишлинского, Москва, РОССИЯ
[2] Московский физико-технический институт, Долгопрудный, РОССИЯ
[3]НИИ механики МГУ имени М.В. Ломоносова, Москва, РОССИЯ
[4] Московский авиационный институт (национальный исследовательский университет), Москва, РОССИЯ
[5] Норвежский университет науки и технологии, Тронхейм, НОРВЕГИЯ
[6] Институт прикладной механики Российской Академии наук, Москва, РОССИЯ
[7] НИУ Московский Государственный строительный университет, Москва, РОССИЯ

Аннотация: Предложена реализация теории многокомпонентного сухого трения [1-15] для анализа динамики некоторых роботизированных систем, таких как робот-бабочка или робот-гуманоид. Поскольку основным управляемым элементом этих систем является сферическая эластичная композитная оболочка, требуется рассчитать распределение нормальных контактных напряжений внутри пятна контакта. Распределение контактного давления для таких элементов построено с использованием уравнения С. А. Амбарцумяна для поперечно-изотропной сферической оболочки. Это уравнение модифицируется путем введения усредненного контактного давления и нормальных перемещений для оболочки. Построение разрешающего интегрального уравнения для контактного давления основано на принципе суперпозиции и методе функций Грина. Для этого строится соответствующая функция Грина, представляющая собой нормальное смещение оболочки как решение проблемы влияния концентрированного давления. Функция Грина, так же, как и контактное давление, ищется в виде разложений в ряды в полиномах Лежандра с учетом дополнительных соотношений для пониженного контактного давления и нормальных перемещений. Используя функцию Грина, строится интегральное уравнение, решающее задачу. В результате задача сводится к определению коэффициентов расширения в ряду пониженного контактного давления. Ограничиваясь конечным числом членов в ряду разложений, используя дискретизацию площади контакта и свойства полиномов Лежандра, задача сводится к решению системы алгебраических уравнений для коэффициентов расширения для пониженного давления. После этого из дополнительного соотношения определяются коэффициенты требуемого расширения контактного давления в ряду в полиномах Лежандра. Для описания условий контакта оболочки с поверхностью используется теория многокомпонентного анизотропного сухого трения, учитывающая комбинированную кинематику движения оболочки (одновременное скольжение, вращение и качение). Коэффициенты модели сухого трения могут быть рассчитаны с помощью простых явных формул [2], основанных на численных экспериментах.

Ключевые слова: сферическая композитная оболочка; контактная задача;
теория многокомпонентного анизотропного сухого трения.

INTRODUCTION

The theory of the multicomponent dry friction is very effective instrument for the correctly describing of effects of the combined dry friction in many engineering systems. One of the distinguished features of this theory is possibility to carry out analytical investigation of the equations of motions. Connection between the parameters, which are defined the force state inside of contact spot, and the kinematical parameters is given by the simple analytical functions. It's so-called the approximate model of the combined dry friction or phenomenological model. Only six numeric's coefficients are required to calculate. These coefficients can be calculated analytically, numerically or defined from the experiments. Procedure of analytical or numerical definitions of the friction model coefficients is based on the calculation of the first moments of the distribution of the normal pressure inside of contact patch. In order to use these results to analyze the dynamics of some robotic systems, such as a butterfly robot or a humanoid robot, it is necessary to calculate the normal pressure inside the contact spot for various composite spherical shells.

In investigation described below the contact pressure distribution is constructed using the S.A. Ambartsumyan's equation for a transversally isotropic spherical shell. This equation is modified by introducing additional relationships for the reduced contact pressure and normal displacements. The construction of the resolving integral equation for the contact pressure is based on the principle of superposition and the method of Green's functions. For this, the corresponding Green's function is constructed, which is the normal displacement of the shell as a solution to the problem of the effect of concentrated pressure. Green's function as well as the contact pressure, it is sought in the form of series expansions in Legendre polynomials, taking into account additional relations for the reduced contact pressure and normal displacements.

Using the Green's function, an integral equation solving the problem is constructed. As a result, the problem is reduced to determining the expansion coefficients in a series of the reduced contact pressure. Restricting ourselves to a finite number of terms in the series of expansions, using the discretization of the contact area and the properties of Legendre polynomials, the problem is reduced to solving a system of algebraic equations for the expansion coefficients for the reduced pressure. After that, from the additional relation, the coefficients of the required expansion of the contact pressure in a series in Legendre polynomials are determined.

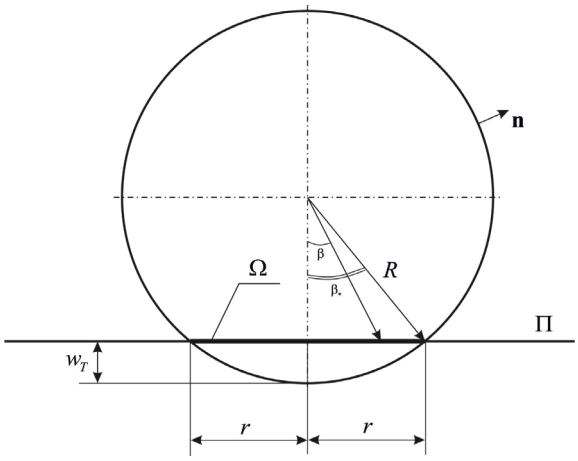

Figure 1. Contact problem

CONTACT PROBLEM SOLUTION

To determine the contact pressure, we pose a static contact problem for a spherical shell of radius R, thickness h and an absolutely rigid reference plane Π [21]. We assume that the shell is made of a transversely isotropic material in such a way that the main direction of elasticity, perpendicular to the plane of isotropy, at each point of the shell coincides with the outer normal $\mathbf{n}$ to the middle surface of the shell.

Contact between shell and reference plane Π occurs along a flat circular area (contact patch) Ω some radius r belonging to the plane Π: $\Omega \in \Pi$ (fig. 1). Taking into account the small size of the contact area $(r \ll R)$ the radius of the contact spot in the zero approximation is determined from the condition of intersection of the undeformed middle surface of the shell

$$r = R\sin\beta_*,\ \beta_* = \arccos\frac{R - w_T}{R}, \qquad (1.1)$$

where w_T - displacement at the frontal point of the shell.

In this case, in the contact area, the normal displacements of the shell are determined as follows (Fig. 1)

$$w = R\left(1 - \cos\beta\right) - w_T. \qquad (1.2)$$

Assuming that the contact problem is axisymmetric, we use the S.A. Ambartsumyan [21] for a transversely isotropic spherical shell, connecting the normal displacements of the shell w with influencing pressure on her p

$$\left[c^2\left(\Delta+1\right)^2 + 1 - h^*\Delta\right]\left(\Delta+2\right)w = \frac{R^2}{Eh}\left(1 - h^*\Delta\right)\left(\Delta + 1 - \nu\right)p, \qquad (1.3)$$

$$\Delta = \frac{1}{\sin\beta}\frac{\partial}{\partial\beta}\left(\sin\beta\frac{\partial}{\partial\beta}\right),$$

$$c^2 = \frac{h^2}{12\left(1-\nu^2\right)R^2},$$

$$h^* = \frac{Eh^2}{10\left(1-\nu^2\right)R^2G'},$$

E - Young's modulus for directions in the plane of isotropy, ν – Poisson's ratio, which characterizes the contraction in the plane of isotropy under tension in the same plane, G' - shear modulus for planes normal to the plane of isotropy.

Note that the structure of equation (1.3) does not allow us to apply expansions in series in Legendre polynomials, since the presence of the operator factor $\Delta + 2$ on the left side turns it to

zero at $n=1$, where n Is the number of a member of the expansion series. To overcome this difficulty, in contrast to the solution proposed in [21], we introduce auxiliary functions of averaged pressure as well as averaged deflection for the shell as follows:

$$p=\left(1+\tfrac{1}{2}\Delta\right)\tilde{p},\quad \tilde{w}=\left(1+\tfrac{1}{2}\Delta\right)w. \qquad (1.4)$$

Then equation (1.3) in new functions takes the form

$$\left[c^2\left(\Delta+1\right)^2+1-h^*\Delta\right]\tilde{w}= =\frac{R^2}{Eh}\left(1-h^*\Delta\right)\left(\Delta+1-\nu\right)\tilde{p}. \qquad (1.5)$$

In this case, the form of equation (1.5) allows us to apply the expansion in series in Legendre polynomials to the solution.
To solve the contact problem, we use the Green's function $G\left(\beta,\xi\right)$, which is a solution to the following equation

$$\left[c^2\left(\Delta+1\right)^2+1-h^*\Delta\right]G\left(\beta,\xi\right)= =\frac{R^2}{Eh}\left(1-h^*\Delta\right)\left(\Delta+1-\nu\right)\delta\left(\beta-\xi\right), \qquad (1.6)$$

where $\delta\left(\beta-\xi\right)$ Is the Dirac delta function.

We expand the required function $G\left(\beta,\xi\right)$ and $\delta\left(\beta-\xi\right)$ in series in Legendre polynomials

$$G\left(\beta;\xi\right)=\sum_{n=0}^{\infty}G_n\left(\xi\right)P_n\left(\cos\beta\right),$$
$$\delta\left(\beta-\xi\right)=\sum_{n=0}^{\infty}\delta_n\left(\xi\right)P_n\left(\cos\beta\right), \qquad (1.7)$$
$$\delta_n\left(\xi\right)=\frac{2n+1}{2}P_n\left(\cos\xi\right)\sin\xi.$$

Substitution of (1.7) into (1.6) taking into account the relation $\Delta P_n\left(\cos\beta\right)=-mP_n\left(\cos\beta\right),\ m=n\left(n+1\right)$ leads to the equation

$$\left[c^2\left(1-m\right)^2+1+h^*m\right]G_n\left(\xi\right)= =\frac{R^2}{Eh}\left(1+h^*m\right)\left(1-m-\nu\right)\delta_n\left(\xi\right).$$

Where does it follow

$$G_n\left(\xi\right)=A_nP_n\left(\cos\xi\right)\sin\xi,$$
$$A_n=R^2\frac{2n+1}{2Eh}\frac{\left(1+h^*m\right)\left(1-m-\nu\right)}{c^2\left(1-m\right)^2+1+h^*m}. \qquad (1.8)$$

Using the Green's function, we obtain an integral connection between normal displacements and the function $\tilde{p}$ [22-26]

$$\tilde{w}\left(\beta\right)=\int_0^{\pi}G\left(\beta,\xi\right)\tilde{p}\left(\xi\right)d\xi. \qquad (1.9)$$

Let's expand $\tilde{p}\left(\beta\right)$ in a series in Legendre polynomials

$$\tilde{p}\left(\beta\right)=\sum_{k=0}^{\infty}\tilde{p}_kP_k\left(\cos\beta\right). \qquad (1.10)$$

Substituting (1.10) into (1.9), we obtain

$$\tilde{w}\left(\beta\right)= =\sum_{n=0}^{\infty}\sum_{k=0}^{\infty}A_n\tilde{p}_kP_n\left(\cos\beta\right)c_{nk}, \qquad (1.11)$$
$$c_{nk}=\int_0^{\pi}P_n\left(\cos\xi\right)P_k\left(\cos\xi\right)\sin\xi d\xi$$

Insofar as $c_{nk}=\frac{2}{2n+1}\delta_{kn}$, where δ_{kn} Is the Kronecker symbol, relation (1.11) takes the form

$$\tilde{w}(\beta)=\sum_{n=0}^{\infty}B_n\tilde{p}_nP_n(\cos\beta),$$
$$B_n=\frac{R^2}{Eh}\frac{(1+h^*m)(1-m-\nu)}{c^2(1-m)^2+1+h^*m}. \quad (1.12)$$

Let us construct a system of linear algebraic equations for the coefficients $\tilde{p}_n$... On the right-hand side of (1.12), we restrict ourselves to taking into account the first $N+1$ terms

$$\tilde{w}(\beta)\approx\sum_{n=0}^{N}B_n\tilde{p}_nP_n(\cos\beta). \quad (1.13)$$

Suppose that displacements $w(\beta)$ set in the contact area $\Omega=\{\beta:\beta\in[0,\beta^*]\}$, where $\beta^*=\arcsin r/R$ - define the boundary of the contact area.

Select in the contact area $N+1$ points with coordinates $\beta_k\in\Omega$, $k=0,1,2,...N$... Replacing the approximate equality (1.13) by the exact one, for each k-th point β_k we obtain an algebraic equation containing $N+1$ unknown $\tilde{p}_n$.Thus, since the number of such equations $N+1$, we get the system from $N+1$ equations for $N+1$ unknown

$$\mathbf{B}\tilde{\mathbf{p}}=\tilde{\mathbf{w}},$$
$$\mathbf{B}=(b_{kn})_{N+1\times N+1},\ \tilde{\mathbf{p}}=(\tilde{p}_n)_{N+1\times 1},$$
$$\tilde{\mathbf{w}}=(\tilde{w}_k)_{N+1\times 1}, \quad (1.14)$$
$$b_{kn}=B_nP_n(\cos\beta_k),$$
$$w_k=w(\beta_k),$$

the solution of which is the vector $\tilde{\mathbf{p}}$ expansion coefficients (1.10).

Desired contact pressure $p(\beta)$ can also be represented as a series expansion in Legendre polynomials

$$p(\beta)=\sum_{n=0}^{\infty}p_nP_n(\cos\beta). \quad (1.15)$$

Representation (1.4) implies a connection between the coefficients p_n and $\tilde{p}_n$

$$p_n=(2-m)\tilde{p}_n, \quad (1.16)$$

from which the first $N+1$ expansion coefficients in a series of the required contact pressure.

As an example, consider a contact problem for a shell with the following parameters: $R=1$ m, $h=1/20$ m, $\nu=0.3$, $E=2\cdot10^{11}$ Pa, $G'=0.7\cdot10^{10}$ Pa, $w_T=0.01R$.

Figure 2 shows the distribution of shell displacements in the contact zone $\Omega=\{\beta:\beta\in[0,\beta^*]\}$

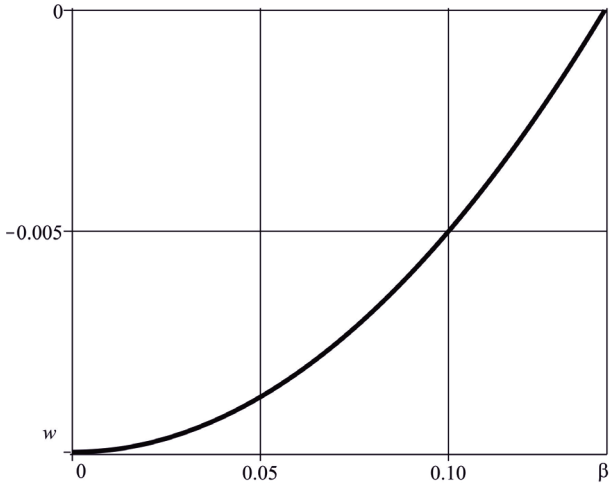

Figure 2. Distribution of displacements over the contact area

Figure 3 shows the distribution of contact pressure as a solution to problem (1.14) - (1.16). The solid curve corresponds to $N=20$, dashed line - $N=30$...

Further improvement of the solution of the contact problem based on the transient function approach [27] could require higher-order shell theories approximating the three-dimensional

stress state in irreducibility domains near contact spot boundaries (e. g. see [28-30]).

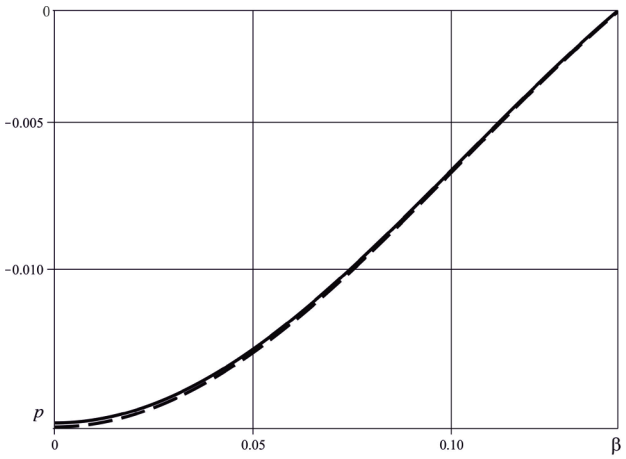

Figure 3. Contact pressure distribution

DRY FRICTION MODEL OF SHELL CONTACT WITH THE ROUGH PLANE

The dynamic interaction of a weakly deformed solid with a rough reference plane is determined by the normal reaction $\mathbf{N}$, the resulting vector of tangential forces $\mathbf{T}$, the rolling resistance moment $\mathbf{M}_\tau$ and the dry friction moment $\mathbf{M}_\nu$ [2]. These values can be determined by integrating the normal contact pressure, as well as the total tangential pressure obtained under the assumption of the validity of the differential form of the Amonton-Coulomb law for a small element of the area inside the contact spot [1-13] along the contact area S.

Taking into account the anisotropy of dry friction, the integral model of the force state inside the contact spot has the form

$$\mathbf{N} = \int_S \sigma_0 \left[\mathbf{e}_3 + \frac{\mathbf{r}_\tau \times (\mathbf{h} \cdot \mathbf{w}_\tau)}{|\mathbf{w}_\tau|} \right] dS$$

$$\mathbf{M}_\tau = \int_S \sigma_0 \mathbf{r}_\tau \times \left[\mathbf{e}_3 + \frac{\mathbf{r}_\tau \times (\mathbf{h} \cdot \mathbf{w}_\tau)}{|\mathbf{w}_\tau|} \right] dS; \qquad (2.1)$$

$$\mathbf{T} = -\int_S \sigma_0 \left[1 + \frac{\mathbf{r}_\tau \times (\mathbf{h} \cdot \mathbf{w}_\tau)}{|\mathbf{w}_\tau|} \cdot \mathbf{e}_3 \right] \frac{\mathbf{f} \cdot (\mathbf{v}_0 - R\mathbf{w}_\tau \times \mathbf{e}_3 + \mathbf{w}_\nu \times \mathbf{r}_\tau)}{|\mathbf{v}_0 + \mathbf{w}_\nu \times \mathbf{r}_\tau|} dS$$

Here $\mathbf{v}_0$ is the longitudinal absolute velocity; $\mathbf{w}_\tau$ angular rolling velocity; $\mathbf{w}_\nu$ angular spinning velocity; $R(M)$ radius of curvature of a rolling body calculated at a point M; $\mathbf{r}_\tau(M)$ radius vector of a point $M \in S$ in the contact plane; $\mathbf{e}_3$ normal unit vector of the contact plane; $\mathbf{h} = h_{\alpha\beta}\mathbf{e}^\alpha \mathbf{e}^\beta$ "rolling friction tensor" for an anisotropic elastic body:

$$\forall \mathbf{w}_\tau = \mathbf{w}_\tau(\mathbf{q}) \quad \mathbf{w}_\tau^{\mathrm{T}} \cdot \mathbf{h} \cdot \mathbf{w}_\tau > 0.$$

A detailed analysis of equations (2.1) was carried out in [2]. In particular, it was shown that in most engineering problems, it is sufficient to consider orthropic dry friction defined by the following friction tensor as it was shown in [2, 5, 10]:

$$\mathbf{f} = f \begin{pmatrix} 1 & 0 \\ 0 & k \end{pmatrix}, \; f \neq 0, \; \kappa \neq 0 \qquad (2.2)$$

where f and κf are the main components of the friction tensor.

It is convenient to write the proposed friction model (2.1) in a coordinate system Oxy, with the origin in the center of the contact spot, such that the corresponding basis vectors $\mathbf{e}_1$ and $\mathbf{e}_2$ are collinear to the main directions of the friction tensor. In addition, it is natural to assume that static contact pressure has the property of axial symmetry: $\sigma_0(x, y) = \sigma_0(\pm x, \pm y)$, and rolling friction is isotropic.

An approximate analytical model of the force inside interaction the contact spot is constructed under the assumption that the rolling shell moves with longitudinal velocity $\mathbf{v}_0 = v\mathbf{e}_1'$ along

the axis of the global stationary coordinate system, with angular velocity of rolling $\mathbf{w}_\tau = -\Omega_r \mathbf{e}_2$ and angular velocity of spinning ω.

It is assumed that the contact area has axial symmetry with a characteristic size of the contact spot R (for example, the diameter of the corresponding set on the plane $\{x, y\}$).

In the presence of motion, tangential stresses arise, leading to distortion of the symmetrical diagram of the distribution of normal contact stresses. Assuming that the displacement of the center of gravity of the contact spot relative to the geometric center is described by a vector $\mathbf{d}$ whose modulus was calculated in [1, 6-12], the symmetry breaking can be represented by the following formula:

$$\sigma(x, y) = \sigma_0(x, y)(1 + d_x x + d_y y)$$

where d_x and d_y are the projections of the vector $\mathbf{d}$ on the axis x and y, respectively.

The resulting friction force vector can be represented as the sum of two components: $\mathbf{T} = T_\mathrm{P}\mathbf{e}_1 + T_\perp \mathbf{e}_2$, where T_P is the longitudinal abut $T_\perp$ is transverse components of the friction force. As it was shown in [1-12], the latter of them arises due to the relationship of friction effects.

As a result, integral representations (2.1) can be substantially simplified, as it was implemented in [1-12].

However, integral relations are too complex to apply to the analysis of the dynamics of real systems, while their approximations by analytical functions are quite accurate and simple at the same time. Using the technique described in detail in previous works [1-12], an approximate analytical model of friction describing the interaction of an elastic rolling shell with a solid surface, in the case of combined kinematics and orthotropic friction, can be presented in the following form:

$$F_\mathrm{P} = \frac{F_0 v}{\sqrt{v^2 + a u^2}}, \quad F_\perp = \frac{\mu_0 k F_0 v u^2}{\sqrt{(v^6 + b\omega^6)}}, \quad M_\nu = \frac{M_0 u}{\sqrt{u^2 + m v^2}} \tag{2.3}$$

Here $u = \omega_\nu R$, F_0 is the longitudinal component of the friction force of the beginning of the motion, but M_0 is the friction torque of the beginning of the motion. The coefficients of the model (2.3) can be calculated using simple explicit formulas [2] based on numerical experiments, the results of which are presented in Fig. 2-3.

CONCLUSIONS

A formulation is proposed and a method is developed for solving the problem of the motion of a composite spherical transversely isotropic shell on a solid surface, taking into account the combined dry friction. Taking into account the assignment of the reduced contact pressure function, S.A. Ambartsumyan's modified equation was used, which allows us to apply series expansions by Legendre polynomials. Using the Green's function, the problem is reduced to solving a system of algebraic equations with respect to the coefficients of decomposition into a series of functions of the reduced contact pressure and displacements. The relationship between the true and reduced contact pressure allows us to determine the coefficients of the contact pressure decomposition series.

To describe the conditions of shell contact with the surface, the theory of multicomponent anisotropic dry friction is used, taking into account the combined kinematics of shell motion (simultaneous sliding, rotation and rolling).

The coefficients of the approximated dry friction model (2.3) can be calculated using simple explicit formulas [2] based on numerical

experiments, the results of which are presented in Fig. 2-3.

ACKNOWLEDGEMENTS

A.A. Kireenkov and G.V. Fedotenkov were supported by the RFBR under the grant Nr. 20-08-01120. Investigations performed by S. I. Zhavoronok were a part of the State Task for Basic Researches Nr. 121112200124-1.

REFERENCES

1. **Kireenkov A., Zhavoronok S.** A Method of Parameters Identification for the Coupled Dry Friction Model for Pneumatic Tires, in: WCCM-ECCOMAS2020. URL https://www.scipedia.com/public/Kireenkov_Zhavoronok_2021a.
2. **Kireenkov A. A., Zhavoronok S. I.** Anisotropic combined dry friction in problems of pneumatics' dynamics // J. Vibration Engineering and Technology, Vol. 8, 365–372 (2020).
3. **Kireenkov A. A., Zhavoronok S. I.** Numeric-Analytical Methods of the Coefficients Definition of the Rolling Friction Model of the Pneumatic Aviation Tire, in: 8th International Conference on Coupled Problems in Science and Engineering, COUPLED PROBLEMS 2019 (2021), pp. 204-212.
4. **Kireenkov A. A., Ramodanov S. M.** Combined Dry Friction Models in the Case of Random Distribution of the Normal Contact Stresses Inside of Contact Patches, in: 8th International Conference on Coupled Problems in Science and Engineering, COUPLED PROBLEMS 2019 (2021), pp. 176-182.
5. **Kireenkov A. A., Zhavoronok S. I.** Implementation of analytical models of the anisotropic combined dry friction in problems of pneumatics' dynamics // MATEC Web of Conferences, Vol. 211 (2018), 08004
6. **Kireenkov A.A., Nushtaev D.V., Zhavoronok S.I.** A new approximate model of tyre accounting for both deformed state and dry friction forces in the contact spot on the background of the coupled model // MATEC Web of Conferences, Vol. 211 (2018), 08003.
7. **Kireenkov A. A.** Improved friction model of the aviation tyre contact with the landing strip // IFAC-PapersOnLine Vol. 51, No. 2, pp. 890-894.
8. **Kireenkov A. A., Zhavoronok S. I.** Coupled Dry Friction Models in Problems of Aviation Pneumatics' Dynamics // International Journal of Mechanical Sciences (2017), Vol. 127, pp. 198-203.
9. **Kireenkov A. A.** Improved theory of the combined dry friction in problems of aviation pneumatics' dynamics, in: Proceedings of the 7th International Conference on Coupled Problems in Science and Engineering, COUPLED PROBLEMS 2017 (2017), pp. 1293-1298.
10. **Zhavoronok S. I., Kireenkov A. A.** On the effect of the anisotropic dry friction and the deformed state of tires on the shimmy initiation, in: Proceedings of the 7th International Conference on Coupled Problems in Science and Engineering, COUPLED PROBLEMS 2017 (2017), pp. 216-226.
11. **Ramodanov S. M., Kireenkov A. A.** Controllability of a rigid body in a perfect fluid in the presence of friction, in: Proceedings of the 7th International Conference on Coupled Problems in Science and Engineering, COUPLED PROBLEMS 2017 (2017), pp.179 – 184.
12. **Kireenkov A. A.** Further development of the theory of multicomponent dry friction, in: COUPLED PROBLEMS 2015 - Proceedings of the 6th International Conference on Coupled Problems in Science and Engineering (2015), pp. 203-209.

13. **Kireenkov A. A., Semendyaev S. V., Filatov V. V.** Experimental study of coupled two-dimensional models of sliding and spinning friction // Mechanics of Solids (2010), Vol. 45, No. 6, pp. 921–930.
14. **Kireenkov A. A.** Combined model of sliding and rolling friction in dynamics of bodies on a rough plane // Mechanics of Solids (2008), Vol. 43, No. 3, pp. 412-425.
15. **Kireenkov A. A.** Coupled models of sliding and rolling friction// Doklady Physics (2008), Vol. 53, No. 4, pp. 233-236
16. **Kireenkov A. A.** Modelling of the force state of contact of a ball rolling along the boundaries of two rails // AIP Conference Proceedings (2021), Vol. 2343,120002.
17. **Kireenkov A.** Influence of the Combined Dry Friction on the Dynamics of the Rigid Ball Moving Along Two parallel Rails, in: 9th edition of the International Conference on Computational Methods for Coupled Problems in Science and Engineering (COUPLED PROBLEMS 2021). URL https://www.scipedia.com/public/Kireenkov_2021b.
18. **Kireenkov A.** Dry Friction Model of a Contact of a Solid Ball Moving Along the Boundaries of Two Rails, in: WCCM-ECCOMAS2020.URL: www.scipedia.com/public/Kireenkov_2021a.
19. **Kireenkov A. A.** Preface: mathematical models and investigations methods of strongly nonlinear systems // AIP Conference Proceedings (2021), Vol. 2343, 120001.
20. **Surov M., Shiriaev A. and al.** Case study in non-prehensile manipulation: Planning and orbital stabilization of one-directional rollings for the `Butterfly robot, in: Proceedings - IEEE International Conference on Robotics and Automation (2015), pp. 1484-1489.
21. **Ambartsumyan S. A.** Theory of Anisotropic Shells, Moscow, Nauka, 1974.
22. **Mikhailova E.Yu., Fedotenkov G.V.** Nonstationary Axisymmetric Problem of the Impact of a Spherical Shell on an Elastic Half-Space (Initial Stage of Interaction) // Mechanics of Solids (2011), Vol. 46, No. 2, pp. 239–247.
23. **Tarlakovskii D. V., Fedotenkov G. V.** Two-Dimensional Nonstationary Contact of Elastic Cylindrical or Spherical Shells // Journal of Machinery Manufacture and Reliability (2014), Vol.43, No.2, pp. 145–152.
24. **Fedotenkov G. V., Mikhailova E. Yu, Kuznetsova El. L., Rabinskiy L. N.** Modeling the unsteady contact of spherical shell made with applying the additive technologies with the perfectly rigid stamp // International Journal of Pure and Applied Mathematics (2016), Vol. 111, No. 2, pp. 331-342.
25. **Mikhailova E. Yu., Tarlakovskii D. V., Fedotenkov G. V.** Transient contact problem for spherical shell and elastic half-space, in: Shell Structures: Theory and Applications, Vol. 4. CRC Press / Balkema, Taylor & Francis Gr., Leiden (2018), pp. 301-304.
26. **Tarlakovskii D. V., Fedotenkov G. V.** Nonstationary 3D motion of an elastic spherical shell // Mechanics of Solids (2015), Vol. 46, No, 5, pp. 779-787.
27. **Fedotenkov G. V., Zhavoronok S. I.** Transient contact of a cylindrical shell and a rigid body // AIP Conference Proceedings (2021), vol. 2343, 120010.
28. **Amosov A. A., Zhavoronok S. I.** An approximate high-order theory of thick anisotropic shells // International Journal for Computational Civil and Structural Engineering (2003), Vol. 1, No. 5, pp. 28-38.
29. **Zhavoronok S. I., Leontiev A. N., Leontiev K. A.** Analysis of thick-walled rotation shells based on legendre polynomials // International Journal for Computational Civil and Structural Engineering (2010), Vol. 6, No. 1-2, pp. 105-111.
30. **Zhavoronok S. I.** A general higher-order shell theory based on the analytical dynamics of constrained continuum systemsin: Shell Structures: Theory and Applications, Vol. 4. CRC Press / Balkema, Taylor & Francis Gr., Leiden (2018), pp. 189-192.

Alexey A. Kireenkov is a Senior Reseacher of the Ishlinsky Institute for Problems in Mechanics of Russian Academy of Sciences (IPMech RAS) and Associate Professor of the high mathematics departments of the Moscow Institute of Physics and Technology (National Investigation University). Address: IPMech RAS, Prospekt Vernadskogo 101, korp.1, 119526, Moscow, Russia. Phone: +7(916)8685839.

Grigory V. Fedotenkov is a Senior Researcher of the Laboratory of dynamical Tests of the Research Institute of Mechanics of Lomonosov Moscow State University, Associate Professor of the Moscow Aviation Institute (National Research University). Phone: +7(916)4598363. Address: 119192, Michurinskiy Prospekt, 1, Moscow, Russia

Anton V. Shiriaev is Professor (full) of the Department of Engineering Cybernetics, Norwegian University of Science and Technology - (NTNU). Phone: +4773590246 Address: Department of Engineering Cybernetics, NTNU, NO-7491 Trondheim, Norway.

Sergey I. Zhavoronok, Ph.D., Leading researcher of the Department of Mechanics of Smart and Composite Materials and Systems, Institute of Applied Mechanics of Russian Academy of Sciences (IAM RAS); Associate Professor of the Department of Informatics and Applied Mathematics of the National Research University MGSU. Address: Leningradskiy Prospekt 7, 125040, Moscow, Russia, IAM RAS. Phone: +7(495) 941-1777; +7(916) 134-2843. e-mail: Zhavoronok@iam.ras.ru

Киреенков Алексей Альбертович – старший научный сотрудник ФГБУН Институт проблем механики им. А.Ю. Ишлинского РАН, доцент кафедры высшей математики Московского физико-технического института (Национального исследовательского университета); ИПМех РАН, 119526, Россия Москва, Проспект Вернадского, 101, корп. 1, тел.: +7 (916) 868-58-39. E-mail: kireenk@ipmnet.ru

Федотенков Григорий Валерьевич – старший научный сотрудник Лаборатории динамических испытаний НИИ механики Московского Государственного университета им. М. В. Ломоносова, 119192, Москва, Россия, Мичуринский проспект, 1; доцент кафедры сопротивления материалов, динамики и прочности машин Московского авиационного института (национального исследовательского университета); тел.: +7 (916) 459-83-63. E-mail: greghome@mail.ru

Ширяев Антон Станиславович – профессор кафедры инженерной кибернетики Норвежского научно-технологического университета; NO-7491 Тронхейм, Норвегия, Норвежский научно-технологический университет, кафедра инженерной кибернетики, тел.: +4 (773) 590-246. E-mail: anton.shiriaev@ntnu.no

Жаворонок Сергей Игоревич, ведущий научный сотрудник отдела механики адаптивных и композиционных материалов и систем ФГБУН Институт прикладной механики РАН, 125040, Россия, Москва, Ленинградский проспект, 7; доцент кафедры информатики и прикладной математики Национального исследовательского Московского государственного строительного университета;
тел.: +7 (916) 134-2843. E-mail: Zhavoronok@iam.ras.ru

DOI:10.22337/2587-9618-2022-18-1-24-39

CONTROL OF HEAVY CONCRETE CHARACTERISTICS AFFECTING STRUCTURAL STIFFNESS

Semen S. Kaprielov [1], Andrey V. Sheinfeld [1], Nikita M. Selyutin [2]

[1] Research Institute of Reinforced Concrete named after A.A. Gvozdev JSC "Research Center "Construction", Moscow, Russia

[2] Enterprise Master Beton LLC, Moscow, Russia

Abstract. New experimental data have been obtained on the strength and deformation characteristics of heavy concrete o strength classes B30-B100 (strength from 36.2 to 115.1 MPa), prepared from self-compacting mixtures using crushed stone from various dense rocks as a coarse aggregate - granite, basalt and gabbro-diabase, as well as crushed stone from gravel.

It has been established that the values of the compressive strength of concrete "R_{bn}" (prism strength) are 24% higher than the normalized indicators given in Table 6.7 of the current set of Building Code of the Russian Federation SP 63.13330.2018. For high-strength concrete on crushed granite of strength classes from B70 to B100, the values of the static modulus of elasticity E_b, which largely determines the stiffness of reinforced concrete structures, exceed by 5-14% the values given in Table 6.11 of SP 63.13330.2018. At the same time, the use of gabbro-diabase or basalt crushed stone as a coarse aggregate instead of granite does not affect the strength and Poison's ratio. However, this allows increasing the static modulus of elasticity of concrete by 9 and 19%, respectively. The values of the dynamic modulus of elasticity of heavy concrete are in the range from 41.1 to 60.4 GPa and exceed the static modulus of elasticity of concrete by 2.2-5.3 GPa depending on the classes of concrete.

The paper shows the possibility of using a less time-consuming method for monitoring the values of the static modulus of elasticity of concrete in structures by determining the dynamic modulus using the calibration dependence E_b - E_d.

The obtained results indicate that the real potential of high-strength concretes is not fully used in structures designed in accordance with normative characteristics R_{bn} and E_b provided for by SP 63.13330.2018. The actual values of these characteristics are higher and can be controlled by technological tricks.

Keywords: High-strength heavy concrete, deformation characteristics of concrete, structural stiffness, crushed stone from dense rocks, modulus of elasticity, Poisson's ratio, compressive strength, organomineral modifier, self-compacting concrete mix.

УПРАВЛЕНИЕ ХАРАКТЕРИСТИКАМИ ТЯЖЁЛОГО БЕТОНА, ВЛИЯЮЩИМИ НА ЖЁСТКОСТЬ КОНСТРУКЦИЙ

С.С. Каприелов [1], А.В. Шейнфельд [1], Н.М. Селютин [2]

[1] НИИЖБ им. А.А. Гвоздева АО «НИЦ «Строительство», г. Москва, Россия

[2] ООО «Предприятие Мастер Бетон», г. Москва, Россия

Аннотация: Получены новые экспериментальные данные о прочностных и деформационных характеристиках тяжёлых бетонов классов по прочности на сжатие В30-В100 (прочностью от 36,2 до 115,1 МПа), приготовленных из самоуплотняющихся смесей с использованием в качестве крупного заполнителя щебня из разных плотных горных пород – гранитного, базальтового и габбро-диабазового, а также щебня из гравия.

Установлено, что значения нормативного сопротивления бетонов осевому сжатию R_{bn} (призменная прочность) на 24 % превосходят нормируемые показатели, приведенные в таблице 6.7 действующего свода правил РФ СП 63.13330.2018. Значения статического модуля упругости E_b, в значительной степени предопределяющего жесткость железобетонных конструкций, для высокопрочных бетонов на гранитном щебне, классов от В70 до В100 превышают на 5-14 % значения, приведенные в таблице 6.11 СП 63.13330.2018. При этом, использование в качестве крупного заполнителя габбро-диабазового или ба-

зальтового щебня взамен гранитного, не влияет на прочность и коэффициент поперечных деформаций, но позволяет повысить статический модуль упругости бетонов на 9 и 19 %, соответственно. Значения динамического модуля упругости тяжелых бетонов находятся в диапазоне от 41,1 до 60,4 ГПа и, в зависимости от классов бетона, превышают статический модуль упругости бетонов на 2,2-5,3 ГПа.
Показана возможность использования менее трудоемкого метода контроля значений статического модуля упругости бетона в конструкциях посредством определения динамического модуля с использованием градуировочной зависимости $E_b - E_d$.
Полученные результаты свидетельствуют о том, что реальный потенциал высокопрочных бетонов не полностью используется при проектировании конструкций с учётом предусмотренных СП 63.13330.2018 нормативных характеристик R_{bn} и E_b, фактические значения которых выше и могут управляться технологическими приёмами.

Ключевые слова: Высокопрочный тяжелый бетон, деформационные характеристики бетона, жёсткость конструкций, щебень из плотных пород, модуль упругости, коэффициент Пуассона, прочность на сжатие, органоминеральный модификатор, самоуплотняющаяся бетонная смесь.

INTRODUCTION

The construction of high-rise buildings and other unique structures predetermined the increasing importance of the deformation characteristics of concrete affecting the stiffness of structures.
Calculations performed for the limit states of both the first and second groups in most cases show that the limiting design factor is not the strength of concrete, but its deformation parameters characterizing the process of deformation and movement of structures under load.
Among several normalized deformation characteristics of concrete, the most significant for the stiffness of structures is the static modulus of elasticity (E_b), which, according to SP 63.13330.2018, is currently tied mainly to strength classes and types of concrete. Other deformation characteristics, according to SP 63.13330.2018, are either tied to the modulus of elasticity (shear modulus ($G = 0.4E_b$), or it is accepted as constant value (ratio of lateral strain to longitudinal one - Poisson's ratio $\nu_b = 0.2$; ultimate compression and tension strain short-term load $\varepsilon_{b0}=0.002$ and $\varepsilon_{bt0}=0.0001$), or not standardized (dynamic modulus of elasticity of concrete E_d).
In a general approximation, the modulus of elasticity of heavy concrete, considering the characteristics of its composition, can be determined by the expression:

$$E_b = E_{cp} \cdot V_{cp} + E_{fa} \cdot V_{fa} + E_{ca} \cdot V_{ca}, \qquad (1)$$

where:
E_{cp}, E_{fa} and E_{ca} are modulus of elasticity of cement stone, fine and coarse aggregates respectively;
V_{cp}, V_{fa} *and* V_{ca} are the specific volumes of cement stone, fine and coarse aggregates in concrete respectively.
A more accurate determination of the modulus of elasticity allows more complex calculation models, which additionally considers other factors that can affect the parameters of the concrete structure - the porosity of the cement stone, the degree of cement hydration, the properties of the contact zone, the properties of coarse aggregate, etc. Examples of such calculation models are given by P.-C. Aitcin [1]. Aitcin notes its' differences associated with the use in the calculations of certain factors depending on the technology of preparation and the material composition of concrete. This indicates the importance of technological factors (the quality of the concrete components and their volume ratio, the method of preparation and the consistency of concrete mixtures) in regulating the most important deformation characteristic - the static modulus of elasticity.
A number of studies, devoted to this issue, show the role of the characteristics of the filler, the mortar part of concrete, the structure of the cement stone and the contact zone in changing the elastic modulus [2-6].

Particularly noteworthy is the study of the deformation characteristics of high-strength concretes of strength classes B60-B100, which are the main structural material of unique structures [7-14].
Studies [15-18] of concretes with high-strength fractionated aggregates and with highly active cement at a reduced water-cement ratio confirmed the pattern represented by expression (1). Increased values of the strength and elasticity modulus of concrete are provided by the high density and strength of the cement stone, high-quality aggregate and its increased concentration, i.e., dense packing in the volume of concrete.
Studies of modified concretes with organo-mineral modifiers of the MB type revealed an important role in changing the elasticity modulus of such cement stone parameters as phase composition (balance of hydrate neoplasms) and porosity, which are regulated by the dosages of additives [10-14]. This allows not only to control the strength and deformation characteristics of high-strength concretes under short-term and long-term loading of structures, but also to derive a corrective function for S.V. Aleksandrovsky and I.E. Prokopovich used to describe the creep measure [13].
The dependences between the deformation characteristics of high-strength concretes and the parameters of the cement stone structure established in [10-12, 19] allow significantly expand the ideas of A.E. Sheikin [20] on the influence of technological factors and the structure of cement stone on the deformation characteristics of concrete. In particular, it has been shown that the values of the static modulus of elasticity for fine-grained concretes of the same class in terms of compressive strength can vary depending on the phase composition and differential porosity of the cement stone [10–13].
If accept that the static modulus of elasticity is a complex and variable parameter, the value of which depends on a number of factors, including the modulus of elasticity and the specific content of concrete components, it seems relevant to assess the influence of the type and quality of large aggregates, the most common in Russia, on deformation characteristics and strength both conventional and modified high-strength heavy concretes. Despite the availability of information on this issue [5-9], the assessment of the significance of the factor of the nature of the aggregate on the deformation characteristics of concrete should probably be decided considering the specific properties of materials and compositions of concrete mixtures.
The purpose of the research was to determine the effect of coarse aggregate made of different rocks on the strength and deformation characteristics of concretes of classes from B30 to B100, prepared from self-compacting mixtures, with the justification of the method for controlling the initial modulus of elasticity of concrete in erected structures.
To achieve the purpose, the following tasks have been solved:
- Determination of strength and deformation characteristics of 7 series of self-compacting concretes of classes B30-B100 at the age of 28 and 90 days. Each of which had the same composition, but was prepared with 4 types of coarse aggregate;
- Establishing the dependences of the deformation characteristics of concretes with various types of coarse aggregates on the class of concrete in terms of compressive strength;
- Evaluation of the obtained results by its comparing with the standard values given in the Building code of the Russian Federation SP 63.13330.2018 “Concrete and reinforced concrete structures. General provisions”, recommended by FIB international standard Model Code MC 2010 and European standard EN 1992-1-1:2004 Eurocode 2;
- substantiation of the method for control of the static modulus of elasticity of concrete in erected structures by establishing a calibration dependence between the values of the static (E_b) and dynamic (E_d) modulus of elasticity of concrete.

1. MATERIALS AND TEST METHODS

1.1. Applied materials

The materials (cement, modifier, microfiller, sand and crushed stone), which satisfy the standards of the Russian Federation and applied in the production of self-compacting concrete mixes for construction projects at the Moscow-City MIBC, were

used for the preparation of concrete in laboratory conditions. In addition, other types of coarse aggregate were used: crushed gravel, gabbro-diabase and basalt crushed stone. The reason for choosing 4 different types of crushed stone was the difference in true density and in parameters characterizing strength, in particular: "mass loss during compression in the cylinder" and "grain content of weak rocks", which allow more accurate than the classification parameter dependent on its "crushability", to evaluate the strength of coarse aggregate.

The characteristics of the materials were as follows:

- Portland cement PC 500-D0-N with a normal density of 24.6% and a C_3A content of 4.9%, which meets the requirements of the RF standard GOST 10178;
- organo-mineral concrete modifier MB10-50S A-II-2, including microsilica (45%), fly ash (45%) and superplasticizer (10%) [21], which meets the requirements of the RF standard GOST R 56178 and TU 5743- 083-46854090-98 amend. No. 1-3;
- microfiller - non-activated mineral powder grade MP-1 (ground limestone) with a particle size of less than 1.25 mm, corresponding to the requirements of the RF standards GOST R 52129 and GOST R 56592;
- SikaPlast E4 superplasticizer based on a mixture of modified lignosulfonates and polycarboxylate esters, which meets the requirements of the RF GOST 24211 standard;
- Class I quartz sand with fineness modulus Mcr = 2.55, with a content of dust and clay particles of 0.95%, corresponding to the requirements of the RF GOST 8736 standard;
- crushed stone from gravel with a fraction of 3-10 mm, corresponding to the requirements of the RF standard GOST 8267;
- crushed stone of granite fraction 5-10 mm, corresponding to the requirements of the RF standard GOST 8267;
- crushed stone gabbro-diabase fraction 5-10 mm, corresponding to the requirements of the RF standard GOST 8267;
- crushed stone basalt fraction 5-10 mm, corresponding to the requirements of the RF standard GOST 8267;
- water for mixing concrete mixtures that meets the requirements of the RF GOST 23732 standard.

Table 1 provides physical and technical characteristics and mineralogical composition of coarse aggregate varieties.

Table 1. Physical and technical characteristics and mineralogical composition of coarse aggregate

Characteristic	*Type of coarse aggregate (crushed stone)*			
	gravel	*granite*	*gabbro-diabase*	*basalt*
1	2	3	4	5
True density, kg/m^3	2650	2670	3070	3000
Mass loss during compression in the cylinder,%	6.02	6.55	3.17	1.03
Breakability grade	1200	1400	1400	1400
The content of lamellar and angular grains, %	7.98	22.0	8.2	28.0
Grain content of weak rocks, %	4.15	1.50	0	0
The content of dust particles, %	0.99	0.96	0.70	0.8
Mineralogical composition, %:				
- organogenic limestone	40.0	-	-	-
- quartz	8.8	-	-	-
- flint	7.7	-	-	-
- dolomite	7.6	-	-	-
- quartzite	4.9	-	-	-
- limestone organogenic silicified	2.8	-	-	-

- tuff sandstone	2.5	-	-	-
- sandstone	1.6	-	-	-
1	2	3	4	5
- iron oxides and hydroxides	0.5	-	-	-
- granite	23.6	54.8		
- granodiorite	-	40.9	-	-
- diorite	-	3.8	-	-
- intensely altered rock (dolerite)	-	0.5	-	-
- intensively altered basalt	-	-	60.5	-
- intensively modified gabbro	-	-	39.5	-
- intensively altered picrobasalt	-	-	-	97.8
- effusive rock intensively altered	-	-	-	2.2

1.2. Compositions and Properties of Concrete Mixes

In laboratory of Research Institute of Reinforced Concrete, 7 series (28 compositions) of concrete from self-compacting mixtures with a cement consumption of 290 to 480 kg/m^3 with the addition of MB modifier and microfiller at a water-binding ratio W / (C + MB) from 0.25 to 0.69 have been prepared. Each series was prepared with 4 types of coarse aggregate - crushed stone from gravel, granite, gabbro-diabase and basalt crushed stone. The compositions of concrete mixtures were selected with the expectation of the same volumetric dosage of each of these materials. Respectively, the actual volume of coarse aggregate in different concrete series was in a narrow range - from 0.310 to 0.335 m^3/m^3. Table 2 presents the compositions and properties of self-compacting concrete mixtures are presented.

Concrete mixtures were prepared in a 60-liter forced-action mixer with mixing of each batch for 5 minutes. The test results of concrete mixtures showed (table 2) that their average density ("γ") depends on the true density of coarse aggregate and varies in a wide range - from 2386 to 2541 kg/m^3. The mobility of mixtures, determined by the spread of a normal cone [22], is in the range from 55 to 70 cm. Considering also the absence of signs of water separation and stratification of mixtures, according to [23], this allows to classify them as self-compacting.

Table 2. Compositions and Properties of Self-Sealing Concrete Mixes

Series number	*Compositions of concrete mixes, kg/m^3*							*Properties of concrete mixtures*			
	C	*MB*	*MP-1*	*P*	*G*	*SP*	*W*	*γ, kg/m^3*	*V_G, m^3/m^3*	*SC, cm*	*W/(C+MB)*
1	290	-	150	820	855[1]/870[2]/ 995[3]/970[4]	3,52	198	2316-2456	0,322-0,326	55-58	0.69
2	300	30	170	835	830[1]/835[2]/960[3]/940[4]	-	176	2341-2471	0,308-0,313	55-59	0.53
3	300	50	180	845	835[1]/850[2]/970[3]/950[4]	-	158	2368-2503	0,314-0,318	60-63	0.45
4	350	65	150	815	820[1]/840[2]/955[3]/930[4]	-	160	2360-2495	0,309-0,311	60-70	0.39
5	420	70	100	825	830[1]/845[2]/955[3]/930[4]	-	161	2406-2531	0,310-0,317	60-68	0.33
6	450	100	50	790	870[1]/875[2]/1005[3]/1000[4]	-	154	2414-2549	0,327-0,333	62-70	0.28
7	480	130	50	725	880[1]/905[2]/1015[3]/985[4]	-	152	2417-2552	0,328-0,339	62-70	0.25

Notes: C is Portland cement; MB is organomineral concrete modifier; MP-1 is microfiller; P is quartz sand; G is crushed stone: 1) gravel, density 2650 kg/m^3, 2) granite, density 2670 kg/m^3, 3) gabbro-diabase, density 3070 kg/m^3, 4) basalt, density 3000 kg/m^3; SP is superplasticizer; W is water, γ is average density of the mixture; V_G is the volume of coarse aggregate in the volume of the concrete mix; SC is the mobility along the spread of a normal cone.

1.3. Object of research and test methods

Six samples-cubes of 100×100×100 mm size have been prepared from concrete mixtures without vibration compaction to determine the cubic compressive strength of concrete (R) at the age of 28 and 90 days according to the standards of the Russian Federation GOST 10180 and GOST 31914. And 6 prism samples of 100 × 100 × 400 mm have been prepared to determine the prism compressive strength of concrete (R_b), static and dynamic modulus of elasticity, Poisson's ratio at the age of 28 and 90 days according to the standards of the Russian Federation GOST 24452, GOST 31914 and [24, 25].

Control samples were stored before testing under normal temperature and humidity conditions (temperature plus 20 ± 2 °C, humidity 95 ± 5%). The determination of the static modulus of elasticity and Poisson's ratio was carried out on a hydraulic press (see Figure 1) using 3 prism samples. The loading of the prism specimens was carried out in steps equal to $0.1R_b$ with holding at each step for 4-5 minutes to a level of 40% of the prism strength.

Figure 1. Tests of prism specimens with determination of the static elasticity modulus and Poisson's ratio of concrete on a hydraulic press

Determination of the dynamic modulus of elasticity (E_d) was carried out on the device Erudite MKIV CNS Farnell Limited (PC 1004) (see Figure 2) using 3 prism specimens. The determination of the dynamic modulus of elasticity of concrete with a length of prism specimens of 400 mm was carried out at a longitudinal resonant oscillation frequency in the range of 4–6 kHz according to the formula of the technical manual [24]:

$$E_d=4\cdot n^2\cdot l^2\cdot\gamma\cdot 10^{-12}, \qquad (2)$$

where: n – is resonant frequency of longitudinal vibrations, Hz; l – is specimen length, mm; γ – is average density of concrete in a sample, kg/m^3.

Figure 2. Tests of prism specimens with determination of the dynamic elasticity modulus of concrete using the Erudite MKIV (PC 1004) device

The value of the static and dynamic modulus of elasticity, as well as the Poisson's ratio at each age, was taken as the average value of the test results of all 3 prism specimens.

The actual class of concrete in terms of compressive strength (B_f) and the compressive strength of prisms (R_{bn}) were determined in accordance with the RF standard GOST 18105, considering the requirements of GOST 31914 for the minimum value of the required strength coefficient K_T = 1.14 (with a coefficient of variation V = 10%) according to the formulas:

$$B_f=\frac{R}{K_T}=\frac{R}{1,14}, \qquad (3)$$

$$R_{bn}=R_b\cdot\left(1\text{-}1,64\cdot\frac{V}{100}\right)=0,836\,R_b, \qquad (4)$$

2. TEST RESULTS AND DISCUSSION

Table 3 presents test results for concretes with various types of coarse aggregates in terms of: average density, cubic (R) and design compressive strength of prisms (R_b), actual class (B_f), compressive strength of prisms (R_{bn}) static E_b) and dynamic (E_d) elastic modulus, and also Poisson's ratio (ν) at the age of 28 and 90 days.

Table 3. Strength and short-term deformation characteristics of concrete

Series and composition number	*Age of concrete. days*	*Average density of concrete. kg/m³*	*Indicators of concrete compressive strength. MPa*				*Deformation characteristics of concrete*		
			R	B_ϕ	R_b	R_{bn}	E_b. *GPa*	E_d. *GPa*	ν
1	2	3	4	5	6	7	8	9	10
1-1	28	2326	36.2	32	35.0	29.3	32.2	37.1	0.207
	90	2332	38.3	33	37.8	31.6	33.6	37.4	0.206
1-2	28	2330	36.5	33	36.2	30.3	32.5	38.1	0.206
	90	2327	40.1	35	38.6	32.3	34.5	39.5	0.207
1-3	28	2448	37.6	33	36.3	30.3	36.0	41.1	0.207
	90	2451	38.1	33	37.6	31.4	37.8	41.5	0.205
1-4	28	2452	38.4	34	36.3	30.3	38.8	42.8	0.204
	90	2448	39.6	35	38.0	31.8	39.3	43.7	0.205
2-1	28	2358	61.0	53	57.2	47.8	38.3	41.8	0.212
	90	2352	65.3	57	60.0	50.2	39.1	42.2	0.208
2-2	28	2378	61.8	54	56.0	46.8	39.2	42.8	0.214
	90	2384	65.4	57	63.4	53.0	40.1	43.7	0.206
2-3	28	2476	62.2	55	58.1	48.6	40.5	44.2	0.223
	90	2481	66.1	58	62.4	52.2	41.4	45.9	0.211
2-4	28	2480	62.8	55	57.8	48.3	44.1	47.3	0.214
	90	2479	67.4	59	61.5	51.4	46.4	48.6	0.206
3-1	28	2363	68.2	60	58.4	48.8	38.8	42.1	0.205
3-2	28	2387	68.0	60	63.7	53.3	39.5	43.5	0.206
3-3	28	2451	70.0	61	61.8	51.7	42.8	48.0	0.209
3-4	28	2502	66.8	59	60.5	50.6	44.8	49.2	0.198
4-1	28	2372	65.6	58	60.4	50.5	38.8	42.3	
	90	2358	76.5	67	71.3	59.6	38.9	42.5	0.207
1	2	3	4	5	6	7	8	9	10
4-2	28	2414	73.8	65	68.6	57.3	40.2	45.3	
	90	2407	80.2	70	74.5	62.3	40.5	45.7	0.198
4-3	28	2483	76.0	67	70.1	58.6	43.0	47.4	
	90	2482	81.8	72	74.9	62.6	43.2	48.0	0.214
4-4	28	2473	73.6	65	68.0	56.8	46.2	51.1	
	90	2496	82.3	72	75.8	63.4	46.5	51.3	0.213
5-1	28	2410	78.2	69	71.8	60.0	42.4	47.7	
	90	2418	82.8	73	76.8	64.2	43.5	48.2	0.220
5-2	28	2432	82.6	72	79.8	66.7	43.2	48.9	
	90	2426	92.5	81	85.3	71.3	44.1	49.4	0.205

5-3	28	2518	87.8	77	82.3	68.8	47.6	50.4	
	90	2523	97.5	85	89.2	74.6	48.0	50.7	0.196
5-4	28	2523	91.4	80	83.7	70.0	51.2	56.5	
	90	2536	101.5	89	93.4	78.1	51.6	56.6	0.210
6-1	28	2412	97.5	86	91.1	76.2	44.8	48.4	
	90	2418	100.4	88	94.5	79.0	45.6	48.8	0.222
6-2	28	2423	100.3	88	92.6	77.4	46.1	50.2	
	90	2426	109.2	96	100.0	83.6	48.0	52.8	0.220
6-3	28	2515	107.0	94	98.2	82.1	51.0	55.0	
	90	2519	111.3	98	104.4	87.3	52.0	55.9	0.228
6-4	28	2532	102.9	90	94.6	79.1	54.1	58.8	
	90	2540	113.1	99	100.5	84.0	56.2	59.9	0.235
7-1	28	2425	100.2	88	95.4	79.8	46.8	50.6	
	90	2430	103.8	91	97.2	81.3	47.0	51.2	0.226
7-2	28	2443	102.8	90	97.2	81.3	47.5	52.9	
	90	2438	114.8	101	104.2	87.1	48.1	53.1	0.230
7-3	28	2520	112.8	99	102.1	85.4	51.6	56.4	
	90	2511	115.1	101	105.0	87.8	52.0	56.6	0.237
7-4	28	2553	108.5	95	104.5	87.4	55.4	60.2	
	90	2544	114.6	101	107.0	89.5	56.4	60.4	0.242

2.1. Average density

The average density of heavy concretes with various types of coarse aggregates varies in a wide range from 2326 to 2553 kg / m^3 and generally corresponds to the trend of changes in the average density of concrete mixes (see Table 2) and in some cases slightly exceeds the standard value up to 1.8%. according to RF Standards GOST 25192 and SP 63.13330.2018 (2000-2500 kg/m^3), however complies with the requirements of EN 206:2013 (2000-2600 kg/m^3).

2.2. Compressive strength of cubes

The cubic compressive strength (R) of all concretes with various types of coarse aggregates at the age of 28 days is in the range from 36.2 to 112.8 MPa and corresponds to the actual compressive strength classes of concrete from B_f32 to B_f99. And in age 90 days, it is in the range from 38.1 to 115.1 MPa and corresponds to the actual classes of concrete in terms of compressive strength from B_f33 to B_f101.

The use of various types of coarse aggregate (crushed stone of gravel, granite, gabbro-diabase and basalt crushed stone) slightly changes the cubic compressive strength of concrete (see Figure 3), which for all concrete compositions ranges from 89 to 111% of the strength of concrete on crushed granite. At the same time, concretes with granite, gabbro-diabase and basalt crushed stone aggregate with a crushability grade of 1400 have approximately the same cubic compressive strength. And on crushed stone of gravel with a crushability grade of 1200, the strength of concrete takes minimum values.

2.3. Compressive strength of prisms

The design prism compressive strength (R_b) of concrete of classes B30 to B100 at the age of 28 days is in the range from 35.0 to 104.5 MPa. And at the age of 90 days it was from 37.6 up to 107.0 MPa, does not depend on the type of

coarse aggregate and is a linear function of the concrete class in terms of compressive strength (see Figure 4).

The experimentally obtained actual values of the concrete prism compressive strength (R_{bn}) are 24% higher than those normalized according to the building code SP 63.13330.2018 (see Figure 4). The calculation of reinforced concrete structures for strength, performed on the basis of the normalized and design characteristics of concrete according to table 6.7 of the building code SP 63.13330.2018, in essence, leads to significant reserves of their bearing capacity.

If we evaluate the above results according to the criterion of the prismatic strength ratio, determined as the ratio of the prismatic compressive strength of concrete to cubic strength ($K_{pp} = R_b / R$), then its actual values are in the range from 0.86 to 0.99 and significantly exceed the values of this coefficient calculated according to the parameters given in SP 63.13330.2018 (from 0.71 to 0.73).

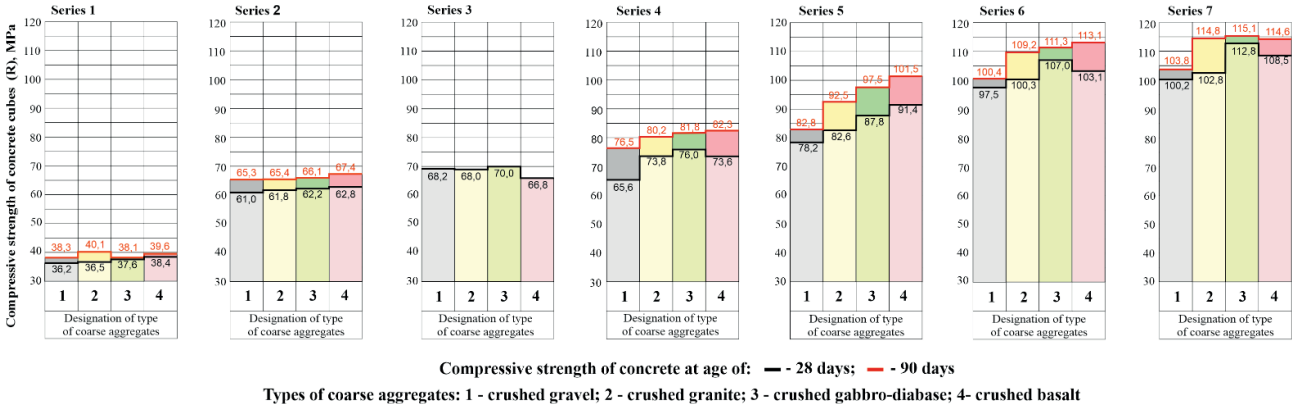

Figure 3. Compressive strength of concrete cubes with various types of coarse aggregates

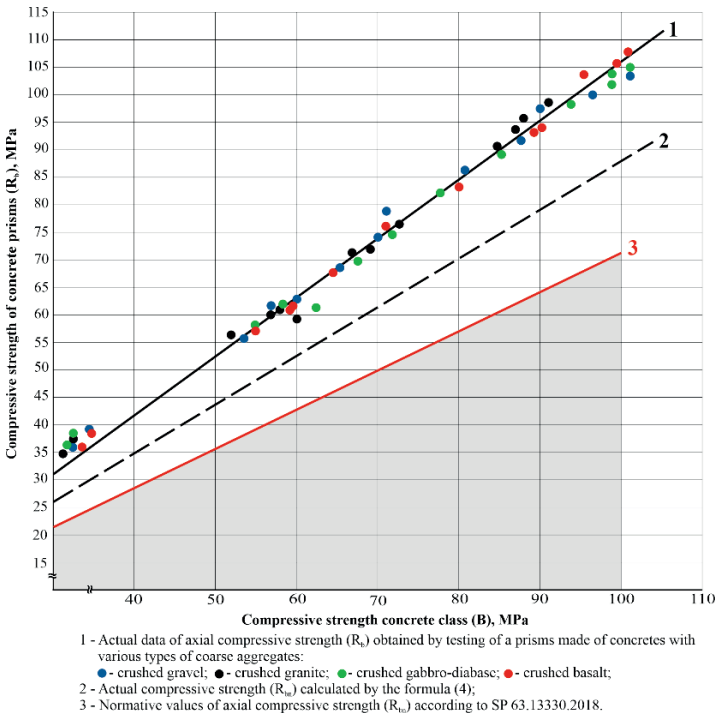

Figure 4. Axial compressive strength of heavy-weight concrete with various types of coarse aggregates

2.4. Elastic modulus

Table 3 and Figure 5 provide the results of determination of static (E_b) and dynamic (E_d) modulus of elasticity and dependencies on the actual classes of concrete (B_f32-B_f101) with compressive strength 36.2 -115.1 MPa with various types of coarse aggregates.

The obtained results (see Figure 5) show that the static and dynamic modulus of elasticity of concrete are directly proportional to the compressive class of concrete and largely depend on the type of coarse aggregate, in particular:

- static modulus of elasticity of heavy concrete with aggregate on crushed stone from gravel of actual classes B_f32-B_f91 (strength 36.2-103.8 MPa) is in the range from 32.2 to 47.0 GPa; the dynamic modulus of elasticity exceeds the static modulus by 3.1-4.9 GPa and is in the range from 37.1 to 51.2 GPa;

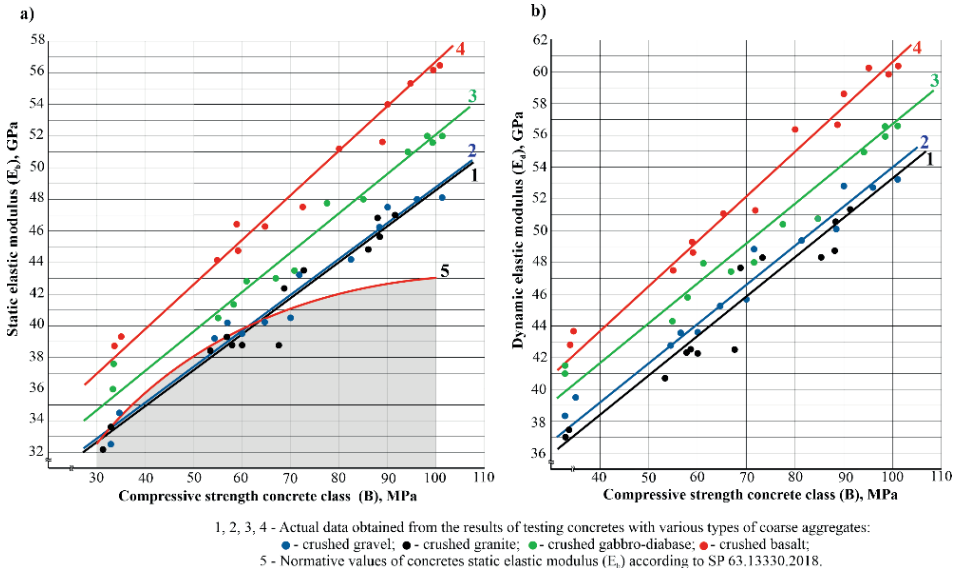

Figure 5. Static (a) and dynamic (b) elastic modules vs compressive strength of concretes of B30-B100 classes

- static modulus of elasticity of heavy concrete with aggregate on crushed granite actual classes B_f33-B_f101 (strength 36.6-114.8 MPa) is in the range from 43.2 to 48.1 GPa; the dynamic modulus of elasticity exceeds the static modulus by 3.2-5.7 GPa and is in the range from 38.1 to 53.1 GPa;
- static modulus of elasticity of heavy concretes with filler on gabbro-diabase crushed stone of actual classes B_f33-B_f101 (strength 37.6-115.1 MPa) is in the range from 36.0 to 52.0 GPa; the dynamic modulus of elasticity exceeds the static modulus by 2.7-5.2 GPa and is in the range from 41.1 to 56.4 GPa;
- static modulus of elasticity of heavy concrete with aggregate on basalt crushed stone of actual classes B_f34-B_f101 (strength 38.4-114.6 MPa) is in the range from 38.8 to 56.4 GPa; the dynamic modulus of elasticity exceeds the static modulus by 2.2-5.3 GPa and is in the range from 42.8 to 60.4 GPa.

Comparison of the experimentally obtained values of the static elastic modulus, and, consequently, the stiffness of reinforced concrete structures made of heavy concrete of compressive strength classes B30-B100, prepared with various types of coarse aggregate, with standardized values showed that:

- the static modulus of elasticity of concretes of classes B30-B70 on ordinary large aggregates (granite crushed stone and gravel crushed stone) corresponds to the values given in SP 63.13330.2018, Model Code MC 2010 and EN 1992-1-1: 2004 Eurocode 2;
- the static modulus of elasticity of high-strength concretes of classes B71-B100 on the same

conventional large aggregates (granite crushed stone and gravel crushed stone) exceeds by 5 ... 14% the values given in SP 63.13330.2018, corresponds to Model Code MC 2010 and is consistent with previously obtained results [10-14, 17, 18];

- the use of gabbro-diabase and basalt crushed stone as a coarse filler allows increasing the static modulus of elasticity of heavy concretes of compressive strength classes B30-B100 by 9 and 19%, respectively, which is consistent with the information given by the FIB in Table 5.1-6 of Model Code 2010, and paragraph 3.1.3 of EN 1992-1-1:2004 Eurocode 2.

The increase in the static modulus of elasticity of concretes on gabbro-diabase and basalt crushed stone in comparison with concretes on granite crushed stone is obviously associated with higher characteristics of the elastic properties of the rocks from which it is obtained. As is known, the elastic modulus of granite is 30-68 GPa, while in denser rocks it is higher: gabbro 60-125 GPa, diabase 80-110 GPa, basalt 20-100 GPa [15, 20, 26].

The same nature of the curves presented in Figures 5a and 5b indicates the presence of a linear dependence of the static modulus of elasticity of concrete not only on the compressive strength, but also on the dynamic modulus of elasticity, which corresponds to the information given in [27]. Based on the data in Table 3, the relationship between the static modulus of elasticity and the dynamic modulus of elasticity of heavy concretes of classes B30-B100 with various types of coarse aggregates was established (Figure 6), which can be expressed by the equation:

$$E_b = 0.982E_d - 3.437, \qquad (5)$$

The indicators of the dependence presented in Figure 6 are as follows: the number of test results (n) - 52; the average value of the static modulus of elasticity (E_{bm}) is 44.1 GPa; calculated standard deviation of the established dependence (S_2) is 1.203 GPa; standard deviation of the static modulus of elasticity actually obtained from the results of concrete testing (S_3) is 0.819 GPa; the root-mean-square deviation of the method used in constructing the dependence was assumed to be $0.02E_{bm}$ (S_4=0.881 GPa); correlation coefficient of the established dependence (r) is 0.99; the error in determining the static modulus of elasticity [(S_2/E_{bm})·100]=1.9%.

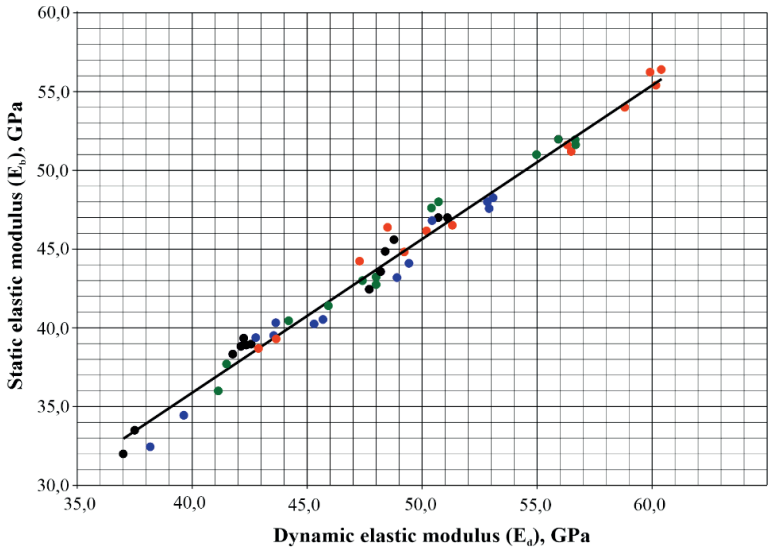

Actual data obtained from the results of testing concretes with various types of coarse aggregates:
● - crushed gravel; ● - crushed granite; ● - crushed gabbro-diabase; ● - crushed basalt;

Figure 6. Dependence between values of static (E_b) and dynamic (E_d) elastic modulus of heavy-weight concretes of B30-B100 classes

The obtained indicators allow using the dependence established in this way to determine the static modulus of elasticity of concrete from core specimens taken from structures, based on the results of a less laborious determination of the dynamic modulus of elasticity, since the value of the correlation coefficient of the dependence is more than 0.7, and the value of the error in determining the initial static modulus of elasticity is less than 15%.

2.5. Poison's ratio

Poisson's ratio of heavy concretes of classes B30-B100 is in the range from 0.196 to 0.242, basically corresponds to the normalized value of the Poisson's ratio $\nu_{b,P}$=0.2) according to clause 6.1.17 of the building code of the Russian Federation SP 63.13330.2018. With an increase in the concrete compressive strength class from B30 to B100, the average Poisson's ratio increases from 0.20 to 0.23 and practically does not depend on the type of coarse aggregate (see Figure 7).

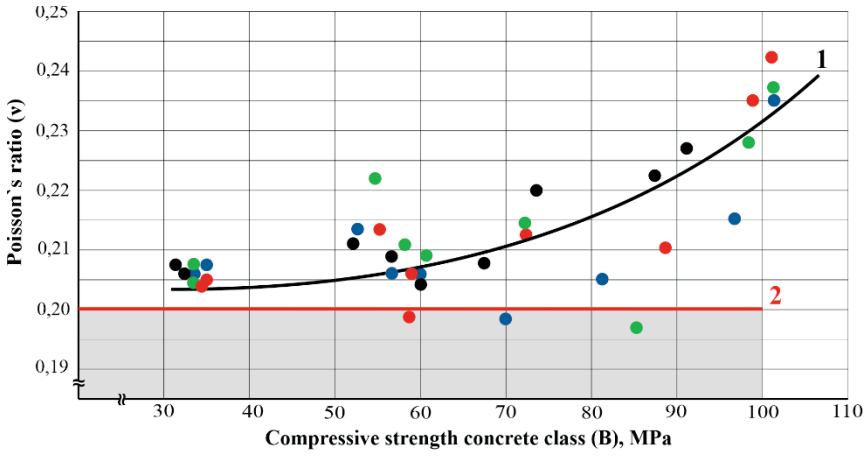

1 - Actual data obtained from the results of testing concretes with various types of coarse aggregates:
● - crushed gravel; ● - crushed granite; ● - crushed gabbro-diabase; ● - crushed basalt;
2 - Normative value of concretes Poisson`s ratio (ν_n) according to SP 63.13330.2018.

Figure 7. Poisson's ratio of concretes of B30-B100 classes

CONCLUSION

1. It is shown the possibility of controlling the strength and deformation characteristics of heavy concretes of classes B30-B100 (strength from 36.2 to 115.1 MPa) prepared from self-compacting mixtures due to technological factors - the use of various types of coarse aggregates and modifiers.
2. Use the crushed stone from more dense and durable rocks - gabbro-diabase or basalt (true density 3000- 3070 kg/m3, modulus of elasticity up to 125 GPa) as a coarse filler instead of crushed stone from gravel or crushed granite (true density 2650-2670 kg / m^3, modulus of elasticity up to 68 GPa), does not lead to significant changes in the cubic and prism compressive strengths of concrete and Poisson's ratio, but allows increasing the static modulus of elasticity of concrete by 9-19%.
3. The values of the dynamic modulus of elasticity of heavy concrete were obtained. This is in the range from 41.1 to 60.4 GPa and, depending on the classes of concrete, exceed the static modulus of elasticity of concrete by 2.2-5.3 GPa. The possibility of using a less time-consuming method for monitoring the values of the static modulus of elasticity of concrete in structures by determining the dynamic modulus

using the calibration dependence E_b - E_d is shown.
4. The obtained results show that the values of the strength and deformation characteristics of modern concretes of classes B30-B100 exceed the standard values given in the code of rules of the Russian Federation SP 63.13330.2018, in particular:
- the actual prism compressive strength is 24% higher than the standard values according to table 6.7 of the building code;
- the static modulus of elasticity of high-strength concretes of classes B80-B100 is 5-14% higher than the standard values according to table 6.11 of the building code.
5. The above is the basis for making appropriate changes to the building code of the Russian Federation SP 63.13330.2018 in terms of increasing the standard values of prism strength and the modulus of elasticity of heavy concrete.
6. The ability to control the values of the modulus of elasticity of heavy concrete by selecting a large aggregate of the appropriate origin and quality should considered when calculating and designing reinforced concrete structures and, as an appropriate addition, is included in the building code of the Russian Federation SP 63.13330.2018. This is in line with the recommendations of CEB-FIP Model Code 2010 and EN 1992-1-1:2004 Eurocode 2.

The authors are grateful to Dr. Krylov S.B., Ph.D., Arleninov P.D., engineer Kolmakova P.S. for participation in the planning of the experiment and in the analysis of the results.

REFERENCES

1. **P.-C. Aitcin** High-Performance Concrete // E & FN Spon, London, 1998.
2. **Qirui Luo, Wei Wang, Zhuangzhuang Sun, Bingjie Wang, Shanwen Xu.** Statistical analysis of mesoscopic concrete with random elastic modulus // Journal of Building Engineering. - 2021. - №101850. - C. 1-15.
3. **Yueyi Gao, Chuanlin Hu, Yamei Zhang, Zongjin Li, Jinlong Pan.** Investigation on microstructure and microstructural elastic properties of mortar incorporating fly ash // Cement and Concrete Composites. - 2017. - №S0958-9465(17)30848-X. - C. 1-30.
4. **Meenakshi Sharma, Shashank Bishnoi.** Influence of properties of interfacial transition zone on elastic modulus of concrete: Evidence from micromechanical modelling // Construction and Building Materials. - 2020. - №1183814. - C. 1-11.
5. **Qinghe Wang, Zhe Li, Yuzhuo Zhang, Huan Zhang, Mei Zhou, Yanfeng Fang** Influence of coarse coal gangue aggregates on elastic modulus and drying shrinkage behaviour of concrete // Journal of Building Engineering. - 2020. - №101748. - C. 1-12.
6. **Nayara S. Klein, Lauri A. Lenz, Wellington Mazer** Influence of the granular skeleton packing density on the static elastic modulus of conventional concretes // Construction and Building Materials. - 2020. - №118086. - C. 1-8.
7. **Hans Beushausen, Thomas Dittmer**. The influence of aggregate type on the strength and elastic modulus of high strength concrete // Construction and Building Materials. - 2015. - №132-139. - C. 132-139.
8. **H. Beshr, A.A. Almusallam, M. Maslehuddin.** Effect of coarse aggregate quality on the mechanical properties of high strength concrete // Construction and Building Materials. - 2003. - №97-103. - C. 97-103.
9. **F.P. Zhou, F.D. Lydon and B.I.G. Barr.** Effect of coarse aggregate quality on the mechanical properties of high strength concrete // Cement and Concrete Research. - 1995. - №177-186. - C. 177-186.
10. **S. Kaprielov, N. Karpenko, A. Sheinfeld, E. Kouznetsov**. Influence of multicomponent modifier containing silica fume, fly ash, superplasticizer and air-entraining agent on structure and deformability of high-strength concrete // Seventh CANMET/ACI International Conference on

Superplasticizers and other chemical admixtures in concrete. Berlin, Germany, 2003, p.p.99-107
11. **S. Kaprielov, N. Karpenko, A. Sheinfeld** On Controlling Modulus of Elasticity and Creep in High-Strength Concrete with Multicomponent Modifier // Eighth CANMET/ACI International Conference on Fly ash, Silica Fume, Slag and Natural Pozzolans in Concrete, Las Vegas, May 23-29,2004, Supplementary Papers, p.p.405-421
12. **Kaprielov S.S., Sheinfeld A.V., Kardumyan G.S.** New modified concretes. - Moscow: LLC "Printing house" Paradise ", 2010. - 258 p.
13. **Karpenko N.I., Kaprielov S.S., Kuznetsov E.N., Sheinfeld A.V., Bezgodov I.M.** Creep measures for high-strength concretes based on MB / RAASN, Bulletin of the Department of Building Sciences. Issue. 8. - M., 2004. - P.203-214.
14. **Smirnov N.V., Antonov E.A., Dmitriev A.I., Kaprielov S.S., Sheinfeld A.V., Zhigulev N.F.** Prospects for the use of concrete with high performance properties in domestic transport construction / Transport construction. - No. 12. - 1998. - P.16-18.
15. **Berg O.Ya., Shcherbakov E.N., Pisanko G.N.** High-strength concrete - Moscow: Stroyizdat, 1971. - 208 p.
16. **Melnik R.A., Fedorchuk V.I., Lubenets I.I**. Mechanical properties of high-strength concrete grades 800 and 1000 / Concrete and reinforced concrete. - No. 8. - 1975. - P.7-10.
17. **Sviridov N.V.** Extra strong cement concrete / Energy construction. - No. 8. - 1991. - P.21-29.
18. **Sviridov N.V., Kovalenko M.G.** Concrete with a strength of 150 MPa on ordinary Portland cements / Concrete and reinforced concrete. - No. 2. - 1990. - P.21-22.
19. **Sheinfeld A.V.** Features of the formation of a hierarchical micro- and nanostructure of cement systems with complex organo-mineral modifiers / Concrete and reinforced concrete. - No. 2. - 2016. - P.16-21.
20. **Sheikin A.E., Chekhovskii Yu.V., Brusser M.I.** Structure and properties of cement concretes - Moscow: Stroyizdat, 1979. - 344 p.
21. **Kaprielov S., Sheinfeld A.** Influence of Silica Fume / Fly Ash / Superplasticizer Combinations in Powder-like Complex Modifiers on Cement Paste Porosity and Concrete Properties. Sixth CANMET/ACI International Conference on Superplasticizers and other Chemical Admixtures in Concrete. Nice, France, October 2000. Proceedings, p.p.383-400.
22. EN 12350-8: 2010 Testing fresh concrete - Part 8: Self compacting concrete - Slump-flow test.
23. EN 206: 2013 Concrete - Specification, performance, production and conformity.
24. Resonant Frequency Testing. Technical Reference Manual / CNS Farnell Limited Elstree Business Center, Elstree Way, Borehamwood, Hertfordshire, WD6 1RX, August 2005. – 24p.
25. Operating instructions. ERUDITE MKIV (PC 1004) / CNS Farnell Limited Elstree Business Center, Elstree Way, Borehamwood, Hertfordshire, England. WD6 1RX, 2004. – 34p.
26. Under the total. ed. prof. Voznesensky A.N. Geology and dams / Moscow; Leningrad: Gosenergoizdat, 1959, Vol. 3 - 1963. - 175 p.
27. **Byung Jae Lee, Seong-Hoon Kee, Taekeun Oh, Yun-Yong Kim** Effect of Cylinder Size on the Modulus of Elasticity and Compressive Strength of Concrete from Static and Dynamic Tests // Hindawi Publishing Corporation Advances in Materials Science and Engineering. - 2015. - №ID 580638. – 12 p.

СПИСОК ЛИТЕРАТУРЫ

1. **P.-C. Aitcin** High-Performance Concrete // E & FN Spon, London, 1998.
2. **Qirui Luo, Wei Wang, Zhuangzhuang Sun, Bingjie Wang, Shanwen Xu.** Statisti-

cal analysis of mesoscopic concrete with random elastic modulus // Journal of Building Engineering. - 2021. - №101850. - С. 1-15.
3. **Yueyi Gao, Chuanlin Hu, Yamei Zhang, Zongjin Li, Jinlong Pan.** Investigation on microstructure and microstructural elastic properties of mortar incorporating fly ash // Cement and Concrete Composites. - 2017. - №S0958-9465(17)30848-X. - С. 1-30.
4. **Meenakshi Sharma, Shashank Bishnoi** Influence of properties of interfacial transition zone on elastic modulus of concrete: Evidence from micromechanical modelling // Construction and Building Materials. - 2020. - №1183814. - С. 1-11.
5. **Qinghe Wang, Zhe Li, Yuzhuo Zhang, Huan Zhang, Mei Zhou, Yanfeng Fang** Influence of coarse coal gangue aggregates on elastic modulus and drying shrinkage behaviour of concrete // Journal of Building Engineering. - 2020. - №101748. - С. 1-12.
6. **Nayara S. Klein, Lauri A. Lenz, Wellington Mazer** Influence of the granular skeleton packing density on the static elastic modulus of conventional concretes // Construction and Building Materials. - 2020. - №118086. - С. 1-8.
7. **Hans Beushausen, Thomas Dittmer** The influence of aggregate type on the strength and elastic modulus of high strength concrete // Construction and Building Materials. - 2015. - №132-139. - С. 132-139.
8. **H. Beshr, A.A. Almusallam, M. Maslehuddin** Effect of coarse aggregate quality on the mechanical properties of high strength concrete // Construction and Building Materials. - 2003. - №97-103. - С. 97-103.
9. **F.P. Zhou, F.D. Lydon and B.I.G. Barr** Effect of coarse aggregate quality on the mechanical properties of high strength concrete // Cement and Concrete Research. - 1995. - №177-186. - С. 177-186.
10. **S. Kaprielov, N. Karpenko, A. Sheinfeld, E. Kouznetsov** Influence of multicomponent modifier containing silica fume, fly ash, superplasticizer and air-entraining agent on structure and deformability of high-strength concrete // Seventh CANMET/ACI International Conference on Superplasticizers and other chemical admixtures in concrete. Berlin, Germany, 2003, p.p.99-107
11. **S. Kaprielov, N. Karpenko, A. Sheinfeld** On Controlling Modulus of Elasticity and Creep in High-Strength Concrete with Multicomponent Modifier // Eighth CANMET/ACI International Conference on Fly ash, Silica Fume, Slag and Natural Pozzolans in Concrete, Las Vegas, May 23-29,2004, Supplementary Papers, p.p.405-421
12. **Каприелов С.С., Шейнфельд А.В., Кардумян Г.С.** Новые модифицированные бетоны. – М.: ООО «Типография «Парадиз», 2010. – 258 стр.
13. **Карпенко Н.И., Каприелов С.С., Кузнецов Е.Н., Шейнфельд А.В., Безгодов И.М.** Меры ползучести высокопрочных бетонов на основе МБ / РААСН, Вестник отделения строительных наук. Вып. 8. - М., 2004. - С.203-214.
14. **Смирнов Н.В., Антонов Е.А., Дмитриев А.И., Каприелов С.С., Шейнфельд А.В., Жигулев Н.Ф.** Перспективы применения бетонов с высокими эксплуатационными свойствами в отечественном транспортном строительстве / Транспортное строительство. - № 12. – 1998. - С.16–18.
15. **Берг О.Я.,Щербаков Е.Н., Писанко Г.Н.** Высокопрочный бетон – Москва: Стройиздат, 1971. – 208 стр.
16. **Мельник Р.А., Федорчук В.И., Лубенец И.И.** Механические свойства высокопрочных бетонов марок 800 и 1000 / Бетон и железобетон. - №8. – 1975. - С.7-10.
17. **Свиридов Н.В.** Особо прочный цементный бетон / Энергетическое строительство. - №8. – 1991. - С.21-29.
18. **Свиридов Н.В., Коваленко М.Г.** Бетон прочностью 150 МПа на рядовых порт-

ландцементах / Бетон и железобетон. - №2. – 1990. - С.21-22.
19. **Шейнфельд А.В.** Особенности формирования иерархической микро- и наноструктуры цементных систем с комплексными органоминеральными модификаторами / Бетон и железобетон. - № 2. – 2016. - С.16-21.
20. **Шейкин А.Е., Чеховский Ю.В., Бруссер М.И.** Структура и свойства цементных бетонов – Москва: Стройиздат, 1979. – 344 стр.
21. **Kaprielov S., Sheinfeld A.** Influence of Silica Fume / Fly Ash / Superplasticizer Combinations in Powder-like Complex Modifiers on Cement Paste Porosity and Concrete Properties. Sixth CANMET/ACI International Conference on Superplasticizers and other Chemical Admixtures in Concrete. Nice, France, October 2000. Proceedings, p.p.383-400.
22. EN 12350-8: 2010 Testing fresh concrete - Part 8: Self compacting concrete - Slump-flow test.
23. EN 206: 2013 Concrete - Specification, performance, production and conformity.
24. Resonant Frequency Testing. Technical Reference Manual / CNS Farnell Limited Elstree Business Center, Elstree Way, Borehamwood, Hertfordshire, WD6 1RX, August 2005. – 24p.
25. Operating instructions. ERUDITE MKIV (PC 1004) / CNS Farnell Limited Elstree Business Center, Elstree Way, Borehamwood, Hertfordshire, England. WD6 1RX, 2004. – 34p.
26. **Под общ. ред. проф. Вознесенского А.Н.** Геология и плотины / Москва; Ленинград: Госэнергоиздат, 1959, Т.3 – 1963. – 175 стр.
27. **Byung Jae Lee, Seong-Hoon Kee, Taekeun Oh, Yun-Yong Kim** Effect of Cylinder Size on the Modulus of Elasticity and Compressive Strength of Concrete from Static and Dynamic Tests // Hindawi Publishing Corporation Advances in Materials Science and Engineering. - 2015. - №ID 580638. – 12 p.

Semen S. Kaprielov, Eng.Sc.D., head of laboratory №16 "Research Institute for Concrete and Reinforced Concrete" named after A.A. Gvozdev, JSC Research Center of Construction, 2-nd Institutskaya str., 6, Moscow, 109428, Russian Federation, tel. +7 (499) 171-0573, e-mail: kaprielov@masterbeton-mb.ru.

Andrey V. Sheynfeld, Eng.Sc.D., deputy head of laboratory №16 "Research Institute for Concrete and Reinforced Concrete" named after A.A. Gvozdev, JSC Research Center of Construction, 2-nd Institutskaya str., 6, Moscow, 109428, Russian Federation, tel. +7 (499) 174-7635, e-mail: sheynfeld@masterbeton-mb.ru.

Nikita M. Selyutin, engineer, «Master Concrete Enterprise» LTD, Saratovskaya str., 31, Moscow, 109518, Russian Federation, tel. +7 (499) 796-16-32, e-mail: selyutin@masterbeton-mb.ru.

Каприелов Семен Суренович, доктор технических наук, заведующий лабораторией №16 НИИЖБ им. А.А. Гвоздева АО «НИЦ Строительство», 109428 Москва, 2-я Институтская ул., д.6, кор.5, тел. +7-499-171-0573, e-mail: kaprielov@masterbeton-mb.ru.

Шейнфельд Андрей Владимирович, доктор технических наук, зам. заведующего лабораторией №16 НИИЖБ им. А.А. Гвоздева АО «НИЦ Строительство», 109428 Москва, 2-я Институтская ул., д.6, кор.5, тел. +7-499-174-7635, e-mail: sheynfeld@masterbeton-mb.ru.

Селютин Никита Михайлович, инженер, ООО «Предприятие Мастер Бетон», 109518 Москва, ул. Саратовская, д.31, +7-499-796-1632, e-mail: selyutin@masterbeton-mb.ru.

International Journal for Computational Civil and Structural Engineering, 18(1) 40–50 (2022)

DOI:10.22337/2587-9618-2022-18-1-40-50

THE EFFECT OF DRAW-OFF ON FILTRATION REGIME OF EARTH-FILL DAM

Nikolay A. Aniskin*, *Stanislav A. Sergeev

National Research Moscow State University of Civil Engineering, Moscow, RUSSIA

Abstract. The article discusses the solution to the problem of transient seepage in relation to cases of rapid drawdown or draw-off, which may be caused by technological necessity or an emergency. This paper provides an overview of research and calculation methods for the problem under consideration. Using the PLAXIS software package, a numerical solution of the filtration problem for a homogeneous soil dam with a drainage prism is obtained. This problem has been repeatedly solved using other methods and computational programs. Comparison of the obtained results with those performed earlier by other methods showed their reliability and good comparability. The obtained results of solving the filtration problem at the next stage of the study of the structure operability can be used to assess the filtration strength of the soils of the dam and the stability of the upstream slope.

Keywords: drawdown, draw-off, filtration flow, depression surface, filtration gradient, slope stability.

ВЛИЯНИЕ СРАБОТКИ ВОДОХРАНИЛИЩА НА ФИЛЬТРАЦИОННЫЙ РЕЖИМ ГРУНТОВОЙ ПЛОТИНЫ

Н.А. Анискин*, *С.А. Сергеев

Национальный исследовательский Московский государственный строительный университет, Москва, РОССИЯ

Аннотация. В статье рассматривается решение задачи неустановившейся фильтрации применительно к случаям быстрой сработки водохранилищ гидроузлов, что может быть вызвано технологической необходимостью или аварийной ситуацией. Дается обзор исследований и методов расчета рассматриваемой задачи. С использованием программного комплекса PLAXIS получено численное решение фильтрационной задачи для грунтовой однородной плотины с дренажной призмой. Данная задача ранее неоднократно решалась с использованием других методов и вычислительных программ. Сравнение полученных результатов с выполненными ранее другими методами показали их достоверность и хорошую сопоставимость. Полученные результаты решения фильтрационной задачи на следующем этапе изучения работоспособности конструкции могут быть использованы для оценки фильтрационной прочности грунтов плотины и устойчивости верхового откоса.

Ключевые слова: сработка водохранилища, фильтрационный поток, депрессионная поверхность, градиент фильтрации, устойчивость откоса.

INTRODUCTION

The operation of earth-fill dams often requires drawdown or draw-off. It can be caused by the technological scheme of the work of a hydraulic structure - the use of water for various purposes, for example, power generation, irrigation or water supply. Also, draw-off can be caused by the need to reduce the current water head in the event of an emergency situation in the hydraulic structure. Such a decrease in the water level, which sometimes occurs at a sufficiently high speed, causes a change in the filtration regime of the earth-fill dam: the position of the depression surface, the direction and magnitude of the velocities and filtration gradients change. These changes can lead to negative consequences: the occurrence of filtration deformations, a decrease in stability and

the collapse of the slope due to the action of the emerging hydrodynamic filtration loads [1-4].

In the practice of hydraulic engineering, there are cases of accidents at structures caused by a rapid drawdown or draw-off [5-7]. As an example, a massive slope collapse at the 116 m high San Luis dam in California occurred in 1981 as a result of lowering the upstream level by 55 m in 120 days during the dry season [5, 6]. A 340 m wide landslide brought down an array of soil with a volume of 310000 m^3 into the reservoir. After repair work, during which 1 100 000 m^3 of soil was additionally poured into the body of the dam, the dam's operability was restored.

An important issue in the design of soil dams is the prediction of the behavior of the structure with changes in water level and ensuring its stability and safety [8, 9]. The solution to this problem has two parts:

1) Solution of transient seepage problem, which makes it possible to determine changes in the position of the depression surface, filtration head, filtration gradients and velocities, distribution of filtration hydrodynamic load in the upper prism of a soil dam.

2) Assessment of the stability of the dam slope, taking into account the results of solving the filtration problem.

In this paper, we consider the solution of transient seepage problem. The paper provides an overview of the development and current state of the issue in solving such problems. The results of the numerical solution of a transient seepage problem for a earth-fill dam with a rapid drawdown or draw-off using the PLAXIS software package are presented. Comparison of the obtained results with the available analytical solution, the results of physical modeling and numerical solution using the FILTR program is given.

METHODS

The solution of the considered filtration problem is based on the theory of transient motion of an incompressible fluid in a non-deformable porous medium. The porous medium is completely saturated with liquid. For the first time, general differential equations describing the process of transient seepage were formulated by N.E. Zhukovsky [10], but due to the complexity of the solution, these equations were used much later. Hydraulic methods based on the Boussinesq equation [11] have received significant development in the practice of calculating transient seepage problems:

$$\frac{\partial H}{\partial t} = \frac{kh_a}{\mu}\left(\frac{\partial^2 H}{\partial x^2} + \frac{\partial^2 H}{\partial y^2}\right) + \frac{\varepsilon}{\mu}, \qquad (1)$$

where H – head, t – time period, k – coefficient of filtration, h_m – average head, μ – water absorption coefficient, ε – soil porosity.

The main assumption adopted in hydraulic theory is the constancy of horizontal filtration velocities along the vertical section.

Boussinesq's hypothesis about the constancy of horizontal velocities along the vertical section of the filtration flow was tested in the works of Musket (1949) (Muskat) [12, 13], and later V. M. Shestakov [14], which showed its inaccuracy.

The main results of the considered filtration calculations are the determination of the position of the depression surface and the values of the head gradients. Many researchers in the late 30s - early 40s of the last century [11] adopted an approximate scheme, according to which it was believed that during the fall of the water level in the head water, the depression curve does not have time to change its position and is in the initial position. Analyzing the picture of filtration movement in the dam slope obtained under this assumption, R. Muller [11] came to the conclusion that the average head gradient near the slope is approximately equal to Sin β (where β is the angle of inclination of the slope surface to the horizon) and is directed along the slope surface. However, further research by numerous authors showed that such a scheme often overestimates filtration gradients and forces and is acceptable for low-permeability soils. The problems associated with the calculations of transient seepage found their development in the works of V. I. Aravin [15], N.

N. Bindeman [16], N. N. Verigin [17], V. M. Dombrovsky [18], G. Kamensky [19], L.S. Leybenson [20], V.S. Lukyanova [21], P.Ya. Polubarinova-Kochina [3, 4], I.A. Charny [22], V.M. Shestakova [14, 23, 24], Musket (1949) (Muskat) [13], H.R. Cedergreen [1], E. Reinius [25] and others.

All studies of transient seepage problems presented above were carried out under certain restrictions, which is caused by the imperfection of the methods used. A homogeneous area was considered, a constant rate of reservoir drawdown was taken, and a set of structures for which the proposed methods could be applied was limited.

Today, a qualitatively higher level of solving such problems is achieved using numerical methods and, first of all, using the finite element method (FEM) [26, 27]. The solution of the filtration problem in most of the used computational programs and complexes is reduced to solving the basic differential equation of the theory of filtration using the known boundary and initial conditions:

$$\frac{\partial}{\partial x}\left(K_x \frac{\partial H}{\partial x}\right)+\frac{\partial}{\partial y}\left(K_y \frac{\partial H}{\partial y}\right)+\frac{\partial}{\partial z}\left(K_z \frac{\partial H}{\partial z}\right)-\mu \frac{\partial H}{\partial t}=0 \qquad (2)$$

where $H=f(x,y,z,t)$ is the required head function in the computational domain, changing in time t; Kx, Ky, Kz - filtration coefficients in the directions of the coordinate axes X, Y, Z; μ - coefficient of soil water loss.

It is assumed that the movement of water between the soil particles occurs when the pores are completely filled with water under the action of a hydraulic gradient from an area with higher pressure to an area with lower pressure. The ability of the soil to conduct a saturated water flow under the influence of a hydraulic pressure gradient is characterized by a filtration coefficient. By value, it is equal to the velocity of the filtration flow with an equal unit of the hydraulic pressure gradient. The problem is to determine the position of the free (depression) flow surface with such a formulation of the task. This is solved by excluding finite elements from the computational domain, for which the value of the filtration head obtained from the solution turns out to be less than their altitude position [26, 27].

In the considered filtration problems, the water level in the head water changes, as a result of which the pores that are not completely filled with water are saturated (when the level rises) or water outflows from them (when the level decreases). These issues (in relation to porous soils) were considered in the works of famous scientists in the field of soil hydrology [28]. The concept of the basic hydrophysical characteristic was introduced as a characteristic of the water-holding capacity of the soil [28]. There are many models that characterize the hydraulic behavior of unsaturated soils [29-31].

The PLAXIS software package used in this work includes modules for performing calculations of steady-state groundwater filtration. The PlaxFlow module allows calculations of transient groundwater filtration. Filtration parameters include the water permeability of the soil (in a saturated state), as well as models and filtration parameters in an unsaturated zone. One of the most common and proven models is used – the Van Genuchten model [31], the basic equation of which relates water saturation to head as follows:

$$S(\phi_p) = S_{res} + (S_{sat} - S_{res})\left[1 + (g_a \left|\phi_p\right|)^{g_n}\right]^{g_c} \qquad (3)$$

where $\phi_p = -\frac{p_w}{\gamma_w}$ и p_w- pore suction pressure, γ_w - unit weight of pore liquid, S_{res} – residual water saturation, which characterizes the part of the liquid remaining in the pores even with high suction, S_{sat} – may be less than one, because pores can be occupied by gas, g_a – a parameter that characterizes the amount of gas that has penetrated into the soil, g_n – parameter characterizing the rate of fluid loss

from the soil, $g_c = \frac{(1-g_n)}{g_n}$ - parameter used in the general Van Genuchten equation.

Further, the paper presents some results of numerical solutions of transient seepage problems performed using the PLAXIS program and their comparison with analytical solutions, results of physical and numerical modeling using the FILTR program [32].

RESEARCH OBJECT

To evaluate the numerical solution of the problem of transient seepage when the water level of the head water changes, obtained using the PLAXIS software package, a test problem was solved, which has solutions by various methods [11, 14, 32]. A homogeneous sand dam with a drainage prism was considered (Fig. 1). The height of the dam is 24.0 m, the upstream slope was laid - 1: 3.0, downstream slope - 1: 1.85. In the downstream fill, drainage is arranged in the form of a drainage fill with a height of 5.0 m. The initial water level of the head water is H_1 = 22.0 m, the water level of the tailwater is constant and equal to h_2 = 3.0 m. The sand filtration coefficient is k = 1.92 m/day, water absorption coefficient μ = 0.2. The drawdown rate is v = 1.0 m/day.

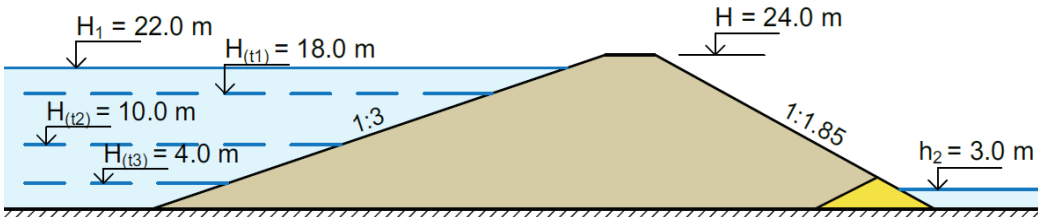

Figure 1. Schematic diagram of an earth dam with a drainage banquet

The moments of time τ = 4 days (drawdown by 4 meters, the permanent water level 18.0 m), τ = 12 days (drawdown by 12 meters, the permanent water level 10.0 m) and τ = 18 days (drawdown by 18 meters, the permanent water level 4.0 m).

RESULTS

The comparison results for the position of the depression surface in the design sections are presented in Fig. 2 and Table 1.

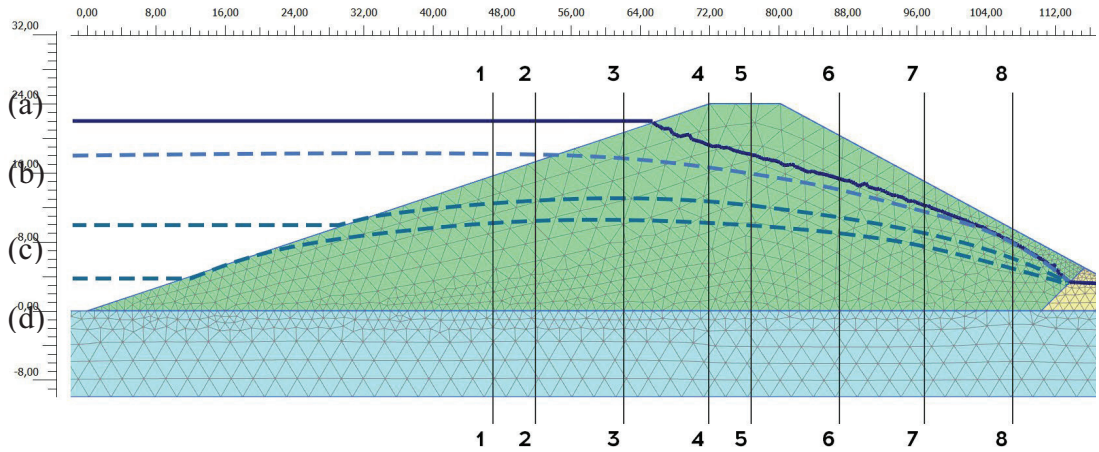

Figure 2. Position of depression curves, where (a) is the normal water level, (b), (c), (d) is the position at times τ = 4, 12, 18 days

A fairly good comparability of the results obtained by all methods can be noted. So, at the moment of time $\tau = 4$ days, the difference in the altitude of the points on the depression surface is in the interval (0.1-0.5) m, which does not exceed 3% of the headwater level.

Table 1. Results for the position of the depression surface in the design sections

Time	*Calculation method*	*Coordinates of the surface points of the depression curve*							
		Design sections							
		1-1	*2-2*	*3-3*	*4-4*	*5-5*	*6-6*	*7-7*	*8-8*
T= 4 days	hydraulic integrator V.S. Lukyanov		18.0	18.0	17.1	16.0	14.3	11.9	8.5
	V.M.Shestakov's method		18.0	17.3	16.8	15.7	13.9	11.6	7.9
	FILTR		18.0	17.8	17.0	16.1	14.4	11.7	7.5
	Plaxis		18,0	17.7	16.7	15.9	14.2	11.6	7.6
T= 12 days	hydraulic integrator V.S. Lukyanov	12.3	13.0	13.5	12.8	12.3	11.2	9.7	7.2
	V.M.Shestakov's method	13.0	13.9	14.0	13.7	13.0	12.0	10.0	7.8
	FILTR	13.1	13.3	13.5	13.0	12.5	11.4	9.3	6.2
	Plaxis	12.6	12.9	13.2	12.9	12.4	10.7	8.9	6.0
T=18 days	hydraulic integrator V.S. Lukyanov	9.5	10.0	10.6	10.5	10.2	9.2	8.2	6.2
	V.M.Shestakov's method	11.6	11.9	12.0	11.5	11.0	10.0	8.9	6.0
	FILTR	10.8	11.0	11.1	10.9	10.5	9.5	8.0	5.5
	Plaxis	10.2	10.4	10.5	10.2	9.7	8.9	7.4	5.1

At the moment of time τ = 18 days, the difference in results at some points increases to 1.5 m (PLAXIS - Shestakov's method in sections 2-2, 3-3). It is possible to note a slight excess of the results for the second and third calculated points in time according to the method of V.M. Shestakov with other methods and good comparability of numerical solutions and modeling on a hydraulic integrator.

Figure 3 shows the distribution of filtration heads for the design points in time, obtained from the solution of the transient seepage problem using the PLAXIS software package.

The obtained pictures of the filtration head distribution allow us to estimate the dynamics of changes in the direction of movement of the filtration flow depending on the water level in the head water. For the moment of time $\tau = 4$ days (Fig. 3, b), in an insignificant part of the upstream slope above the drawdown mark of 18.0 m, there was an outflow of water and drainage of the soil. Movement in the entire calculated area below the depression surface is directed from the upstream slope to the downstream fill side. By the moment of time τ = 12 days (Fig. 3, c) in the center of the soil massif of the dam, an area with increased head is formed relative to the area adjacent to the upstream slope of the dam. This indicates the occurrence of the movement of the filtration flow towards the upstream slope of the dam.

With a further decrease in the water level (Fig. 3, d), the head distribution does not change and the movement of water from the center to the upstream slope continues.

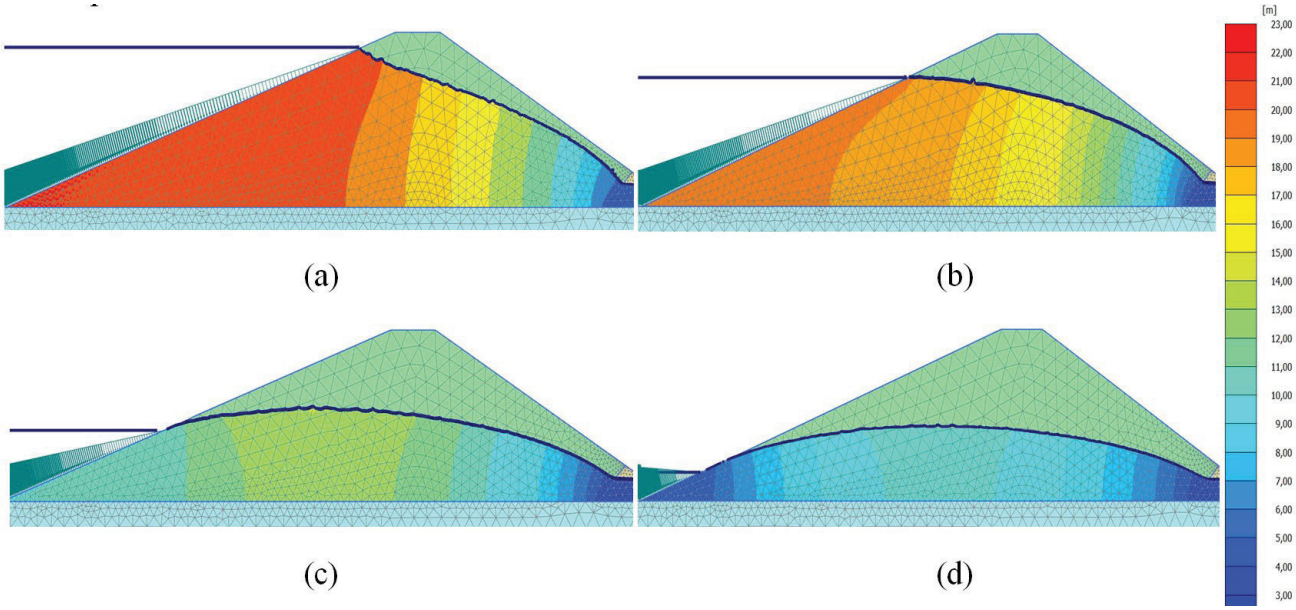

Figure 3. Distribution of filtration head, where (a) - the normal water level, (b), (c), (d) is the position at times τ = 4, 12, 18 days

The occurrence of a filtration flow directed towards the head water during the drawdown negatively affects the stability of the slope [7-9]. To assess the stability, it is necessary to know the distribution over the calculated area of the volumetric hydrodynamic load, which is directly proportional to the filtration gradient. As a result of solving the considered problem using the PLAXIS calculation complex, distributions of filtration gradients were obtained at calculated time points. Table 2 shows the values of the components of the filtration gradients and their comparison with the results of calculations in FILTR. Fig. 4 shows the results of calculations in the form of a distribution of horizontal components of the filtration gradient.

Table 2. Results of calculations of the components of the filtration gradient

Time	*Software package*	*Component of the filtration gradient*			
		upstream slope		*downstream slope*	
		horizontal, i_x	*vertical, i_y*	*horizontal, i_x*	*vertical, i_y*
normal water level	FILTR	-0.01	0.02	-0.52	0.72
	Plaxis	-0.001	0.02	-0.6	0.55
T= 4 days	FILTR	0.04	-0.12	-0.43	0.71
	Plaxis	0.02	-0.17	-0.57	0.51
T= 12 days	FILTR	0.31	0.07	-0.33	0.59
	Plaxis	0.25	-0.1	-0.39	0.34
T= 18 days	FILTR	0.32	0.09	-0.26	0.46
	Plaxis	0.31	-0.1	-0.29	0.23

The results of calculations in two computing complexes showed a fairly good comparability of the results. Thus, at the initial moment of time (Fig. 4, a), the horizontal components of the filtration gradient change quite smoothly from a value close to zero near the upstream slope to a value of ~ -0.52 at the outlet of the filtration flow into the drainage prism (the "-" sign corresponds to the direction of the horizontal component of the velocity towards the downstream fill). Throughout the massif, the vertical component of the gradient is positive, which corresponds to the direction of the vector of the vertical component of the velocity to the base of the dam. At the outlet of the filtration flow into the drainage prism, its value reaches 0.72.

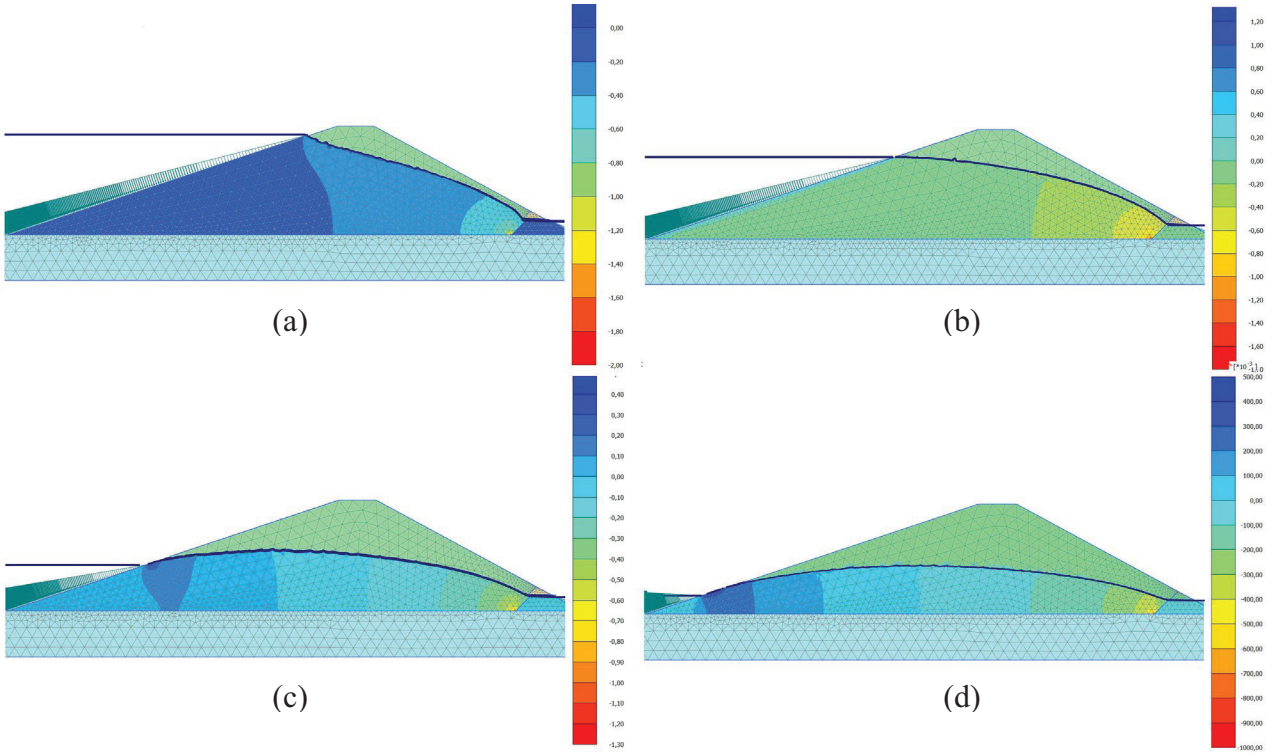

Figure 4. Distribution of horizontal components of the filtration gradient in the Plaxis software package where (a) - the normal water level, (b), (c), (d) is the position at times τ = 4, 12, 18 days

The obtained distributions of filtration gradients for other calculated cases (Fig. 4, b, c, d) are qualitatively and quantitatively comparable (Table 2). The values and places of occurrence of the maximum gradients are revealed: at the surface of the upper slope near the exit point of the depression surface and at the inlet of the filtration flow into the drainage prism.

The results of the numerical solution of the transient seepage problem can be further used to assess the stability of the slopes of a earth dam.

CONCLUSIONS

1. The numerical solution of the transient seepage problem obtained using PLAXIS is quite reliable. This is confirmed by good comparability with the results of other solution methods: on a hydraulic integrator, according to V.S. Shestakov's method.
2. A good agreement was obtained between the results of the numerical solution using the FILTR software (using the "classical" solution of the basic differential equation of the filtration theory) and the PLAXIS software (using the

Van Genuchten soil water absorption-water loss model).

3. The used technique and computational complex allows obtaining a reliable detailed picture of changes in the position of the depression curve, filtration gradients and velocities with a decrease in the water level.

4. The obtained results of solving the transient seepage problems are necessary to assess the filtration strength of the elements of ground dams and to check the stability of the slopes of the construction, since in the case of rapid drawdown or draw-off, additional hydrodynamic forces that worsen it arise.

REFERENCES

1. **Cedergreen H.R.** Seepage, drainage and flow nets. (2nd Edition). John Wiley & Sons, Inc.New-York – London-Sidney-Toronto, 1977
2. **Reddi, L.N.**: Seepage in Soils Principles and Applications, Hoboken (NJ): John Wiley & Sons, 2003
3. **Polubarinova-Kochina P.Ya.** About unsteady groundwater movements. Dokl. USSR Academy of Sciences, 1950, vol. 75, No. 3
4. **Polubarinova-Kochina P.Ya.** Theory of groundwater movement. State Publishing House of Technical and Theoretical Literature, Moscow, 1952.
5. **Stark, T. D., Jafari, N. H., Zhindon, J. S. L., & Baghdady, A.** (2017). Unsaturated and Transient Seepage Analysis of San Luis Dam. Journal of Geotechnical and Geoenvironmental Engineering, 143(2), 04016093
6. **Alonso, E. E., & Pinyol, N. M.** (2016). Numerical analysis of rapid drawdown: Applications in real cases. Water Science and Engineering, 9(3), p. 175–182
7. **Vandenberge, D. R.** (2014). Total Stress Rapid Drawdown Analysis of the Pilarcitos Dam Failure using the Finite Element Method. Frontiers of Structural and Civil Engineering, 8(2), p. 115–123
8. **Berilgen, M. M.** (2007). "Investigation of stability of slopes under drawdown conditions," Computers and Geotechnics, 34, p. 81-91.
9. **Zomorodian, A., Abodollahzadeh, S. M.**: Effect of Horizontal Drains on Upstream Slope Stability during Rapid Drawdown Condition, International Journal of Geology, 2010, Issue 4, Volume 4, pp. 85
10. **Zhukovsky N.E.** Theoretical research on the movement of subsurface waters. Zh. RFHO, 1889, vol. 21, issue 1
11. **Shestakov V.M.** Determination of hydrodynamic forces in earthworks and slopes when levels fall in the streams. Collection "Issues of filtration calculations of hydraulic structures", VODGEO, 1956, No. 2.
12. Development of research on filtration theory in the USSR. Institute of Problems of Mechanics of the USSR Academy of Sciences, Institute of Hydrodynamics of the USSR Academy of Sciences, VNIIG named after B.E.Vedeneev, Research Institute of Natural Gases, M., "Science"
13. **Musket M.** The seepage of water throught dams with vertical faces. Phisics, 1935, v.6
14. **Shestakov V.M.** Some issues of modeling of transient seepage. Collection "Issues of filtration calculations of hydraulic structures", VODGEO, 1956, No. 2
15. **Aravin V.I., Moshkova M.A.** Investigation on a slit tray of the influence of the shape of the water seal with unsteady filtration. Izv. VNIIG, 1964, vol.76
16. **Bindeman N.N.** Hydrogeological calculations of groundwater retention and filtration from storage. M., Ugletekhizdat, 1951
17. **Verigin N.N.** On groundwater flows with local enhanced infiltration. Dokl. USSR Academy of Sciences, 1950, vol.70, No. 5.
18. **Dombrovsky V.M.** Simplified calculation of the depression curve with a decrease in

the level of the head water, "Hydrotechnical construction", No. 2, 1947
19. **Kamensky G.N.** Equations of unsteady groundwater movement in finite differences and their application to the study of backwater phenomena. Izv. USSR Academy of Sciences, OTN, 1940, No. 4
20. **Leibenzon L.S.** The movement of natural liquids and gases in a porous medium. M.-L., Gostekhizdat, 1947
21. **Lukyanov V.S.** Hydraulic devices for technical calculations, "Izvestiya AN SSSR", dep. tech. Sciences, No. 2, 1939
22. **Charny I.A.**Underground hydromechanics. M.-L., Gostekhizdat, 1948
23. **Shestakov V.M.** Filtration calculation of earthen dams and cofferdam in case of fluctuations of the ponds. Hydraulic engineering, 1953, No. 7, pp. 36-39
24. **Shestakov V.M.** Calculation of depression curves in earthen dams and dams with a decrease in the water level. Hydraulic engineering, 1954, no. 4, p. 32-36
25. **Reinius E.** The stability of the upstream slope of earth dams, Stockholm, 1948.
26. **Aniskin N.A., Antonov A.S.** Development geo-seepage models for solving seepage problems of large dam's foundations, on an example of ANSYS Mechanical APDL, Advanced Materials Research Vols. 1079-1080 (2015) pp 198-201
27. Al-Labban, Salama, Seepage and Stability Analysis of the Earth Dams under Drawdown Conditions by using the Finite Element Method" (2018). Electronic Theses and Dissertations, 2004-2019. 6157.
28. **Terleev V.V., Narbut M.A., Topazh A.G., Mirchel V.** Modeling of hydrophysical properties of soil as a capillary-porous body and improvement of the Mualem-Van Genuchten method: theory. Agrofizika, 2014, No. 2 (14), pp. 35 -44
29. **Kosugi K.** 1999. General model for unsaturated hydraulic conductivity for soil with lognormal pore-size distribution. Soil Sci. Soc. Am. J. 63:270-277
30. **Mualem Y.** 1976. A new model for predicting hydraulic conductivity of unsaturated porous media. Water Resour. Res. 12:513-522.
31. **Van Genuchten, M.Th.** 1980. A closed form equation for predicting the hydraulic conductivity of unsaturated soils. Soil Sci. Soc. Am. J. 44:892-989.
32. **Aniskin N.A.** Transient seepage in earth dams and foundations. Collection "Vestnik MGSU", 2009, No. 2, pp. 70-79

СПИСОК ЛИТЕРАТУРЫ

1. **Cedergreen H.R.** Seepag, drainage and flow nets. (2nd Edition). John Wiley & Sons, Inc.New-York – London-Sidney-Toronto, 1977
2. **Reddi, L.N.:** Seepage in Soils Principles and Applications, Hoboken (NJ): John Wiley & Sons, 2003
3. **Полубаринова-Кочина П.Я.** О неустановившихся движениях грунтовых вод. Докл. АН СССР, 1950, т.75, №3
4. **Полубаринова-Кочина П.Я.** Теория движения грунтовых вод. Гос. Издательство технико-теоретической литературы, М., 1952.
5. **Stark, T. D., Jafari, N. H., Zhindon, J. S. L., & Baghdady, A.** (2017). Unsaturated and Transient Seepage Analysis of San Luis Dam. Journal of Geotechnical and Geoenvironmental Engineering, 143(2), 04016093
6. **Alonso, E. E., & Pinyol, N. M.** (2016). Numerical analysis of rapid drawdown: Applications in real cases. Water Science and Engineering, 9(3), 175–182.
7. **Vandenberge, D. R.** (2014). Total Stress Rapid Drawdown Analysis of the Pilarcitos Dam Failure using the Finite Element Method. Frontiers of Structural and Civil Engineering, 8(2), 115–123.
8. **Berilgen, M. M.** (2007). "Investigation of stability of slopes under drawdown

conditions," Computers and Geotechnics, 34, 81-91.
9. **Zomorodian, A., Abodollahzadeh, S. M**.: Effect of Horizontal Drains on Upstream Slope Stability during Rapid Drawdown Condition, International Journal of Geology, 2010, Issue 4, Volume 4, pp. 85.
10. **Жуковский Н.Е.** Теоретическое исследование о движении подпочвенных вод. Ж. РФХО, 1889, т.21, вып.1.
11. **Шестаков В.М.** Определение гидродинамических сил в земляных сооружениях и откосах при падении уровней в бьефах. Сб. «Вопросы фильтрационных расчетов гидротехнических сооружений», ВОДГЕО, 1956, №2
12. Развитие исследований по теории фильтрации в СССР. Институт проблем механики АН СССР, Институт гидродинамики СО АН СССР, ВНИИГ им. Б.Е.Веденеева, ВНИИ Природных газов, М., «Наука»
13. **Musket M.** The seepage of water throught dams with vertical faces. Фильтрация воды через дамбы с вертикальными стенками. Phisics, 1935, v.6
14. **Шестаков В.М.** Определение гидродинамических сил в земляных сооружениях и откосах при падении уровней в бьефах. Сб. «Вопросы фильтрационных расчетов гидротехнических сооружений», ВОДГЕО, 1956, №2
15. **Аравин В.И., Мошкова М.А.** Исследование на щелевом лотке влияния формы водоупора при неустановившейся фильтрации. Изв. ВНИИГ, 1964, т.76
16. **Биндеман Н.Н.** Гидрогеологические расчеты подпора грунтовых вод и фильтрации из водохранилищ, м., Углетехиздат, 1951
17. **Веригин Н.Н.** О течениях грунтовых вод при местной усиленной инфильтрации. Докл. АН СССР, 1950, т.70, №5
18. **Домбровский В.М.** Упрощенный расчет кривой депрессии при снижении горизонта верхнего бьефа, «Гидротехническое строительство», №2, 1947
19. **Каменский Г.Н.** Уравнения неустановившегося движения грунтовых вод в конечных разностях и применения их к исследованию явлений подпора. Изв. АН СССР, ОТН, 1940, №4
20. **Лейбензон Л.С.** Движение природных жидкостей и газов в пористой среде. М.-Л., Гостехиздат, 1947
21. **Лукьянов В.С.** Гидравлические приборы для технических расчетов, «Известия АН СССР», отд. техн. наук, №2, 1939
22. **Чарный И.А.** Подземная гидромеханика. М.-Л., Гостехиздат, 1948.
23. **Шестаков В.М.** Фильтрационный расчет земляных плотин и перемычек при колебании бьефов. Гидротехническое строительство, 1953, №7, с.36-39.
24. **Шестаков В.М.** Расчет кривых депрессии в земляных плотинах и дамбах при понижении горизонта водохранилища. Гидротехническое строительство, 1954, №4, с. 32-36.
25. **Reinius E.** The stability of the upstream slope of earth dams, Stockholm, 1948.
26. **Aniskin N.A., Antonov A.S.** Development geo-seepage models for solving seepage problems of large dam's foundations, on an example of ANSYS Mechanical APDL, Advanced Materials Research Vols. 1079-1080 (2015) pp. 198-201
27. Al-Labban, Salama, Seepage and Stability Analysis of the Earth Dams under Drawdown Conditions by using the Finite Element Method" (2018). Electronic Theses and Dissertations, 2004-2019. 6157
28. **Терлеев В. В., Нарбут М. А., Топаж А. Г., Миршель В.** Моделирование гидрофизических свойств почвы как каппилярно-пористого тела и

усовершенствование метода Муалема-Ван Генухтена: теория. Агрофизика, 2014, №2(14), с. 35 -44.
29. **Kosugi K.** 1999. General model for unsaturated hydraulic conductivity for soil with lognormal pore-size distribution. Soil Sci. Soc. Am. J. 63:270-277.
30. **Mualem Y.** 1976. A new model for predicting hydraulic conductivity of unsaturated porous media. Water Resour. Res. 12:513-522.
31. **Van Genuchten, M.Th.** 1980. A closed form equation for predicting the hydraulic conductivity of unsaturated soils. Soil Sci. Soc. Am. J. 44:892-989.
32. **Анискин Н.А.** Неустановившаяся фильтрация в грунтовых плотинах и основаниях. Сборник «Вестник МГСУ», 2009, №2, с.70-79.

Aniskin Nikolay Alexeyevich, Professor, DSc, Acting Director of the Institute of Hydrotechnical and Power Engineering (IGES) of the National Research Moscow State University of Civil Engineering (NRU MGSU), 129337, Russia, Moscow, Yaroslavskoe shosse, 26, phone +7 (495) -287-49-14 ext. 14-19, e-mail: Aniskin@mgsu.ru

Sergeev Stanislav Alexeyevich, PhD, Associate Professor of the Department of Hydraulics and Hydraulic Engineering, Researcher at the Scientific and Educational Center "Geotechnics" of the National Research Moscow State University of Civil Engineering (NRU MGSU), 129337, Russia, Moscow, Yaroslavskoe shosse, 26, phone +7 (495) -287-49-14 ext. 14-19, e-mail: SergeevSA@mgsu.ru

Анискин Николай Алексеевич, профессор, доктор технических наук, исполняющий обязанности директора Института гидротехнического и энергетического строительства (ИГЭС) Национального исследовательского Московского государственного строительного университета (НИУ МГСУ), 129337, г. Москва, Ярославское ш., д. 26, тел. +7 (495)-287-49-14 доб.14-19. e-mail: Aniskin@mgsu.ru

Сергеев Станислав Алексеевич, кандидат технических наук, доцент кафедры «Гидравлики и гидротехнического строительства», научный сотрудник Научно-образовательного центра «Геотехника» Национального исследовательского Московского государственного строительного университета (НИУ МГСУ) 129337, г. Москва, Ярославское ш., д. 26, тел. +7 (495)-287-49-14 доб.14-19 e-mail: SergeevSA@mgsu.ru

International Journal for Computational Civil and Structural Engineering, 18(1) 51–60 (2022)

DOI:10.22337/2587-9618-2022-18-1-51-60

FORECASTING AND DETERMINING OF COST PERFORMANCE INDEX OF TUNNELS PROJECTS USING ARTIFICIAL NEURAL NETWORKS

Oday Hammoody [1], Jumaa A. Al-Somaydaii [2], Faiq M.S. Al-Zwainy [3], Gasim Hayder [4]

[1]Civil Engineering Department, University of Technology, Baghdad, IRAQ
[2] College of Engineering, Al-Anbar University, Anbar, IRAQ
[3] Forensic DNA for Research and Training Center, Al-Nahrain University, Baghdad, IRAQ
[4] Institute of Energy Infrastructure (IEI), Universiti Tenaga Nasional (UNITEN), Selangor, MALAYSIA

Abstract. Construction projects, especially tunnel projects in the Arab world, suffer from poor documentation of data and information, and therefore there is a difficulty in estimating the budget or total costs or indicators of earned value, and with the advancement of artificial neural networks, the urgent need arises to estimate the earned value indicators for tunnels projects in the absence or lack of data required for the purpose of estimating costs and durations together. Objective: The primary aim of the current study is to introduce Artificial Intelligence (AI) in conducting statistical approach for earned value management of the tunnels projects. Methodology: The study was based on the assurance of different variables that effect on the Earned Value Management (EVM) of the tunnels projects that involves historical data in Iraq and Jordan. Five independent variables were randomly selected (Actual Cost AC, Planning Value PV, Earned Value EV, Actual Duration AD and Planning Duration PD), which were all around characterized for each tunnel project, and one dependent variable Cost Performance Index (CPI) was selected. NEUFRAME V.5 Program was selected, which is the premier neural network simulation environment. The methodology of ANN embraced for finding best network architecture and inside parameters that control and monitoring the preparation procedure which did by utilizing the default parameters of the NEUFRAME programming package. Results: The experimentation results reveal that, Mean Absolut Percentage Error (MAPE) and Average Accuracy percentage (AA) generated by ANN model (CPI) were found to be 9.6% and 90.368%, respectively. Therefore, the ANN model (CPI.model.1) shows a magnificent concurrence with the real estimations.

Keywords: Forecasting, artificial neural networks, tunnel project, cost performance index.

ПРОГНОЗИРОВАНИЕ И ОПРЕДЕЛЕНИЕ ИНДЕКСА ЭФФЕКТИВНОСТИ ЗАТРАТ ДЛЯ ПРОЕКТОВ ТУННЕЛЕЙ С ИСПОЛЬЗОВАНИЕМ ИСКУССТВЕННЫХ НЕЙРОННЫХ СЕТЕЙ

Одай Хаммуди [1], Джумаа А. Аль-Сомайдаии [2], Фаик М.С. Аль-Звайни [3], Гасим Хайдер [4]

[1] Факультет гражданского строительства, Технологический университет, Багдад, ИРАК
[2] Инженерный колледж, Университет Аль-Анбар, Анбар, ИРАК
[3] Научно-исследовательский и учебный центр судебно-медицинской экспертизы ДНК, Университет Аль-Нахрейн, Багдад, ИРАК
[4] Институт энергетической инфраструктуры (IEI), Национальный университет Тенага (UNITEN), Селангор, МАЛАЙЗИЯ

Аннотация. Строительные проекты, особенно проекты туннелей в арабском мире, страдают от плохого документирования данных и информации, и поэтому возникают трудности с оценкой бюджета, или общих затрат, или показателей заработанной стоимости. С развитием искусственных нейронных сетей становится актуальной оценка показателей заработанной стоимости для проектов тоннелей в связи с отсутствием или недостатком данных, необходимых для комплексной оценки затрат и сроков выполнения работ. Цель исследования: Основная цель настоящего исследования является внедрение искусственного интеллекта (ИИ) для применения статистического подхода к управлению заработанной стоимостью проектов строительства туннелей. Методология: В исследовании выполнено обоснование различных переменных, влияющих на управление заработанной стоимостью (EVM) проектов туннелей, которые включают исторические данные в Ираке и Иордании. Были случайным образом выбраны пять независимых переменных (фактическая стоимость AC, плановая стоимость PV, заработанная стоимость EV, фактическая продолжительность AD и планируемая продолжительность PD), которые были всесторонне охарактеризованы для каждого проекта туннеля, а также была выбрана одна зависимая переменная - индекс эффективности затрат (CPI). Была выбрана программа NEUFRAME V.5, которая является ведущей средой моделирования искусственных нейронных сетей (ANN). Методология ANN использовалась для поиска лучшей сетевой архитектуры и внутренних параметров, которые контролируют и управляют процедурой подготовки, используя параметры по умолчанию пакета программирования NEUFRAME. Результаты. Результаты экспериментов показывают, что средняя абсолютная ошибка в процентах (MAPE) и средний процент точности (AA), полученные с помощью модели ANN (CPI), составляют 9,6% и 90,368% соответственно. Таким образом, модель ANN (CPI.model.1) показывает хорошее совпадение с реальными оценками.

Ключевые слова: прогнозирование; искусственная нейронная сеть; проекты туннелей; индекс эффективности затрат.

1. INTRODUCTION

From numerous decades, earned value management has happened to an extraordinary significance in the space of engineering industry. Managing the earned worth administration subject beginnings from the commencement of thought in the brain of the proprietor or the engineer and proceeds for the duration of the life of the task. Earned Value is a notable task the executive's apparatus that utilizes data on cost, duration and work execution to build up the present status of the undertaking. By methods for a couple of straightforward rates, it permits the supervisor to extrapolate current patterns to foresee their presumable last impact. The technique depends on a rearranged model of a task however end up being valuable by and by of cost control. It is being created to account better for schedule and time stages [1].

There are a lot of definitions for Earned Value Management (EVM), (Zhuo, 2005) defined EVM as an effective method of combination control to the scope, schedule and cost of the project [2]. EVM is a method of project management, which facilitates project control and provides support in forecasting final cost [3]. VM is an administration system for project execution monitoring. EVM coordinates cost, and timetable control under a similar structure, and it gives execution changes, and records which permit chiefs to distinguish over-expenses and deferrals [4]. EVM can offer many benefits to construction companies. They include [5, 6]:

1) Accurate estimate of task culmination and total cost.
2) Objective measurement of accomplishments against cost and schedule,
3) Early alerts to deferrals and overruns.
4) Information about schedule and cost variances during the course of the project.
5) Minimizing little changes in plan that can turn out to be huge after some time (scope creep) and that can lessen gainfulness.
6) Improvement in the control of contract performance.
7) Demonstrating a competitive advantage and improving customer goodwill.

2. RESEARCH OBJECTIVES

The primary goal of this study was, to present a factual methodology for earned value management of the construction tunnels projects. This target can be done during following advances:
1) An overview of EVM in engineering project management.
2) Identify the variables' that have an effect on the earned value management of tunnels projects.
3) Developing a mathematically model for earned value management using the Artificial Neural Network technique (ANN), to predict the Cost Performance Index (CPI) in tunnels projects
4) Verification and approval of the scientific model created.
5) Illation of a simply mathematical formula in order to estimating the CPI of tunnels projects.
6) Finding the value of accuracy of the mathematical formula, and the explained of the value of the correlation between predicting CPI (calculated), and CPI as actual value.

3. RESEARCH METHODOLOGY

Current methodology utilizes to accomplish the current study objectives can be abridged as follow advances:
1) Theoretical Survey: Theoretical survey was made to review the development of ANN on the EVM in project management field. The concept of the neural networks, and concept of earned value management, which include the review of literatures involving references, distractions, articles, handbooks and web-site relating to the task of research especially that are related to the construction projects sector.
2) Field Work Included Four Stages:
a) Preliminary stage, involves data description and identification, which describes the factors affecting the application of predicting the earned value for tunnels project, It is worth noting that the method of collecting historical data is a direct method through continuous field visits to spending projects under implementation, and it is the same method used in reference [7]
b) Secondary stage includes building of the ANN model to estimating Cost Performance Index (CPI).
c) Thirdly stage presents the verification and validation of the ANN model;
d) In the final stage, conclusions are drawn for this study and the results are discussed.

4. APPLICATION OF ARTIFICIAL NEURAL NETWORK IN EARNED VALUE MANAGEMENT

One of the most powerful and popular multilayer feed forward network is trained with back-propagation. The training of the developed network is conducted by back-propagation algorithm which was developed and involves only four stages; the feed forward stage of the input training patterns, the calculation and back-propagation stage of the associated error, and the adjustment stage of the weights [8].
Main aim of this study is to develop artificial neural networks model to predict and estimate the earned value indicators of tunnel projects in Iraq and Jordan. To attain this, there was a requirement to determine the factors that react the efficiency for tunnel projects. Therefore, the researchers in this study are attempting building and evaluation EVM model through the following stages:
1) Chose Software of ANN
2) Diagnostics of ANN model factors.
3) Building and evaluation of the developed ANN models
4) Validation of the developed ANN model

4.1. Neuframe Software Applications

The reproduction of neural system on a NEUFRAME program exhibits its hidden numerical equations in a basic with completely control-able structure. A few applications that help the foundation of neural systems like

SPSS, MATLAB and NeuroSolutions; however, this examination was chosen NEUFRAME Program, where NEUFRAME is the head neural system reproduction condition. The NEUFRAME run gives a simple to-utilize, visual, object-situated way to deal with critical thinking utilizing savvy advances. It gives highlights to empower organizations to research and apply clever innovations from introductory experimentation through structure installed applications utilizing programming segments. NEUFRAME is an incorporated gathering of knowledge Technology instruments that incorporate ANN rationale that permit putting the intensity of artificial neural lattice to turn on beginning of black box. Fig. 1 shows the schematic of the NEUFRAME V.5 program which is worked to decide the connection between the autonomous factors (information) and ward factors (yield) [9].

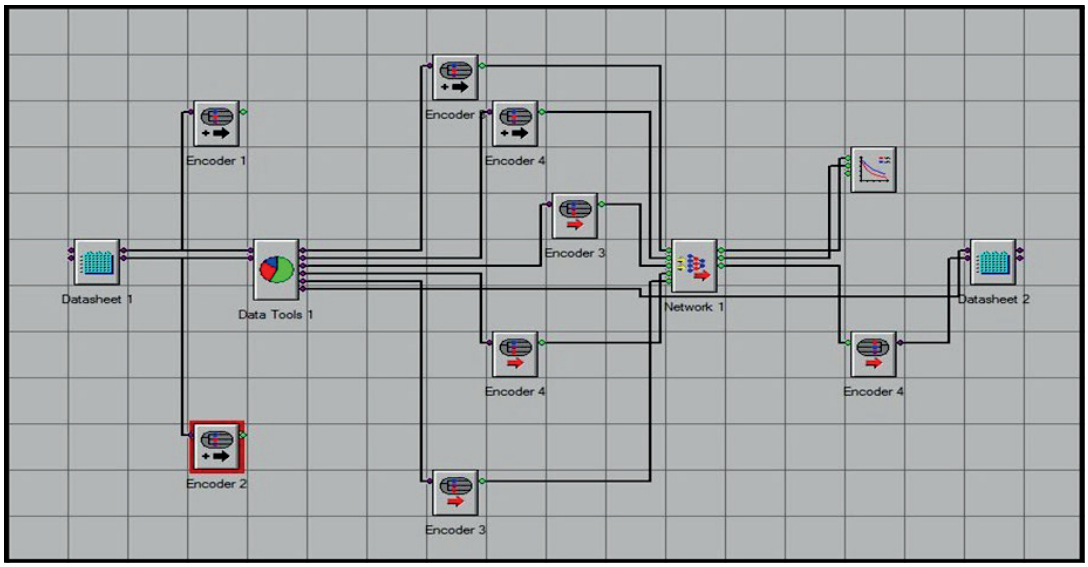

Figure 1. NEUFRAME V.5 interface (Researcher)

4.2. Diagnostics of ANN Model Factors

This study embraces historical information investigation as the establishment to this technique. In addition, the utilization of verifiable information helps with giving a connection between the principle factors influencing the earned value parameters of the tunnels projects to make estimates for new projects. Therefore, historical data of tunnels projects were collected, which were done between 2005 and 2017 in Ministry of Housing and construction in Kurdistan of Iraq, with Amman Municipality in Jordan, as shown in Fig. 2.

Figure 2. Tunnel Project in Amman (Researcher)

Six factors were painstakingly chosen and were all around characterized for each tunnel project. These illustrative factors can be ordered into two sorts: dependent and independent factors.

1) Dependent variables (factors): Cost Performance Index (CPI) is defined as the dependent factor and each individual tunnel project is used as the basic unit of the surveillance.

2) Independent variables (factors): After building up the reliant factors which are to be anticipated by neural system model, it was important to create autonomous factors to clarify any variety in project cost. Only five variables were adopted in this study as independent variables as follows:

a) F1: AC, Actual Cost.
b) F2: EV, Earned Value.
c) F3: PV, Planning Value,
d) F4: AD, Actual Duration.
e) F5: PD, Planning Duration,

4.3. Development of CPI-ANN Model

Neural Network (NN) models should be in an efficient way to improve its presentation. Such strategy needs address main considerations, for example, advancement of model inputs, information and data division and pre-handling, improvement of model design (architecture), model enhancement (training and preparing), halting standards, and model approval (validation). An organized procedure for building up the model has been utilized to tackle the current issue. This methodology fuses four principle stages:

a) Inputs and output Model
b) data division and pre-handling
c) Architecture of ANN Model
d) Equation of ANNs Model

4.3.1. Development of Model Inputs and Outputs

The determination of model info factors that have the most noteworthy effect on the model execution is a significant advance in creating ANN models. Introducing as enormous number of info factors as conceivable to ANN models for the most part builds the system size, bringing about a decline in preparing speed, and a decrease in the effectiveness of the system. Various strategies have been proposed to help the determination of info factors, for example, Method of prior knowledge: in view of earlier information, the suitable information factors can be chosen. This Methodology is basically used for the field of undertaking the board, and is received in this examination. As a primer stage to neural system displaying, the current issue needs to distinguish and label the information as info or as yield. NEUFRAME v.4 gives Microsoft Excel sheet, which is utilized through this progression. The independent factors influencing the issue are recognized and considered as (N) input parameters, which are spoken to by hubs at the info cushion of a neural system. The output of the model is Cost Performance Index (CPI).

4.3.2. Data and Information Division

Information and data pre-preparing is significant for utilizing ANN efficacious. It figures out what data is introduced to make the model during the preparation phase [10, 11]. In this way, the following stage in the advancement of ANN models is separating the accessible raw-data into three subsets, training, testing and validation sets. Learning was performed on the preparation set, which utilized for evaluating the loads while the cross-approval set was utilized for speculation that is to create best model for concealed models. In any case, the test set is utilized for estimating the speculation capacity of the system and assessed arranges execution. The complete accessible information is 45 tunnel projects that are isolated arbitrarily into three sets with the accompanying proportion:

a) Training set: includes (30) projects equal to (67%).
b) Testing set: includes (10) projects equal to (22%).
c) Validation set: includes (5) projects equal to (11%).

4.3.3. Model Architecture

One of the most significant and hard errands in the improvement of ANN models into decide the model engineering. For the most part, there is no immediate and exact method for deciding the most suitable number of neurons to remember for each concealed layer, and this issue turns out to be increasingly confounded as the quantity of shrouded layers in the system increments. Since ANN has one hidden layer can rough any persistent capacity, giving that adequate

connection weights are utilize. Only one hidden layer was used to build CPI model. The methodology embraced for finding the ideal ANN design and interior parameters that mentoring the preparation procedure that were completed by utilizing the default parameters of the NEUFRAME package with one hidden layer and one hidden node. Also, a learning rate is (0.30), also, momentum term is (0.90), and hidden layer had sigmoid transfer functions and output layer had sigmoid transfer functions. Results were summarized in Table 1 for the CPI model.

Table 1: Effect of Parameters on ANN Performance

ANN Model for CPI			
Nodes	Learning Rate	Momentum term	
1	0.3	0.9	
Transfer functions			
Hidden layers		Output layers	
Sigmoid		Sigmoid	
Error %	Error of Training	Error of Testing	Correlation Coefficient
	4.50	5.40	0.88

4.3.4. Equation of CPI Model

The modest number of comradeship (connection) weights got by NEUFRAME for the ideal ANNs model (CPI model) empowers the system to be converted into relative straightforward equation. To exhibit this, the structure of ANNs model as appeared in Fig. 3, while connection weights and limit plane (bais) are condensed in Table 2.

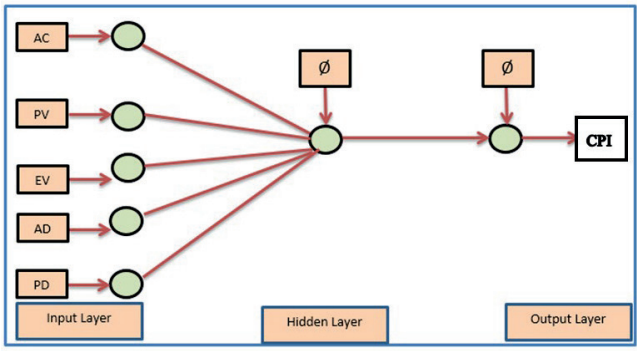

Figure 3. Architecture of the CPI Model (Researcher)

Table 2. Weight and Bais in ANN Optimal

weight from nodes input layer to nodes in hidden layer					
W_1=1	W_2=2	W_3=3	W_4= 4	W_5= 5	W_6=6
2.88	2. 55	0.77	1.88	0.66	2.44
Hidden layer threshold Θ_j			Output layer threshold Θ_j		
1.44			2.33		

Utilization the association weight with Baises as in Table (2), calculate CPI can be expressed as follow equation:

$$CPI = \{1/[1+e(2.33+2.44 \tanh (x))]+0.81\} \quad (1)$$

Where:

$$X = [1300 + (2.88*AC) + (2.55*PV) + (0.77*EV) + (1.88*AD) + (0.66*PD)] \quad (2)$$

A numerical model is given to more readily clarify the execution of the recipe. The condition was tried against the information

utilized in the CPI model preparing, data and information as in below:

AC= 25,898,722 $
EV= 25,555,077 $
PV= 22,365,353 $
AD= 275 day
PD= 310 day

The estimated value using equation (1) was (0.854), compares well with actual value (measured value), (CPI=0.961). The difference is very little; this shows the strength of the predicted neural network developed in this research, as will be seen in the next section.

4.3.5. Validation of the Developed CPI-ANN Model

The synopsis of registering Cost Performance Index (CPI) by ANN for confirmation of assessing models is appeared in the following Table 3. Where section (2) presents actual Cost Performance Index that has been gotten from tunnels projects under development in Iraq, and section (3) speaks to assess Cost Performance Index subsequent to applying ANN condition on them, where ANN condition is acquired by NEUFRAME V.4, and the correlation between the actual and estimated Cost Performance Index is appeared.

Correlation coefficient through columns (Actual CPI and measure CPI by ANN is 75.0%), in this way it very well may be presumed that this model shows a decent concurrence with the genuine estimations, as shown in Fig. 4. Where, Y-axes represent Actual CPI, X-axes represent Estimated CPI.

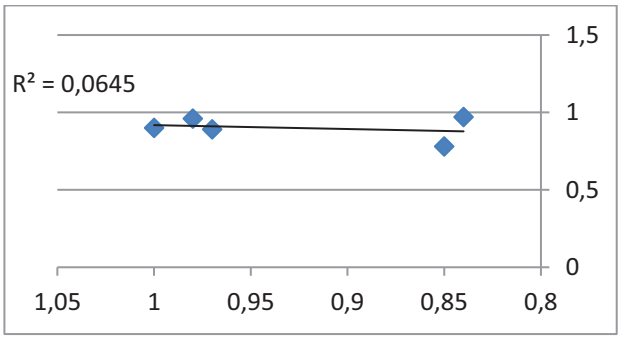

Figure 4. Comparison of Predicted and Observed CPI for Validation Data

The description of five (5) observations of tunnels projects (variables) was shown in Table 4.

Table 3. Validation of the developed ANN model

Projects	Actual CPI	Estimate CPI by ANN
1	0.96	0.98
2	0.78	0.85
3	0.90	1.0
4	0.97	0.84
5	0.89	0.97

Table 4. Verification for CPI Model.

Project.	AC	PV	EV	AD	PD	CPI
1	21,889,822	20,567,354	21,556,078	395	355	0.98
2	98,511,540	105,978,004	87,977,501	360	495	0.85
3	18,889,197	15,281,994	17,280,998	405	405	1.0
4	23,299,665	25,112,254	25,781,671	370	495	0.84
5	28,622,733	29,660,594	27,779,457	355	315	0.97

In this way it very well may be presumed that this model shows a decent concurrence with the genuine estimations.

a) Mean Absolute Percentage Error (MAPE): According to (Aidan et al, 2020) and (Jasim et al, 2020) error of mean absolute percentage is designate by the next equation [12, 13]:

$$MAPE = \{ \sum_{i=1}^{n} \frac{|A-E|}{A} * 100 \ \% \backslash n \ \} \quad (3)$$

Table 5. Mean Absolute Percentage Error (MAPE)

Projects	Actual CPI	Estimate CPI by ANN	MAPE%
1	0.96	0.98	18.68
2	0.78	0.85	5.46
3	0.90	1.0	6.60
4	0.97	0.84	6.54
5	0.89	0.97	10.88
MAPE%			48.16/5=9.6

b) Average Accuracy (AA %):
According to (Zamim et al, 2019) and (Jaber et al, 2020) Average Accuracy performance is defined as (100−MAPE) %. Average Accuracy (AA) can be designate by the next equation [14, 15, 16]:

AA %= 100-MAPE% = 100-9.6 = 90.368% (4)

Discussion the results in current study are specified in Table (6). MAPE % and average AA % created by ANN model (CPI) were originated to be 9.6% and 90.368% respectively. Therefore, it can be summarized that CPI-ANN model shows an excellent agree within the raw data.

Table 6. Conclusion of the Comparative Study

Details	CPI- ANN model
MAPE	9.6%
AA	90.368%
R	0.75
R^2	0.5625

5. CONCLUSIONS

Earned Value is exceptionally amazing asset to assessment execution for tunnels projects.. There is shortcoming in chronicling information and records in development and construction sector for Iraqi and Jordan. Methodology is primarily relied upon the assurance of different components that influence the EVM of the tunnels projects extends that includes historical information. In addition, five independent factors were arbitrarily chosen which were very much characterized for individual construction tunnel project and one only depended variable (CPI) was chosen. Information gathered was examined and the exploration issue recognized. In this manner, supervised learning algorithm was utilized for preparing the ANN. This relies upon the back-propagation algorithm, which is a kind of supervised learning algorithms that generally utilized in project management. The data was divided randomly into three sets: training set, testing set and cross validation set according to these percentage 67 %, 22 % and 11 % respectively for model (CPI). ANN technique was used to find the optimum model, which included one only hidden layer together, one only neuron with sigmoid transfer function, also, the output neuron had a sigmoid transfer function. Accuracy performances of the optimum model are 90.368% and Mean Absolute Percentage Error (MAPE) 9.6%. This study recommends the necessity of adopting artificial neural networks in estimating earned value in construction projects in general and tunnel projects in particular, as they are considered an important, simple and accurate method in planning and cost control work.

The Availability of Data
The datasets generated during and/or analysed during the current study are available from the corresponding authors on reasonable request.

Conflicts of Interest
All authors have no conflicts of interest or intersection of interest.

ACKNOWLEDGMENT

All the authors extend their sincere thanks and appreciation and great gratitude to all officials at

Al-Nahrain University, University of Technology, Anbar University, AlMaarif University College in Iraq, as well as Universiti Tenaga Nasional (UNITEN) in Malaysia for their support for this manuscript financially and morally. Thanks are extended to all the engineers who provided advice and guidance throughout the completion of the manuscript.

Author Contributions

Oday Hammoody contributed to the planning, enforcement, and writing of the manuscript, Faiq M. S. Al-Zwainy presented the original idea and contributed to model design and prescribe the manuscript. Jumaa A. building the ANN model and performed the computations. Gasim Hayder helped supervise the manuscript. All authors discussed the results and contributed to the final manuscript.

REFERENCES

1. **Jumaa A. AL-Somaydaii and HADI S. M. Aljumaily FAIQ M. S. AL-Zwainy,** "tilization Multifactor Linear Regression Technique for Prediction the Earned Value in Bridges Projects", *Journal of Engineering and Applied Sciences*, Vol. 13, No. 7, pp:1676-1682, 2018.
2. **Zhang Z.** "Project management". Beijing: Science-Publishing Inc; 2005, p. 168–173.
3. **Lipke W., Zwikael O., Henderson K., Anbari F.,** 2009. "Prediction of project outcome the application of statistical methods to earned value management and earned schedule performance indexes", International Journal of Project Management. Vol. 1, No. 27, pp: 400-407, 2018.
4. **Pajares J., López-Paredes A**., 2011. "An extension of the EVM analysis for project monitoring: The Cost Control Index and the Schedule Control Index". International Journal of Project Management. Vol. 1, No. 29, pp: 615-621, 2011.
5. **Koster K., Wallace D., Kinder J., Bell C.,** "Earned Value Management for Dummies", Deltek Special Edition, Wiley Publishing, Inc. 2011.
6. **Faiq. M. S. Al-Zwainy, Rafaa H. Al-Suhaily, Zuher S.,** "Project Management and Artificial Neural Networks: Fundamental and Application", LAP LAMBERT Academic Publishing, 2015.
7. **Faiq Ms Al-Zwainy, Shakir A Salih, Mohammed R Aldikheeli**, "Prediction of residual strength of sustainable self-consolidating concrete exposed to elevated temperature using artificial intelligent technique", International Journal of Applied Science and Engineering, Vol. 18, No. 2, pp. 42-60, 2012.
8. **Faiq M. S. Al-Zwainy,** "The Use of Artificial Neural Networks for Productivity Estimation of finish Works for Building Projects", Journal of Engineering and Development, Vol. 16, No. 2, pp. 1-15, 2021.
9. **Faiq M. S. Al-Zwainy**, "The Use of Artificial Neural Network for Estimating Total Cost of Highway Construction Projects", a thesis submitted to the Civil Engineering Department, College of Engineering, Baghdad University, Ph.D., 2009.
10. **Faiq M. S. Al-Zwainy And Ibrahim A. Aidan,** "Forecasting the cost of structure of infrastructure projects utilizing artificial neural network model (highway projects as case study)", Indian Journal of Science and Technology, Vol. 10, No. 20, pp. 1-12, 2017.
11. **Jumaa A. Al-Somaydaii,** "Development Mathematical Model for Brick Works Productivity by Using Support Vector Machine", International Journal of Applied Engineering Research, Vol. 11, No. 23, pp:11126-11131, 2016.
12. **Ibrahim A. Aidan, Duaa Al-Jeznawi, Faiq M. S. Al-Zwainy,** "Predicting Earned Value Indexes in Residential Complexes' Construction Projects Using Artificial

Neural Network Model", International Journal of Intelligent Engineering and Systems, Vol. 13, No. 4, pp. 248-259, 2020.
13. **Nidal A. Jasim, Shelan M. Maruf, Hadi S. M. Aljumaily, Faiq M. S. Al-Zwainy,** "Predicting Index to Complete Schedule Performance Indicator in Highway Projects Using Artificial Neural Network Model", Archives of Civil Engineering, Vol. 66, No. 3, pp. 541-554, 2020.
14. **Salah Kh. Zamim, Nora S. Faraj, Ibrahim A. Aidan, Faiq M. S. Al-Zwainy, Mohammed A. Abdulqader, and Ibraheem A. Mohammed**, "Prediction of dust storms in construction projects using intelligent artificial neural network technology", Periodicals of Engineering and Natural Sciences, Vol. 7, No. 4, pp. 1659-1666, 2019.
15. **Firas Kh. Jaber, Nidal A. Jasim, Faiq M. S. Al-Zwainy,** "Forecasting techniques in Construction industry: Earned value indicators and performance models", Scientific Review Engineering and Environmental Sciences, Przegląd Naukowy Inżynieria i Kształtowanie Środowiska, Vol. 29, No. 2, pp. 234-554, 2020.
16. **Doseva, Nadezhda and Chakyrova, Daniela.** "Life Cycle Cost Optimization of Residential Buildings in Bulgaria: a Case Study of the Building Envelope" Civil and Environmental Engineering, vol.17, no.1, 2021, pp.107-116. https://doi.org/10.2478/cee-2021-0012

Oday Hammoody. Civil Engineering Department, University of Technology, Sinaa Str., 10066, Baghdad, Iraq.

Jumaa A. Al-Somaydaii. College of Engineering, Al-Anbar University, Ramadi City, 31001, Anbar, Iraq.

Faiq M. S. Al-Zwainy. Forensic DNA for Research and Training Center, Al-Nahrain University, Al-Jadraia, 10072, Baghdad, Iraq. Corresponding author: faiq.al-zwainy@eng.nahrainuniv.edu.iq, faiqalzwainy@gmail.com

Gasim Hayder. Institute of Energy Infrastructure (IEI), Universiti Tenaga Nasional (UNITEN), Jalan Ikram-Uniten, 43000, Kajang, Selangor, Malaysia.

Одай Хаммуди. Факультет гражданского строительства, Технологический университет, ул. Синаа, 10066, Багдад, Ирак.

Джумаа А. Аль-Сомайдаии. Инженерный колледж, Университет Аль-Анбар, город Рамади, 31001, Анбар, Ирак.

Фаик М.С. Аль-Звайни. Научно-исследовательский и учебный центр судебно-медицинской экспертизы ДНК, Университет Аль-Нахрейн, Аль-Джадрайя, 10072, Багдад, Ирак. Автор, ответственный за переписку: faiq.al-zwainy@eng.nahrainuniv.edu.iq, faiqalzwainy@gmail.com

Гасим Хайдер. Институт энергетической инфраструктуры (IEI), Национальный университет Тенага (UNITEN), Джалан Икрам-Унитен, 43000, Каджанг, Селангор, Малайзия.

DOI:10.22337/2587-9618-2022-18-1-61-71

NUMERICAL MODELING OF CYCLOTRON FLOW ACCELERATION MODES IN AERODYNAMIC MODULES OF SOLAR AEROBARIC POWER PLANTS

Alexander A. Soloviev [1], Dmitry A. Soloviev [2, 3], Liubov A. Shilova [4]

[1] Moscow State University named after M.V. Lomonosov, Moscow, RUSSIA
[2] Institute of Oceanology named after P.P. Shirshov of Russian Academy of Sciences, Moscow RUSSIA;
[3] Joint Institute for High Temperatures RAS (JIHT RAS), Moscow, RUSSIA
[4] National Research Moscow State University of Civil Engineering (NRU MGSU), Moscow, RUSSIA

Abstract. When constructing solar aerobaric power plants, it is necessary to develop effective ways to accelerate convective flows initiated by the action of a high-temperature working fluid heated due to the concentration of solar radiation, accumulation of dissipated heat losses and the use of the greenhouse effect. As an option for organizing the flow in the aerodynamic module of the solar aerobaric power plants, article considered a diagram of the cyclotron acceleration of the flow during horizontal and vertical transfer of convective air currents formed in cells containing alternately located cold and hot side boundaries and differently heated upper and lower bases.

Keywords: numerical modeling, RES, aerodynamic modules, solar radiation.

ЧИСЛЕННОЕ МОДЕЛИРОВАНИЕ РЕЖИМОВ ЦИКЛОТРОННОГО УСКОРЕНИЯ ПОТОКА В АЭРОДИНАМИЧЕСКИХ МОДУЛЯХ ГЕЛИОАЭРОБАРИЧЕСКИХ ЭЛЕКТРОСТАНЦИЙ

А.А. Соловьев [1], Д.А. Соловьев [2, 3], Л.А. Шилова [4]

[1] МГУ имени М.В. Ломоносова, Москва, РОССИЯ
[2] Институт океанологии имени П.П. Ширшова РАН, Москва, РОССИЯ
[3] Объединённый институт высоких температур РАН (ОИВТ РАН), Москва, РОССИЯ
[4] Национальный исследовательский Московский государственный строительный университет (НИУ МГСУ), Москва, РОССИЯ

Аннотация. При строительстве гелиоаэробарических электростанций необходима разработка эффективных способов ускорения конвективных потоков, инициированных воздействием высокотемпературного рабочего тела, нагретого благодаря концентрации солнечной радиации, аккумулированию рассеиваемых теплопотерь и использованию парникового эффекта. В качестве варианта организации потока в аэродинамическом модуле ГАБТЭС на основе методов численного моделирования рассматривается схема циклотронного ускорения потока при горизонтальном и вертикальном переносе конвективных воздушных течений, формирующихся в ячейках, содержащих попеременно расположенные холодные и горячие боковые границы и различно нагретые верхние и нижние основания.

Ключевые слова: численное моделирования, ВИЭ, аэродинамические модули, солнечная радиация.

INTRODUCTION

Traditional renewable energy technologies include direct photovoltaic converters of electrical energy [1]. Also, it is known the usage of the parabolic mirrors which concentate solar rays and heat a high-temperature coolant. The energy of this coolant is directed to Stirling engines [2].

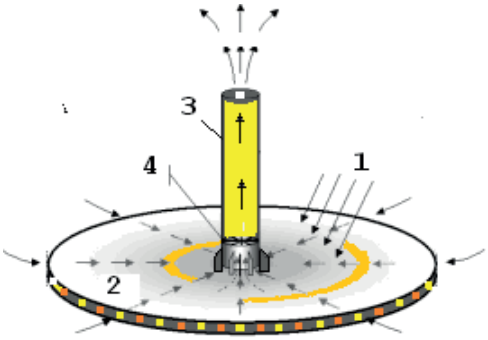

Figure 1. Scheme of generating artificial wind in the 'Solar Chimney' power plant. 1- solar radiation; 2- solar collector; 3- draft pipe; 4- turbine with an electric generator.

Wind turbines use natural wind flows without any modernization. In solar aerobaric power plants (SABPP) of the Solar Chimney type shown in Fig. 1, the artificially generated air flow is created due to the ascending convection of air heated in a solar greenhouse (collector) [3]. The technology for solar energy converting to electricity through the energy of artificial wind is less known in world practice than semiconductor and wind power plants or geothermal plants with a steam-gas thermodynamic cycle. However, in recent years, more and more works have appeared related to the study of issues of increasing the efficiency of this type of power plants [4] - [6]. These works also include the assessment of the effectiveness of such power plants' combined use not only for generating electricity, but also for obtaining fresh water [7], and for the removal of man-made pollution from the air of large cities [8], [9]. At SABPP of the "Solar Chimney" type, air heating and heat accumulation is carried out in a solar collector (greenhouse), which is formed by a horizontal soil surface and a translucent roof (Fig. 1). A draft tube is installed along the central axis of the greenhouse, where a turbine generator is placed, which converts the energy of convective movements of heated air into electrical energy. The main amount of thermal energy released by the infrared component of solar radiation goes into the atmosphere above the draft tube through the inner cavity of it and the turbine. The accumulation of thermal energy for the night period is carried out, in particular, due to the installation of containers with water on the surface of the solar collector.

The physical foundations of the conversion of solar energy in this case are as follows. The temperature difference between the air mass at the base and at the top of the pipe creates a steady-state convective air flow velocity. The magnitude of this speed is determined by the internal resistance of the air outlet duct, the main value of which falls on a turbine with a coupled electric generator. The inclination of the turbine blades during the axial flow of the stream, its friction against the surface of the blades and the generator load determine the air resistance of the turbine mainly. The flow rate in the pipe is constant during axial vertical movement of air masses due to the continuity of the flow. The temperature can also be considered practically the same throughout the movement of air in the pipe with low heat losses. As a result, the main amount of heat energy is released through the turbine into the atmosphere.

An analysis of such structures using solar energy with transformation into a laminar-convective flow of ascending air flows indicates a relatively low value of the coefficient of utilization of solar radiation energy entering the collector territory [10], [11]. This is due to the fact that the process of converting the energy of radiant heating of the greenhouse air environment into the energy of streams is carried out in the Solar Chimney

structures only within the framework of vertical convection, without using the energy formed during horizontal advection. This is the basis of all known to date "greenhouse" solar energy complexes. Therefore, in the estimates of the solar energy conversion coefficient, it is necessary to state the relatively low efficiency of generating of artificial wind, which is a source of electricity [12].

FORMULATION OF THE PROBLEM AND METHODS FOR INVESTIGATION

Among the possible decisions that can ensure an increase in the efficiency of energy generation of currents excited by solar heating, the most important is to transform air flow into a controlled tornado rotating the turbine [13], [14]. With an appropriate trajectory, such a flow will contain two components of motion and velocity - axial (vertical) and tangential (rotation in a plane perpendicular to the pipe axis). A feature of an artificial tornado should also be local vortices in the form of a system of high-speed rotating air vortex bundles filling the cross-section of the flow in the pipe before entering the turbine. These vortices cause the hydrodynamic instability of turbulent flow in the pipe and collector and can significantly increase the energy of the process and the efficiency of converting thermal energy into useful energy generated by the turbine [15].

One of the tasks in the construction of solar aerobaric power plants is the development of effective ways to accelerate convective flows initiated by the action of a high-temperature working fluid heated due to the concentration of solar radiation, the accumulation of dissipated heat losses and the use of the greenhouse effect. As an option for organizing the flow in the aerodynamic module SABPP, we further consider the scheme of cyclotron acceleration of the flow during horizontal and vertical transfer of convective air streams formed in cells containing alternately located cold and hot side boundaries and differently heated upper and lower bases. Fig. 2 shows a diagram of such a method for accelerating a convective flow.

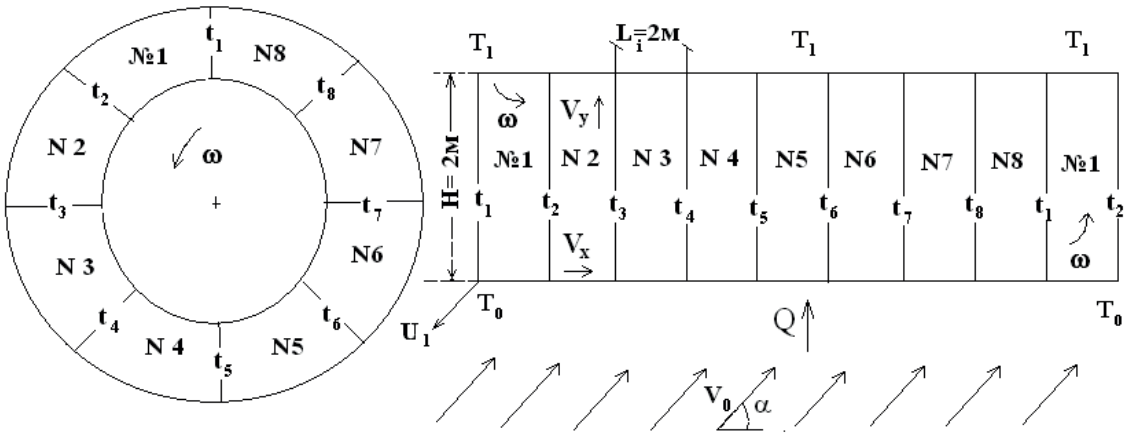

Figure 2. Scheme of the acceleration of the convective flow during the passage of air masses swirling with an angular velocity ω through the cells with alternately heated and cooled side walls. The wind flow entering the cells has a velocity $V_0(V_x, V_y, U)$. *The heat flux entering the channel from the lower boundary equals* Q, *the temperature of the lower boundary is* T_0, *the upper boundary is* T_1. *The cold side walls of the convective cells of the module have a temperature* t_{2i+1}, *the hot side boundaries are* t_{2i}, *the numbers of the cells are* $i = 0,1,2...n$.

The following system of differential equations [12] was used for the model theoretical calculation of the parameters of the convectively swirling flow arising in the annular channel of the aerodynamic module SABPP.

$$\frac{\partial V_i}{\partial t}+V_j\frac{\partial V_i}{\partial x_j}=-\frac{1}{\rho_0}\frac{\partial P}{\partial x_i}+\nu\frac{\partial^2 V_i}{\partial x_j\partial x_j}+g\frac{(T-T_\infty)}{T_\infty}\delta_{i3}-2\omega(V_1\delta_{i2}-V_2\delta_{i1}), \quad (1)$$

$$\frac{\partial T}{\partial t}+V_j\frac{\partial T}{\partial x_j}=\lambda\frac{\partial^2 T}{\partial x_j\partial x_j}, \quad (2)$$

$$\frac{\partial V_i}{\partial x_i}=0. \quad (3)$$

Here U_i is component of velocity vector (i,j=1,2,3); ω is angular swirling of vortex at the periphery of the system; T is an internal temperature; T_∞ is an external temperature; P is a pressure; ρ_0 is an air density under normal conditions; ν and λ are viscosity and thermal conductivity factors respectively; δ_{ij} is Kronecker delta. The density depends on the temperature as follows (4):

$$\rho(T)=[1-\beta(T-T_0)]. \quad (4)$$

In this equation, the properties of the medium were characterized by the coefficient of thermal expansion: $\beta=-1/\rho_0(\partial\rho/\partial T)$.

The boundary conditions of the problem were formulated as follows:

1) The heat flux between the lower and upper boundaries, respectively heated to temperatures T_0 and T_1, was taken equal to $Q=-c_0\rho\lambda\,\partial(T_0-T_1)/\partial X_3$, where c_0 is heat capacity of air.

2) a wind velocity flow V_0 was introduced into the system of cells at an angle α to the horizon through the lower surface of the module.

3) At the lateral odd boundaries of the cells of the energy-dynamic channel, temperatures t_{2i+1} were set that were lower in absolute value with respect to the temperatures t_{2i} of the lateral even sides of the numbered cells $i=0,1,2...n$.

At the initial moment of time, the movement in the system was assumed to be absent, and the temperatures outside T_∞ and inside T were known.

An additional rotation with an angular velocity ω was imparted to the air flow in the system of cells. The momentum exchange coefficients were determined according to the well-known Kolmogorov relation obtained from the averaged equation of the balance of turbulent energy.

The problem has been solved numerically using the MATLAB software, which is a fourth-generation high-level programming language and an interactive environment for numerical calculations, visualization and programming. The calculation was carried out for an aerodynamic channel with a length of 10 m, a height of 2.0 m, an outer radius of 2.0 m and an inner radius of 1.0 m. The system of equations (1) - (3) was transformed to a dimensionless form. All values were normalized to the scale of length H, temperature - $\sqrt{\frac{1}{\beta}}$, speed - $\sqrt{gH}$, time - $\sqrt{\frac{H}{g}}$.

Numerical analysis was performed using the finite difference method.

Table 1 presents the main parameters of the problem, which remained unchanged in numerical calculations.

Table 1. The main parameters of the problem.

Parameter	Designation	Value
Vertical dimension	H	2 m
Horizontal dimension	L	10 m
Channel outer radius	R	2,0 m
Internal radius of the channel	r	1,0 m
Dimensionless vertical step	Δz	0.0625
Dimensionless horizontal step	Δx	0.052
Dimensionless time step	Δt	1
Peripheral vorticity	ω	0.05 s^{-1}
Air density	ρ	1,29 kg/m^3
Heat capacity of air	c_o	1007 J//kg degree
Number of time steps	N	1000

In the first series of calculations, the conditions for the formation of a flow through the cells in 18 hours were analyzed. Table 2 shows the conditions of the first series of numerical experiment.

Table 2. Initial conditions of the problem (the first series of numerical calculations).

Parameter	Value
t11	20 °C
t12	80 °C
t13	18 °C
t14	100 °C
t15	16 °C
t16	120 °C
Q	500 W /m^2
To	100 °C
T	20 °C
T_1	40 °C
T_∞	20 °C
α	30 °
Vo	5m/s
n	5

The numerical calculation grid includes the number of points along the X3 axis equal to N = 16 and the number of points along the horizontal axis M = 96. The dimensionless step

of dimensions in the vertical direction was designated Δz and Δx horizontally. The dimensionless time step was denoted as. The total number of time steps Δt_{Σ} varied depending on the specific conditions of the problem.

NUMERICAL SIMULATION RESULTS

Fig. 3 shows the distribution of the temperature established over time inside the channel along the flow.

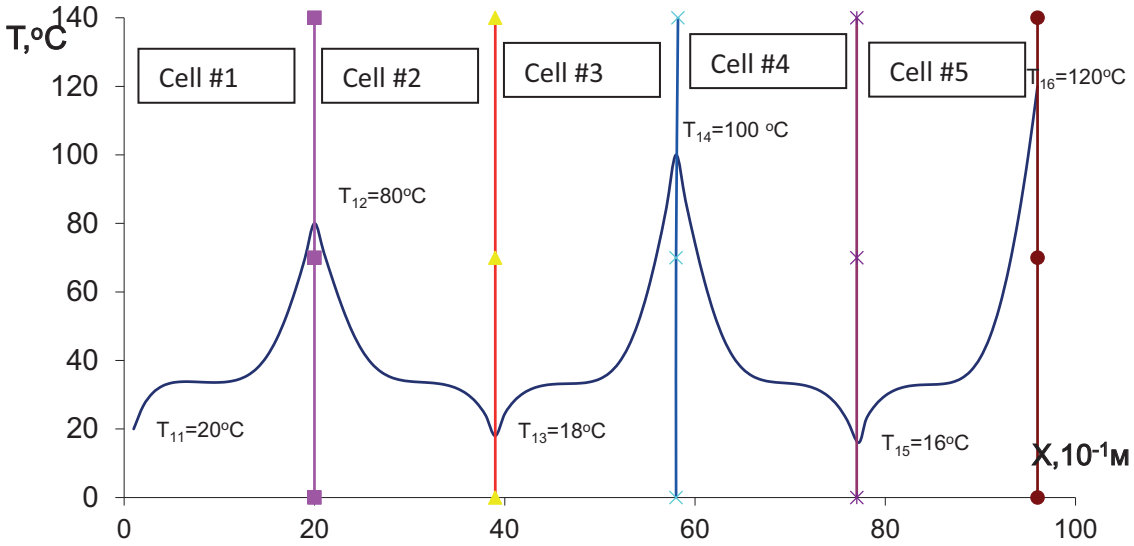

Figure 3. The temperature distribution in the cells convective SABPP aerodynamic channel in the first series of numerical experiment

Speed change along the direction of horizontal convective transport is given in Fig. 4. The figure shows that the steady-flow mode exiting aerodynamic cellular module completed through almost 5 hours after start heating. Subsequently the flow rate, which is formed at the outlet of the module, remains unchanged.

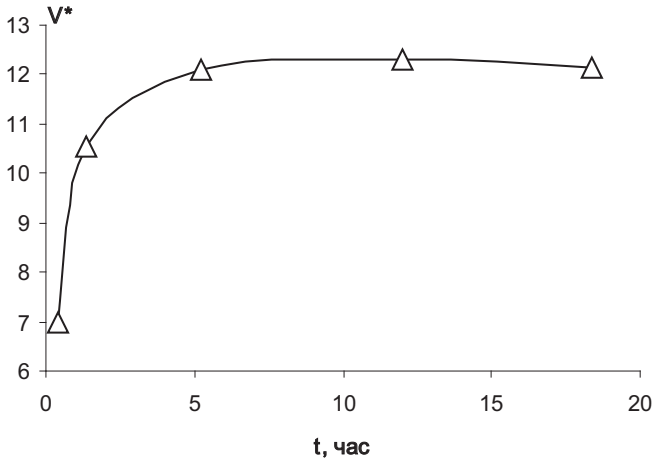

Figure 4. Numerical experiment data (series 1). The speed was normalized to a value in the incoming wind flow module

The transfer rate of air masses noticeably increases when they move through convective cells between cold and hot walls. For example, see Fig. 5.

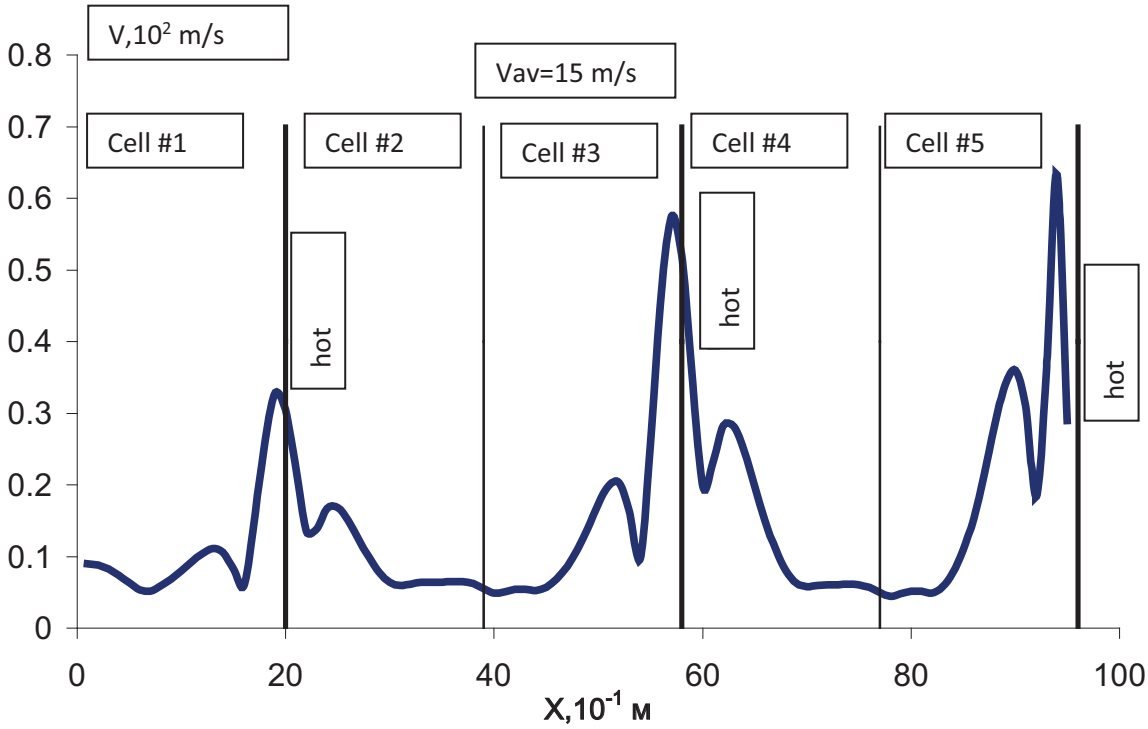

Figure 5. Change in flow rate when moving through alternately heated and cooled convective cells. The numerical calculation data refer to the moment 26 minutes after the heating is turned on

Fig. 6 illustrates the nature of air movement between the cells. It shows streamlines. At the cold wall, circulation occurs in a vertical plane with counterclockwise rotation. Near the heated wall, the circulation movement changes direction (Fig. 6).

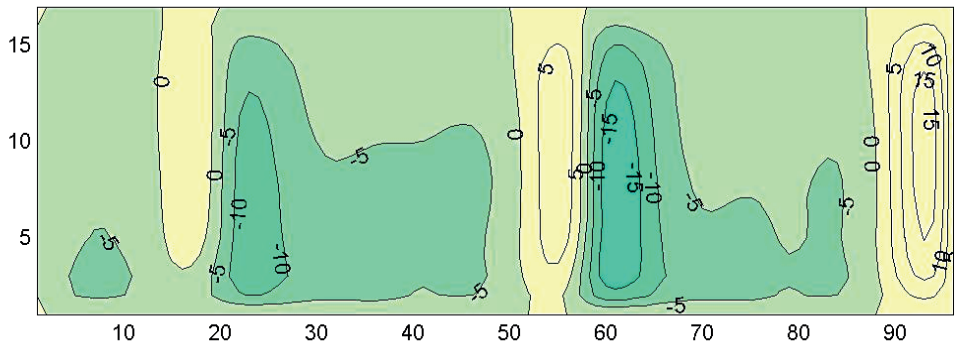

Figure 6. Streamline pattern in a vertical section of an aerodynamic module with alternately heated and cooled side walls. The values given on the isolines correspond to the circulation of the speed, expressed in normalized units, referred to the value of the circulation of the wind speed at the radius of the channel

An essential sign of a circulating increase in velocity in an aerodynamic channel with convective cells is the acceleration of the flow. This is evidenced by the calculation results shown in Fig. 7.

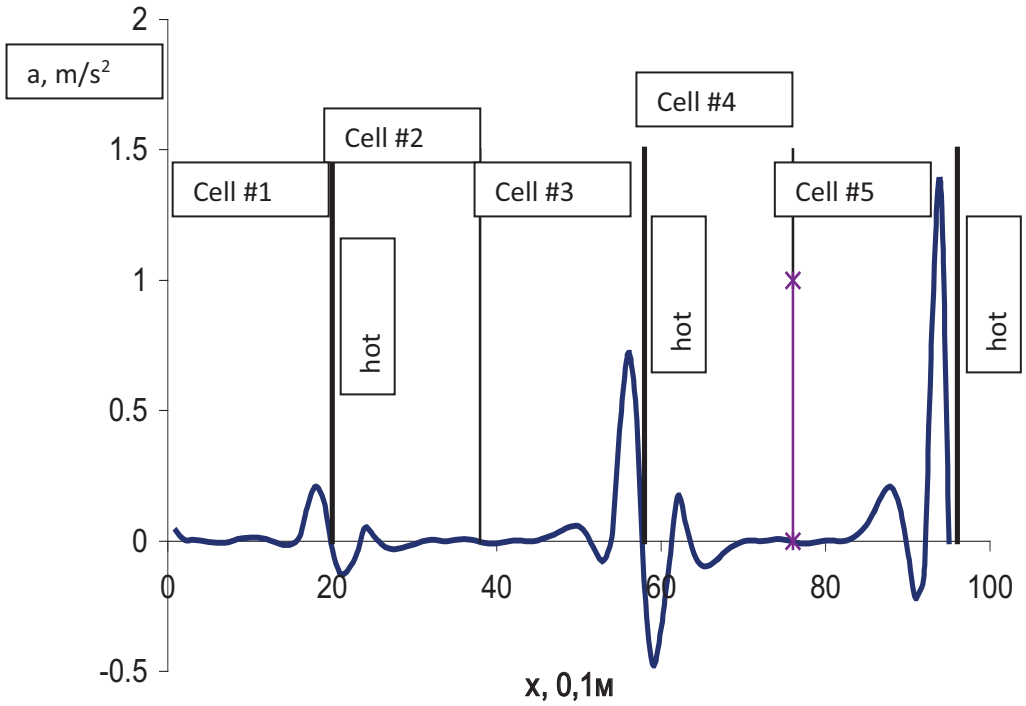

Figure 7. Change in the flow acceleration along the path of air movement through the convective cells of the aerodynamic module

It is accelerated in odd cells, in which the transfer movement of air masses goes in the direction from the cold side wall of the channel to the hot one. Moreover, as the cell number grows, the acceleration value increases. According to the calculation results for the conditions of series 1 of the numerical experiment (see Table 1), the change in acceleration a in odd cells ($i = 0,1,2....n$) of the SABPP aerodynamic channel separated by hot and cold partitions is determined by the following relation

$$a = 0,303 \cdot (2i + 1) - 0,163 \qquad (5)$$

If the number of cells in the channel is 8, then the flow acceleration will reach a value equal to 2.6 m / s^2 in the last section.

In cells, where convective flow is transferred from a hot wall to a cold one, the air movement downstream slows down. However, in general, the tendency to accelerate the flow in the direction of convective transfer prevails over deceleration. The empirical trend formula for calculating the acceleration **a** (m / s^2) in the channel with the outer radius **R** (m) is as follows:

$$a = 0,094 \cdot R - 0,0355 \qquad (6)$$

From the relation (6), it follows that with the outer radius of the aerodynamic channel with the height H = 2m and the outer radius R less than 0.37 m, the flow will practically slow down.

CONCLUSIONS

Numerical modeling of the approach for acceleration of convective flows initiated by solar heating of air masses in the aerodynamic module of helioaerobaric power plants with horizontal and vertical transfer of convective air streams formed in cells containing alternately located cold and hot side boundaries and differently heated upper and lower bases has been carried out. An analysis of several series of numerical experiments was carried out. This shown the optimal conditions for the intensification formed in the flow cells with a decreasing and increasing temperature difference between the walls along the flow were determined.

According to the results of experiments, it can be concluded for the studied heating and cooling options that the proposed method for intensifying flows in the SABPP aerodynamic module divided into differently heated and side walls allows to increase the speed of the forming current an order in relation to the natural wind speed and obtain a cyclotron flow acceleration of the order of 2.6 m/s^2. The variant of the aerodynamic module SABPP with a multicellular structure of heating and a convective flow passing through it can be recommended for practical implementation.

ACKNOWLEDGMENT

The study was carried out within the framework of the State Assignment (registration number # 075-00460-21-00, 0128-2021-0003).

REFERENCES

1. Turkenburg W.C., Faaij A., others. Chapter 7: Renewable energy technologies // World energy assessment: energy and the challenge of sustainability. New York: UNDP, 2000. C. 228–506.
2. Kongtragool B., Wongwises S. A review of solar-powered Stirling engines and low temperature differential Stirling engines // Renewable and Sustainable energy reviews. 2003. № 2(7). C. 131–154.
3. Al-Kayiem H.H., Aja O.C. Historic and recent progress in solar chimney power plant enhancing technologies // Renewable and Sustainable Energy Reviews. 2016. (58). C. 1269–1292. DOI:10.1016/J.RSER.2015.12.331.
4. Long T., Zheng D., Li W., Li Y., Lu J., Xie L., Huang S. Numerical investigation of the working mechanisms of solar chimney coupled with earth-to-air heat exchanger (SCEAHE) // Solar Energy. 2021. (230). C. 109–121. DOI:10.1016/j.solener.2021.10.029.
5. Omara A.A.M., Mohammed H.A., Al Rikabi I.J., Abuelnour M.A., Abuelnuor A.A.A. Performance improvement of solar chimneys using phase change materials: A review // Solar Energy. 2021. (228). C. 68–88. DOI:10.1016/J.SOLENER.2021.09.037.
6. RahimiLarki M., Abardeh R.H., Rahimzadeh H., Sarlak H. Performance analysis of a laboratory-scale tilted solar chimney system exposed to ambient crosswind // Renewable Energy. 2021. (164). C. 1156–1170. DOI:10.1016/J.RENENE.2020.10.118.
7. Rahdan P., Kasaeian A., Yan W.M. Simulation and geometric optimization of a hybrid system of solar chimney and water desalination // Energy Conversion and Management. 2021. (243). C. 114291. DOI:10.1016/J.ENCONMAN.2021.114291.
8. Liu Y., Ming T., Peng C., Wu Y., Li W., de Richter R., Zhou N. Mitigating air pollution strategies based on solar chimneys // Solar Energy. 2021. (218). C. 11–27. DOI:10.1016/J.SOLENER.2021.02.021.
9. Ming T., Gui H., Shi T., Xiong H., Wu Y., Shao Y., Li W., Lu X., de Richter R. Solar chimney power plant integrated with a photocatalytic reactor to remove atmospheric methane: A numerical analysis

// Solar Energy. 2021. (226). C. 101–111. DOI:10.1016/J.SOLENER.2021.08.024.
10. Kasaeian A.B., Molana S., Rahmani K., Wen D. A review on solar chimney systems // Renewable and Sustainable Energy Reviews. 2017. (67). C. 954–987. DOI:10.1016/J.RSER.2016.09.081.
11. Pradhan S., Chakraborty R., Mandal D.K., Barman A., Bose P. Design and performance analysis of solar chimney power plant (SCPP): A review // Sustainable Energy Technologies and Assessments. 2021. (47). C. 101411. DOI:10.1016/J.SETA.2021.101411.
12. Solovyev A., Solovyev D., Shilova L. Solar-vortex power plants: Principles of effective work and technical requirements on the preparation of initial data for design // MATEC Web of Conferences. 2018. (196). C. 04075. DOI: 10.1051/matecconf/201819604075.
13. Soloviev A. A. Sinergeticheskiye yavleniya v tropicheskikh tsiklonakh i tornado [Synergetic phenomena in tropical cyclones and tornadoes] // Istoriya i metodologiya yestestvennykh nauk, ser. Fizika. 1988. No. 34, pp. 53–62.
14. Solovyev A.A., Solovyev D.A., Shilova L.A. The innovative solar energy conversion technologies: solar convective-vortex power systems // OP Conf. Series: Materials Science and Engineerin. 2021. № 1030 (2021). C. 012162. DOI:10.1088/1757-899X/1030/1/01216.
15. Chabanov A.I., Sobolev V.M., Soloviev A.A., Gorodov M.I., Erokhov N.M., Filipenko E.S. Solnechnyy intensifitsirovannyy teplichnyy kompleks [Solar intensified greenhouse complex] // Izobreteniya i poleznyye modeli. 2005. No. 32, pp. 33–43.

СПИСОК ЛИТЕРАТУРЫ

1. Turkenburg W.C., Faaij A., others. Chapter 7: Renewable energy technologies // World energy assessment: energy and the challenge of sustainability. New York: UNDP, 2000. C. 228–506.
2. Kongtragool B., Wongwises S. A review of solar-powered Stirling engines and low temperature differential Stirling engines // Renewable and Sustainable energy reviews. 2003. № 2(7). C. 131–154.
3. Al-Kayiem H.H., Aja O.C. Historic and recent progress in solar chimney power plant enhancing technologies // Renewable and Sustainable Energy Reviews. 2016. (58). C. 1269–1292. DOI:10.1016/J.RSER.2015.12.331.
4. Long T., Zheng D., Li W., Li Y., Lu J., Xie L., Huang S. Numerical investigation of the working mechanisms of solar chimney coupled with earth-to-air heat exchanger (SCEAHE) // Solar Energy. 2021. (230). C. 109–121. DOI:10.1016/j.solener.2021.10.029.
5. Omara A.A.M., Mohammed H.A., Al Rikabi I.J., Abuelnour M.A., Abuelnuor A.A.A. Performance improvement of solar chimneys using phase change materials: A review // Solar Energy. 2021. (228). C. 68–88. DOI:10.1016/J.SOLENER.2021.09.037.
6. RahimiLarki M., Abardeh R.H., Rahimzadeh H., Sarlak H. Performance analysis of a laboratory-scale tilted solar chimney system exposed to ambient crosswind // Renewable Energy. 2021. (164). C. 1156–1170. DOI:10.1016/J.RENENE.2020.10.118.
7. Rahdan P., Kasaeian A., Yan W.M. Simulation and geometric optimization of a hybrid system of solar chimney and water desalination // Energy Conversion and Management. 2021. (243). C. 114291. DOI:10.1016/J.ENCONMAN.2021.114291.
8. Liu Y., Ming T., Peng C., Wu Y., Li W., de Richter R., Zhou N. Mitigating air pollution strategies based on solar chimneys // Solar Energy. 2021. (218). C. 11–27. DOI:10.1016/J.SOLENER.2021.02.021.
9. Ming T., Gui H., Shi T., Xiong H., Wu Y., Shao Y., Li W., Lu X., de Richter R. Solar

chimney power plant integrated with a photocatalytic reactor to remove atmospheric methane: A numerical analysis // Solar Energy. 2021. (226). C. 101–111. DOI:10.1016/J.SOLENER.2021.08.024.
10. Kasaeian A.B., Molana S., Rahmani K., Wen D. A review on solar chimney systems // Renewable and Sustainable Energy Reviews. 2017. (67). C. 954–987. DOI:10.1016/J.RSER.2016.09.081.
11. Pradhan S., Chakraborty R., Mandal D.K., Barman A., Bose P. Design and performance analysis of solar chimney power plant (SCPP): A review // Sustainable Energy Technologies and Assessments. 2021. (47). C. 101411. DOI:10.1016/J.SETA.2021.101411.
12. Solovyev A., Solovyev D., Shilova L. Solar-vortex power plants: Principles of effective work and technical requirements on the preparation of initial data for design // MATEC Web of Conferences. 2018. (196). C. 04075. DOI:10.1051/matecconf/201819604075.
13. Соловьев А.А. Синергетические явления в тропических циклонах и торнадо // История и методология естественных наук, сер Физика. 1988. № 34. С. 53–62.
14. Solovyev A.A., Solovyev D.A., Shilova L.A. The innovative solar energy conversion technologies: solar convective-vortex power systems // OP Conf. Series: Materials Science and Engineerin. 2021. № 1030 (2021). C. 012162. DOI:10.1088/1757-899X/1030/1/01216.
15. Чабанов А.И., Соболев В.М., Соловьев А.А., Городов М.И., Ерохов Н.М., Филипенко Е.С. Солнечный интенсифицированный тепличный комплекс // Изобретения и полезные модели. 2005. № 32. С. 33–43.

Alexander A. Solovyev, professor, academician of the RIA, MV Lomonosov Moscow State University, Faculty of Geography, Renewable Energy Research Laboratory, 119991, GSP-1, Moscow, Lenin Hills, d. 1, Bldg. 19, Moscow State University, e-mail: asolovev@geogr.msu.ru

Dmitry A. Solovyev, Senior Researcher, Candidate of Physical and Mathematical Sciences, Shirshov Institute of Oceanology, Russian Academy of Sciences, 36, Nahimovskiy prospekt, Moscow, Russia, 117997; Senior Researcher (part-time) of Laboratory No. 12, Joint Institute of High Temperatures of the Russian Academy of Sciences (JIHT RAS), 125412, Moscow, Izhorskaya Street, 13, building 2, solovev@ocean.ru, Tel.: +7(499)1247928

Liubov A. Shilova, Candidate of Technical Sciences, Senior Lecturer Department of information systems technology and automation in construction, Moscow State University of Civil Engineering (National Research University) (MGSU), 26 Yaroslavskoye Shosse, Moscow, 129337, Russian Federation, ShilovaLA@mgsu.ru

Соловьев Александр Алексеевич, д-р физ.-мат. наук, профессор, академик РИА, заведующий НИЛ возобновляемых источников энергии географического факультета МГУ им. М.В. Ломоносова, 119991, ГСП-1 г. Москва, Ленинские горы, д. 1, корп. 19, e-mail: asolovev@geogr.msu.ru, +7 (495) 939-42-57

Соловьев Дмитрий Александрович, кандидат физ.-мат. наук, научный сотрудник лаборатории взаимодействия океана и атмосферы и мониторинга климатических изменений, Институт океанологии имени П.П. Ширшова РАН, 117997, Москва, Нахимовский проспект, д. 36; старший научный сотрудник (по совместительству) лаборатории №12, Объединённый институт высоких температур РАН (ОИВТ РАН), 125412, г. Москва, ул. Ижорская, д.13, стр.2, solovev@ocean.ru, +7-499-1247928

Шилова Любовь Андреевна, канд. техн. наук, доцент кафедры ИСТАС Национального исследовательского Московского государственного строительного университета (НИУ МГСУ), 129337, г. Москва, ул. Ярославское ш., д.26, ShilovaLA@mgsu.ru, +7(495) 287-49-14

International Journal for Computational Civil and Structural Engineering, 18(1) 72–81 (2022)

DOI:10.22337/2587-9618-2022-18-1-72-81

THE LOOP RESULTANT METHOD FOR STATIC STRUCTURAL ANALYSIS

Vladimir V. Lalin, Huu H. Ngo

Peter the Great St. Petersburg Polytechnic University, St. Petersburg, Russian Federation

Abstract: This work deals with the loop resultant method applied to linear static response of statically indeterminate rod-systems. The method uses the representation of this system in the form of a union of statically indeterminate loops. An algorithm for construction the flexibility matrix of the system is proposed. The unknowns of a system are the loop resultants. This method is based on the use of compatibility equations of deformations, the general solution of homogeneous equations of equilibrium is obtained by transposition of the compatibility matrix. The advantages of this method are the number and location of zero blocks and non-zero blocks of the system flexibility matrix depend only on the numbering of loops. Application of this method is considered for analysis of structural frame.

Keywords: force method; loop resultant method; flexibility matrix; compatibility equation of deformations; statically indeterminate system.

МЕТОД КОНТУРНЫХ УСИЛИЙ В СТАТИКЕ СТЕРЖНЕВЫХ СИСТЕМ

В.В. Лалин, Х.Х. Нго

Санкт-Петербургский политехнический университет Петра Великого, г. Санкт-Петербург, РОССИЯ

Аннотация: В работе рассматривается метод расчета статически неопределимых стержневых систем, основанный на представлении системы в виде объединения статически неопределимых контуров. Предложен алгоритм построения матрицы податливости системы. Неизвестными в системе уравнений являются усилия в контурах. Основой метода являются уравнения совместности деформаций, общее решение однородных уравнений равновесия получается транспонированием матрицы совместности. Рассмотрен пример расчета статически неопределимой рамы. Достоинством метода является то, что структура матрицы разрешающей системы уравнений, то есть количество и расположение в ней нулевых и ненулевых блоков зависит только от нумерации контуров.

Ключевые слова: метод сил; метод контурных усилий; матрица податливости; уравнения совместности деформаций; статически неопределимая система.

1. INTRODUCTION

Most of the engineering structures in civil engineering are statically indeterminate systems [1,2], which are omnipresent nowadays. For determining the structural responses the force method and the displacement method [1-3] have already been applied successfully in hand-computation of static and dynamic analysis. However for hand calculations, solving a system of equations of more than 10 unknowns was a major challenge. Thus, matrix calculus was developed to write an algorithm (or a programme) in a programming language and it is used on a digital electronic computer for automation of the solution of the system of equations [4]. Through the matrix approaches and the finite element method [4,5] achieved reliable results in structural analysis. However, most of current programmes use the displacement method or the mixed method [5,6].

Besides that, the first matrix approaches have been applied to improvement and automation of the force method [7-12]. Many algorithms of the force method have been studied to apply to structural design, such as an efficient analysis for cyclically symmetric space truss structures using an orthogonal self-stress matrix [13], a new structural analysis and optimization algorithm for determining the minimum weight of structures under displacement and stress constraints [14], the genetic algorithm for nonlinear analysis and optimal design of structures [15].

Within the algorithm of the integrated force method [16,17] the compatibility conditions are used. The papers [18-20] are also noticed that the use of the compatibility conditions is important for the automatic proccess of the force method. An efficient algorithm of the force method, which was called the loop resultant method, was developed by [21], this method will be discussed in more detail in next sections.

2. FORMULATION OF THE FLEXIBILITY MATRIX

We formulate the different flexibility matrices for element-rod (ER) which are based on their strain energy as the following formula:

$$W = \frac{1}{2}\int_0^L \left[\frac{N^2(s)}{EA} + \frac{Q^2(s)}{kGA} + \frac{M^2(s)}{EI} \right] ds \,. \qquad (2.1)$$

Let's find the integral of (3.1), we have

$$W = \frac{1}{2}\sigma^T \cdot \Lambda \cdot \sigma \,, \qquad (2.2)$$

where L is the length of the element-rod, EA is the axial stiffness, kGA is the shear stiffness, EI is the bending stiffness.

The element-rod with rigid nodes, namely the type I, has the matrix (3x1) of internal forces $\sigma^T=[F_x\ F_y\ M]$ at any point A is shown as in Figure 2.1. The point A is any point, but the point A is the same point for all elements. Rigid cantilevers connect the element nodes with the point A. Thus, the bending moment M(s), the shear force Q as well as the axial force N of the element-rod are obtained, respectively:

$$M(s) = -(y(s) - y_A)F_x + \\ + (x(s) - x_A)F_y + M, \qquad (2.3)$$

$$Q = F_x n_x + F_y n_y \,, \qquad (2.4)$$

$$N = F_x t_x + F_y t_y \,. \qquad (2.5)$$

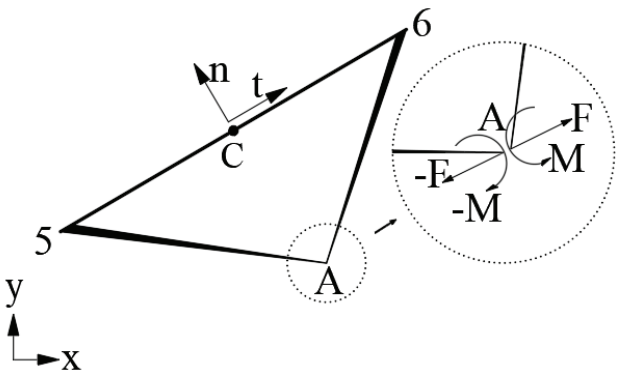

Figure 2.1. The nodal resultant of the element-rod (the type I)

Here C is the center point of the element-rod; t and n are the unit tangent and the unit normal vectors of the element-rod, respectively; F_x, F_y, n_x, n_y and t_x, t_y are the projections of three vectors F, n and t, respectively.

The type I (an element-rod with rigid ends), the type II (an element-rod hinged at one end and rigid at the other) and the type III (an element-rod with hinged ends) are shown in Figure 2.2.

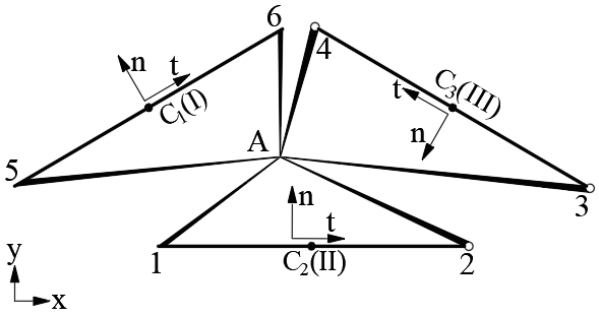

Figure 2.2. The different types of the elementrod

The flexibility matrices Λ of individual element-rods depend on their types. The flexibility matrix Λ (3x3) of the first type (its the shortest path from node 5 to node 6) can be expressed as

$$\Lambda_{(I)} = Q \cdot \tilde{\Lambda} \cdot Q^T + \tilde{\Lambda}_A, \qquad (2.6)$$

where the diagonal flexibility matrix for the horizontal element-rod cooresponding to the natural coordinate system can be described as below

$$\tilde{\Lambda} = diag\left\{\frac{L}{EA}; \left(\frac{L}{kGA} + \frac{L^3}{12EI}\right); \frac{L}{EI}\right\}, \qquad (2.7)$$

The orthogonal matrix (3x3) of a rotational element-rod is

$$Q = \begin{bmatrix} t_x & n_x & 0 \\ t_y & n_y & 0 \\ 0 & 0 & 1 \end{bmatrix} \qquad (2.8)$$

and the adding matrix (3x3) of the vector C_1A is

$$\tilde{\Lambda}_A = \frac{L}{EI}\begin{bmatrix} y^2 & -x \cdot y & -y \\ -x \cdot y & x^2 & x \\ -y & x & 0 \end{bmatrix}, \qquad (2.9)$$

here $x=x_{C1}-x_A$; $y=y_{C1}-y_A$ are the coordinates of a vector C_1A.

The second type of the element-rod hinged at one end, which is linked by a shortest path from node 1 to node 2, has the matrix (2x1) of internal forces $\sigma^T=[F_x\ F_y]$ and its the flexibility matrix (2x2) is expressed as:

$$\Lambda_{(II)} = \begin{bmatrix} \Lambda_{11} & \Lambda_{12} \\ \Lambda_{21} & \Lambda_{22} \end{bmatrix}, \qquad (2.10)$$

where $\Lambda_{11} = L\left(\frac{t_x^2}{EA} + \frac{t_y^2}{kGA} + L^2\frac{t_y^2}{3EI}\right)$;

$$\Lambda_{12} = \Lambda_{21} = Lt_x t_y\left(\frac{1}{EA} - \frac{1}{kGA} - \frac{L^2}{3EI}\right);$$

$$\Lambda_{22} = L\left(\frac{t_y^2}{EA} + \frac{t_x^2}{kGA} + L^2\frac{t_x^2}{3EI}\right).$$

An element-rod with hinged ends is a third type in which two nodes 3, 4 are connected by one shortest path, has the matrix (1x1) of internal forces $\sigma=t_xF_x+t_yF_y$, its the flexibility matrix is presented as

$$\Lambda_{(III)} = \frac{L}{EA}. \qquad (2.11)$$

The following kinematical variable *e* are energy conjugated with internal forces σ: $e^T=[e_x\ e_y\ \varphi]$, where e_x e_y - are relative displacements of the ends of the cantilevers at the point A, φ - is relative angle of rotation of the ends of the cantilevers at the point A.

3. THE BASIC LOOPS and COMPATIBILITY CONDITIONS

For the loop resultant method, Figure 3.1 shows two simple types of structural open-loop and closed-loop, which can be characterized by parameter: the degree of statically indeterminate loop, denoted by n^i_{st}.

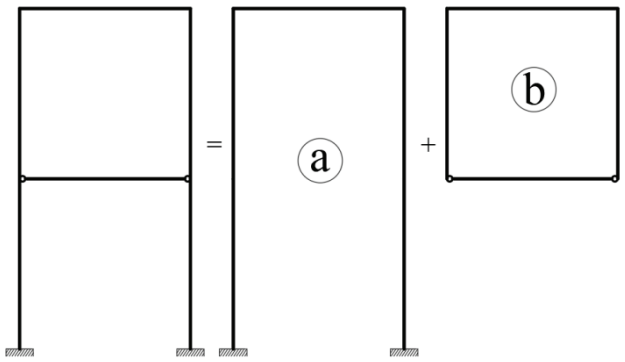

Figure 3.1. Two basic loops a (n^a_{st} =3), b (n^b_{st} =1)

In the following, we consider two principal rules to be applied for the process in building an algorithm.

Rule 1: The sum of the degree of each statically indeterminate loop $\sum n_{st}^{i}$ should be equal to the total degree of entire statically indeterminate structure n_{st}.

$$n_{st} = \sum_{i} n_{st}^{i} = n_{st}^{a} + n_{st}^{b} + ... + n_{st}^{i}. \qquad (3.1)$$

Rule 2: Selected loops can have one or several common element-rods and vice verca, but it is necessary to satisfy the condition of completeness of each loop, i.e. the individual element-rod must appear at least once in the basic loops.

The algorithm of the loop resultant method can be described in the following steps:

Step 1. Choose basic loops.

Step 2. Determine the flexibility matrix of element-rods Λ_i.

Step 3. Construct the flexibility block diagonal matrix

$$\Lambda = diag\{\Lambda_i\}. \qquad (3.2)$$

Step 4. Establish the compatibility matrix B.

Step 5. Complete the flexibility matrix of the framed structure

$$L = B \cdot \Lambda \cdot B^{T}. \qquad (3.3)$$

Step 6. Solve the system of equations

$$L \cdot X = -B \cdot e_o. \qquad (3.4)$$

Step 7. Compute the internal forces

$$\sigma = B^{T} \cdot X. \qquad (3.5)$$

We note that for the current algorithm, B^T is the transpose of a matrix B; X is the loop resultant matrix of the system; e_o is the initial deformations of the system.

To construct the compatibility matrix B, we consider the relationship of the deformation between different element-rods of the structural loop (Figure 3.1) using two transformation matrices H_1, H_2.

$$H_2 \cdot (e_1 + e_2 + e_3 - e_4) = 0, \qquad (3.6)$$

where $H_2 = [t_{cx} \quad t_{cy} \quad (-y \cdot t_{cx} + x \cdot t_{cy})]$; t_c is the unit vector which passes through the two hinges; t_{cx}, t_{cy} are the projections of the vector t_c; $x = x_A - x_C$, $y = y_A - y_C$. Thus the compatibility matrix B (1x12) is

$$B = [H_2 \quad H_2 \quad H_2 \quad -H_2]. \qquad (3.7)$$

When the loop has only one hinge, the compatibility matrix B (2x12) is

$$B = [H_1 \quad H_1 \quad H_1 \quad -H_1]. \qquad (3.8)$$

here $H_1 = \begin{bmatrix} 1 & 0 & -y \\ 0 & 1 & x \end{bmatrix}$; $x = x_A - x_H$, $y = y_A - y_H$; H denotes the hinged position.

When the loop has not hinge, the compatibility matrix B (3x12) is

$$B = [I \quad I \quad I \quad -I]. \qquad (3.9)$$

where I is identity (3x3) matrix.

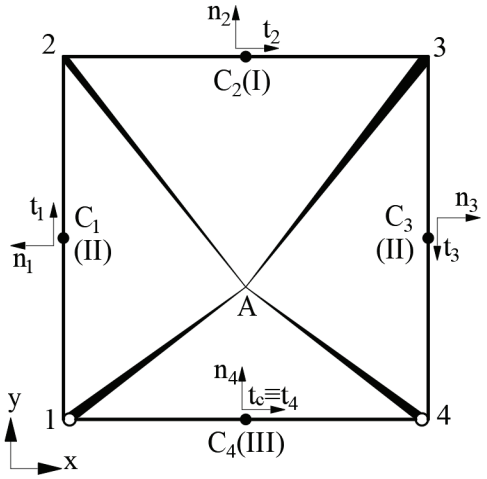

Figure 3.1. The basic loop

4. THE NUMERICAL EXAMPLE

The example is shown in Figure 4.1. The flexural rigidity EI is constant, the Young's modulus is $E=3\cdot10^7$ kN/m^2, the sizes of a rectangular cross-section are b=200 mm, h=200 mm, L=2 m. Determine the bending moments of structural frame under external loads P_1=8 kN, P_2=4 kN.

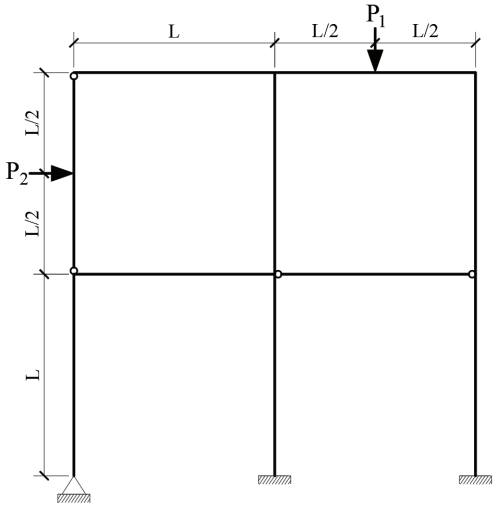

Figure 4.1. The framed structure under dead loads P_1 and P_2

First, the loop resultant method requires the component of information system which is shown in Figure 4.2, includes the point A, the type of the ER, the coordinate of the center point of the ER.

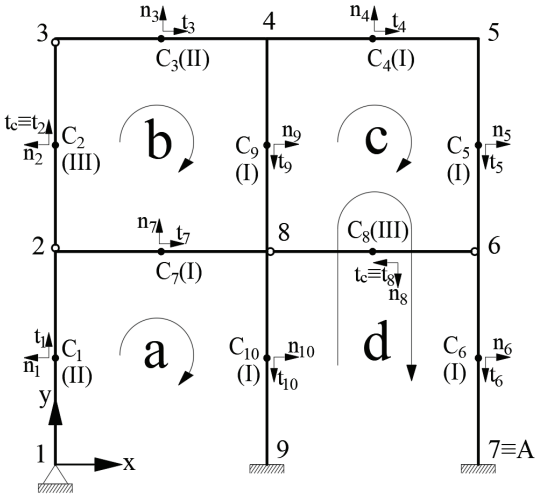

Figure 4.2. The four loops

In the loop resultant method basic loops may be chosen as shown in Figure. 4.3, which has four statically indeterminate loops: n_{st}^a=2, n_{st}^b=1, n_{st}^c=1, n_{st}^d=3.

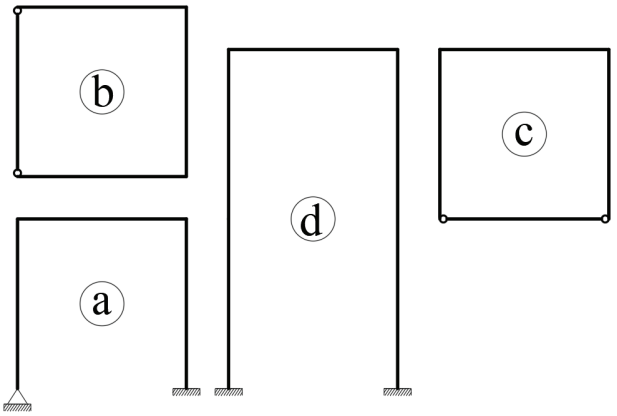

Figure 4.3. Selected basic loops.

Now, we consider the selected loops in Figure 4.3, which are reduced to the statically determinate loops in Figure 4.4, and we then calculate bending moments M_{Pi} (Figure 4.4) of the loops caused by external loads. When the basic loop subjected to external loads, it is necessary that the added internal forces allow it to reach balance, which can be mutually excluded in the whole system.

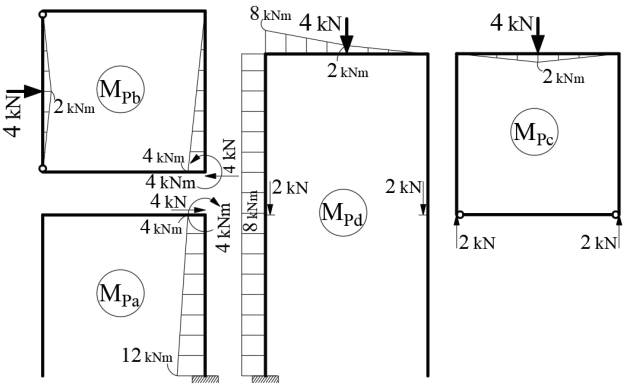

Figure 4.4. Bending moments M_{Pi} of loop fragments

Next, we compute bending moments on statically determinate loops caused by unit force in the direction of the desired deformation as in

Figuge 4.5 (their bending moment diagrams are shown in Figures 4.6, 4.7).

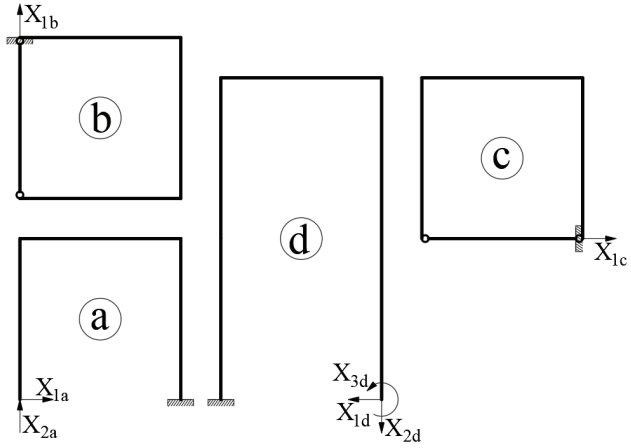

Figure 4.5. The loops subjected to unit force

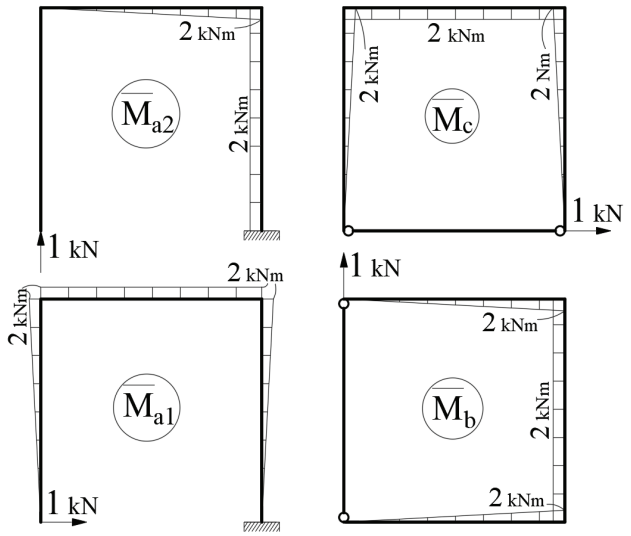

Figure 4.6. The loops a, b, c in the unit state

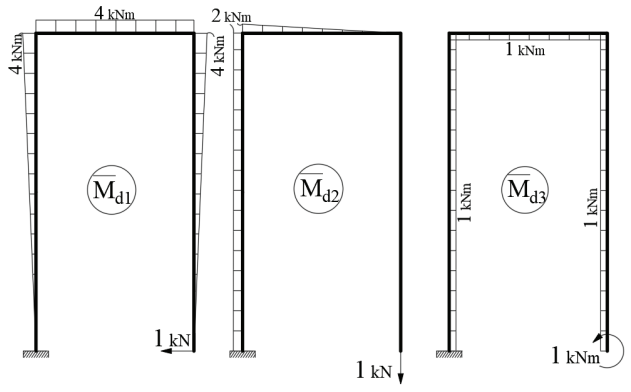

Figure 4.7. The loop d in the unit state

For calculating the initial deformations e_o, it is necessary to construct bending moment diagrams $\bar{M}_{ij}$ due to unit primary unknowns X_{ij}, j = 1, 2, 3, i = a, b, c, d and diagrams M_{Pi} due to external load.

The components of the matrix deformation Be_o are a set of displacements and rotations of basic loops, which are calculated by the formula.

$$\Delta_{ji,Pi} = \sum \int \frac{\bar{M}_{ji} \cdot M^*_{Pi}}{EI} dS\,, \tag{4.1}$$

The matrix deformation Be_o may be constructed for all structure

$$(Be_o)^T=[\Delta_{1a,Pa}\ \ \Delta_{2a,Pa}\ \ \Delta_{1b,Pb}\ \ \Delta_{1c,Pc}\ \ \Delta_{1d,Pd}\ \Delta_{2d,Pd}\ \ \Delta_{3d,Pd}]. \tag{4.2}$$

In our case we get

$$(Be_o)^T=(1/EI)\times[-29.33\ 64\ 40\ \ -26.67\ \ 104\ 110.67\ -56]. \tag{4.3}$$

In structural frame, we consider only the bending moment, i.e. the axial flexibility (1/EA) and the shear flexibility (1/kGA) are equal to zero. The corresponding flexibility matrices (2.6), (2.10), (2.11) are

$$\Lambda_{(I)} = \frac{L}{EI}\begin{bmatrix} (\frac{L^2}{12}t_y^2 + \frac{y^2}{EI}) & -(\frac{L^2}{12}t_x t_y + xy) & -y \\ & (\frac{L^2}{12}t_x^2 + x^2) & x \\ symm. & & 1 \end{bmatrix},$$

$$\Lambda_{(II)} = \begin{bmatrix} \frac{L^3}{3EI}t_y^2 & -\frac{L^3}{3EI}t_x t_y \\ symm. & \frac{L^3}{3EI}t_x^2 \end{bmatrix},\ \Lambda_{(III)} = 0 \tag{4.4}.$$

So the flexibility matrix Λ_i for each element-rod of the frame can be calculated by using the formulas (4.4).

$$\Lambda_1=\begin{bmatrix}2.7 & 0.0\\ 0.0 & 0.0\end{bmatrix},\ \Lambda_2=0,$$

$$\Lambda_3=\begin{bmatrix}0.0 & 0.0\\ 0.0 & 2.7\end{bmatrix},\ \Lambda_4=\begin{bmatrix}32 & 8.0 & -8.0\\ 8.0 & 2.7 & -2.0\\ -8.0 & -2.0 & 2.0\end{bmatrix},$$

$$\Lambda_5=\begin{bmatrix}18.7 & 0 & -6.0\\ 0.0 & 0 & 0.0\\ -6.0 & 0 & 2.0\end{bmatrix},\Lambda_6=\begin{bmatrix}2.7 & 0 & -2.0\\ 0.0 & 0 & 0.0\\ -2.0 & 0 & 2.0\end{bmatrix},$$

$$\Lambda_7=\begin{bmatrix}8.00 & 12.0 & -4.0\\ 12.0 & 18.7 & -6.0\\ -4.0 & -6.0 & 2.0\end{bmatrix},\ \Lambda_8=0,$$

$$\Lambda_9=\begin{bmatrix}18.7 & 12.0 & -6.0\\ 12.0 & 8.0 & -4.0\\ -6.0 & -4.0 & 2.0\end{bmatrix},\Lambda_{10}=\begin{bmatrix}2.7 & 4.0 & -2.0\\ 4.0 & 8.0 & -4.0\\ -2.0 & -4.0 & 2.0\end{bmatrix}.$$

After the flexibility matrices of element-rods are found, the following block diagonal matrix must be established.

$\Lambda=(1/EI)\times\mathrm{diag}\{\Lambda_1;\ \Lambda_2\ ;\Lambda_3;\ \Lambda_4;\ \Lambda_5;\ \Lambda_6;\ \Lambda_7;\ \Lambda_8;\ \Lambda_9;\ \Lambda_{10}\}$.

Using the formula (3.7), (3.8), (3.9), we construct the compatibility matrix B (7x24) for the whole system:

$$B=\begin{bmatrix}H_1 & 0 & 0 & 0 & 0 & 0 & H_1 & 0 & 0 & H_1\\ 0 & H_2 & H_2 & 0 & 0 & 0 & H_2 & 0 & H_2 & 0\\ 0 & 0 & 0 & H_2 & H_2 & 0 & 0 & H_2 & H_2 & 0\\ 0 & 0 & 0 & I_{3\times3} & I_{3\times3} & I_{3\times3} & 0 & 0 & I_{3\times3} & I_{3\times3}\end{bmatrix},\qquad(4.9)$$

where I_{nxn} is the unit matrix of size nxn.
Using the formula (3.3) for the flexibility matrix of structural frame, we have

$$L=\frac{1}{EI}\begin{bmatrix}13.33 & -8.00 & 4.00 & 0.00 & -2.67 & -4.00 & 2.00\\ -8.00 & 10.67 & -2.67 & 0.00 & 4.00 & 8.00 & -4.00\\ 4.00 & -2.67 & 13.33 & -4.00 & 12.0 & 8.00 & -4.00\\ 0.00 & 0.00 & -4.00 & 13.33 & -29.3 & -8.00 & 8.00\\ -2.67 & 4.00 & 12.00 & -29.3 & 74.7 & 24.0 & -24.0\\ -4.00 & 8.00 & 8.00 & -8.00 & 24.0 & 18.67 & -10.0\\ 2.00 & -4.00 & -4.00 & 8.00 & -24.0 & -10.0 & 10.00\end{bmatrix}.\qquad(4.10)$$

The solution of equations (3.4) leads to following results.
The loop resultants are

$$X=[-793.776\quad -2687.37\quad -677.853\quad -283.478\quad 925.688\quad -4937.73\quad 1923.37].\qquad(4.11)$$

According to the formula (3.5) we get the stress resultant as

$$\begin{aligned}\sigma=[&-793.776\quad -2687.37\quad -677.853\quad 0.0000\quad -677.853\quad 1209.17\\ &-4937.73\quad 2490.33\quad 1209.17\quad -4937.73\quad 2490.33\quad 925.688\\ &-4937.73\quad 1923.37\quad -793.776\quad -2009.51\quad 8038.05\quad 283.478\\ &-1209.17\quad 4259.88\quad -5201.74\quad -1719.46\quad 2250.37\quad -12672.8].\end{aligned}\qquad(4.12)$$

The final bending moment which are shown in Table 4.1, may be calculated by the formula $M_{final} = M_{Pn} + M$, where $M_p = \Sigma M_{Pi}$ (Figure 4.4), M is calculated by formula (2.3).

Table 4.1. The bending moments of the structural frame.

№ ER	Bending moments M_P (N·m)	Bending moments of the resultant system M (N·m)	Bending moments M_{final} (N·m)
1s	0.000000	0.0000000	0.0000000
1e	0.000000	-1587.550	-1587.550
2s,2e	0.000000	0.0000000	0.0000000
2m	-2000.00	0.0000000	-2000.000
3s	0.000000	0.0000000	0.0000000
3e	0.000000	-1355.700	-1355.700
4s	-8000.00	+7529.120	-470.8800
4m	0.000000	+2591.390	+2591.390
4e	0.000000	-2346.330	-2346.330
5s	0.000000	-2346.330	-2346.330
5e	0.000000	+71.99000	+71.99000
6s	0.000000	+71.99000	+71.99000
6e	0.000000	+1923.370	+1923.370
7s	0.000000	+1587.550	+1587.550
7e	0.000000	-2431.470	-2431.470
8s,8e	0.000000	0.0000000	0.0000000
9s	+8000.00	-8884.830	-884.8300
9e	+12000.0	-11303.16	+696.8400
10s	+12000.0	-13734.63	-1734.630
10e	+20000.0	-17173.56	+2826.44

We note that the numbers 1…10 describe the ordinal ERs; the value of the bending moment at the start, middle and end of the ER are denoted by s, m and e, respectively.

5. CONCLUSIONS

It is well know that the classical force method is not easily fully automated. In the present paper the technique, the so-called loop resultant method, is used to automate the classical force method by using an algorithm, which may be constructed the computationally easy way to static analysis for statically indeterminate structures.

The extension of this algorithm that could be applied to dynamic analysis is still under investigation.

REFERENCES

1. **Marti P.** Theory of structures, fundamentals framed structures, plates and shells. Wilhelm Ernst & Sohn, 2013, 677 p.
2. **Timoshenko S.P., Young D.H.** Theory of structures. McGraw-Hill, Inc., 2nd edition, 1965, 627 p.
3. **Kinney J.K.** Indeterminate structure analysis. Addison-wesley publising company, INC. Reading, Massachetts, U.S.A., 1st edition, 1962, 651 p.
4. **Karnovsky I.A., Lebed O.I.** Advanced methods of structural analysis. Springer New York DordrechtHeidelberg London, 2010, 589 p., ISBN 978-1-4419-1046-9.
5. **Zienkiewicz O.C., Taylor R.L., Fox D.D.** The finite element method for solid and structural mechanics. Elsevier Ltd., 7th edition, 2014, 617 p., ISBN: 978-1-85617-634-7.
6. **Gatica G.N.** A Simple Introduction to the Mixed Finite Element. Springer, 2014, 142 p., ISBN 978-3-319-03694-6.
7. **Wehle L.B., Lansing W.** A method for reducing the analysis of complex redundant structures to a routine procedure. // Journal of The Aeronautical Sciences. 1952, Vol. 19, pp. 677-684.
8. **Patnaik N.** An integrated force method for discrete analysis. // International Journal for Numerical Methods in Engineering, Vol. 6, 1973, pp. 237-251.
9. **Rozin L.A.** Sterzhnevyye sistemy kak sistemy konechnykh elementov [About the Rod-systems as the Finite Element Systems. СПб, СПбГТУ, 1975, 237 p. (in Russian).

10. **Felippa C.A.** Will the force method come back?. // Journal of Applied Mechanics, 1987, Vol. 54, pp. 728-729.
11. **Spiliopoulos K.V., Souliotis P.G.** Automatic collapse load analysis of regular plane frames using the force method. // Computers & Structures, Vol. 64, 1997, pp. 531-540.
12. **Felippa C.A., Park K.C.** A direct flexibility method. // Computer Methods in Applied Mechanics and Engineering, Vol. 149, 1997, pp. 319-337.
13. **Koohestani K.** An orthogonal self-stress matrix for efficient analysis of cyclically symmetric space truss structures via force method. // International Journal of Solids and Structures, 2011, pp. 227-233.
14. **Sedaghati R., Esmailzadeh E.** Optimum design of structures with stress and displacement constraints using the force method. // International Journal of Mechanical Sciences, 2003, pp. 1369-1389.
15. **Kaveh A., Rahami H.** Nonlinear analysis and optimal design of structures via force method and genetic algorithm. // Computers and Structures, 2006, pp. 770-778.
16. **Patnaik N., Hopkins A., Halford R.** Integrated force method solution to indeterminate structural mechanics problems. National Aeronautics and Space Administration, Washington, DC 20546-0001, 2004, 180 p.
17. **Wang Y., Senatore G.** Extended integrated force method for the analysis of prestress-stable statically and kinematically indeterminate structures. // International Journal of Solids and Structures, Vol. 202, 2020, pp. 798-815.
18. **Lalin V.V.** Uravneniya sovmestnosti deformatsiy kak osnova algoritmizatsii metoda sil dlya sterzhnevykh sistem [About Compatibility Equations of Deformation as the Basis for Algoritmization of the Force Method for Rod-systems]. // SPb, SPbGTU, 1992, pp. 96-111 (in Russian).
19. **Patnaik S.N., Coroneos R. M., Hopkins D.A.** Compatibility conditions of structural mechanics. // International journal for numerical methods in engineering, 2000, pp. 685-704.
20. **Patnaik S.N.** Compatibility Condition in Theory of Solid Mechanics (Elasticity, Structures, and Design Optimization). NASA Center for Aerospace Information, 2007, 43p.
21. **Lalin V.V., Rozin L.A., Bugayeva T.N.** Metod konturnykh usiliy v statike sterzhnevykh sistem [About the Loop Resultant Method for Static Analysis of the Rod-systems]. // News of higher educational institutions. Construction., 1998, Vol. 10, pp. 15-24 (in Russian).

СПИСОК ЛИТЕРАТУРЫ

1. **Marti P.** Theory of structures, fundamentals framed structures plates and shells. Wilhelm Ernst & Sohn, 2013, 677 p.
2. **Timoshenko S.P., Young D.H.** Theory of structures. McGraw-Hill, Inc., 2nd edition, 1965, 627 p.
3. **Kinney J.K.** Indeterminate structure analysis. Addison-wesley publising company, INC. Reading, Massachetts, U.S.A., 1st edition, 1962, 651 p.
4. **Karnovsky I.A., Lebed O.I.** Advanced methods of structural analysis. Springer New York DordrechtHeidelberg London, 2010, 589 p., ISBN 978-1-4419-1046-9.
5. **Zienkiewicz O.C., Taylor R.L., Fox D.D.** The finite element method for solid and structural mechanics. Elsevier Ltd., 7th edition, 2014, 617 p., ISBN: 978-1-85617-634-7.
6. **Gatica G.N.** A Simple Introduction to the Mixed Finite Element. Springer, 2014, 142 p., ISBN 978-3-319-03694-6.
7. **Wehle L.B., Lansing W.** A method for reducing the analysis of complex redundant structures to a routine procedure. // Journal of The Aeronautical Sciences. 1952, Vol. 19, pp. 677-684.

8. **Patnaik N.** An integrated force method for discrete analysis. // International Journal for Numerical Methods in Engineering, Vol. 6, 1973, pp. 237-251.
9. **Розин Л.А.** Стержневые системы как системы конечных элементов. СПб, СПбГТУ, 1975, 237 с.
10. **Felippa C.A.** Will the force method come back?. // Journal of Applied Mechanics, 1987, Vol. 54, pp. 728-729.
11. **Spiliopoulos K.V., Souliotis P.G.** Automatic collapse load analysis of regular plane frames using the force method. // Computers & Structures, Vol. 64, 1997, pp. 531-540.
12. **Felippa C.A., Park K.C.** A direct flexibility method. // Computer Methods in Applied Mechanics and Engineering, Vol. 149, 1997, pp. 319-337.
13. **Koohestani K.** An orthogonal self-stress matrix for efficient analysis of cyclically symmetric space truss structures via force method. // International Journal of Solids and Structures, 2011, pp. 227-233.
14. **Sedaghati R., Esmailzadeh E.** Optimum design of structures with stress and displacement constraints using the force method. // International Journal of Mechanical Sciences, 2003, pp. 1369-1389.
15. **Kaveh A., Rahami H.** Nonlinear analysis and optimal design of structures via force method and genetic algorithm. // Computers and Structures, 2006, pp. 770-778.
16. **Patnaik N., Hopkins A., Halford R.** Integrated force method solution to indeterminate structural mechanics problems. National Aeronautics and Space Administration, Washington, DC 20546-0001, 2004, 180 p.
17. **Wang Y., Senatore G.** Extended integrated force method for the analysis of prestress-stable statically and kinematically indeterminate structures. // International Journal of Solids and Structures, Vol. 202, 2020, pp. 798-815.
18. **Лалин В.В.** Уравнения совместности деформаций как основа алгоритмизации метода сил для стержневых систем. // СПб, СПбГТУ, 1992, с. 96-111.
19. **Patnaik S.N., Coroneos R. M., Hopkins D.A.** Compatibility conditions of structural mechanics. // International journal for numerical methods in engineering, 2000, pp. 685-704.
20. **Patnaik S.N.** Compatibility Condition in Theory of Solid Mechanics (Elasticity, Structures, and Design Optimization). NASA Center for Aerospace Information, 2007, 43p.
21. **Лалин В.В., Розин Л.А., Бугаева Т.Н.** Метод контурных усилий в статике стержневых систем. // Изв. вузов. Строительство, 1998, с. 15-24.

Vladimir V. Lalin, Dr.Sc., Professor, Institute of Civil Engineering, Peter the Great St. Petersburg Polytechnic University (SPbPU); 29 Polytechnicheskaya, St. Petersburg, 195251, Russian Federation; phone: +7(921) 319-98-78; Email: vllalin@yandex.ru.

Нии Н. Ngo, Postgraduate; Peter the Great St. Petersburg Polytechnic University (SPbPU); 29 Polytechnicheskaya, St. Petersburg, 195251, Russian Federation; phone: +7(952)276-57-85; Email: hieupolytech1993@gmail.com.

Лалин Владимир Владимирович, доктор технических наук, профессор, Инженерно-строительный институт, Санкт-Петербургский политехнический университет Петра Великого (СПбПУ); 195251, г. Санкт-Петербург, ул. Политехническая, д. 29; телефон: +7(921) 319-98-78; Email: vllalin@yandex.ru.

Нго Хыу Хиеу, аспирант, Инженерно-строительный институт, Санкт-Петербургский политехнический университет Петра Великого (СПбПУ); 195251, г. Санкт-Петербург, ул. Политехническая, д. 29; телефон: +7(952) 276-57-85; Email: hieupolytech1993@gmail.com.

International Journal for Computational Civil and Structural Engineering, 18(1) 82–91 (2022)

DOI:10.22337/2587-9618-2022-18-1-82-91

ASSESSMENT OF THE INFLUENCE OF THE ROTATIONAL COMPONENTS OF SEISMIC ACTION ON THE SSS OF A MULTISTOREY REINFORCED CONCRETE BUILDING

Andrej A. Reshetov, Ekaterina M. Lokhova

Moscow State University of Civil Engineering (National Research University), Moscow, RUSSIA

Abstract. The urgent task of earthquake-resistant construction is to improve the methods of calculating the seismic effect. Currently, most calculations for seismic effects are made taking into account only the translational components of the earthquake. However, seismic soil rotations make a tangible contribution to the dynamic response of structures that are sensitive to the wave effect of seismic impact. Modern studies show that building structures have a spatial nature of work, and in calculations for seismic loads, in addition to three translational components, it is necessary to consider the impact on buildings and structures from additional three rotational components. The purpose of this work is to assess the influence of rotational components on the stress-strain state of a multielement reinforced concrete building. In the course of the work, calculations of a reinforced concrete building were made without taking into account and taking into account the rotational components of the seismic impact, based on the results of which a comparative analysis was made. The calculation for the earthquake was performed by an explicit direct dynamic method of central differences in the LS-DYNA software in six settings: the action of the translational component is set along the X axis; the action of the translational component is set along the X axis and rotational component – relative to the Y axis; the action of the translational component is set along the Y axis; the action of the translational component is set along the Y axis and rotational component – relative to the X axis; the impact of three translational components; the action of three translational and three rotational components. As a result of a comparative analysis of the obtained displacements and stresses, it was concluded that taking into account rotational components does not make a tangible contribution to the SSS of the building under consideration.

Keywords: Accounting For Rotational Components, Method Of Central Differences, Earthquake-Resistant Construction, Nonlinear Dynamic Methods.

ОЦЕНКА ВЛИЯНИЯ РОТАЦИОННЫХ КОМПОНЕНТ СЕЙСМИЧЕСКОГО ВОЗДЕЙСТВИЯ НА НДС МНОГОЭТАЖНОГО ЖЕЛЕЗОБЕТОННОГО ЗДАНИЯ

А.А. Решетов, Е.М. Лохова

Национальный исследовательский Московский государственный строительный университет, Москва, РОССИЯ

Аннотация. Актуальной задачей сейсмостойкого строительства является совершенствование методов расчёта на сейсмическое воздействие. В настоящее время большинство расчетов на сейсмические воздействия производятся с учетом только поступательных компонент землетрясения. Однако сейсмические ротации грунта дают ощутимый вклад в динамическую реакцию сооружений, чувствительных к волновому эффекту сейсмического воздействия Современные исследования показывают, что строительным конструкциям присущ пространственный характер работы, а при расчётах на сейсмические нагрузки помимо трёх поступательных компонент, необходимо рассмотрение воздействия, оказываемого на здания и сооружения от дополнительных трёх ротационных компонент. Целью данной работы является оценка влияния ротационных компонент на напряженно-деформированное состояние многоэлементного железобетонного здания. В ходе работы были произведены расчеты железобетонного здания без учёта и с учётом ротационных компонент сейсмического воздействия, по результатам которых был произведен сравнительный анализ. Расчет на землетрясение был произведен явным прямым динамическим методом центральных разностей в ПК LS-DYNA в шести постановках: воздействие поступательной компоненты задано вдоль оси X; воздействие поступательной компоненты задано вдоль оси X и ротационной относи-

тельно оси Y; воздействие поступательной компоненты задано вдоль оси Y; воздействие поступательной компоненты задано вдоль оси Y и ротационной относительно оси X; воздействие трёх поступательных компонент; воздействие трёх поступательных и трёх ротационных компонент. В результате сравнительного анализа полученных перемещений и напряжений был получен вывод о том, что учёт ротационных компонент не вносит ощутимого вклада в НДС рассматриваемого здания.

Ключевые слова: Учет компонентов вращения, метод центральных разностей, сейсмостойкие конструкции, нелинейные динамические методы.

1. INTRODUCTION

About a third of the population of the Russian Federation lives in seismically active regions, while earthquakes rank third after typhoons and floods in terms of damage caused. Hundreds and thousands of people die during destructive earthquakes. Reducing the negative consequences of earthquakes is possible thanks to the approaches of earthquake-resistant construction, one of the tasks of which is to determine and study the processes of interaction between buildings and their foundations. Currently, when calculating for an earthquake, only translational components are taken into account, while a number of works of scientists, in particular Yu P Nazarov [1–4], shows that when designing in seismic regions for all buildings and structures, it is also necessary to take into account rotational components seismic impact.

The first mention of rotational vibrations of the base area was the monograph by A G Nazarov [1]. The monograph specifies that the considered elementary area of the base has six degrees of freedom, which consist of three translational and three rotational, from which it follows that the vibrations made by the elementary platform are decomposed into translational and rotational. Ten years later, the first analytical description of rotational vibrations was made by N M Newmark [5], where the relationship between the torsion of the structure and the rotational component of the seismic action was shown. A number of works by N M Newmark [5-7] laid the foundation for further studies of the properties of fields of seismic activity. As a result of research by V V Lee and M D Trifunac [8], the possibility of obtaining synthetic rotational accelerograms using exact physical dependencies describing the propagation of elastic waves was stated, a description of one of the methods for calculating the rotational components was made. The accelerograms obtained by this method have realistic properties and resemble the real rotational motion of the soil foundation.

The purpose of this study is to assess the influence of rotational component on the stress-strain state of a reinforced concrete building.

2. MATERIALS AND METHODS

The dynamic method used in this work is based on the equation of motion, which has the following form:

$$M \cdot \ddot{u} + C\,\dot{u} + K \cdot u = f^{a}, \qquad (1)$$

where:

M – system mass matrix;

C – damping matrix;

K – system stiffness matrix;

f^{a} – vector of external influences.

The explicit method of central differences is used in the work. The solution of the differential equation (1) is reduced to a system of nonlinear differential equations at each step of time integration. Integration of the equation of motion can be performed both according to explicit and implicit schemes, but the most effective method is considered to be the explicit method of central differences implemented in the LS-DYNA software and used in this work.

Let each time step $\Delta t_i = \Delta t$, then the expressions for the central differences of the derivatives of

the displacement at the time t_i can be written in the following form:

$$\dot{u}_i = \frac{u_{i+1} - u_{i-1}}{2\Delta t}; \quad \ddot{u}_i = \frac{u_{i+1} - 2u_i + u_{i-1}}{(\Delta t)^2}. \tag{2}$$

Substituting equation (2) in (1) for a linear elastic system, we get:

$$m\frac{u_{i+1} - 2u_i + u_{i-1}}{(\Delta t)^2} + c\frac{u_{i+1} - u_{i-1}}{2\Delta t} + ku_i = p_i, \tag{3}$$

where it is assumed that u_i and u_{i-1} are known from the solution for the previous time steps.
Moving these known ones to the right side, we get the following equation:

$$\left[\frac{m}{(\Delta t)^2} + \frac{c}{2\Delta t}\right]u_{i+1} = p_i - \left[\frac{m}{(\Delta t)^2} - \frac{c}{2\Delta t}\right]u_{i-1} - \left[k - \frac{2m}{(\Delta t)^2}\right]u_i. \tag{4}$$

Let us replace with variables:

$$\tilde{k} = \frac{m}{(\Delta t)^2} + \frac{c}{2\Delta t}; \quad \tilde{p}_i = p_i - \left[\frac{m}{(\Delta t)^2} - \frac{c}{2\Delta t}\right]u_{i-1} - \left[k - \frac{2m}{(\Delta t)^2}\right]u_i. \tag{5}$$

Then (5) can be written in the following form:

$$\tilde{k}u_{i+1} = \tilde{p}_i. \tag{6}$$

The method of finding u_{i+1} at a time point $i+1$ based on the equilibrium of equation (1) at time i without using the same equation at a time $i+1$ is called explicit. To calculate u_{-1}, we use formula (2) for $i = 0$ and we get:

$$\dot{u}_0 = \frac{u_1 - u_{-1}}{2\Delta t}; \quad \ddot{u}_0 = \frac{u_1 - 2u_0 + u_{-1}}{(\Delta t)^2}. \tag{7}$$

$$u_{-1} = u_0 - \Delta t(\dot{u}_0) + \frac{(\Delta t)^2}{2}\ddot{u}_0. \tag{8}$$

$$\ddot{u}_0 = \frac{p_0 - c\dot{u}_0 - ku_0}{m}. \tag{9}$$

The object of the study is a monolithic reinforced concrete structure with a cross arrangement of girders. The height of the building is 8 floors (24 m). The dimensions of the structure in the plan are 20.4 m in width and length. Vertical load-bearing elements are presented in the form of columns located with a pitch of 6 m in one direction and 9 m in the other (Fig. 1). In the course of the development of the scheme, the following sections and thicknesses were adopted: a square section of 0.4 × 0.4 (h) m for columns, a rectangular section of 0.4 × 0.5 (h) m for girders, the thickness of the floors was taken equal to 0.2 m. The design parameters of the material are taken as for concrete B25: modulus of elasticity E = $3 \cdot 10^{10}$ Pa, density ρ = 2500 kg/m³, attenuation coefficient c = 0,05 of the critical, Poisson's ratio = 0.2. In addition to its own weight, all slabs are subject to a vertical force equal to 200 kg·s/m².
The calculation of the structure for seismic action was carried out in the LS-DYNA software, where an explicit method of integrating the equation of motion was implemented. Columns and girders were modelled with finite elements of the BEAM type, slabs – with flat finite elements of the SHELL type. The material type is set as ELASTIC. Constant vertical loads are specified with the BODY_Z function. All nodes of intersections of girders, columns and slabs are rigid, and the finite element mesh of girders and slabs is joint. The step of dividing all finite elements is taken equal to 0.3 m. In total, the model contains 46400 finite elements, 4784 of which are bar (BEAM), and 41616 are flat four-node (SHELL).
Modelling of the seismic impact was carried out with the assumption that the structure under study is located on some absolutely rigid platform (Fig. 2) for which the dependences of accelerations/velocities/displacements on time are set. All rotational components are calculated according to the integral model. Damping was simulated in proportion to the strain rate.

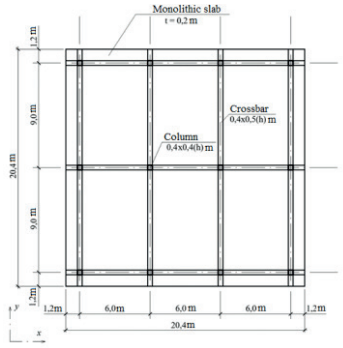

Figure 1. Constructive floor plan of the building under study

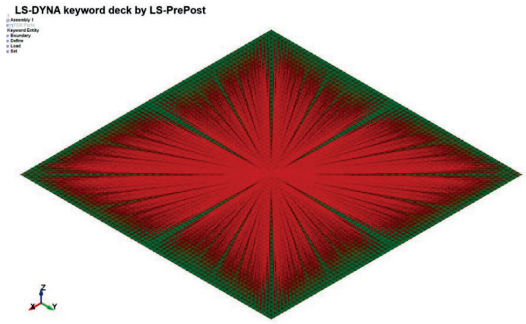

Figure 2. General view of the platform model in the design scheme

All nodes of the platform model in Fig. 2 are combined into one absolutely rigid nodal body with a central main node for which the diagrams of the dependence of translational and rotational accelerations on time were set.

As the analysed calculation results, the work considers nodal displacements of nodes numbered 13071 (central), 15383 (extreme) relative to the centre of the platform located on the upper slab and the forces in the lower finite element (B 9253) of the extreme corner column. A general view of the design scheme of the building under study in the LS-DYNA software is shown in Fig. 3.

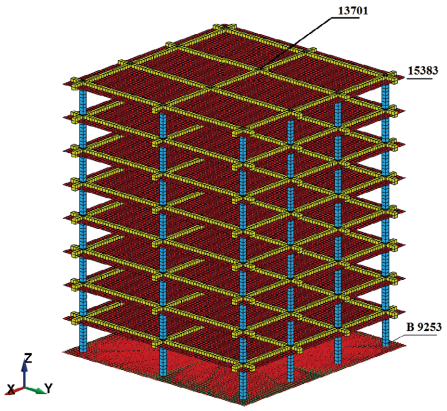

Figure 3. General view of the design scheme

2.1 Calculation from accounting the rotational component relative to the Y axis

In the course of the work, a calculation was carried out taking into account the rotational component relative to the Y axis, which included the following calculations:

1. Taking into account one translational component the action of which is directed along the X axis.

2.Taking into account two components, where one is translational along the X axis, and the other arises from the translational one along the X axis, rotational component — relative to the Y axis. Accelerograms of a given seismic action are shown in Fig. 4-5 for translational and rotational actions, respectively.

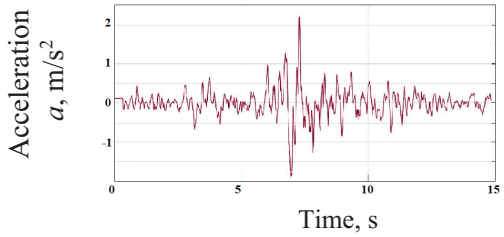

Figure 4. Accelerogram of translational motion along the X-axis

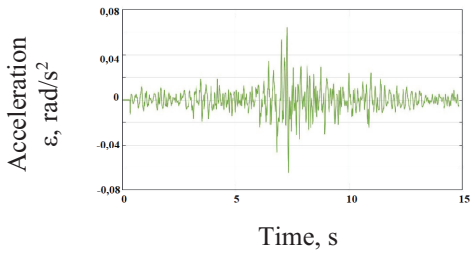

Figure 5. Accelerogram of rotational movement with respect to the Y-axis from the action ax

2.2 Calculation from accounting the rotational component relative to the X axis

In the course of the work, a calculation was also carried out taking into account the rotational component relative to the X axis, which included the following calculations:
1. Taking into account one translational component the action of which is directed along the Y axis.

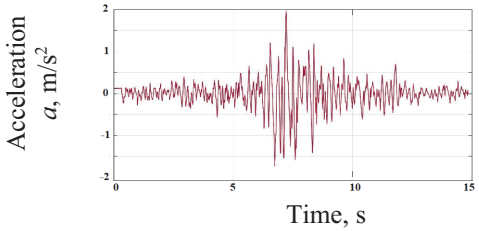

Figure 6. Accelerogram of translational motion along the Y-axis

2.Taking into account two components, where one is translational along the Y axis, and the other arises from the translational one along the Y axis, rotational component — relative to the X axis. Accelerograms of a given seismic action are shown in Fig. 6-7 for translational and rotational actions, respectively.

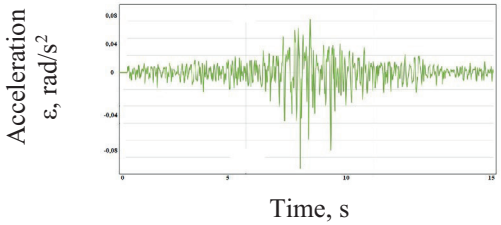

Figure 7. Accelerogram of rotational movement with respect to the X-axis from the action a_y

2.3 Calculation from accounting the six rotational components

Also in the course of the work, a calculation was made for a six-component seismic action, which included the following calculations:
1. Taking into account three translational components the action of which is directed along three mutually perpendicular axes.

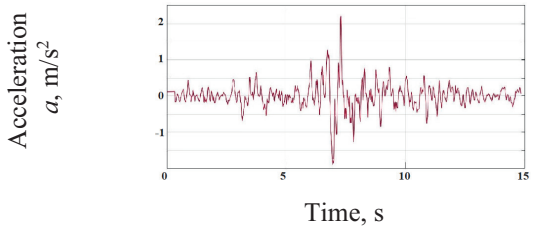

Figure 8. Accelerogram of translational motion along the X-axis

2. Taking into account six components, where three are translational, and the other three are rotational and arise from translational.
Accelerograms of a given seismic action are shown in Fig. 8-10 for translational and in Fig. 11-13 for rotational actions.

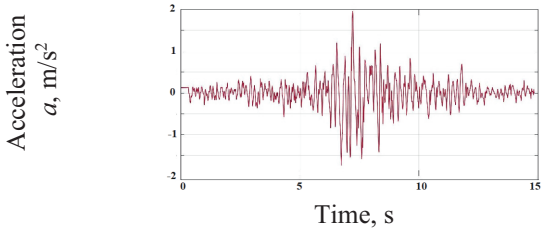

Figure 9. Accelerogram of translational motion along the Y-axis

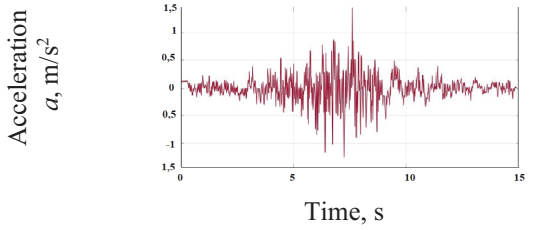

Figure 10. Accelerogram of translational motion along the Z-axis

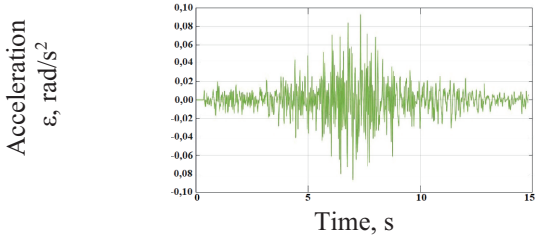

Figure 11. Accelerogram of rotational movement with respect to the X-axis from the action a_y, a_z

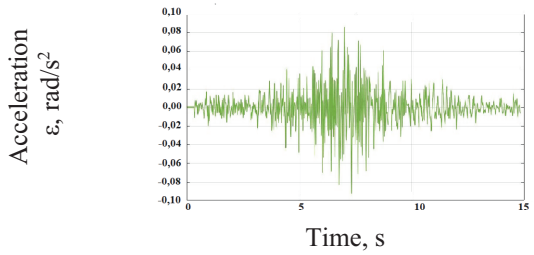

Figure 12. Accelerogram of rotational movement with respect to the Y-axis from the action a_x, a_z

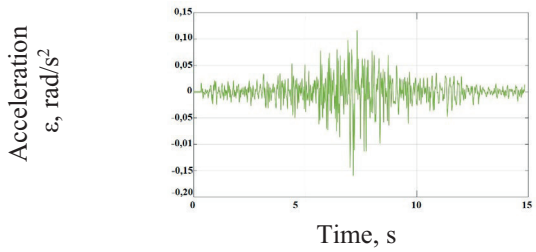

Figure 13. Accelerogram of rotational movement with respect to the Z-axis from the action a_y, a_x

3. RESULTS

Fig.14–16 reflect the results (for calculation from item 2.1) obtained, the comparison of the maximum and minimum values of which are given in Table 1. Fig.17–19 reflect the results (for calculation from item 2.2) obtained, the comparison of the maximum and minimum values of which are given in Table 2. Fig.20–26 reflect the results (for calculation from item 2.3) obtained, the comparison of the maximum and minimum values of which are given in Table 3.

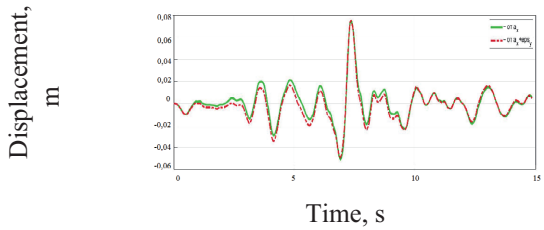

Figure 14. Graphical comparison of displacement values of node No 13071 along the X axis

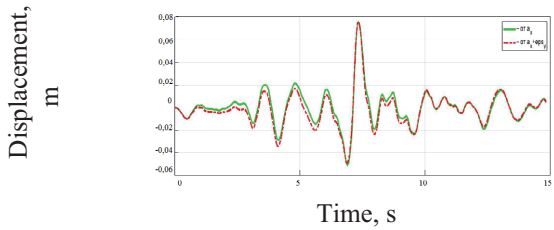

Figure 15. Graphical comparison of displacement values of node No 15383 along the X axis

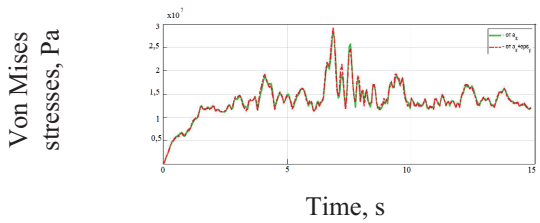

Figure 16. Graphical comparison of von Mises stresses of element B9253

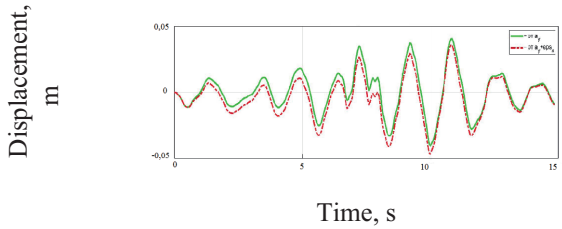

Figure 17. Graphical comparison of displacement values of node No 13071 along the Y axis

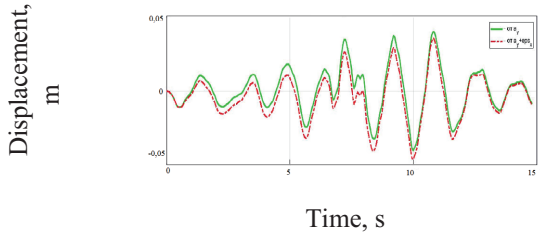

Figure 18. Graphical comparison of displacement values of node No 15383 along the Y axis

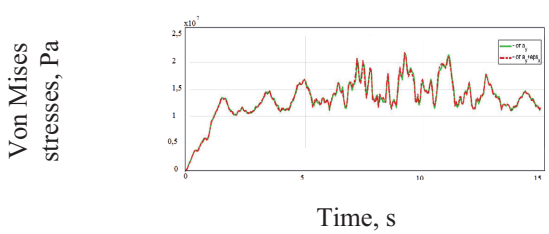

Figure 19. Graphical comparison of von Mises stresses of element B9253

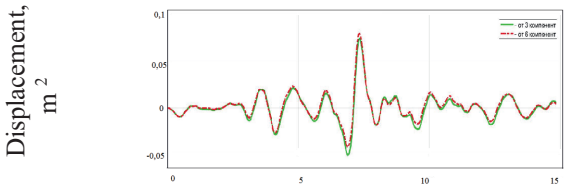

Figure 20. Graphical comparison of displacement values of node No 13071 along the X axis

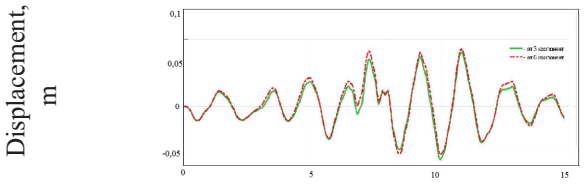

Figure 21. Graphical comparison of displacement values of node No 13071 along the Y axis

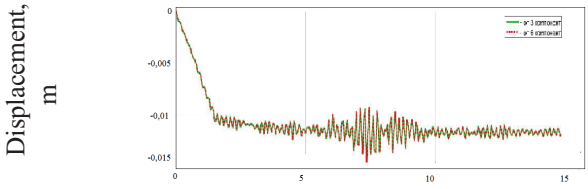

Figure 22. Graphical comparison of displacement values of node No 13071 along the Z axis

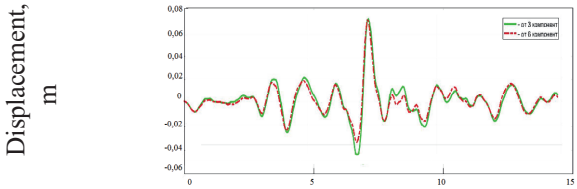

Figure 23. Graphical comparison of displacement values of node No 15383 along the X axis

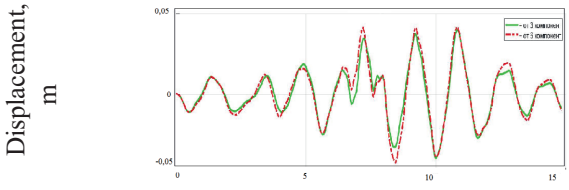

Figure 24. Graphical comparison of displacement values of node No 15383 along the Y axis

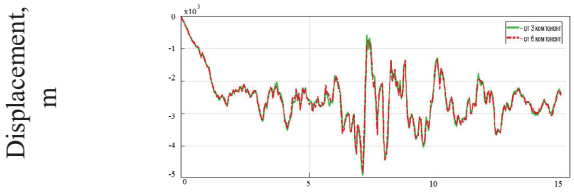

Figure 25. Graphical comparison of displacement values of node No 15383 along the Z axis

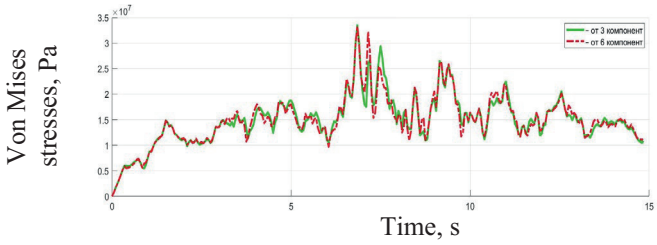

Figure 26. Graphical comparison of von Mises stresses of element B9253

Table 1. Comparison of the maximum and minimum values of displacements and stresses from accounting ε_y

		From the action a_y	From the action $a_y + \varepsilon_x$	Difference
Node 13071	u_y^{max}, m	$4{,}02 \cdot 10^{-2}$	$3{,}56 \cdot 10^{-2}$	11,44 %
	u_y^{min}, m	$-4{,}05 \cdot 10^{-2}$	$-4{,}64 \cdot 10^{-2}$	12,72 %
Node 15383	u_y^{max}, m	$4{,}05 \cdot 10^{-2}$	$3{,}57 \cdot 10^{-2}$	13,45 %
	u_y^{min}, m	$-4{,}04 \cdot 10^{-2}$	$-4{,}64 \cdot 10^{-2}$	12,93 %
Element 9253	σ_M^{max}, Pa	$2{,}17 \cdot 10^{7}$	$2{,}18 \cdot 10^{7}$	0,49 %

Table 2. Comparison of the maximum and minimum values of displacements and stresses from accounting ε_x

		From the action a_x	From the action $a_x + \varepsilon_y$	Difference
Node 13071	u_x^{max}, m	$7{,}48 \cdot 10^{-2}$	$7{,}47 \cdot 10^{-2}$	0,13 %
	u_x^{min}, m	$-5{,}11 \cdot 10^{-2}$	$-4{,}91 \cdot 10^{-2}$	4,07 %
Node 15383	u_x^{max}, m	$7{,}52 \cdot 10^{-2}$	$7{,}51 \cdot 10^{-2}$	0,13 %
	u_x^{min}, m	$-5{,}10 \cdot 10^{-2}$	$-4{,}90 \cdot 10^{-2}$	4,08 %
Element 9253	σ_M^{max}, Pa	$2{,}88 \cdot 10^{7}$	$2{,}91 \cdot 10^{7}$	0,95 %

Table 3. Comparison of the maximum and minimum values of displacements and stresses from taking into account three and six rotational components

		3 components	6 components	Difference
Node 13071	u_x^{max}, m	$7{,}48 \cdot 10^{-2}$	$8{,}01 \cdot 10^{-2}$	7,09 %
	u_x^{min}, m	$-5{,}11 \cdot 10^{-2}$	$-4{,}23 \cdot 10^{-2}$	20,80 %
	u_y^{max}, m	$4{,}02 \cdot 10^{-2}$	$4{,}28 \cdot 10^{-2}$	6,07 %
	u_y^{min}, m	$-4{,}05 \cdot 10^{-2}$	$-3{,}66 \cdot 10^{-2}$	10,66 %
	u_z^{max}, m	$-9{,}27 \cdot 10^{-4}$	$-9{,}28 \cdot 10^{-4}$	0,11 %
	u_z^{min}, m	$-1{,}47 \cdot 10^{-2}$	$-1{,}48 \cdot 10^{-2}$	0,67 %
Node 15383	u_x^{max}, m	$7{,}49 \cdot 10^{-2}$	$7{,}37 \cdot 10^{-2}$	1,63 %
	u_x^{min}, m	$-5{,}14 \cdot 10^{-2}$	$-3{,}76 \cdot 10^{-2}$	26,7 %
	u_y^{max}, m	$3{,}98 \cdot 10^{-2}$	$4{,}15 \cdot 10^{-2}$	4,09 %
	u_y^{min}, m	$-4{,}02 \cdot 10^{-2}$	$-4{,}27 \cdot 10^{-2}$	5,85 %
	u_z^{max}, m	$-5{,}82 \cdot 10^{-4}$	$-7{,}58 \cdot 10^{-4}$	23,22 %
	u_z^{min}, m	$-4{,}88 \cdot 10^{-3}$	$-4{,}80 \cdot 10^{-3}$	1,67 %
Element 9253	σ_M^{max}, Pa	$3{,}35 \cdot 10^{7}$	$3{,}33 \cdot 10^{7}$	0,60 %

4. CONCLUSION

For the buildings considered in the work of a relatively simple geometric shape that are not related to structures of increased number of storeys, taking into account the rotational components of the seismic effect leads to a decrease in the horizontal displacements of the upper mark to 27%, an increase in vertical displacements to 23% and an increase in stresses by 0.6%.

The results of the study are agreement with similar works [1-4] and allow us to conclude that the influence of the rotational components on the stress-strain state of the building under study is insignificant.

The calculation for a monolithic reinforced concrete 8-floor building, taking into account the rotational components of the seismic effect, was carried out in the LS-DYNA software and according to the data obtained in Fig. 14–26 and Tables 1–3, we can conclude that for buildings of relatively simple geometric shape that are not related to structures of increased number of storeys, with significant plan symmetry, when calculating the seismic effect, it is possible to neglect the effect of the rotational component, since they do not suffer from such dangerous phenomena as swinging about two horizontal axes or twisting relative to the vertical one, and the effect of rotational components on such structures does not make a tangible contribution to the stress-strain state.

However, this does not mean that the same conclusion can be drawn for high-rise buildings and

structures of complex geometric shapes, significant asymmetry and developed in plan. Thus, further work on the study of the spatial work of buildings involves a detailed study based on modern calculation methods, which should ensure the required reliability and safety of building structures designed in seismic regions.

REFERENCES

1. **Yu.P. Nazarov and E.V. Poznyak.** Foundations, foundations and soil mechanics, 6, pp. 32-36 (2015).
2. **Yu. P. Nazarov,** Development of methods for calculating structures as spatial systems for seismic impact: Doctor of Science thesis (TsNIISK named after Kucherenko), p. 452 (1999).
3. **Yu.P. Nazarov,** Analytical foundations for calculating structures for seismic effects, (Moscow: Nauka), p. 468 (2010).
4. **Yu.P. Nazarov,** Design models of seismic impacts (Science) p. 414 (2012).
5. **N. Newmark**, Torsion in symmetrical building (Engineering, Santiago) pp 19 – 32 (2004).
6. **N. Newmark N. and E. Rosenblueth,** Fundamentals of Earthquake (New York : Prentice-Hall), p. 640 (1971).
7. **N. M. Newmark**, Journal of the Engineering Mechanics Division, 3, pp. 67-94. (1959).
8. **Lee V.W., Trifunac M. D**. Torsional accelerograms (Soil. Dyn. Earthq.) pp. 132-139 (1985).
9. **Trifunac M. D.** A note on rotational components of earthquake motions on ground surface for incident body waves // Soil Dynamics and Earthquake Engineering. – 1982. – Vol. 1, № 1. – P. 11-19.
10. **O.V. Mkrtychev. and A.A. Reshetov,** Seismic Loads in the Calculation of Buildings and Structures (Moscow: ASV publishing house), p.140 (2017).
11. **O.V. Mkrtychev and G.A. Jinchvelashvili,** Problems of accounting for nonlinearities in the theory of seismic stability (theory and misconceptions), (Moscow: ASV publishing house, 2014), p. 192
12. **De La Llera J.C., Chopra A.K**., Earthquake Engineering and Structural Dynamics, Vol. 23, pp. 1003-1022 (1994).
13. **O.V. Mkrtychev and E.M. Lokhova,** IOP Conf. Ser.: Mater. Sci. Eng. 1015 012038 (2021).
14. **Thomson W. T**. Theory of vibration with applications 4th edition (New Jersey.: Prentice-Hall), p. 143 (1993).
15. **E.V. Poznyak** Development of methods of the wave theory of seismic stability of building structures: Doctor of Science thesis (TsNIISK named after Kucherenko), p. 281 (2018).
16. **Basu D., Whittaker A.,** Journal of Engineering Mechanics, 138,9., pp. 1141–1156 (2012).
17. **Luco J.E.** Earthquake Engineering and Structural Dynamics, 4, pp. 207–219, (1976)
18. **O. Yu Eshchenko and V. A. Demchenko**, Assessment of the seismic resistance of buildings and structures (Krasnodar: KubGAU), p. 91 (2019).

СПИСОК ЛИТЕРАТУРЫ

1. **Назаров Ю.П., Е.В. Позняк**. Оценка ротационных компонент сейсмического движения грунта // Основания, фундаменты и механика грунтов, №6, с. 32-36 (2015).
2. **Назаров Ю.П.** Разработка методов расчёта сооружений как пространственных систем на сейсмическое воздействие (ЦНИИСК им. Кучеренко), с. 452 (1999).
3. **Назаров Ю.П.** Аналитические основы расчета сооружений на сейсмические воздействия, (М.: Наука), с. 468 (2010).
4. **Назаров Ю.П**. Расчётные модели сейсмических воздействий (М.: Наука) с. 414 (2012).
5. **N. Newmark,** Torsion in symmetrical building (Engineering, Santiago) pp 19 – 32 (2004).

6. **N. Newmark N. and E. Rosenblueth**, Fundamentals of Earthquake (New York: Pren-tice-Hall), p. 640 (1971).
7. **N. M. Newmark**, Journal of the Engineering Mechanics Division, 3, pp. 67-94. (1959).
8. **Lee V.W., Trifunac M. D**. Torsional accelerograms (Soil. Dyn. Earthq.) pp. 132-139 (1985).
9. **Trifunac M. D.** A note on rotational components of earthquake motions on ground sur-face for incident body waves // Soil Dynamics and Earthquake Engineering. – 1982. – Vol. 1, № 1. – P. 11-19.
10. **Мкртычев О.В., Решетов А.А.** Сейсмические нагрузки при расчете зданий и сооружений (Москва, АСВ), p.140 (2017).
11. **Мкртычев О.В., Джинчвелашвили Г.А**. Проблемы учета нелинейностей в теории сейсмостойкости, (М. : МГСУ), с. 192 (2014).
12. **De La Llera J.C., Chopra A.K.,** Earthquake Engineering and Structural Dynamics, Vol. 23, pp. 1003-1022 (1994).
13. **O.V. Mkrtychev and E.M. Lokhova**, IOP Conf. Ser.: Mater. Sci. Eng. 1015 012038 (2021).
14. **Thomson W. T.** Theory of vibration with applications 4th edition (New Jersey.: Prentice-Hall), p. 143 (1993).
15. **Позняк Е. В.** Развитие методов волновой теории сейсмостойкости строительных конструкций (ЦНИИСК им. Кучеренко), с. 281 (2018).
16. **Basu D., Whittaker A.,** Journal of Engineering Mechanics, 138,9., pp. 1141–1156 (2012).
17. **Luco J.E.** Earthquake Engineering and Structural Dynamics, 4, pp. 207–219, (1976).
18. **Ещенко О.Ю., Демченко В.А.** Оценка сейсмостойкости зданий и сооружений 4-е издание (Краснодар, КубГау), с. 91 (2019).

Reshetov Andrey Alexandrovich, Candidate of Technical Sciences, engineer of the Research Center "Reliability and Seismic Resistance of Structures" Moscow State University of Civil Engineering (National Research University). 129337, Russia, Moscow, Yaroslavskoe shosse, 26. E-mail: andrew331@bk.ru.

Lokhova Ekaterina Mikhailovna, postgraduate student of the National Research Moscow State University of Civil Engineering, engineer of the Research Center "Reliability and Seismic Resistance of Structures", National Research University "Moscow State University of Civil Engineering" (NRU MGSU). 129337, Russia, Moscow, Yaroslavskoe shosse, 26. E-mail: elm97@mail.ru.

Решетов Андрей Александрович, кандидат техничеких наук, инженер Научно-исследовательского центра «Надежность и сейсмостойкость сооружений» (НИЦ НиСС), Национального исследовательского университета «Московский государственный строительный университет» (НИУ МГСУ). 129337, Россия, г. Москва, Ярославское шоссе, д. 26. E-mail: andrew331@bk.ru.

Лохова Екатерина Михайловна, аспирант Национального исследовательского Московского государственного строительного унивеситета, инженер Научно-исследовательского центра «Надежность и сейсмостойкость сооружений» (НИЦ НиСС), Национального исследовательского университета «Московский государственный строительный университет» (НИУ МГСУ). 129337, Россия, г. Москва, Ярославское шоссе, д. 26. E-mail: elm97@mail.ru.

DOI:10.22337/2587-9618-2022-18-1-92-98

CALCULATIONS OF 3D ANISOTROPIC MEMBRANE STRUCTURES UNDER VARIOUS CONDITIONS OF FIXING

Anatoly I. Bedov [1], Ruslan F. Vagapov [2], Azat I. Gabitov [2], Alexander S. Salov [2]

[1] National Research Moscow State University of Civil Engineering, Moscow, RUSSIA
[2] Ufa State Petroleum Technological University, Ufa, RUSSIA

Abstract: A unified approach in solving equilibrium problems of standard cells of membrane structures made of various absolutely flexible materials, including anisotropic (orthotropic) materials is presented in this paper. The objects of study are rectangular membranes under various conditions of fixing and/or supporting. The problems were considered in a geometrically nonlinear formulation, with the deformations and the squares of the rotation angles thereunder being considered to be comparable with each other, but small compared to unity. A resolving system of differential equations in partial derivatives written in displacements is obtained therewith. These equations combining with the presented boundary conditions are numerical models of a number of fragments of real membrane structures. The closed nonlinear system of equations was integrated using the discrete braking method. Therewith both longitudinal and transverse vibrations of anisotropic masses were analyzed using a conditional dynamic model to select the initial values of the displacements. The problem of equilibrium of a square isotropic membrane with a free boundary under a uniformly distributed load is presented as an example. The resulting graphs and tables show the distribution of forces and displacements. They may be used for calculating membrane structures. The developed technique may be applied to those values of the initial parameters under which the calculations have not yet been made.

Keywords: membranes, membrane structures, geometrically nonlinear formulation, dimensionless form of resolving equations, compliant contour, free boundary, absolutely rigid fixing, peculiar points, method of undetermined reduction factors, discrete braking method, uniaxial state of stress zone, displacement equation, dynamic models, anisotropic masses.

РАСЧЕТЫ ПРОСТРАНСТВЕННЫХ АНИЗОТРОПНЫХ МЕМБРАННЫХ КОНСТРУКЦИЙ ПРИ РАЗЛИЧНЫХ УСЛОВИЯХ ЗАКРЕПЛЕНИЯ

А.И. Бедов [1], Р.Ф. Вагапов [2], А.И. Габитов [2], А.С. Салов [2]

[1] Национальный исследовательский Московский государственный строительный университет, Москва, РОССИЯ
[2] Уфимский государственный нефтяной технический университет, Уфа, РОССИЯ

Аннотация: В работе в геометрически нелинейной постановке сформулирован единый подход к решению задач равновесия типовых ячеек мембранных конструкций из различных, абсолютно гибких, в том числе и анизотропных (ортотропных) материалов. Объектами исследования являются прямоугольные мембраны при различных условиях закрепления и/или подкрепления. Задачи рассматривались в геометрически нелинейной постановке, согласно которой деформации и квадраты углов поворота считаются соизмеримыми между собой, но малыми по сравнению с единицей. При этом получена разрешающая система дифференциальных уравнений в частных производных, записанная в перемещениях. Эти уравнения в комбинации с представленными краевыми условиями являются численными моделями ряда фрагментов реальных мембранных конструкций. Замкнутая нелинейная система уравнений интегрировалась с использованием метода дискретных торможений. При этом для выбора начальных значений смещений с помощью условной динамической модели анализировались продольные и поперечные колебания анизотропных масс. В качестве примера представлена задача равновесия квадратной изотропной мембраны со свободным краем под равномерно распределенной нагрузкой. Полученные при этом графики и таблицы показывают распределение усилий и смещений.

Они могут быть использованы при расчетах мембранных конструкций. Для тех значений исходных параметров, при которых вычисления еще не проводились, можно прибегнуть к разработанной методике.

Ключевые слова: мембраны, мембранные конструкции, геометрически нелинейная постановка, безразмерный вид разрешающих уравнений, податливый контур, свободный край, абсолютно жесткое закрепление, особенные точки, метод неопределенных коэффициентов приведения, метод дискретных торможений, складчатая зона, уравнения в перемещениях, динамические модели, анизотропные массы.

INTRODUCTION

Membrane structures widely applied in construction practice are implemented in materials with various properties and structure (metal sheet, polymer films, technical fabrics, etc.). When calculating, such structures are divided into standard cells being the anisotropic membranes either fixed and/or supported on four, three or two sides [6, 8, 13, 14, 16-18].

A vast amount of references [15] is devoted to the solution of equilibrium problems for rectangular membranes fixed along a contour or along two boundaries, with a detailed review thereof being considered herein [2].

This article is devoted to the calculation of rectangular orthotropic membranes with different fixing conditions.

Therewith the load was assumed to be uniformly distributed. The problem is considered in a geometrically nonlinear formulation, whereby the deformations and the squares of the rotation angles are considered to be comparable with each other, but small as compared to unity [1, 3, 4]. The following geometric relations correspond to these conditions:

$$\varepsilon_x = K_u \frac{\partial u}{\partial x} + \left(\frac{1}{2}\right) K_w^2 \left(\frac{\partial w}{\partial x}\right)^2;$$
$$\varepsilon_y = K_v \frac{\partial v}{\partial y} + \left(\frac{1}{2}\right) K_w^2 \left(\frac{\partial w}{\partial y}\right)^2; \quad (1)$$
$$\gamma_{xy} = K_u \frac{\partial u}{\partial y} + K_v \frac{\partial v}{\partial x} + K_w^2 \frac{\partial w}{\partial x}\frac{\partial w}{\partial y}.$$

To give a more convenient dimensionless form to the resolving system and the subsequent solution the method of undetermined reduction factors [5, 6] is used here [5, 6]: $U = K_u au$, $V = K_v av, W = K_\omega aw$, where K_u, K_v, K_w – are unknown yet arbitrary constants, u, v, w – are dimensionless functions proportional to displacements in the direction of the coordinate axes (Fig. 1).

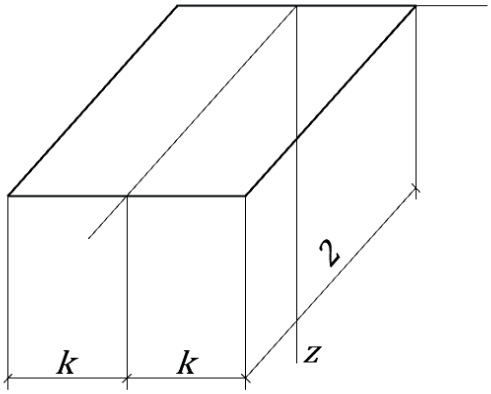

Figure 1. Original membrane scheme

The orthotropy axes of the membrane material were considered to be oriented parallel to the sides thereof, thereby enabling to simplify the physical relations to the form:

$$\varepsilon_x = \lambda n_x - \nu n_y;$$
$$\varepsilon_y = -\nu n_x + n_y, \gamma_{xy} = \frac{n_{xy}}{\mathrm{g}}. \quad (2)$$

Here and elsewhere, a number of dimensionless parameters are used:

$$n_x = N_x/(E_y H);\ n_y = N_y/(E_y H);$$
$$\mu(\lambda - \nu^2) = 1;\ \alpha = \mu\nu + \mathrm{g}; \quad (3)$$
$$\mathrm{g} = G_{xy}/E_y;\ k = b/a.$$

where, N_x, N_y, N_{xy} – are forces; $2a, 2b$ и H – are the plan dimensions and the membrane thickness, respectively; $E_x, E_y, G_{xy}, \nu_{xy}, \nu_{yx}$, – are elastic characteristics of the material.

Let us assume that the structures of the considered membranes and the nature of loading thereof do not allow for uniaxial state of stress zones. Equilibrium equations in a similar formulation are:

$$\frac{\partial n_x}{\partial x}+\frac{\partial n_x}{\partial y}=0;\ \frac{\partial n_{xy}}{\partial x}+\frac{\partial n_y}{\partial y}=0;$$
$$\left[n_x\frac{\partial^2 w}{\partial x^2}+n_y\frac{\partial^2 w}{\partial y^2}+2n_{xy}\frac{\partial^2 w}{\partial x\partial y}\right]K_w^3E_yH=-qa. \quad (4)$$

A resolving system written in displacements may be obtained under (1)-(4) after a number of transformations

$$\mu\frac{\partial^2 u}{\partial x^2}+g\frac{\partial^2 u}{\partial y^2}+\alpha\frac{\partial^2 v}{\partial x\partial y}+\alpha\frac{\partial w}{\partial y}\frac{\partial^2 w}{\partial x\partial y}+$$
$$+\mu\frac{\partial w}{\partial x}\frac{\partial^2 w}{\partial x^2}+g\frac{\partial w}{\partial x}\frac{\partial^2 w}{\partial y^2}=0;$$
$$\alpha\frac{\partial^2 u}{\partial x\partial y}+\mathrm{g}\frac{\partial^2 v}{\partial x^2}+\alpha\frac{\partial w}{\partial x}\frac{\partial^2 w}{\partial x\partial y}+g\frac{\partial w}{\partial y}\frac{\partial^2 w}{\partial x^2}+$$
$$+\mu\lambda\frac{\partial w}{\partial y}\frac{\partial^2 w}{\partial y^2}+\mu\lambda\frac{\partial^2 v}{\partial y^2}=0; \quad (5)$$
$$\mu\left[\frac{\partial u}{\partial x}+\frac{1}{2}\left(\frac{\partial w}{\partial x}\right)^2+\nu\frac{\partial v}{\partial y}+\frac{\nu}{2}\left(\frac{\partial w}{\partial x}\right)^2\right]\frac{\partial^2 w}{\partial x^2}$$
$$+2g\left[\frac{\partial u}{\partial y}+\frac{\partial v}{\partial x}+\frac{\partial w}{\partial x}\frac{\partial w}{\partial y}\right]\frac{\partial^2 w}{\partial x\partial y}$$
$$+\mu\left[\nu\frac{\partial u}{\partial x}++\frac{\nu}{2}\left(\frac{\partial w}{\partial x}\right)^2+\frac{1}{\lambda}\frac{\partial v}{dy}+\frac{1}{2\lambda}\left(\frac{\partial w}{\partial y}\right)^2\right]\frac{\partial^2 w}{\partial y^2}=-1.$$

This system was used in numerical calculations. Equations (10) combined with boundary conditions may be interpreted as a model of a number of standard cells in membrane structures found in actual designing.

Therefore, we had a system of three equations for displacements written in a specific dimensionless form that in the case of an isotropic membrane coincides with the system of resolving equations obtained by M. S. Kornishin [11] for plates, with the cylindrical rigidity thereof tending to zero.

A closed nonlinear system composed of equations (5) and the corresponding boundary conditions (Table 1) was integrated by the discrete braking method [10, 19]. Application of this method in solving 3D problems is known to deal with unacceptable costs of computer time, since the integration step must be small due to stability limitations associated with a large difference in the periods of longitudinal and transverse oscillations, being avoided by introducing anisotropic masses of simpler forms than in paper [12] to the dynamic models. Information on the hypothetical laws of variation of the required functions Q was included to these conditional concepts (Fig. 2), in addition to the weight factors p.

Table 1. Main kinds of boundary conditions

Kind of support contour	Boundary conditions at		
	$x=0$	$y=\kappa$	$x=2$
Absolutely rigid	$u_0=0$	$u_\kappa=0$	$u_2=0$
	$v_0=0$	$v_\kappa=0$	$v_2=0$
	$w_0=0$	$w_\kappa=0$	$w_2=0$
Three sides are absolutely rigid, with the one being free	$u_0=0$	$u_\kappa=0$	$n_{x2}=0$
	$v_0=0$	$v_\kappa=0$	$n_{xy2}=0$
	$w_0=0$	$w_\kappa=0$	$n_{y2}\cdot\frac{\partial^2 w}{\partial y^2}=0$
Flexible, of symmetrical cross section	$\eta_\kappa\cdot\frac{\partial^4 u}{\partial y^4}=n_{x0}+[\Sigma n_{y\kappa}-n_{xy0}]\cdot\frac{\partial^2 u}{\partial y^2}$	$\psi_\kappa\cdot\frac{\partial u}{\partial x}=\Sigma n_{x0}-n_{xy\kappa}$	$\eta_\kappa\cdot\frac{\partial^4 u}{\partial y^4}=n_{x2}+[\Sigma n_{y\kappa}-n_{xy2}]\cdot\frac{\partial^2 u}{\partial y^2}$
	$\psi_\kappa\cdot\frac{\partial v}{\partial y}=\Sigma n_{y\kappa}-n_{xy0}$	$\eta_\kappa\cdot\frac{\partial^4 v}{\partial x^4}=n_{y\kappa}+[\Sigma n_{x0}-n_{xy\kappa}]\cdot\frac{\partial^2 v}{\partial x^2}$	$\psi_\kappa\cdot\frac{\partial v}{\partial y}=\Sigma n_{y\kappa}-n_{xy2}$
	$\eta_\kappa\cdot\frac{\partial^4 w}{\partial y^4}=n_{x0}\cdot\frac{\partial w}{\partial x}+$ $+[\Sigma n_{y\kappa}-n_{xy0}]\cdot\frac{\partial^2 w}{\partial y^2}$	$\eta_\kappa\cdot\frac{\partial^4 w}{\partial x^4}=n_{y\kappa}\cdot\frac{\partial w}{\partial y}+$ $+[\Sigma n_{x0}-n_{xy\kappa}]\cdot\frac{\partial^2 w}{\partial x^2}$	$\eta_\kappa\cdot\frac{\partial^4 w}{\partial y^4}=n_{x2}\cdot\frac{\partial w}{\partial x}+$ $+[\Sigma n_{y\kappa}-n_{xy2}]\cdot\frac{\partial^2 w}{\partial y^2}$

The symbols $\eta_к = \frac{E_к I_к}{E_y}$ u $\psi_к = \frac{E_к A_к}{E_y}$ are used in the table to denote the relative rigidity of the contour for bending and compression. An appropriate combination of the given boundary conditions enables obtaining of a mathematical model of any kind of support for membrane structures [3, 7, 8].

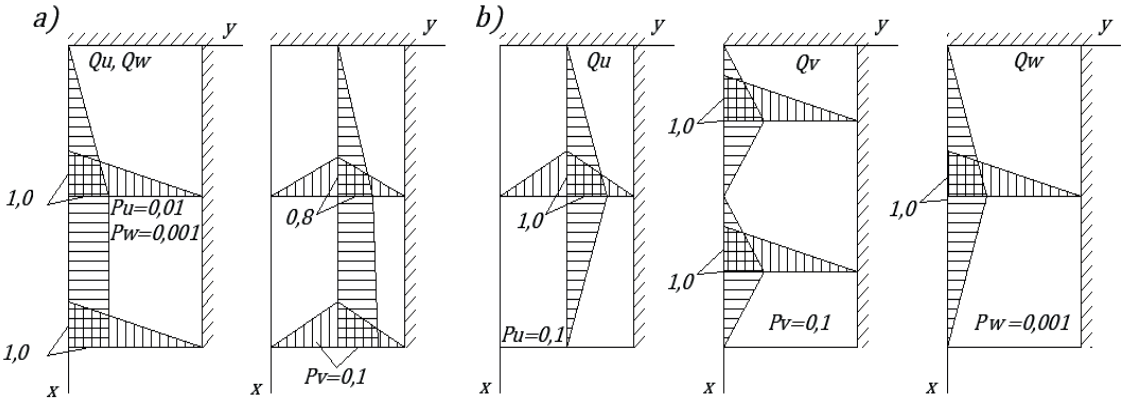

Figure 2. Characteristics of anisotropy of conditional masses of dynamic models

As a result of the numerical solution of the difference analogues of the above equations, the values of the displacement components at all points were obtained. Therewith, central differences with an error of the reminder term of the order of the second degree of strength were used on a square net; extrapolation of the desired functions beyond the contour was made by means of the Lagrange polynomial. The final solutions for displacements may be presented in dimensional form as necessary:

$$U = u\left(\frac{qa}{E_y H}\right)^{\frac{2}{3}} a;\ V = v\left(\frac{qa}{E_y H}\right)^{\frac{2}{3}} a;\qquad W = w\left(\frac{qa}{E_y H}\right)^{\frac{2}{3}} a, \tag{6}$$

with one being able to proceed therefrom to dimensional forces to get a full view of the stress-strain behavior.

The problem of equilibrium of a square isotropic membrane with a free boundary under a uniform load is presented as an example. Half of the membrane only was examined because of the symmetry. Continuous characteristics with reasonable ordinates were received (Fig. 3). In a small neighborhood of the extreme right point of the free boundary, there were jumps of normal n_x, n_y and tangential n_{xy} forces to be explained by ambiguity thereof at this peculiar point. An analysis of the graphs enables conditional division of the area of the deformed membrane in the direction of the x axis into three zones: the first one (in the neighborhood of the y axis) - here all the characteristics behave as in a membrane with four absolutely rigid boundaries; the second one (central part) is a zone where the pattern of the stress-strain behavior is similar to that in the case of a cylindrical bend; the third one (in the neighborhood of the free boundary) - the most of the characteristics have extreme values.

Rectangular membranes with one free boundary were also calculated for various aspect ratios. The free boundary at k > 1.5 was found not to affect the stress state of the membrane in the neighborhood of the opposite rigidly fixed side. Therewith, the stress and strain fields have been slightly changed as compared with a similar membrane rigidly fixed on four sides.

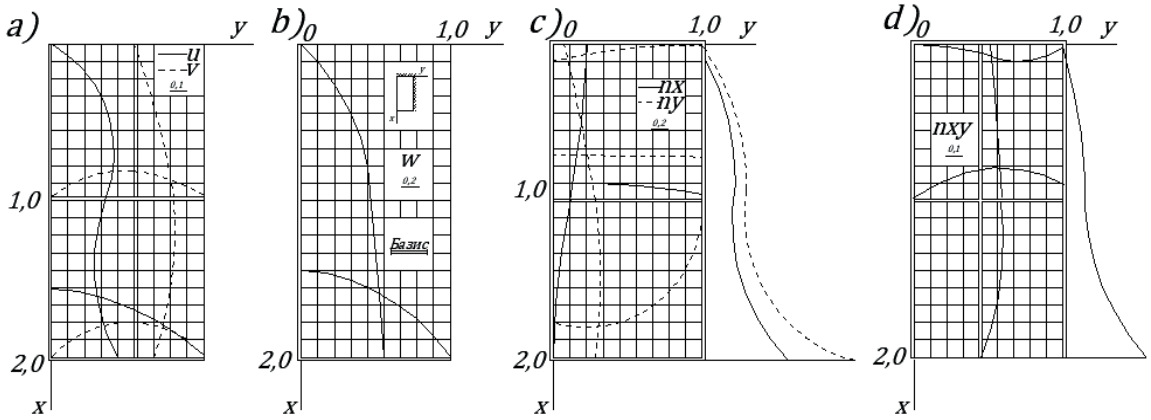

Figure 3. Characteristic functions of deformations in the plane of the membrane (а), displacements in the vertical direction (б), normal components of the stress state (в), and shear components (г)

CONCLUSION

In conclusion we note that the graphs and tables obtained show the nature of the distribution of forces and displacements in membranes for a quite wide range of changes in the main parameters of structures thereof. They may be used in calculations of membrane systems. For the same values of the parameters for which the calculations were not made you may use the developed methodology and the finished program.

ACKNOWLEDGMENTS

The experimental research was partially made at the Research and Educational Center for Innovative Technologies (RECIT) under FSBEI of Higher Education Ufa State Petroleum Technological University. RECIT performs research and testing of a wide range of construction materials and products: cement- and gypsum-based binders, aggregates, concrete, mortars, bricks, masonry blocks, cellular concrete, rebars, under the Certificate for assessment the state of measuring instruments in the laboratory No. TsSM RB.OSI.ST.03022, issued by the Center for Standardization and Metrology of the Republic of Bashkortostan.

REFERENCES

1. **Bedov A., Vagapov R., Gabitov A., Salov A.** // Nonlinear problems of equilibrium for axisymmetric membranes // APEM 2021. IOP Conf. Series: Materials Science and Engineering 11674 (2021) 012009.
2. **Vagapov R.F.** // Review of papers on the theory of membrane calculation // Ufa Petroleum Institute. - Ufa, 1987. - 40 p. Dep. in VNIIIS, 1988, No. 7964.
3. **Vagapov R.F.** Equilibrium of rectangular orthotropic membranes with a free boundary // Structural Analysis. - 1990. - No.1. P.62-65.
4. **Vagapov R.F., Grigoriev A.S., Konovalov M.B., Trushina V.M.** // Problems of equilibrium of membranes and membrane structures // Proceedings of the 14th All-Union Conference on the Theory of Plates and Shells. - Tbilisi, 1987. P. 255-260.
5. **Grigoriev A.S., Trushina V.M., Shadrin V.A.** // Equilibrium of rectangular and round orthotropic membranes at large

deflections // Current problems in Mechanics and Aviation. - M., 1982. - P. 106-113.
6. **Demenev M.G.** Development of coating structures with the application of membrane panels // PhD Tech.Thesis M.: 1990. P.234.
7. **Bedov A.I., Gabitov A.I., Gaisin A.M., Salov A.S., Chernova A.R.** CAD technologies under thermal properties analysis of wall cladding of framed buildings. IOP Conference Series: Materials Science and Engineering: Volume 465, 2018.VII International Symposium Actual Problems of Computational Simulation in Civil Engineering 1–8 July 2018, Novosibirsk, Russian Federation. P.1-8.
8. **Eremeev P.G., Tusnin A.R.** Influence of the eccentric fixing of the membrane to the support contour on the redistribution of forces in the system // Structural Analysis. 1990. - No.1. P. 8-13.
9. **Eremeev P.G.** // 3D thin sheet metal structures of coatings. M: ASV, 2006. P.560.
10. **Kislooky V.N.** // Algorithm for the numerical solution of problems of statics and dynamics of nonlinear systems // Applied Mechanics. - Kyiv, 1966. - Vol. 2. - Issue. 6. P. 87-92.
11. **Kornishin M.S.** // Nonlinear problems of the theory of plates and depressed shells and methods for solution thereof. – M.: Science, 1964. P. 192
12. **Malyi V.I., Dolzhnikov I.L., Alyautdinov M.I., Kulikov V.L.** // Calculation of membrane coatings with a flexible contour // Structural Analysis. – 1981. No. 2. P. 18-22
13. Membrane constructions of buildings and structures: Reference. Under general editorship of V.I. Trofimov and P.G. Eremeeva; Central Research Institute of Building Structures named after V.A. Kucherenko. M.: Stroyizdat, 1990. P.446.
14. **Novikov Yu.N.** // Architectural membrane structures [Electronic resource]: - Access mode: http://www.flexpro.ru / text.htm
15. **Perelmuter A.V., Slivker V.I.** // Calculation models of structures and the possibility of analysis thereof. - M.: DMK Press, 2007. P.600.
16. Pneumatic building structures // Ermolov V.V. et al. - M:. Stroyizdat, 1983. P.439.
17. **Tusnin A.R.** Development of structures for the membrane coating of industrial buildings // PhD Tech. Thesis M.: 1989. P. 219.
18. **Trofimov V.I., Mikulin V.B., Pritsker A.Ya., Reusov V.A., Semyonov V.T.** // Membrane constructions of buildings and structures. Kyiv: Budivelnik, 1986. P.177.
19. **Vinichenko V., Ryazanova V.A., Gabitov A.I., Udalova Y.A., Salov A.S.** Efflorescence processes in exterior wall surface of buildings // Materials Science Forum 968 MSF, 2019. P. 115-121.

Bedov Anatoly Ivanovich, PhD of Engineering, Professor of the Department of Reinforced Concrete and Stone Structures National Research Moscow State University of Civil Engineering; 26, Yaroslavskoe Shosse, Moscow, 129337, Russia; E-mail: gbk@mgsu.ru

Vagapov Ruslan Fanilevich, PhD of Engineering, Assistant Professor of Building Constructions Department Institute of Architecture and Civil Engineering Ufa State Petroleum Technological University; street of Mendeleeva, the house 195, Ufa, 450080, Russia; E-mail: vagapov.rf@gmail.com

Gabitov Azat Ismagilovich, Doctor of Engineering, Professor of Building Constructions Department Institute of Architecture and Civil Engineering Ufa State Petroleum Technological University; street of Mendeleeva, the house 195, Ufa, 450080, Russia; E-mail: azat7@ufanet.ru

Salov Alexander Sergeevich, PhD of Engineering, Assistant Professor of Highways and Structural Engineering Department Institute of Architecture and Civil Engineering Ufa State Petroleum Technological University; street of Mendeleeva, the house 195, Ufa, 450080, Russia; E-mail: salov@list.ru

Бедов Анатолий Иванович, кандидат технических наук, профессор кафедры железобетонных и каменных конструкций Национального исследовательского Московского государственного строительного университета; 129337, Россия, г. Москва, Ярославское шоссе, д. 26; E-mail: gbk@mgsu.ru

Вагапов Руслан Фанилевич, кандидат технических наук, доцент кафедры строительных конструкций Архитектурно-строительного института Уфимского государственного нефтяного технического университета; 450080, Россия, г. Уфа, ул. Менделеева 195; E-mail: vagapov.rf@gmail.com

Габитов Азат Исмагилович, доктор технических наук, профессор кафедры строительных конструкций Архитектурно-строительного института Уфимского государственного нефтяного технического университета; 450080, Россия, г. Уфа, ул. Менделеева 195; E-mail: azat7@ufanet.ru

Салов Александр Сергеевич, кандидат технических наук, доцент кафедры автомобильных дорог и технологии строительного производства Архитектурно-строительного института Уфимского государственного нефтяного технического университета; 450080, Россия, г. Уфа, ул. Менделеева 195; E-mail: salov@list.ru

International Journal for Computational Civil and Structural Engineering, 18(1) 99–108 (2022)

DOI:10.22337/2587-9618-2022-18-1-99-108

ANALYSIS OF THE MOISTURE CONTENT EFFECT ON THE SPECIFIC INDEX AND DAMAGE ACCUMULATION KINETICS IN THE STRUCTURE OF POLYMERIC MATERIALS DURING NATURAL CLIMATIC AGING

Vladimir P. Selyaev, Tatyana A. Nizina, Dmitry R. Nizin, Nadezhda S. Kanaeva

National Research Ogarev Mordovia State University, Saransk, RUSSIA
Russian Academy of Architecture and Building Science Research Institute of Building Physics, Moscow, RUSSIA

Abstract. We present the results analyzing the climatic resistance of epoxy polymers obtained on the basis of a modified Etal-247 resin cured by Etal-45M under the effect of natural climatic factors in a temperate continental climate. The kinetics of damage accumulation in the structure of polymer samples under tensile loads was studied on the basis of the results obtained using the author's method. The essence of the technique was to determine the coordinates of the "critical" points of deformation curves based on the time series fractal analysis methods, recorded with a high readings frequency (0.01 s). To estimate the level of accumulated failures leading to the destruction of samples under tensile loads, we used a parameter defined as the ratio of the number of points with a fractality index less than 0.5 to the total number of points on deformation curves (until reaching the level of "critical" tensile stresses). Time intervals of 0.16 seconds were studied with analyzed area shifted with a step of 0.01 sec. A specific index is proposed that characterizes the accumulated number of damages in the polymer sample structure per unit of its strength. Its achievement leads to the destruction of the composite under study. We have determined the moisture state effect and climatic aging duration on the damage accumulation kinetics in the polymer sample structure under tensile loads.

Keywords: climatic aging, polymers, moisture content, damage accumulation, specific index, fractal analysis.

АНАЛИЗ ВЛИЯНИЯ ВЛАГОСОДЕРЖАНИЯ НА УДЕЛЬНЫЙ ПОКАЗАТЕЛЬ И КИНЕТИКУ НАКОПЛЕНИЯ ПОВРЕЖДЕНИЙ В СТРУКТУРЕ ПОЛИМЕРНЫХ МАТЕРИАЛОВ В ПРОЦЕССЕ НАТУРНОГО КЛИМАТИЧЕСКОГО СТАРЕНИЯ

В.П. Селяев, Т.А. Низина, Д.Р. Низин, Н.С. Канаева

Национальный исследовательский Мордовский государственный университет им. Н.П. Огарёва, г. Саранск, РОССИЯ
Научно-исследовательский институт строительной физики РААСН, г. Москва, РОССИЯ

Аннотация. Представлены результаты анализа климатической стойкости эпоксидных полимеров, получаемых на основе модифицированной смолы Этал-247, отверждаемой Этал-45М, под действием натурных климатических факторов в условиях умеренно-континентального климата. Изучена кинетика накопления повреждений в структуре полимерных образцов под действием растягивающих нагрузок на основе результатов, полученных с помощью авторской методики. Сущность методики заключалась в определении координат «критических» точек кривых деформирования на основе методов фрактального анализа временных рядов, фиксируемых с высокой частотой снятия показаний (0.01 сек.). Для оценки уровня накопленных отказов, приводящих к разрушению образцов под действием растягивающих нагрузок, использовался показатель, определяемый как отношение числа точек с индексом фрактальности, меньшим 0,5, к общему числу точек кривых деформирования (до достижения «критических» уровней растягивающих напряжений). Исследовались временные интервалы продолжительностью 0.16 секунд со смещением

анализируемой области с шагом 0.01 сек. Предложен удельный показатель, характеризующий накопленное число повреждений в структуре полимерных образцов к единице его прочности, достижение которого приводит к разрушению исследуемого композита. Выявлено влияние влажностного состояния и длительности климатического старения на кинетику накопления повреждений в структуре полимерных образцов под действием растягивающих нагрузок.

Ключевые слова: климатическое старение, полимеры, влагосодержание, накопление повреждений, удельный показатель, фрактальный анализ.

1. INTRODUCTION

Polymer materials are widely used almost in all existing industries. By analogy with other materials, the main requirement for polymer-based products and structures is to ensure uninterrupted operation throughout the entire service life. However, the solution to this problem is extremely complicated under the effect of natural climatic factors, as practically all products and structures are exposed to the effect thereof, regardless of their functional purpose. This is due to the high complexity of climatic effects both for analysis and for replication in laboratory conditions with sufficient accuracy and completeness [1 – 6].

Since the complete reproduction of the environment impact in artificial conditions at the moment is not possible due to the insufficient level of instrumental and technical development, the main source of reliable information on the phenomena that arise in the polymer structure during climatic aging are natural climatic studies [7 – 13]. One of these phenomena is the reversibility of changes in the physical and mechanical properties of epoxy polymers, depending on the content of adsorbed moisture. According to the data given in the scientific literature, as well as the author's studies [14 – 16], the spread of strength parameters in the limiting moisture states (moisture saturated and dried) reaches 30% for polymer composites and 50% for unfilled epoxy resin-based polymers. As a result, during the operation of polymer composites, one should take into account both irreversible changes in properties caused by degradation of the surface layers of the product, disordering of filler fibers, photodestruction and chemical transformations of the polymer matrix, as well as reversible changes caused by the processes of sorption and desorption of atmospheric moisture.

The aim of this work is to quantitatively assess the kinetics of damage accumulation in the structure of epoxy polymer samples exposed to natural climatic factors, depending on their duration, the level of applied mechanical impacts, and the polymer material moisture state.

2. METHODS AND MATERIALS

The objects of the study were samples based on Etal-247 resin and Etal-45M hardener by ENPTs EPITAL JSC. Etal-247 is a modified epoxy resin with a mass fraction of epoxy groups of at least 21.4÷22.8% and a Brookfield viscosity at 25 °C in the range of 650÷750 cP. Etal-45M hardener is a mixture of aromatic and aliphatic di- or polyamines modified with salicylic acid.

The samples were subjected to natural exposure on the test stands of the environmental and meteorological monitoring laboratory, construction technologies and examinations of the Ogarev National Research Mordovia State University (Saransk, temperate continental climate). Physicomechanical parameters were determined for samples in a control state, as well as after 67, 151, 306, 531 and 765 days of natural exposure.

The samples were conditioned in accordance with GOST 12423-2013 “Plastics. Conditioning and Testing of Samples”. To establish the effect of the moisture state on the change in the physical and mechanical parameters of epoxy polymers under natural climatic factors, a series of 36 samples exposed in parallel was divided into 3 equal batches tested: immediately after re-

moval from the test site (series "without conditioning"); after moistening to constant weight at a relative humidity of 98±2% ("moisture-saturated" series) and after drying to constant weight at 60 °C ("dried" series) in accordance with GOST R 56762-2015 "Polymer Composites. Method for Determining Moisture Absorption and Equilibrium State".

Mechanical tensile tests of samples (type 2 according to GOST 11262-2017) (ISO 527-2: 2012) "Plastics. Tensile Testing Method") were made using an AGS-X series tensile testing machine with TRAPEZIUM X software. Test temperature was 23±2 °C and relative air humidity of 50±5%. The tensile testing machine clamp movement speed was 2 mm/min.

Quantitative values of accumulated failures are determined on the basis of the author's technique, which allows determining the coordinates of critical points of deformation curves "$\sigma - \varepsilon$" built by methods of fractal analysis [17 – 20]. As "critical" points, we consider the points of the deformation curves for which the $\mu(\sigma, \varepsilon)$ fractality index values calculated over the previous short time intervals using the least coverage method, are less than 0.5. Time intervals of 0.16 seconds were studied with analyzed area shifted with a step equal to 0.01 sec.

To estimate the level of accumulated failures leading to the destruction of samples under tensile loads, we used a parameter defined as the ratio of the number of points with a fractality index less than 0.5 to the total number of points on deformation curves (until reaching the destructing level of tensile stresses)

$$\omega(\sigma, \varepsilon) = \frac{m_{\mu(\sigma,\varepsilon)}}{n_{\mu(\sigma,\varepsilon)}} \cdot 100\%, \qquad (1)$$

where $m_{\mu(\sigma,\varepsilon)}$ is the number of points of the studied series for which the condition $\mu(\sigma, \varepsilon) < 0.5$ is satisfied; $n_{\mu(\sigma,\varepsilon)}$ is the total number of analyzed points.

To take into account the effect of changes in the strength parameters of polymers on the value of accumulated failures (until the sample reaches maximum tensile stresses), we introduce specific index θ defined as [13]

$$\theta = \frac{\omega}{R_s}, \qquad (2)$$

where ω is the relative number of accumulated damages determined according to (1) when the sample reaches the level of maximum tensile stresses [%]; R_s is the tensile strength of polymeric materials [MPa].

3. RESULTS AND DISCUSSION

The change in the sample mass after drying and moistening according to the above modes is shown in Fig. 1. Depending on the moisture state of the samples after being removed from the test stands during drying and moistening to constant weight, a decrease and increase in the weight of the samples by 0.67÷1.35% and 0.88÷1.94%, respectively, is observed. Depending on the duration of natural climatic aging, the range of change in the sample mass ranged (the sum of absolute values of the mass increase and decrease) from 2.09% to 2.73%, and the highest value was recorded for the samples in the control state.

According to the results of the studies, it was established (Fig. 1, 2) that an increase in the moisture content of the control samples from 0.79 to 2.72% (moisture-saturated state) leads to a decrease in the ultimate tensile strength from 37.3 to 26.7 MPa, which corresponds to a residual strength of 71.5% (of the control values in an equilibrium-moisture state). Natural exposure of polymer samples of the studied composition without additional drying and moistening is accompanied by a decrease in strength parameters for the entire exposure time (765 days) by no more than 15%. In this case, the moisture saturation of the samples contributes to an additional decrease in the tensile strength, reaching 24÷35% of the initial value (before the beginning of natural exposure).

The strength parameters of dried samples with the duration of natural climatic exposure not exceed-

ing 306 days, are higher than those for samples not subjected to additional drying. Such restoration of properties is referred to as a reversible change in strength parameters due to the elimination of free moisture. In addition, with an increase in the natural exposure duration, we observed a gradual narrowing of the range of variation of the polymer sample strength parameters in the moisture-saturated and dried states. For time intervals of 531 and 765 days, the difference is only 0.3÷0.65 MPa (Fig. 2, a). At the same time, the tensile strength for samples not subjected to additional conditioning is 15-18% higher than the same parameter in the limiting moisture states. Obviously, for a given natural climatic impact duration, the presence of sorbed moisture in the polymer matrix structure acts as a mechanism that compensates for irreversible changes. At the same time, for the state of samples aged more than 531 days, it is obvious that there is a certain point of optimum moisture content corresponding to the highest ultimate tensile strength value. By analogy with the plasticizing effect of moisture, one can assume a gradual decrease in the contribution of the considered synergistic effect analyzed in [20], from the maximum value at the point corresponding to the moisture-saturated state to zero at the point corresponding to the dried state.

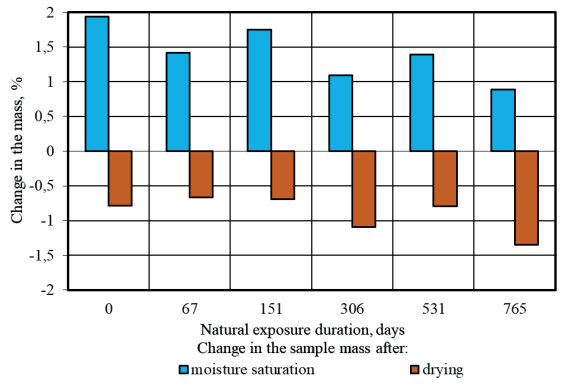

Figure 1. Change in the mass (%)of Etal-247 + Etal-45M polymer samples during their drying and moisture saturation to constant mass

Accumulation curves of failures depending on the level of applied stresses and elongation in tension for control samples in different moisture conditions after natural climatic exposure are shown, respectively, in Fig. 3 and 4. Numerical values of the levels of accumulated failures corresponding to the achievement of the maximum tensile loads by the samples are given in Table 1. It was found that the limiting level of accumulated damage for all types of moisture state of samples of the studied composition varies from 5.06 to 6.05%, increasing in the series: dried (5.06÷5.61%), moisture-saturated (5.23÷6.01%), without additional conditioning (5.53÷6.05%). The analysis results show (Fig. 3, a) that curves of failure rate accumulation depending on the level of applied stress for samples in equilibrium-moisture or dry states are similar. Moisture saturation of the samples leads to a significant (up to two times) acceleration of the process, depending on the level of applied stresses.

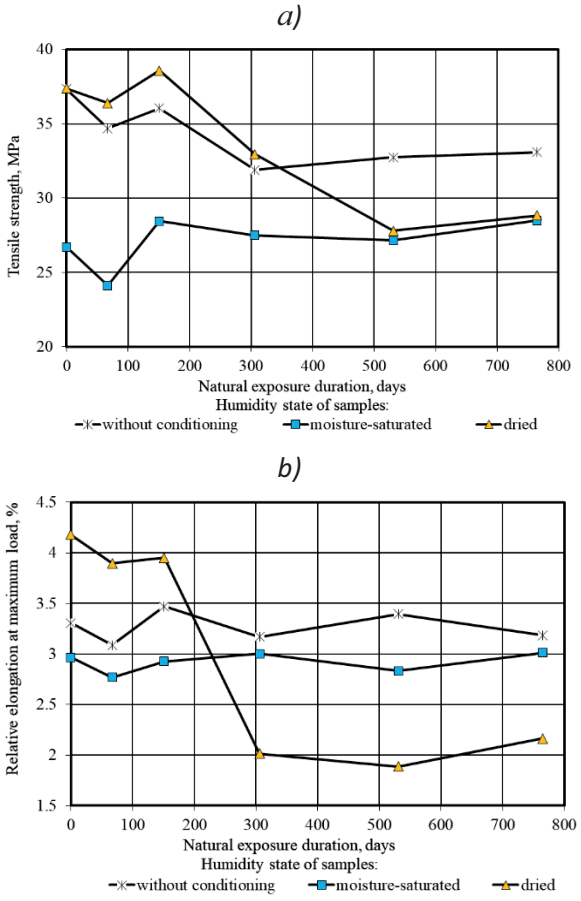

Figure 2. Change in elastic-strength parameters (a – tensile strength; b – relative elongation at maximum load) of polymer samples of the composition Etal-247 + Etal-45M during natural climatic aging in three moisture states (without conditioning, moisture-saturated, dried)

Table 1. Change in the cumulative failure rate of epoxy polymer (Etal-247+Etal-45M) during natural climatic aging in three moisture conditions (without conditioning, moisture-saturated, dried).

Humidity state of samples	Natural exposure duration, days					
	0	67	151	306	531	765
without conditioning	5,69	6,05	5,71	5,76	5,72	5,53
moisture-saturated	6,01	5,61	5,23	5,64	5,50	5,86
dried	5,53	5,61	5,51	5,06	5,43	5,54

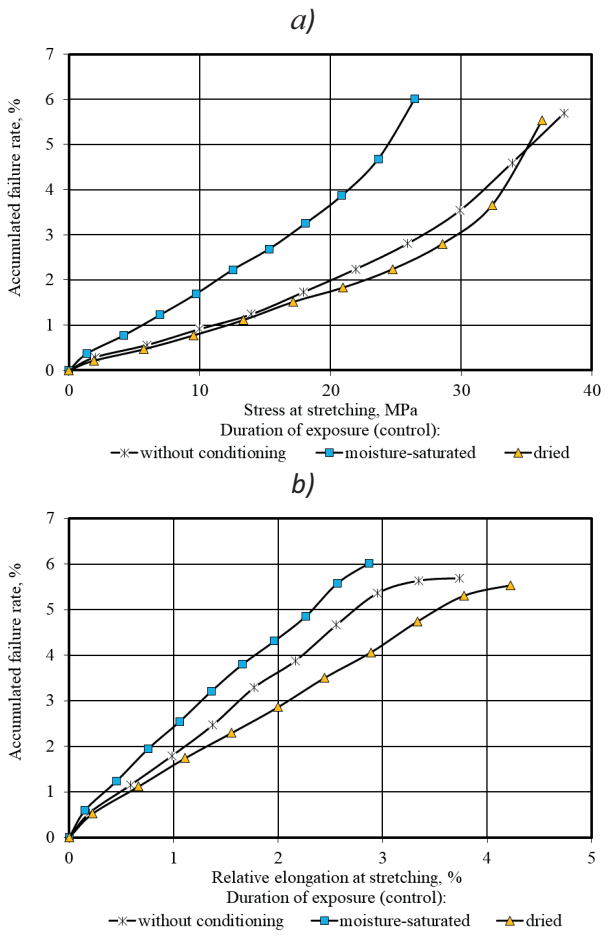

Figure 3. Failure accumulation curves for a series of polymer samples (Etal-247+Etal-45M) in different moisture states depending on the level of applied stresses (a) and relative elongations at stretching (b)

Analysis of changes in the curves for epoxy polymers (Etal-247 + Etal-45M) (Fig. 4) after natural exposure in a temperate continental climate for 765 days indicates that the nature of damage accumulation depending on the level of applied stresses for samples in equilibrium-humidity and moisture-saturated states are similar, especially at levels of tensile stresses not exceeding 40-50% of destructive ones. Moisture saturation of the samples after climatic aging over the entire studied time interval also leads to an acceleration of damage accumulation in comparison with the samples not subjected to additional conditioning. The greatest changes in the damage accumulation kinetics, depending on the natural exposure duration, were recorded for dried samples (Fig. 4, e, f). Thus, an increase in the climatic impact terms of up to 306 days and more leads to a significant acceleration of damage accumulation even at low stresses (Fig. 4, e). At the same time, the shape of the curve “accumulated failure rate –tensile stress” also changes – from concave to close to linear.

An analysis of similar curves for a series of dried samples plotted depending on the level of elongation under tension (Fig. 4, f) also clearly shows the change in the nature of damage accumulation. When physically bound water is removed from the studied epoxy polymer structure exposed to the natural factors site for 306 days or more, brittle fracture of the samples under tensile loads is observed.

The correlation dependence between specific index θ and the ultimate tensile strength of the epoxy polymer (Etal-247 + Etal-45M) in various moisture states (equilibrium-humidity, moisture-saturated and dried) with a sufficiently high reliability ($R^2 = 0.856$) is approximated by an exponential dependence (Fig. 5 , a) of the form

$$\theta = 0.492 \times \exp(-0.031 \times R_s). \quad (3)$$

Approximating the correlation dependence "$\theta - \Delta\varepsilon_s$" (Fig. 5, b) by the equation (without taking into account the data for dried samples after climatic exposure with a duration of 306, 531 and 765 days)

$$\theta = 0.484 \times \exp(-0.296 \times \Delta\varepsilon_s) \quad (4)$$

the reliability drops to 0.684.

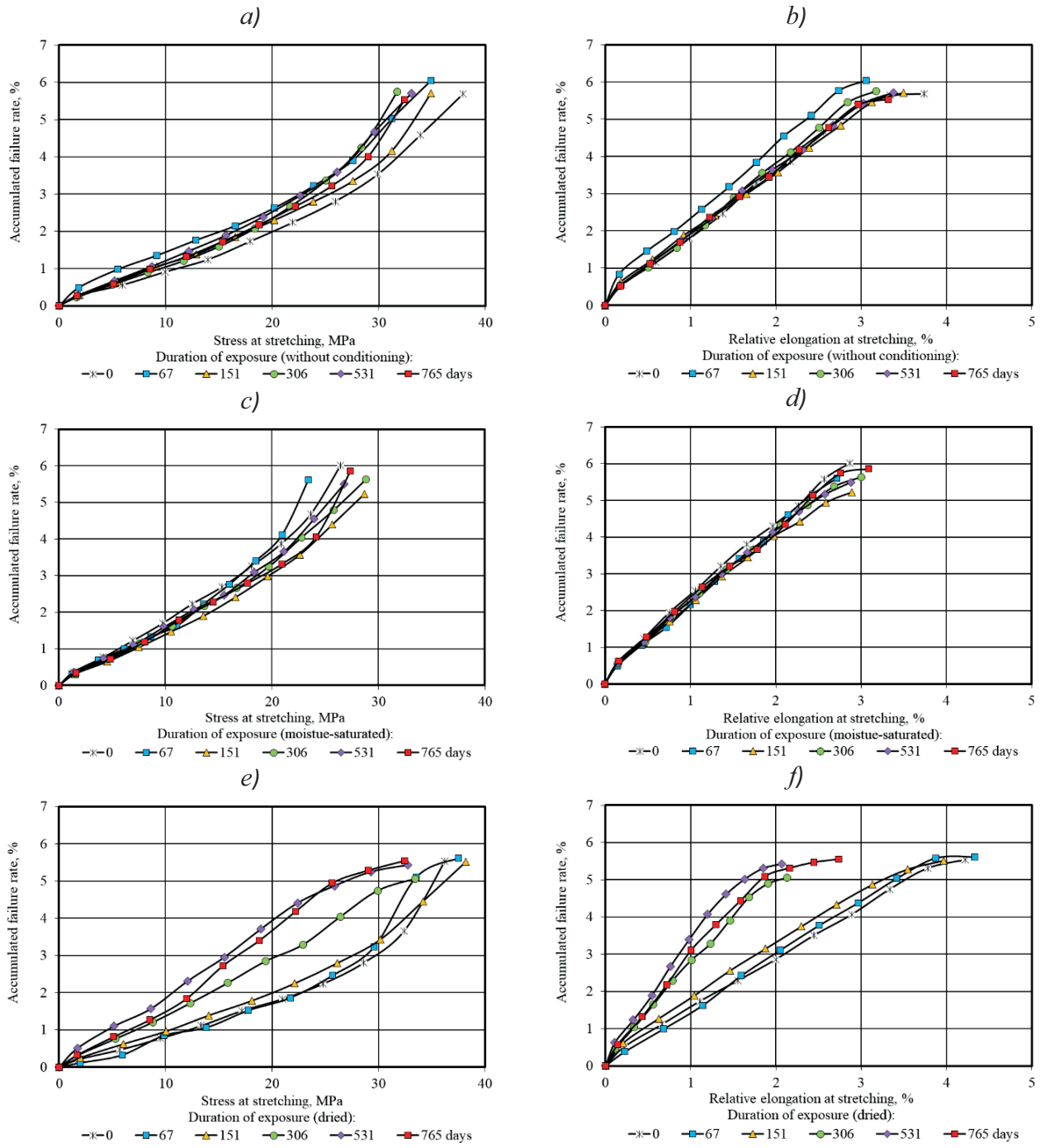

Figure 4. Failure accumulation curves for a series of polymer samples (Etal-247+Etal-45M) during natural aging in different moisture states (a, b – without conditioning; c, d – moisture-saturated; e, f – dried) depending on the level of applied stresses(a, c, e) and relative elongations at stretching (b, d, f)

The possibility of approximating the correlation dependences shown in Fig. 5 (a) by for all series of the studied composition depending on the moisture state of the samples and the duration of natural exposure, confirms the advisability of using specific index θ as a quantitative charac-

teristic of assessing the level of accumulated damage, where its achievement leads to the destruction of polymers. In this case, the analysis of Fig. 5 (b) is an additional confirmation of the change in the mechanism of destruction for samples, with aging duration exceeding 306 days.

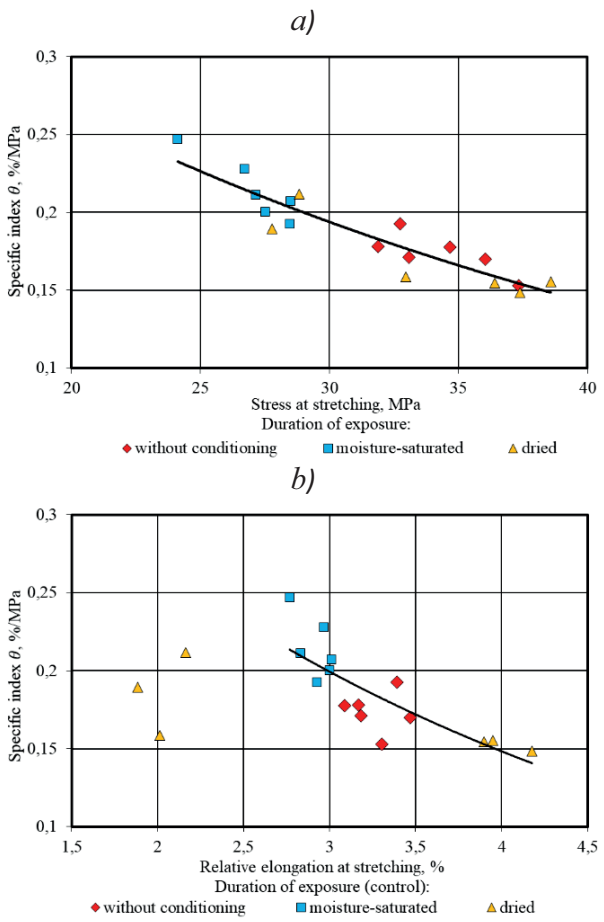

Figure 5. Correlation dependences between the specific index of the number of damages θ and elastic-strength characteristics (a – tensile strength; b – tensile elongation) of an epoxy polymer (Etal-247 + Etal-45M) in different moisture conditions.

4. CONCLUSION

The analysis of the research results showed that the sorbed moisture content is the main source of reversible changes in the elastic-strength parameters of polymer material samples. When the exposure time does not exceed 306 days, the decrease in the ultimate strength of the samples in the moisture-saturated state varies in the range from 16 to 34% of the analogous parameters for the dried samples. An increase in the duration of natural climatic exposure to 531 days and more leads to a change in the nature of the effect of adsorbed moisture on the strength parameters of epoxy polymers (Etal-247 + Etal-45M). In particular, the tensile strength of the samples tested immediately after removing the samples from the test benches (without additional conditioning) is 15-18% higher than the strength parameters in the limiting (moisture-saturated and dried) moisture states.

A sharp decrease in the deformative characteristics of the dried samples was also revealed when the time of natural exposure reached 306 days or more. The climatic effect in the time interval from 151 to 306 days is characterized by a two-fold decrease in the relative elongation during stretching of the dried samples (Fig. 2), which is presumably due to their additional embrittlement due to the removal of sorbed moisture, which in this case plays the role of a compensator for irreversible changes in the polymer matrix structure during natural climatic aging. In this case, a change in the damage accumulation kinetics is also observed depending on the level of applied tensile stresses.

REFERENCES

1. **Collins T.A.** Moisture management and artificial ageing of fibre reinforced epoxy resins // Composite Structures 5. Elsevier applied science. 1989. Pp. 213-239.
2. **Efimov V.A., Kirillov V.N., Dobryanskaya O.A., Nikolaev E.V., Shvedkova A.K.** Methodological issues of conducting full-scale climatic tests of polymer composite materials. Aviacionnye materialy i tekhnologii. 2010. 4(17). Pp. 25–31.
3. **Lettieri M., Frigione M.** Natural and artificial weathering effects on cold-cured epoxy resins // Journal of Applied Polymer

Science, 2011. Vol. 119, Is.3. Pp. 1635-1645.

4. **Marouani S., Curtil L., Hamelin P.** Ageing of carbon/epoxy and carbon/vinyl ester composites used in the reinforcement and/or the repair of civil engineering structures // Composites Part B: Engineering, 2012. Vol. 43, Is. 4. Pp. 2020-2030.
5. **Kablov E.N., Startsev V.O.** Climatic aging of aviation polymer composite materials: I. Influence of significant factors // RUSSIAN METALLURGY (METALLY). 2020. Vol. 4. Pp. 364–372.
6. **Startsev V.O.** Methods for studying the aging of polymer binders. Klei. Germetiki. Tekhnologii. 2020. 9. Pp. 16–26.
7. **Babenko F.I., Gerasimov A.A.** Mechanisms of destruction and strength of structural plastics in cold climates taking into account aging // Nauka I obrazovanie. 2006. 1. Pp. 84–87.
8. **Pavlov N.N.** Starenie plastmass v estestvennyh i iskusstvennyh usloviyah [Aging of plastics in natural and artificial conditions]. Moscow, Khimiya, 1982. 224 p. (in Russian).
9. **Filatov I.S.** Klimaticheskaya ustojchivost' polimernyh materialov [Climatic stability of polymer materials]. Moscow, Nauka, 1983. 214 p. (in Russian).
10. **Kong E.S.-W.** Physical Aging in Epoxy Matrices and Composites // Advances in Polymer Science, 1980. Vol. 80. Pp. 125–171.
11. **Nizin D.R., Nizina T.A., Selyaev V.P., Chernov A.N., Gorenkova A.I.** Natural Climatic Aging of Epoxy Polymers Tasking into Account the Seasonality Impact // Key engineering materials. 2019. Vol. 799. Pp. 159–165.
12. **Startsev O.V., Erofeev V.T., Selyaev V. P.** Klimaticheskie ispytaniya stroitel'nyh materialov [Climatic tests of building materials]. Moscow, ASV, 2017. 558 p. (in Russian).
13. **Nizina T.A., Selyaev V.P., Nizin D.R.** Klimaticheskaya stojkost' epoksidnyh polimerov v umerenno kontinental'nom klimate: monografiya [Climatic stability of epoxy polymers in a temperate continental climate]. Saransk. MRSU, 2020. 188 p. (in Russian).
14. **Startsev V.O., Lebedev M.P., Khrulev K.A., Molokov M.V., Frolov A.S., Nizina T.A.** Effect of outdoor exposure on the moisture diffusion and mechanical properties of epoxy polymers // Polymer testing. 2018. 65. Pp. 281-296.
15. **Startsev V.O., Plotnikov V.I., AntipovYu.V.** Reversible effects of the influence of moisture in determining the mechanical properties of PCM under climatic influences. Trudy VIAM. 2018. 5. Pp. 110–118.
16. **Selyaev V.P., Startsev V.O., Nizina T.A., Startsev O.V., Nizin D.R., Molokov M.V.** Analysis of the plasticizing effect of moisture on the climatic stability of epoxy polymers modified with the aliphatic diluent Etal-1 // Vestnik Privolzhskogo territorial'nogo otdeleniya RAASN, 2018. 21. Pp. 200–205.
17. **Nizina T.A., Nizin D.R., Kanaeva N.S., Kuznetsov N.M., Artamonov D.A.** Applying the Fractal Anaysis Methods for the Study of the Mechanisms of Deformation and Destruction of Polymeric Material Samples Affected by Tensile Stresses // Key engineering materials. 2019. 799. Pp. 217–223.
18. **Nizina T.A., Nizin D.R., Kanaeva N.S.** Statistical Analysis of the Frequency of Damage Accumulation in the Structure of Epoxy Composites Under Tensile Loads // Lecture Notes in Civil Engineering. 2020. Vol. 95. Pp. 1–8.
19. **Nizina T.A., Selyaev V.P., Nizin D.R., Kanaeva N.S.** Quantitative analysis of the kinetics of damage accumulation in the structure of polymer materials under tension // Stroitel'stvo i rekonstrukciya, 2020. 2. Pp. 77–89.
20. **Nizina T.A., Kanaeva N.S., Nizin D.R.** The effect of moisture state on kinetics of

damage accumulation in the structure of epoxy polymer samples under tensile stresses // Lecture Notes in Civil Engineering. 2021. 151. Pp. 208–214.

СПИСОК ЛИТЕРАТУРЫ

1. **Collins T.A.** Moisture management and artificial ageing of fibre reinforced epoxy resins // Composite Structures 5. Elsevier applied science. 1989. – Pp. 213-239.
2. **Ефимов В.А., Кириллов В.Н., Добрянская О.А., Николаев Е.В., Шведкова А.К.** Методические вопросы проведения натурных климатических испытаний полимерных композиционных материалов // Авиационные материалы и технологии. Москва, 2010. № 4(17). – С. 25–31.
3. **Lettieri M., Frigione M.** Natural and artificial weathering effects on cold-cured epoxy resins // Journal of Applied Polymer Science, 2011. Vol. 119, Is.3. – Pp. 1635-1645.
4. **Marouani S., Curtil L., Hamelin P.** Ageing of carbon/epoxy and carbon/vinyl ester composites used in the reinforcement and/or the repair of civil engineering structures // Composites Part B: Engineering, 2012. Vol. 43, Is. 4. – Pp. 2020-2030.
5. **Kablov E.N., Startsev V.O.** Climatic aging of aviation polymer composite materials: I. Influence of significant factors // RUSSIAN METALLURGY (METALLY). 2020. Vol. 4. – Pp. 364–372.
6. **Старцев В.О.** Методы исследования старения полимерных связующих // Елеи. Герметики. Технологии. 2020. №9. – С. 16–26.
7. **Бабенко Ф.И.Ю Герасимов А.А.** Механизмы разрушения и прочность конструкционных пластмасс в холодном климате с учетом старения // Наука и образование. Якутск, 2006. № 1. – С. 84–87.
8. **Павлов Н.Н.** Старение пластмасс в естественных и искусственных условиях. М.: Химия, 1982. – 224 с.
9. **Филатов И.С.** Климатическая устойчивость полимерных материалов. М.: Наука, 1983. – 214 с.
10. **Kong E.S.-W.** Physical Aging in Epoxy Matrices and Composites // Advances in Polymer Science, 1980. Vol. 80. – Pp. 125–171.
11. **Nizin D.R., Nizina T.A., Selyaev V.P., Chernov A.N., Gorenkova A.I.** Natural Climatic Aging of Epoxy Polymers Tasking into Account the Seasonality Impact // Key engineering materials. 2019. Vol. 799. – Pp. 159–165.
12. Климатические испытания строительных материалов / под общ. ред. д-ра техн. наук проф. О.В. Старцева, акад. РААСН д-ра техн. наук проф. В.Т. Ерофеева, акад. РААСН д-ра техн. наук проф. В.П. Селяева. – М.: Издательство АСВ, 2017. – 558 с.
13. **Низина Т.А., Селяев В.П., Низин Д.Р.** Климатическая стойкость эпоксидных полимеров в умеренно континентальном климате: монография. – Саранск: Изд-во Мордов. ун-та, 2020. – 188 с.
14. **Startsev V.O., Lebedev M.P., Khrulev K.A., Molokov M.V., Frolov A.S., Nizina T.A.** Effect of outdoor exposure on the moisture diffusion and mechanical properties of epoxy polymers // Polymer testing. 2018. Т. 65. – С. 281-296.
15. **Старцев В.О., Плотников В.И., Антипов Ю.В.** Обратимые эффекты влияния влаги при определении механических свойств ПКМ при климатических воздействиях // Труды ВИАМ. 2018. №5. – С. 110–118.
16. **Селяев В.П., Старцев В.О., Низина Т.А., Старцев О.В., Низин Д.Р., Молоков М.В.** Анализ пластифицирующего воздействия влаги на климатическую стойкость эпоксидных полимеров, модифицированных алифатическим разбавителем Этал-1 // Вестник Приволжского территориального отделения РААСН. Вып. 21. – Нижний Новгород: ННГАСУ, 2018. – С. 200–205.

17. **Nizina T.A., Nizin D.R., Kanaeva N.S., Kuznetsov N.M., Artamonov D.A.** Applying the Fractal Anaysis Methods for the Study of the Mechanisms of Deformation and Destruction of Polymeric Material Samples Affected by Tensile Stresses // Key engineering materials. 2019. Vol. 799. – Pp. 217–223.
18. **Nizina T.A., Nizin D.R., Kanaeva N.S.** Statistical Analysis of the Frequency of Damage Accumulation in the Structure of Epoxy Composites Under Tensile Loads // Lecture Notes in Civil Engineering. 2020. Vol. 95. – Pp. 1–8.
19. **Низина Т.А., Селяев В.П., Низин Д.Р., Канаева Н.С.** Количественный анализ кинетики накопления повреждений в структуре полимерных материалов при растяжении // Строительство и реконструкция. 2020. №2. – С. 77–89.
20. **Nizina T.A., Kanaeva N.S., Nizin D.R.** The effect of moisture state on kinetics of damage accumulation in the structure of epoxy polymer samples under tensile stresses // Lecture Notes in Civil Engineering. 2021. Vol. 151. – Pp. 208–214.

Vladimir P. Selyaev, Academician of Russian Academy of Architecture and Construction Sciences, Professor, Dr.Sc., Head of department "Building Structures", National Research Ogarev Mordovia State University; Russia, 430005, Saransk, Sovetskaya str., 24; phone +7(834) 247-71-56, e-mail: ntorm80@mail.ru.

Tatyana A. Nizina, Advisor of the Russian Academy of Architecture and Construction Sciences, Professor, Dr.Sc., Professor of department "Building Structures", National Research Ogarev Mordovia State University; Russia, 430005, Saransk, Sovetskaya str., 24; phone +7(917) 993-63-89, e-mail: nizinata@yandex.ru.

Dmitry R. Nizin, Candidate of Technical Sciences, Engineer of the Research Laboratory of Ecological and Meteorological monitoring, construction technologies and expertise, National Research Ogarev Mordovia State University; Russia, 430005, Saransk, Sovetskaya str., 24; phone +7(927) 184-84-22, e-mail: nizindi@yandex.ru.

Nadezhda S. Kanaeva, graduate student of department "Building Structures", National Research Ogarev Mordovia State University; Russia, 430005, Saransk, Sovetskaya str., 24; phone +7((987) 691-96-20, e-mail: aniknadya@yandex.ru.

Селяев Владимир Павлович, академик РААСН, доктор технических наук, профессор, заведующий кафедрой «Строительные конструкции» Национального исследовательского Мордовского государственного университета им. Н.П. Огарёва; Россия, 430005, г. Саранск, ул. Советская, 24; тел.: +7(834) 247-71-56, e-mail: ntorm80@mail.ru.

Низина Татьяна Анатольевна, советник РААСН, доктор технических наук, профессор, профессор кафедры «Строительные конструкции» Национального исследовательского Мордовского государственного университета им. Н.П. Огарёва; Россия, 430005, г. Саранск, ул. Советская, 24; тел.: +7(917) 993-63-89, e-mail: nizinata@yandex.ru.

Низин Дмитрий Рудольфович, кандидат технических наук, инженер научно-исследовательской лаборатории эколого-метеорологического мониторинга, строительных технологий и экспертиз Национального исследовательского Мордовского государственного университета им. Н.П. Огарёва; Россия, 430005, г. Саранск, ул. Советская, 24; тел.: +7(927) 184-84-22, e-mail: nizindi@yandex.ru.

Канаева Надежда Сергеевна, аспирант кафедры «Строительные конструкции» Национального исследовательского Мордовского государственного университета им. Н.П. Огарёва; Россия, 430005, г. Саранск, ул. Советская, 24; тел.: +7(987) 691-96-20, e-mail: aniknadya@yandex.ru.

International Journal for Computational Civil and Structural Engineering, 18(1) 109–118 (2022)

DOI:10.22337/2587-9618-2022-18-1-109-118

ON THE LOSS OF STABILITY AND POSTCRITICAL EQUILIBRIUM OF COMPRESSED THIN-WALLED ANGLE BARS

Gaik A. Manuylov, Sergey B. Kosytsyn, Maxim M. Begichev

Russian University of Transport, Moscow, RUSSIA

Abstract: Angle bars in compression are quite common in building and transport structures. However, the peculiarities of their behavior during the loss of stability and in supercritical equilibrium have not been sufficiently studied even within the limits of elastic deformations. The paper shows solutions for the stability of symmetric and asymmetric rods with an angle profile. The development of post-critical deformations is shown. The features of the behavior of the rods, obeying the hypotheses of V.Z. Vlasov.

Keywords: stability, geometric nonlinearity, finite element method, angle bar, buckling.

О ПОТЕРЕ УСТОЙЧИВОСТИ И ЗАКРИТИЧЕСКОМ РАВНОВЕСИИ СЖАТЫХ ТОНКОСТЕННЫХ СТЕРЖНЕЙ УГОЛКОВОГО ПРОФИЛЯ

Г.А. Мануйлов, С.Б. Косицын, М.М. Бегичев

Российский университет транспорта, г. Москва, РОССИЯ

Аннотация: Стержни уголкового профиля, работающие на сжатие, довольно часто встречаются в строительных и транспортных конструкциях. Однако особенности их поведения при потере устойчивости и в закритическом равновесии изучены недостаточно даже в пределах упругих деформаций. В работе приведены расчеты на устойчивость симметричных и несимметричных стержней с уголковым профилем. Показано развитие послекритических деформаций. Показаны особенности поведения стержней, подчиняющегося гипотезам В.З. Власова.

Ключевые слова: устойчивость, геометрическая нелинейность, метод конечных элементов, стержни уголкового сечения, потеря устойчивости.

Angle bars in compression are quite common in building and transport structures [1-3]. However, the peculiarities of their behavior during the loss of stability and in supercritical equilibrium have not been sufficiently studied even within the limits of elastic deformations. In this case, the choice of the examined model of the beam turns out to be essential [4-8]. There are two options here:

1) The beam is considered as thin-walled, complying with the hypotheses of V.Z. Vlasov [8];

2) The beam is examined without the stiffening hypotheses of Vlasov.

The analysis of its equilibrium states is carried out numerically, using the FEM, taking into account the effects of geometric nonlinearity [9].

Examining the model of a thin-walled Vlasov rod by M. Pignataro and his collaborators [10, 11] using the expansion of the total potential energy up to cubic terms, and investigating the possibility of making the slope angle of the bifurcation curve vanish at the bifurcation point, obtained the necessary conditions for the stability of the supercritical equilibrium of the thin-walled beams in general and of the angle bars, in particular. The authors of this work numerically investigated the angle bars from the M. Pignataro's work (and those close to them in geometry). However, slightly different results were obtained.

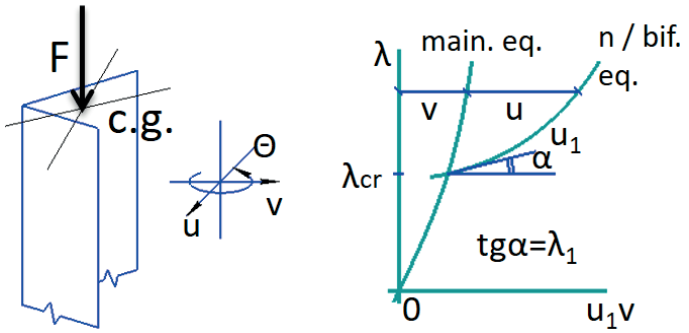

Figure 1. Branching of bifurcation curve

First, let us briefly outline the results of M. Pignataro and his co-workers concerning the stability of the thin-walled Vlasov beams supercritical equilibrium.

We assume that the curve of the "new" post-bifurcation equilibrium $\lambda(v)$ branches off from the curve of the basic equilibrium λ (ν) at the bifurcation point $(\lambda = \lambda_{cr})$ (Fig. 1). The parametric representation of the curves λ (ε) and $u(\varepsilon)$ gives the expansions

$$\lambda(\varepsilon) = \lambda_{cr} + \lambda_1 \varepsilon + \lambda_2 \varepsilon^2/_2 + \cdots$$
$$u(\varepsilon) = 0 + \dot{u}\varepsilon + \ddot{u}/_2 \varepsilon^2 + \cdots$$

The dots above denote derivatives with respect to ε; the subscripts correspond to the derivatives with respect to the coordinate. Here, the proper form $v_1 = \dot{u}$, the potential energy in critical equilibrium is

$$P_c(u) = \frac{1}{2} P_c'' u^2 + \frac{1}{6} P_c''' u^3 + \cdots$$

The slope of the tangent to the curve of the "new" equilibria at the bifurcation point is λ_1 [10, 11] (Fig. 1)

$$\lambda_1 = tg\ \alpha = -P_c''' u_1^3 / 2\dot{P}_c'' u_1^2$$

If $\lambda_1 = tg\ \alpha \neq 0$, then the bifurcation diagram is asymmetric and the supercritical equilibrium is unstable. The system will be sensitive to initial imperfections.

On the contrary, the necessary condition for the stability of the initial post-bifurcation equilibrium is the equality to zero λ_1. This is possible if the cubic term is zero.

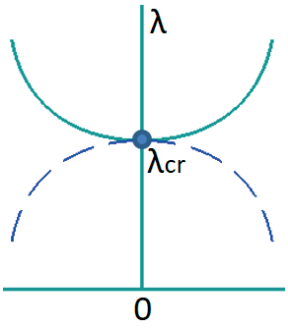

Figure 2. Symmetrical stable bifurcation diagram

$$P_c''' u_1^3 = 0$$

Then the bifurcation diagram is symmetric. It will determine a stable initial post-bifurcation equilibrium if the curvature of the curve of the "new" equilibrium is positive $(\lambda_2 > 0)$, where [10, 11] (Fig. 2)

$$\lambda_2 = \frac{\frac{1}{3} P_c'''' u_1^4 + P_c''' u_1^2 v_2}{\dot{P}_c'' u_1^2}, \text{ (for } \lambda_1 = 0)$$

The expression for the cubic term $\frac{1}{6} P_c''' v_1^3$ according to M. Pignataro is

$$\frac{1}{6} P_c''' u_1^3 = -\frac{1}{2} \int_0^l EI_{c\omega} \theta''(\theta')^2 + EI_{cx} u''(\theta')^2 + EI_{cy} v''(\theta')^2 - EI_x u' v' \theta' + EI_y v' u' \theta' | dz$$

Where $I_{c\omega}$, I_{cx}, I_{cy} are known integral geometric characteristics of a thin-walled beam section.
Under hinged boundary conditions at the ends of the beam, the eigenform is determined by a sinusoid with amplitudes $A_u, A_v \; and \; A_\theta$

$$u_1 = \dot{u}_c = [A_u, A_v, A_\theta] \sin {}^{\pi z}/_{l}$$

The expression for the cubic term in the expansion of the potential energy in terms of these amplitudes of its own form is

$$\frac{1}{6}P_c\dot{u}_1^3 = \frac{\pi^2 E}{3l^2}\left[I_{c\omega}A_\theta^3 + \left(I_{cx}A_v + I_{cy}A_u\right)A_\theta^2 + 2\left(I_y - I_x\right)A_u A_v A_\theta\right]$$

This expression is valid for any asymmetrical section. Therefore, for such a section, the cubic term is not equal to zero

$$\frac{1}{3}P_c'''u_1^3 \neq 0,$$

If $I_{c\omega}A_\theta^3 \neq 0$, or $I_{cx}A_v A_\theta^2 \neq 0$, or $I_{cy}A_u A_\theta^2 \neq 0$, or $\left(I_y - I_x\right)A_u A_v A_\theta \neq 0$. It turns out that a thin-walled hinged Vlasov beam with an asymmetric section has an unstable initial post-bifurcation equilibrium and will be sensitive to initial imperfections.
If the beam has one axis of symmetry and λ_{1c} is the critical buckling load in this plane, and λ_{2c} and λ_{3c} are the critical loads of flexural-torsional loss of stability from the symmetry plane, then for simple (not multiple) critical loads ($\lambda_{1c} \neq \lambda_{2c} \neq \lambda_{3c}$), or if $\lambda_{2c} = \lambda_{3c}$ the cubic term of the expansions is equal to zero ($P_c'''u_1^3 = 0$). Therefore, the bifurcation diagram is symmetric (and, most likely, stable). This is explained by the fact that in this case the amplitudes of the eigenmodes are

$$u_1^a = \begin{bmatrix} 0 \\ A_{v1} \\ 0 \end{bmatrix}, u_2^a = \begin{bmatrix} A_{u2} \\ 0 \\ A_{\theta 2} \end{bmatrix}, u_3^a = \begin{bmatrix} A_{u3} \\ 0 \\ A_{\theta 3} \end{bmatrix}$$

Since due to the symmetry

$$I_{c\omega} = I_{cx} = 0;\; I_{cy} \neq 0$$

then

$$\frac{1}{6}P_c u_1^3 = -\frac{\pi^2 E}{3l^2}\left[I_{cy}A_v A_\theta^2 + 2\left(I_y - I_x\right)A_u A_v A_\theta\right]$$

This expression equals to zero because there is no eigenform with all non-zero components.
If $\lambda_{1c} = \lambda_{2c}$ or $\lambda_{1c} = \lambda_{3c}$, then there is an eigenform u_{*c} in the form of a linear combination of u_{1c} and u_{2c} or u_{1c} and u_{3c}, which can have all components that are not equal to zero

$$u_{*c} = \begin{bmatrix} cA_{u2} \\ A_{v2} \\ cA_{\theta 2} \end{bmatrix} \neq 0$$

Then $\frac{1}{3}P_c'''u_*^3 \neq 0$, and the supercritical equilibrium of a beam with one symmetry plane will be unstable. The bifurcation diagram is asymmetric, and such a beam will be sensitive to initial imperfections.
Finally, if the beam section has two symmetry axes, then

$$I_{c\omega} = I_{cx} = I_{cy} = 0$$

and the expression for the cubic term is greatly simplified

$$\frac{1}{6}P_c'''u_1^3 = \frac{\pi^2 E}{3l^2}\left(I_y - I_x\right)A_u A_v A_\theta$$

The eigenforms' aplitudes

$$u_1^a = \begin{bmatrix} A_u \\ 0 \\ 0 \end{bmatrix}, u_2^a = \begin{bmatrix} 0 \\ A_v \\ 0 \end{bmatrix}, u_3^a = \begin{bmatrix} 0 \\ 0 \\ A_\theta \end{bmatrix}$$

For simple critical loads, it is obvious that $P_c'''u_1^3 = 0$ and the bifurcation diagram is symmetric. If $\lambda_{1c} = \lambda_{2c} = \lambda_{3c}$, then an eigenform with all nonzero components is possible in the form of a linear combination.

$$u_* = c_1 u_{1c} + c_2 u_{2c} + c_3 u_{3c} = \begin{bmatrix} c_1 A_u \\ c_2 A_v \\ c_3 A_\theta \end{bmatrix} \neq 0$$

Then the product $A_u A_v A_\theta \neq 0$. However, multiple critical loads are possible only when $I_y - I_x = 0$. Because of this, $P_c''' u_*^3 = 0$, and the bifurcation diagram of a beam with 2 planes of symmetry is always symmetric. Intuitively, it seems that this diagram also always determines a stable initial supercritical equilibrium. However, a rigorous proof requires considering an explicit expression for the quartic term $\frac{1}{24} P'''' u_1^4$. M. Pignataro and his collaborators gave [10, 11] several examples of imperfection sensitivity curves for beams with a section in the form of an equal- and unequal-angle bar, as well as with a section in the form of a T-beam. The dimensions of the one-axis symmetry beams were selected so that the corresponding critical loads were twofold. Initial imperfections are sinusoidal bends with amplitudes α, β, γ. These imperfections were specified in various combinations (Fig. 3, 4). For a bar with a cross-section in the form of an equal-angle bar, the largest drop in critical loads caused imperfection with the same amplitudes in all directions (Fig. 4).

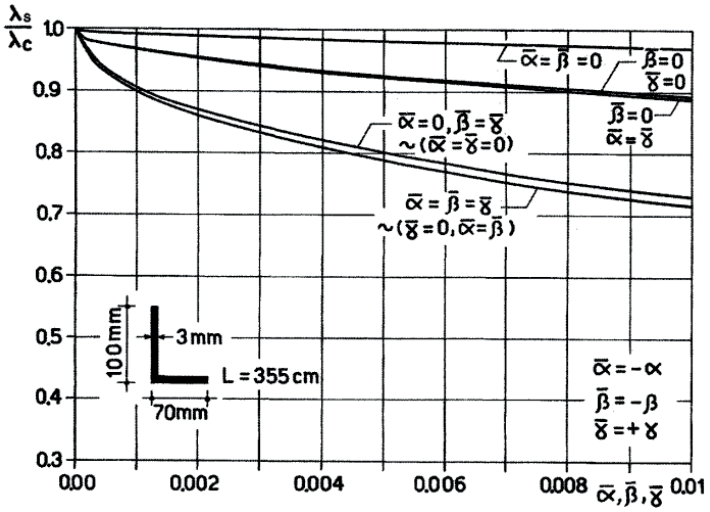

Figure 3. Dependence of critical loads on the values of combinations of initial imperfections for an asymmetric angle bar

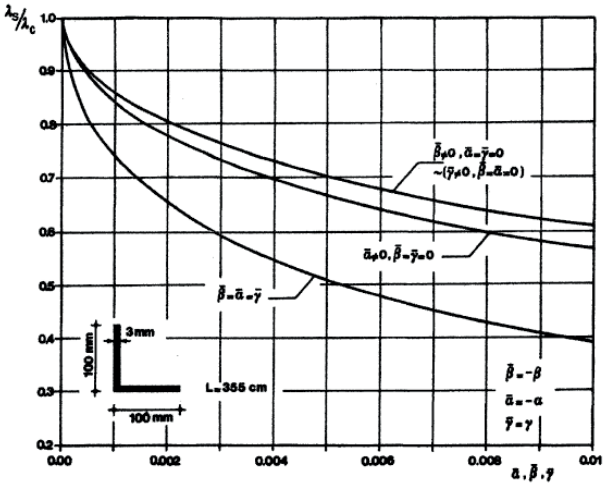

Figure 4. Dependence of critical loads on the values of combinations of initial imperfections for a symmetric angle bar

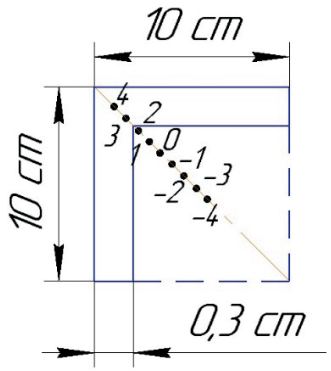

Figure 5. Cross-section of the beam

The authors of this work investigated the post-critical equilibrium of a hinged beam 355 cm long with a cross-section in the form of an equal-angle bar 10 × 10 × 0.3 cm. Such a beam was also studied by M. Pignataro and his collaborators, but as one by Vlasov.

There were rigid plates at the ends of the beam, which did not interfere with the rotation of the end sections. The compressive force was applied along the axis of the section symmetry (at the center of gravity or with an eccentricity of displacement Δe = 0.8 cm, Fig. 5).

Linear calculation of critical loads showed that the first two of them are quite close to each other (torsional $P_{cr\,1} = 39{,}3\ kN$, bending Euler $P_{cr2} = 39{,}34\ kN$). It would seem that the mutual influence of the corresponding closely related forms should significantly affect the beam's post-critical behavior.

However, similar beams of a different length (250 cm, 405 cm) with simple first critical loads showed equilibrium diagrams similar in character to the equilibrium diagram of a beam 355 cm long (Fig. 6). According to this figure, when the compressive load is displaced from the gravity center along the symmetry axis towards the edge (i.e., 1, 2, 3, and 4), the transverse displacements develop smoothly until the limit points are reached. After that, the deformation of "flattening" of the corner section begins to develop on the unstable branch. In this case, the flanges of the corner do not experience additional compression.

When the load shifts towards the center of the geometric contour 10×10 cm (points -1, -2, -3, -4, Fig. 5, 6), then there is a catastrophic drop in the maximum values of the compressive load due to the local loss of stability development of the corner flanges as compressed plates with free edges (Fig. 7).

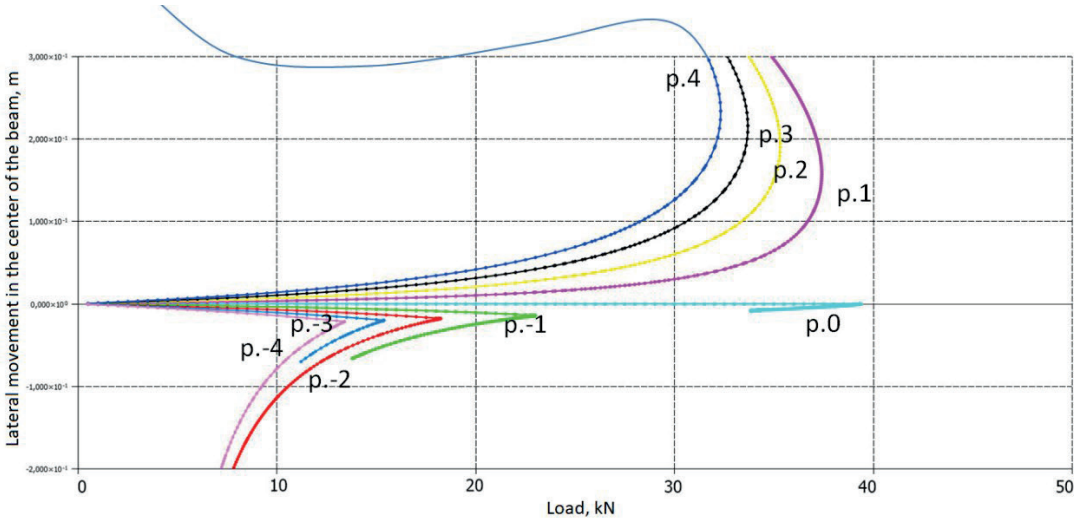

Figure 6. Deformation curves of symmetric angle bar (355 cm) under compression

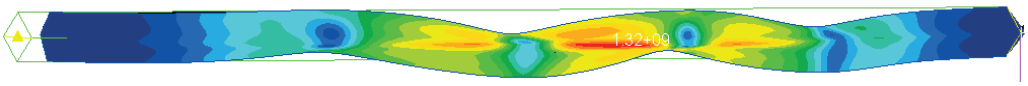

Figure 7. Local loss of stability of flanges

The obtained result testifies to the extreme sensitivity of angle bars to the location of the concentrated compressive load application point. When displaced diagonally from the center of gravity by 3.48 cm, the maximum load decreased by 3 times in comparison with the bifurcation one (Fig. 8). This is an unpleasant result of the buckling shapes interaction for engineers. If a concentrated compressive force must be applied at the point of the angle symmetry axis, then this point can only be between the edge and the angle section gravity center.

For a similar angle bar of a smaller length (l = 250 cm, Fig. 9), the nature of the equilibrium diagrams will not change.

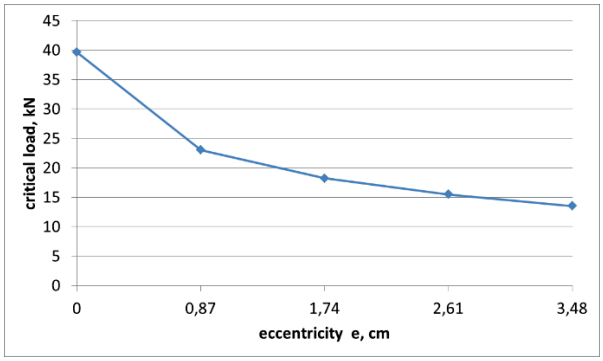

Figure 8. Influence of the location of compressive load application point for a symmetric angle bar on the critical loads

Only the maximum loads at the limiting points increased significantly when the force P was shifted towards the edge. But for such a beam, the critical forces are simple, and they differ significantly from each other.

For a longer rod (l = 405 cm) with the same cross-section, the first critical force $P_{cr\,1} = 31{,}55\ kN$ determines the bending form of buckling, and only the tenth one ($P_{cr\,10} = 37{,}85\ kN$) corresponds to the torsional loss of stability form. The maximum loads at the limiting points decreased slightly. However, the nature of the maximum loads fall at the moment of wave formation did not change ($^{\max P_{-4}}/_{\max P_0} = {}^{12{,}5}/_{32} = 0{,}39$).

Finally, let us consider the effect of transverse diaphragms (from 1 to 15) on the character of the hinged angle bar 355 cm long equilibrium curves (Fig. 10). This was an attempt to successively transform the FE-model of a "usual" beam into a Vlasov beam model with an invariable contour. With three or more diaphragms (Fig. 10), the maximum critical load of the central beam slightly increased (up to ~ 41.5 kN).

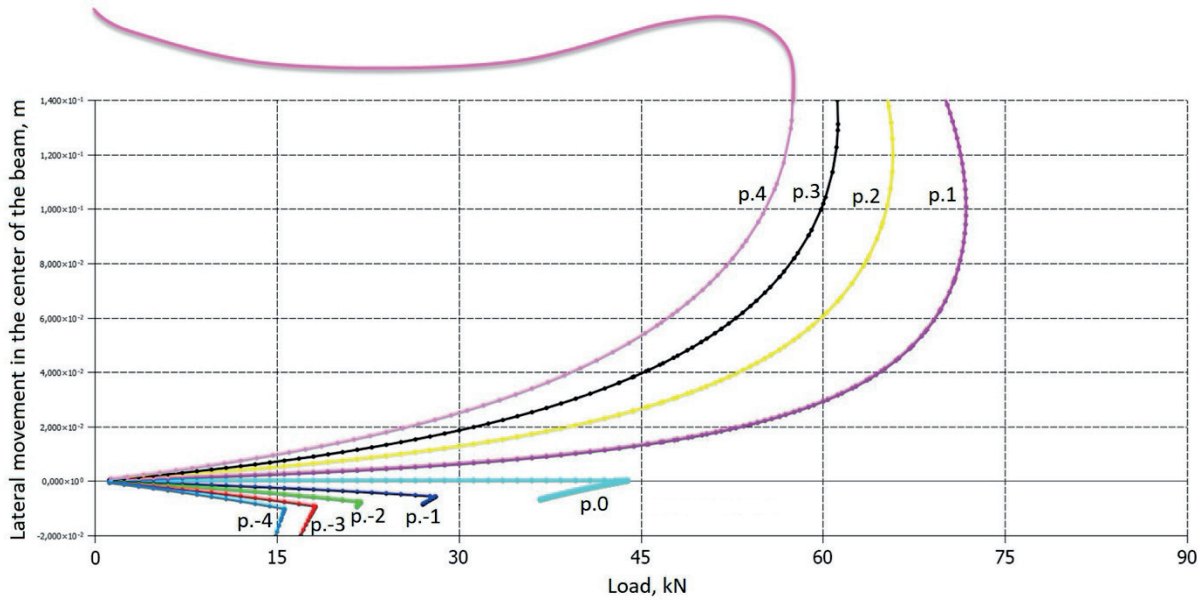

Figure 9. Deformation curves of symmetric angle bar (250 cm) under compression

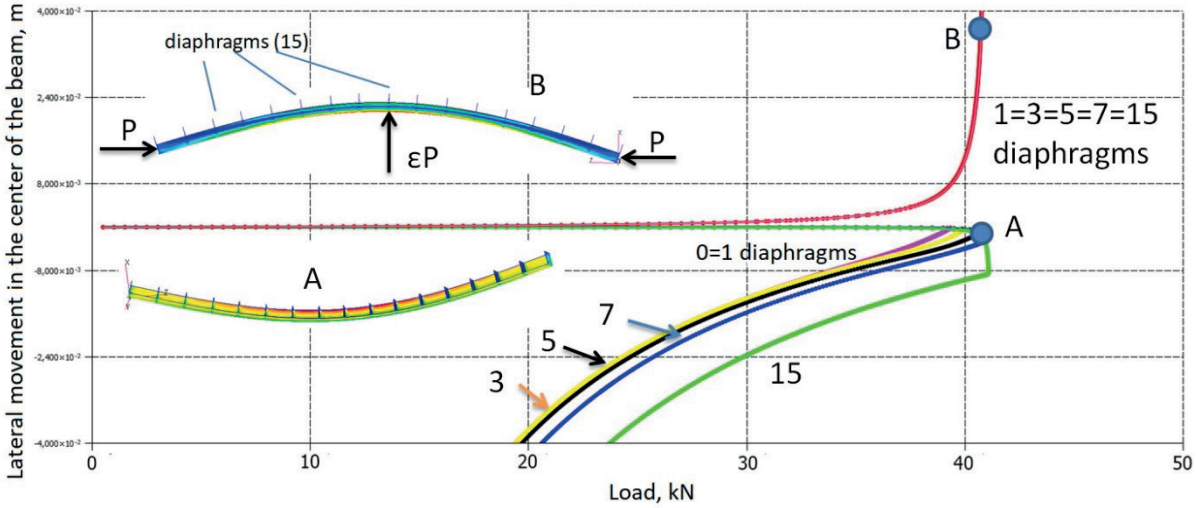

Figure 10. Deformation curves of symmetric angle bar (355 cm) with diaphragms under compression

However, with all the quantitative variants of the diaphragms (3, 5, 7, 15), the supercritical equilibrium was unstable and rather sharply decreasing in terms of the load. A small torque at the end of the beam was used as a disturbance. Under flexural disturbance by a small transverse force εP_1 (Fig. 10, edge in the compressed bending zone), the deflections developed up to the limiting point along the same curve, regardless of the diaphragms number. In general, the examined angle bar with diaphragms has an asymmetric bifurcation diagram.

In contrast, cantilever angle bars have a symmetrical stable post-bifurcation pattern up to the secondary bifurcation load (wave formation) in the flanges.

The Vlasov model of a thin-walled bar does not allow taking into account the actually observed contour deformation and secondary local wave formation in the profile flanges bifurcation effects.

We begin to study the features of equilibrium curves for cantilever beams by considering the stability problem for a steel cantilever beam 200 cm long with a cross-section in the form of a non-equilateral corner 3×2×0.3 cm (Fig. 11).

This rod has the first 5 bending eigenforms.

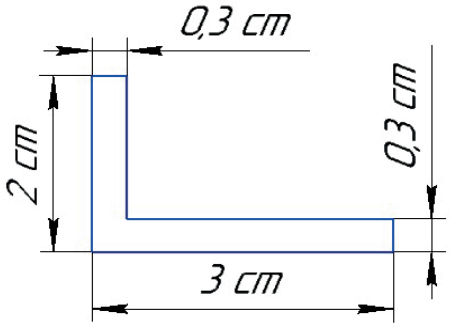

Figure 11. Cross-section of the cantilever beam

The compression load on the beam was applied as uniformly distributed over the end section of the free end. Solutions using the FEM (NASTRAN) showed that the bifurcation diagram of this cantilever rod is symmetric (the red and blue curves are the same and growing up to the moment of wave formation). Consequently, the post-critical equilibrium of such a beam is stable (Fig. 12) up to the moment of local wave formation near the bottom edge from the side of compressed fibers (Fig. 13). This wave formation is provoked by the interaction of two loss of stability forms: general and local. As soon as local wave formation occurs, the load reaches its maximum at the limiting point and then drops sharply (Fig. 12). It is clear that within the Vlasov model framework, the described forms interaction effect cannot be captured.

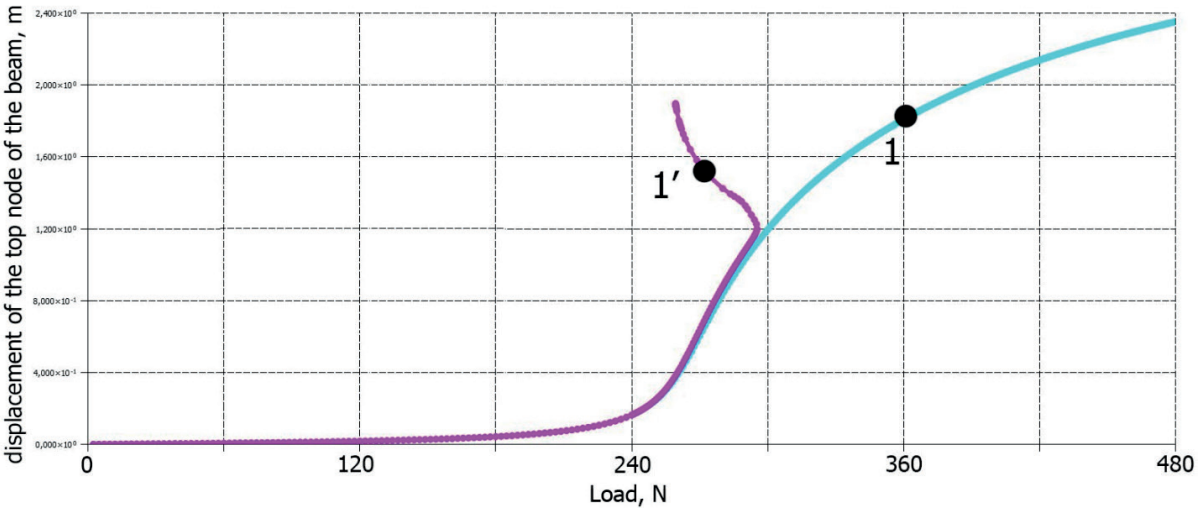

Figure 12. Deformation curves of fixed asymmetric angle bar (200 cm) under compression

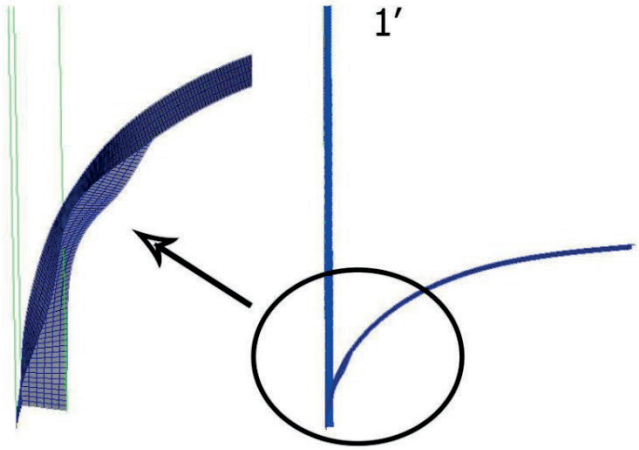

Figure 13. Local wave formation

Interesting results were obtained by the authors when calculating a compressed cantilever angle bar with a symmetric section of 10 ×10 ×0.3 cm and a length of 450 cm. The initial post-bifurcation equilibrium was stable up to the moment of wave formation in compressed flanges (point 1 in Fig. 14). At this point, a wave-like stress distribution is observed. Further, the equilibrium of the corner becomes unstable and the load drops sharply. If the transverse perturbation acts in the opposite direction (the flanges are stretched), then the equilibrium curve reaches the limiting point (point 1') along the same curve as in the first case.

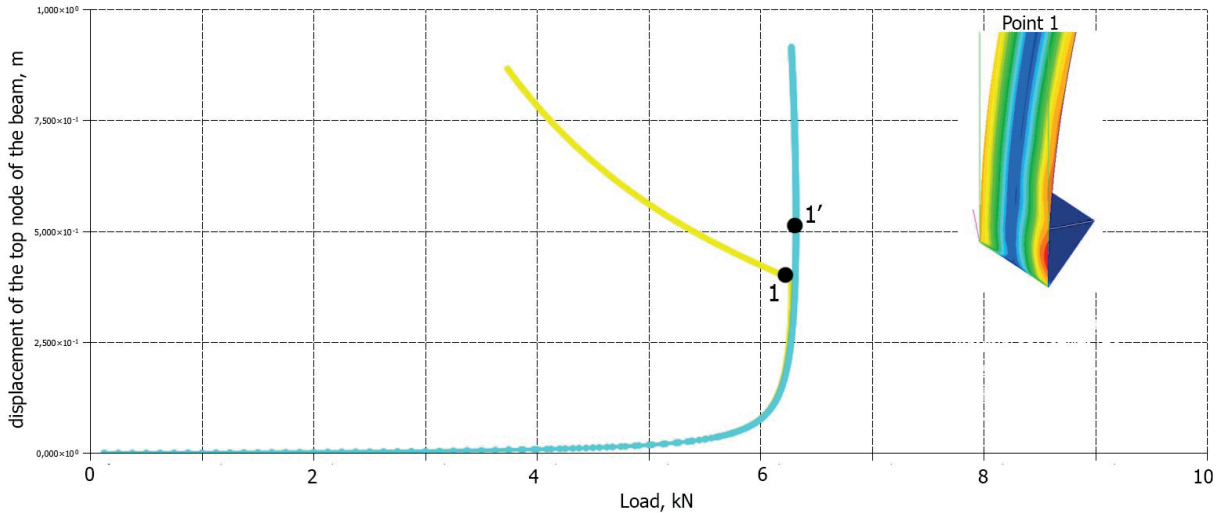

Figure 14. Deformation curves of fixed asymmetric angle bar (450 cm) under compression

Here, as in the previous example, before the waveform load, the bifurcation diagram of such a cantilever beam is symmetrical and stable (as opposed to hinged supported bars with an angle section).

Where does the limit point on the equilibrium curve come from? The authors believe that this is due to the deformation of the contour by the type of "flattening" of the angle bar near the bottom edge, where the greatest supercritical bending moment develops. Flattening reduces the bending stiffness of the corner section.

CONCLUSION

1. Compressed elastic thin-walled angle bars hinged at the ends have an asymmetric bifurcation diagram. Therefore they are extremely sensitive to bending imperfections, which cause additional compression of the zones located near the free edges of the flanges.
2. Compressed elastic cantilever beams of the angle bar have an initial post-bifurcation equilibria diagram that is symmetric and stable up to the load of wave formation in the flanges (secondary bifurcation, which is the result of the interaction of natural forms).
3. The energy theory of post-bifurcation behavior of the Vlasov thin-walled beam, constructed by M. Penyatoro and his collaborators, unfortunately, cannot capture all the important features (local wave formation, “flattening” of sections, etc.) of the development of supercritical stress-strain state of a real thin-walled beam.

REFERENCES

1. **Ilina A.A.** Prochnost i ustoychivost stal'nykh izgibayemykh elementov s regulyarnoy i neregulyarnoy shakhmatnoy perforatsiyey stenki: dissertatsiya na soiskaniye stepeni kand.tekhn. nauk: 05.23.01 / Ilina Anna Aleksandrovna. — Nizhniy Novgorod. – 2004.
2. **Mitchin R.B.** Mestnaya ustoychivost stenki i optimizatsiya stalnoy perforirovannoy balki: dissertatsiya na soiskaniye stepeni kand. tekhn. nauk: 05.23.01 / Mitchin Roman Borisovich. — Lipetsk. – 2003.
3. **Sinelnikov A.S.** Prochnost prosechno-rastyazhnogo profilya pri szhatii: dissertatsiya na soiskaniye stepeni kand. tekhn. nauk: 05.23.01 / Vatin N. I.. — Sankt-Peterburg. – 2015.
4. **Belyy G.I., Astakhov I.B.** Prostranstvennaya ustoychivost elementov konstruktsiy iz stal'nykh kholodnognutykh profiley // Montazhnyye i spetsialnyye raboty v stroitel'stve. — 2006. — Vol. 9.
5. **Tusnin A.R.** Chislennyy raschet konstruktsiy iz tonkostennykh sterzhney otkrytogo profilya.— Moskva: ASV. – 2009. — 143 p
6. **Crisan A., Ungureanu V., Dubina D.** Behaviour of cold-formed steel perforated sections in compression. Part 1— Experimental investigations. ThinWalled Structures. – 2012. – p. 86-96.
7. **Panovko Y.G., Gubanova I.I.** Ustoychivost i kolebaniya uprugikh sistem: Sovremennyye kontseptsii, paradoksy i oshibki. Stability and oscillations of elastic systems: Paradoxes, fallacies, and new concepts (in Russian). 6 ed. Moscow: KomKniga. – 2007.
8. **Vlasov V.Z.** Tonkostennyye uprugiye sterzhni. Moscow: Fizmatgiz. – 1959. – 574 p.
9. **Manuylov G.A., Begichev M.M.** On the reinforcement of thin-walled cold-drawn C-channel beams. IOP Conf. Series: Journal of Physics: Conf. Series. – 1425 (2020) . – 012031
10. **Pignataro M., Rizzi N., Luongo A.** Stability, Bifurcation and Postcritical Behaviour of Elastic Structures (Developments in Civil Engineering 39) Amsterdam: Elsevier Science. – 1991. – 355 p.
11. **Pignataro M., Gioncu V.** Phenomenological And Mathematical

Modelling Of Structural Instabilities. Wien; New York : Springer. – 2005. – 336 p.

СПИСОК ЛИТЕРАТУРЫ

1. **Ильина А.А.** Прочность и устойчивость стальных изгибаемых элементов с регулярной и нерегулярной шахматной перфорацией стенки: диссертация на соискание степени канд.техн. наук: 05.23.01 / Ильина Анна Александровна. — Нижний Новгород. – 2004.
2. **Митчин Р.Б.** Местная устойчивость стенки и оптимизация стальной перфорированной балки: диссертация на соискание степени канд. техн. наук: 05.23.01 / Митчин Роман Борисович. — Липецк. – 2003.
3. **Синельников А.С.** Прочность просечно-растяжного профиля при сжатии: диссертация на соискание степени канд. техн. наук: 05.23.01 / Ватин Н. И.. — Санкт-Петербург. – 2015.
4. **Белый Г.И., Астахов И.Б.** Пространственная устойчивость элементов конструкций из стальных холодногнутых профилей. Монтажные и специальные работы в строительстве. — 2006. — Т. 9.
5. **Туснин А.Р.** Численный расчет конструкций из тонкостенных стержней открытого профиля.— Москва: АСВ. – 2009. — 143 с
6. **Crisan A., Ungureanu V., Dubina D.** Behaviour of cold-formed steel perforated sections in compression. Part 1— Experimental investigations. ThinWalled Structures. – 2012. – p. 86-96.
7. **Пановко Я.Г., Губанова И.И.** Устойчивость и колебания упругих систем. Современные концепции, парадоксы и ошибки. 6-е издание. М.: КомКнига. – 2007.
8. **Власов В.З.** Тонкостенные упругие стержни. М.: Физматгиз. – 1959. – 574 с.
9. **Manuylov G.A., Begichev M.M.** On the reinforcement of thin-walled cold-drawn C-channel beams. IOP Conf. Series: Journal of Physics: Conf. Series. – 1425 (2020) . – 012031
10. **Pignataro M., Rizzi N., Luongo A.** Stability, Bifurcation and Postcritical Behaviour of Elastic Structures (Developments in Civil Engineering 39) Amsterdam: Elsevier Science. – 1991. – 355 p.
11. **Pignataro M., Gioncu V.** Phenomenological And Mathematical Modelling Of Structural Instabilities. Wien; New York : Springer. – 2005. – 336 p.

Gaik A. Manuylov, Ph.D., Associate Professor, Department of Structural Mechanics, Russian University of Transport; 127994, Russia, Moscow, 9b9 Obrazcova Street; phone/fax +7(499)972-49-81.

Sergey B. Kosytsyn, Dr.Sc., Professor, Head of Department of Theoretical Mechanics, Russian University of Transport; 127994, Russia, Moscow, 9b9 Obrazcova Street; phone/fax: +7(499) 978-16- 73; E-mail: kositsyn-s@yandex.ru, kositsyn-s@mail.ru

Maxim M. Begichev, Ph.D., Associate Professor, Department of Theoretical Mechanics, Russian University of Transport; 127994, Russia, Moscow, 9b9 Obrazcova Street; phone/fax: +7(499) 978-16-73; E-mail: noxonius@mail.ru

Мануйлов Гайк Александрович, кандидат технических наук, доцент, доцент кафедры «Строительная механика» Российского университета транспорта; 127994, г. Москва, ул. Образцова, 9, стр. 9; тел./факс +7(499) 972-49-81

Косицын Сергей Борисович, доктор технических наук, профессор, заведующий кафедрой «Теоретическая механика» Российского университета транспорта; 127994, г. Москва, ул. Образцова, 9, стр. 9; тел./факс +7(499) 978-16-73; E-mail: kositsyn-s@yandex.ru, kositsyn-s@mail.ru

Бегичев Максим Михайлович, кандидат технических наук, доцент кафедры «Теоретическая механика» Российского университета транспорта; 127994, г. Москва, ул. Образцова, 9, стр. 9; тел./факс +7(499) 978-16-73; E-mail: noxonius@mail.ru

International Journal for Computational Civil and Structural Engineering, 18(1) 119–128 (2022)

DOI:10.22337/2587-9618-2022-18-1-119-128

NUMERICAL ASSESSMENT OF CARRYING CAPACITY AND ANALYSIS OF PILOT BARETT BEHAVIOR IN GEOLOGICAL CONDITIONS OF VIETNAM

Rashid A. Mangushev [1], Nadezhda S. Nikitina [2], Le Van Chong [1], Ivan Yu. Tereshchenko [3]

[1] Saint-Petersburg State University of Architecture and Civil Engineering, Saint-Petersburg, RUSSIA
[2] National Research Moscow State University of Civil Engineering, Moscow, RUSSIA
[3] LLC "GIPROATOM", Moscow, RUSSIA

Abstract: The article provides an analysis and comparison of the bearing capacity of barrett piles in difficult geological conditions at a construction site in Hanoi - Vietnam based on the results of analytical calculations using various methods. In particular, it contains calculation results according to Building Code of Russian Federation SP 24.13330.2011 "Pile foundations" [1], by numerical modeling of the pile operation under load using the PLAXIS 3D and MIDAS GTS NX software package, based on the results of field tests with piles (static load method). It is noted that the bearing capacity of bored piles and barret piles, according to the results of full-scale static tests with a limiting settlement of 40 mm, is in good agreement with the numerical solution (with the adopted soil model Hardening Soil (HS)) and with the calculation by the analytical method according to the strength characteristics of the soil base

Keywords: pile-barrett, settlement-load dependence, bearing capacity, FEM, analytical solution, mathematical modeling

ЧИСЛЕННАЯ ОЦЕНКА И АНАЛИЗ РАБОТЫ НЕСУЩЕЙ СПОСОБНОСТИ СВАЙ-БАРЕТТ В ИНЖЕНЕРНО-ГЕОЛОГИЧЕСКИХ УСЛОВИЯХ ВЬЕТНАМА

Р.А. Мангушев [1], Н.С. Никитина [2], Ле Ван Чонг [1], И.Ю. Терещенко [3]

[1] Санкт-Петербургский государственный архитектурно-строительный университет (СПбГАСУ), г. Санкт-Петербург, РОССИЯ
[2] Национальный исследовательский Московский государственный строительный университет (НИУ МГСУ), г. Москва, РОССИЯ
[3] ООО "ГИПРОАТОМ", г. Москва, РОССИЯ

Аннотация: В статье приводится анализ и сопоставление несущей способности свай-баретт в сложных инженерно-геологических условиях на строительной площадке в г.Ханоя - Вьетнам по результатам аналитических расчетов по различным методикам, в частности, по СП 24.13330.2011 «Свайные фундаменты» [1], путем численного моделирования работы сваи под нагрузкой с использованием программного комплекса PLAXIS 3D и MIDAS GTS NX, по результатам полевых испытаний сваями (метод статических нагрузок). Отмечено, что несущая способность буронабивных свай и свай-баррет по результатам натурных статических испытаний при ограничении предельной осадки 40 мм, хорошо согласуется с численным решением (с принятой моделью грунта Hardening Soil (HS)) и с расчетом аналитическим методом по прочностным характеристикам грунтового основания.

Ключевые слова: свая-баретта, зависимость осадка-нагрузка, несущая способность, МКЭ,аналитическое решение, математическое моделирование

INTRODUCTION

Currently, high-rise buildings are being actively erected in large metropolitan areas of the world [4]. At the same time, the constructive safety of these structures is largely ensured by a reliable foundation, including during construction on soft soils [14]. The choice of the type of foundation is a very important stage, and it is made at the design stage on the basis of geological survey documents. The foundation structure requires a significant part of the cost of a high-rise structure.

Features of geotechnical conditions define special requirements for the design of zero cycle structures for such facilities [5]. In this regard, barrett piles are increasingly used as deep foundations, which can perceive significant longitudinal and transverse forces due to the increased bearing capacity both in material and in soil compared to alternative types of pile foundations [6].

To calculate the bearing capacity of bored piles on the ground and before testing the piles with a static load, one should assign the main structural parameters of the underground structure and apply various calculation methods of analytical and numerical calculations for limit states [4] at the stage of preliminary design of pile foundations.

In this regard, it is important to carry out a comparative analysis of the results of numerical modeling of the interaction of the bearing capacity of barrett piles in soft soils using various soil models (MC and HS) in the PLAXIS 3D, MIDAS GTS NX software systems and analytical calculations in accordance with the results of field tests [one].

Many scientists have dealt with the design and operation of barrett foundations, including in conditions of soft soils [8–13]. At the same time, it should be taken into account that a special approach is required to calculate the bearing capacity of piles, taking into account the stress-strain state of the enclosing soil mass [9,13,14].

Such a comparative analysis was carried out during the construction of a high-rise building with a developed underground part in the city of Hanoi, Vietnam where, as foundations, barrettes with a section of 800x2800 mm and a length of 37 meters were designed.

MATERIALS AND METHODS

According to the results of geological surveys, the explored depth of the foundation at the construction site in Hanoi - Vietnam has a depth of 61 m and consists of 9 soil layers. Physicomechanical and strength characteristics of soils are shown in Table 1.

Table 1. Physical and mechanical properties of soils

Layer Number	Soil	h, m	γ, kN/m^3	I_L	e	φ, degree	c, kPa	E, MPa
1	Bulk packed soil	1.6	16.00	-	-	-	-	-
2	Fluid clay	16.1	17.00	1.408	1.246	6.30	7.00	1.50
3	Fine sand	5.1	19.00	0.350	0.771	30.00	-	13.5
4	Fluid-plastic clay	10.2	17.20	0.811	1.171	18.00	9.10	15.0
5	Fine sand	3.0	19.20	0.350	0.746	30.00	-	13.5
6	Soft-plastic loam	3.4	17.80	0.695	1.002	7.40	9.60	5.00
7	Fine sand	1.0	19.10	0.035	0.755	30.00	-	13.5
8	Fluid-plastic loam	4.8	17.50	0.930	1.082	8.00	9.50	3.00
9	Gravel and pebble soil	>15.8	20.10	0.300	0.524	38.00	2.00	50.0

The barrette pile operates under indentation load within a depth of 37.00 m, from an elevation of -14.90 m to -51.90 m.

In accordance with Russian standards [1], the bearing capacity of hanging piles is determined depending on the physical and mechanical properties of the foundation soil and the depth of the pile. In accordance with paragraph 7.2.6 [1] it is presented in the following general form:

$$F_d = f(I_L, e, D, L), \qquad (1)$$

where I_L is a soil flow rate;
e is soil porosity coefficient;
D is pile trunk diameter, m;
L is pile-laying depth in the ground, m

The correct choice of the base soil model and its input parameters is of particular importance [7] In numerical geotechnical modeling.

We performed mathematical modeling of the test step by step in several stages:

1. Formation of the initial stress-strain state of the soil mass;
2. Development of the foundation pit;
3. Arrangement of barret piles;
4. Loading of the barrette (see Fig. 1).

A gradual application of a vertical indentation load to the experimental barrette was carried out by 2500 kN at each stage.

Mathematical modeling of changes in the stress-strain state of the soil mass in the process of virtual testing of the experimental barrette pile was carried out using the geotechnical software PLAXIS 3D and MIDAS GTS NX in a spatial setting.

The software package implements several soil models, in particular: Mohr-Coulomb model (MC, Coulomb-Mohr model), Soft Soil Model (soft soil model), Hardening Soil Model (hardening soil model), Soft Soil Creep (soft soil model with taking into account creep), Hardening Soil with Small Strain (model of hardening soil taking into account the stiffness of small deformations), Modified Cam-clay (modified model of Cam-clay, MCC), etc.

It is known that each of these models has its own advantages and disadvantages. In more detail, we considered two models most often used in geotechnical design:

- ideal-elastoplastic model Mohr-Coulomb;
- Elastoplastic model of the hardening soil Hardening Soil.

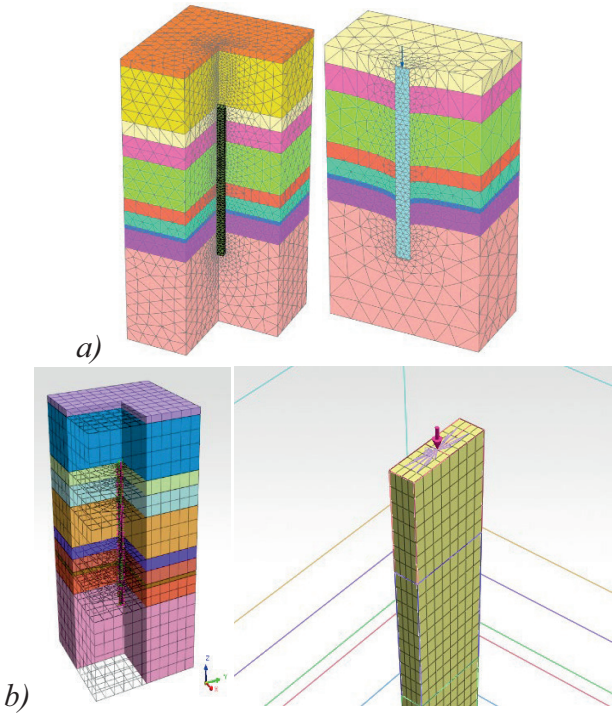

Figure 1. FE model:
a) PLAXIS 3D; b) MIDAS GTS NX

After assigning the parameters of the pile foundation, full-scale tests with the vertical static load of a single barrette with a section of 800x2800 mm and a length of 37 meters were made and carried out at the construction site. The tests were carried out in accordance with Standard of Rusian Federation GOST 20276-2012 [3] using hydraulic jacks using the Top-Down method up to a maximum load of N = 30 MN.

TEST RESULTS AND COMPARISON

Based on the results of full-scale tests, we construct graphs of the dependence of settlement on

time for each stage of the load [14]. The condition of the maximum settlement of the pile head under a load of 40 mm is achieved at a vertical load $F_{d,site}$ = 27500 kN (see Fig. 2). This value is taken as the bearing capacity of the barrette on the ground.

Analytical calculations have shown the value of the total bearing capacity of this barrette equal to $F_{d,calc1}$ = 27285 kN. At the same time, 77% fell on the heel of the pile and only 23% on the side surface.

Considering the significant thickness of weak soils with a low modulus of deformation within the barrett trunk, we note that the pile settlement under load will play a significant role in the formation of its overall bearing capacity. Therefore, it was decided to limit the bearing capacity on the ground by the maximum settlement of a single pile, equal to 40 mm, similar to field and numerical tests in accordance with the provisions of the Russian Geotechnical Construction Standard [2].

The deformed model diagram and vertical displacements at an intermediate stage of testing (at P = 20,000 kN) for various soil models are shown in Figures 3-4.

Table 2 presents the results of determining the bearing capacity of a barrette on the ground by analytical and numerical methods in comparison with the results of field tests.

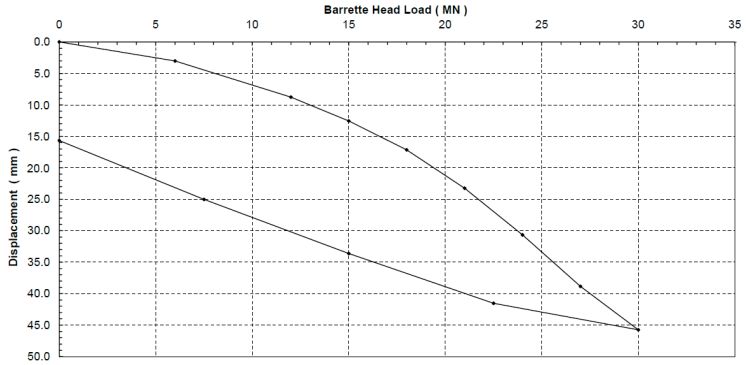

Figure 2. Results of full-scale static tests of barrette piles

a) *b)*

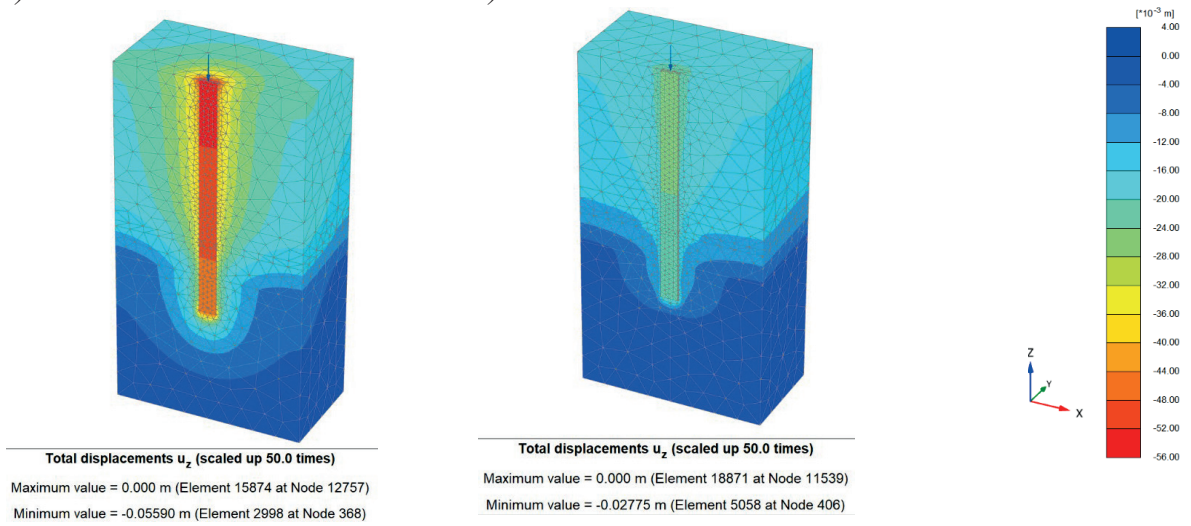

Figure 3. Deformed state and vertical displacements of the FE model in PLAXIS 3D: a) Mohr-Coulomb; b) Hardening Soil

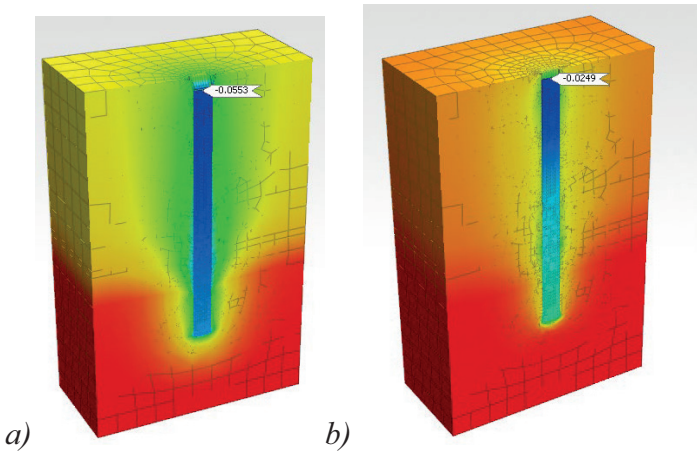

Figure 5. Deformed state and vertical displacements of the FE model in MIDAS GTS NX: a) Mohr-Coulomb; b) Hardening Soil

Table 2. Bearing capacity of pile-barrets by various methods

	Methodology for calculating the bearing capacity of piles on the ground	Bearing capacity of the pile on the ground, kN
	Field test results, $F_{d,site}$	27500
	Analytical classical method [1], $F_{d,calc1}$	27285 (-1%)
Considering unloading	PLAXIS 3D software for Hardening Soil, $F_{d1,HS}$	23700 (-13,8%)
	MIDAS GTS NX software for Hardening Soil, $F_{d2,HS}$	23600 (-14%)
Taking into account unloading	PLAXIS 3D software for Mohr-Coulomb, $F_{d1,MC}$	14500 (-47%)
	MIDAS GTS NX software for Mohr-Coulomb, $F_{d2,MC}$	16440 (-40%)

The combined load-settlement graph for the various considered methods for determining the bearing capacity of the barrette is shown in Figure 5.

Thus, the results of field tests of the bearing capacity of barrette piles with a section of 800×2800 mm and a length of 37 m in comparison with the results of numerical and analytical calculations using various programs showed the following:

• for 13.8 - 14.0%, the results of field tests turned out to be higher than the bearing capacity of the piles than in the numerical modeling in PLAXIS 3D and MIDAS GTS NX programs using the HS model;

• for 40.0 - 47.0%, the results of field tests turned out to be higher than the bearing capacity of piles in numerical modeling in PLAXIS 3D and MIDAS GTS NX programs using the MC model;

• 1.0% higher than the bearing capacity of piles, calculated from the results of analytical methods using tabular soil resistance [1].

It is clearly seen from the given example that the results of mathematical modeling of testing a barrette in a deep pit differ significantly from the graphs of barrett displacement under static load when using different soil models (MC and HS). This discrepancy can be explained by the fact that after the development of the bottom of the pit, part of the subgrade is unloaded and the subsequent loading is performed along the secondary branch "unloading-reloading", which is not taken into account in the MC model.

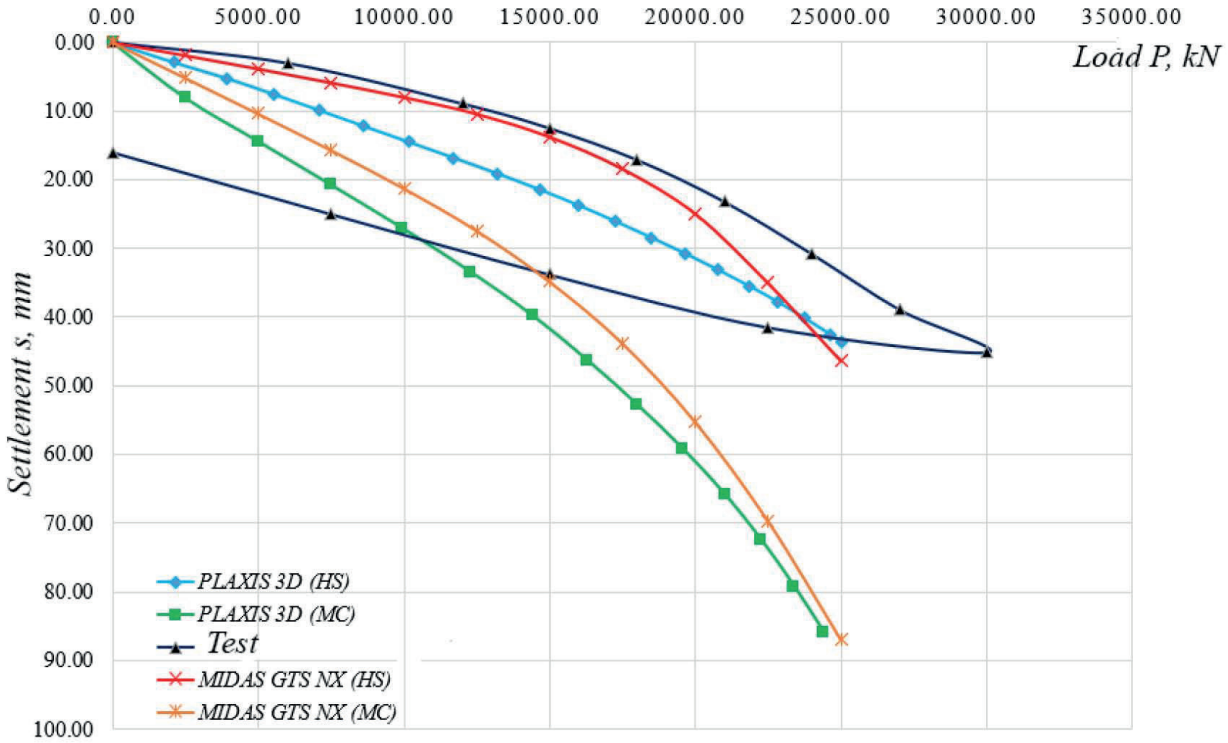

Figure 6. Combined diagram Load vs. Settlement

CALIBRATION OF GEOMECHANICAL MODEL PARAMETERS

Comparison of the calculation results using the Hardening Soil model showed good convergence in bearing capacity with field data (Table 2). At the same time, the model developed in the Midas GTS NX software package most accurately describes the behavior of the barrett under load (Fig. 5). However, the graphs begin to diverge in the range of loads of 15000-25000 kN, in which the piles are supposed to work as part of the foundation of a high-rise building. Therefore, in order to obtain reliable results in further geotechnical calculations, it is necessary to adjust the parameters of the mathematical model.

The characteristics of the soil and the characteristics of the contact elements along the barrett-soil boundary make a significant contribution to the nature of the load-settlement curve.

Russian standards [2] do not allow adjusting the strength parameters of soils for calculations based on the first limiting state. The deformation parameters of the model depend on the strength [15]; therefore, the model was calibrated by adjusting the interface elements.

Judging by the graph of the numerical test (Fig. 6), weak soil layers subjected to plastic flow during shear along the "pile-soil" boundary after reaching the load value of 15,000 kN. Part of the efforts are transferred to stronger and tougher soils, in particular, gravel-pebble soil, within which the calibration of the parameters of work on the lateral surface was carried out.

In the software package Midas GTS NX, the deformation and strength characteristics of the "interface" elements were assigned taking into account the coefficient of strength and stiffness reduction at the material boundary R = 0.6 for all types of soils, adopted in accordance with the Russian code of rules for pile foundations [1]. However, there is no value of

the coefficient of work on the lateral surface of the piles for coarse-grained soils and it is proposed to determine it empirically in the document [1].

The work on the side surface of the barrette in coarse soil is better than in sand, given its structure. After adjusting the parameters of the interface elements, taking into account $R = 0.8$ within the gravel-pebble soil (Fig. 6). It was possible to almost accurately describe the behavior of the barrette under load (Fig. 7).

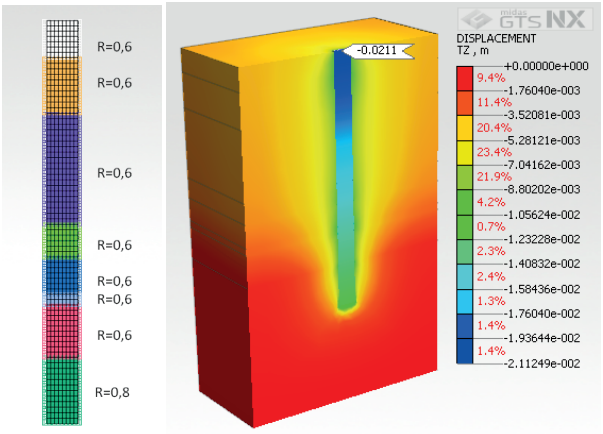

Figure 6. Assigned R-factors after calibration and calculation results

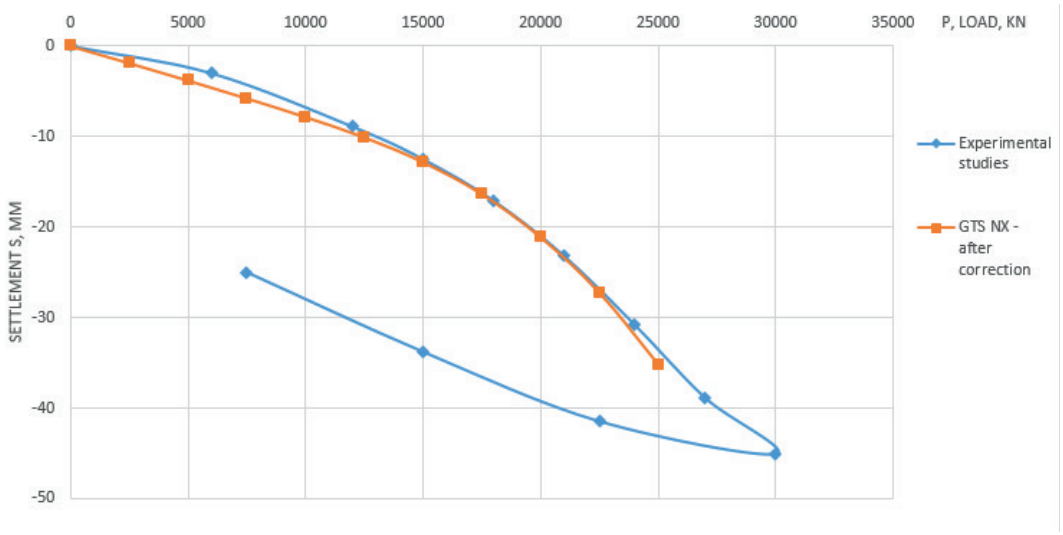

Figure 7. Load vs.settlement plots based on the results of the corrected model calculation and the results of field tests

CONCLUSIONS

As a result of the studies, it was found that modeling the bearing capacity of a pile-barrets with a section of 800x2800 mm and a length of 37 meters along the soil, performed in a software package using the HS model for soil conditions in Hanoi, Vietnam, showed values close to the results of static field tests.

The presented method of numerical calculations using the HS soil model in the PLAXIS 3D and MIDAS GTS NX programs describes the results of static field tests for construction sites with a large thickness of soft soils with sufficient accuracy for practical purposes.

To perform the final numerical calculations of the pile foundations of high-rise buildings, it is necessary to calibrate the numerical model based on the results of field tests. It is recommended to adjust the parameters of the interface elements for the "barrette-ground" contact. The value of the coefficient of reduction of strength and stiffness of contact elements for barrett in coarse soils is recommended to be used higher than in sands.

REFERENCES

1. Building Code of Russian Federation SP 24.13330.2011. Svod pravil. Svaynyye fundamenty. Aktualizirovannaya redaktsiya SNiP 2.02.03-85. [SP 24.13330.2011. Pile foundations. Updated edition of SNiP 2.02.03-85]
2. Building Code of Russian Federation SP 22.13330.2016. Svod pravil. Osnovaniya zdaniy i sooruzheniy. Aktualizirovannaya redaktsiya SNiP 2.02.01-83*. [SP 22.13330.2016 Soil bases of buildings and structures. Updated edition of SNiP 2.02.01-83*].
3. Standard of Russian Fedration GOST 20276-2012. Grunty. Metody polevogo opredeleniya kharakteristik prochnosti i deformiruyemosti. [GOST 20276-2012. Soils. Field methods for determining the strength and strain characteristics]
4. **Shulyat'yev, O. A.** Osnovaniya i fundamenty vysotnykh zdaniy : Nauchnoye izdaniye [Soils and foundations of high-rise buildings: Scientific publication] / O. A. Shulyat'yev. – 2nd edition, remastered and added. - Moscow : Publishing house ASV, 2020. - 442 p.
5. Proyektirovaniye osnovaniy, fundamentov i podzemnykh sooruzheniy: uchebnoye i prakticheskoye posobiye [Design of soils, foundations and underground structures: educational and practical manual] / R. A. Mangushev, A. I. Osokin, V. V. Konyushkov [i dr.].; Under ed. corr. member of RAACS, Dr. of Tech. Sc., Professor R.A. Mangushev. - Moscow: Publishing house ASV, 2021. - 632 p.
6. Svai i svaynyye fundamenty. Konstruirovaniye, proyektirovaniye, tekhnologii [Piles and pile foundations. Designing, designing, technologies] / R. A. Mangushev, A. L. Gotman, V. V. Znamenskiy, A. B. Ponomarev; Under ed. corr. member of RAACS, Dr. of Tech. Sc., Professor R.A. Mangushev. 2nd edition. Moscow : Publishing house ASV, 2018. – 320 p.
7. Osnovy chislennogo modelirovaniya v mekhanike gruntov i geotekhnike: uchebno-metodicheskoye posobiye [Fundamentals of numerical modeling in soil mechanics and geotechnics: teaching aid] / A. Z. Ter-Martirosyan, V. V. Sidorov, Ye. S. Sobolev, I. N. Luzin – Moscow : Publishing MISI – MGSU, 2020. – 91 p.
8. **Mangushev, R. A.** Analytical and numerical methods for determining the carrying capacity of a pile barett on weak soils in deep pits / R. A. Mangushev, N. S. Nikitina, Le Chung Khiyeu, I. YU. Tereshchenko. // IJCCSE. 2021. – Vol. 17, No 3. - Pp. 94-101.
9. **Mangushev, R. A.** Evaluation and analysis of bearing capacity of bores piles and deep laid pile-barrette for a high-rise building on loose grounds based on calculations and field tests / R. A. Mangushev, N. S. Nikitina // IJCCSE. 2018. – Vol. 14, No 2. - Pp. 109-116.
10. **Mangushev, R. A.** Chislennyye, analiticheskiye i polevyye metody otsenki nesushchey sposobnosti svay i svay-barret glubokogo zalozheniya v slabykh gruntakh Sankt-Peterburga [Numerical, analytical and field methods for assessing the bearing capacity of piles and pile-barrets of deep laying in soft soils of St. Petersburg] / R. A. Mangushev // Proceeding of International Conf.; SPbGASU. – SPb., 2012. - Pp. 44-52.
11. **Sidorov, V. V.** Issledovaniye vzaimodeystviya barret s osnovaniyem s uchetom ikh razmera i formy [Research of interaction of a

barret with a base taking into account their size and shape] / V. V. Sidorov, K. YU. Stepanishchev // Vestnik PNIPU. Stroitel'stvo i arkhitektura. – 2017. - No 3. – 78-88.

12. **Rybnikova, I. A** Opyt primeneniya barettnykh fundamentov [Experience of using barrette foundations] / I. A. Rybnikova, A. M. Rybnikov// Vestnik Belgorodskogo gosudarstvennogo tekhnologicheskogo universiteta im. V.G. Shukhova. - 2016. - No 4. - Pp. 23-27.
13. **Van Thanh Tran** Studying and calculating the bearing capacity of barrette piles based on comparison with O-cell test / Van Thanh Tran // Tạp chí Xây dựng Việt Nam 59 (625). - Pp. 232-236.
14. **Schanz T., Vermeer P.A., Bonnier P.G.** The hardening soil model: formulation and verification // Proceedings of the International Plaxis symposium “Beyond 2000 in computational geotechnics”. Rotterdam: Balkema, 1999 P. 281–296.

СПИСОК ЛИТЕРАТУРЫ

1. СП 24.13330.2011. Свод правил. Свайные фундаменты. Актуализированная редакция СНиП 2.02.03-85.
2. СП 22.13330.2016. Свод правил. Основания зданий и сооружений. Актуализированная редакция СНиП 2.02.01-83*.
3. ГОСТ 20276-2012. Грунты. Методы полевого определения характеристик прочности и деформируемости.
4. **Шулятьев, О. А.** Основания и фундаменты высотных зданий : Научное издание / О. А. Шулятьев. Изд. 2-е, перераб. и доп. - М. : Издательство АСВ, 2020. - 442 с.
5. Проектирование оснований, фундаментов и подземных сооружений: учебное и практическое пособие / Р. А. Мангушев, А. И. Осокин, В. В. Конюшков [и др.].; Под ред. чл.-корр. РААСН, д-ра техн. наук, профессора Р.А. Мангушева. – М.: Издательство АСВ, 2021. – 632 с.
6. Сваи и свайные фундаменты. Конструирование, проектирование, технологии / Р. А. Мангушев, А. Л. Готман, В. В. Знаменский, А. Б. Пономарев; Под ред. чл.-корр. РААСН, д-ра техн. наук, профессора Р.А. Мангушева. - Изд. 2-е, стер. М. : Издательство АСВ, 2018. - 320 с.
7. Основы численного моделирования в механике грунтов и геотехнике [Электронный ресурс] : учебно-методическое пособие / А. З. Тер-Мартиросян, В. В. Сидоров, Е. С. Соболев, И. Н. Лузин – М. : Издательство МИСИ – МГСУ, 2020. – 91 с.
8. Аналитические и численные методы определения несущей способности свай-баррет на слабых грунтах в глубоких котлованах / Р. А. Мангушев, Н. С. Никитина, Ле Чунг Хиеу, И. Ю. Терещенко. Текст : электронный // Международный журнал по расчету гражданских и строительных конструкций (журнал IJCCSE). 2021. Том 17 № 3. – С. 94-101.
9. **Мангушев, Р. А.** Оценка и анализ несущей способности буронабивных свай и свай-баррет глубокого заложения для высотного здания на слабых грунтах по результатам расчетов и полевых испытаний / Р. А. Мангушев, Н. С. Никитина. – Текст : электронный // Международный журнал по расчету гражданских и строительных конструкций (журнал IJCCSE). – 2018. – Том 14 № 2. – С. 109-116.
10. **Мангушев, Р. А.** Численные, аналитические и полевые методы оценки несу-

щей способности свай и свай-баррет глубокого заложения в слабых грунтах Санкт-Петербурга / Р. А. Мангушев. – Текст : электронный // сборник статей международной научно-технической конференции; СПбГАСУ. – СПб., 2012. – С. 44-52.

11. **Сидоров, В. В.** Исследование взаимодействия баррет с основанием с учетом их размера и формы / В. В. Сидоров, К. Ю. Степанищев. - Текст : электронный // Вестник ПНИПУ. Строительство и архитектура. – 2017. – № 3. – С. 78-88.
12. **Рыбникова, И. А** Опыт применения бареттных фундаментов / И. А. Рыбникова, А. М. Рыбников. – Текст : электронный // Вестник Белгородского государственного технологического университета им. В.Г. Шухова. - 2016. – № 4. – С. 23-27.
13. **Van Thanh Tran** Studying and calculating the bearing capacity of barrette piles based on comparison with O-cell test / Van Thanh Tran // Tạp chí Xây dựng Việt Nam 59 (625). – C. 232-236.
14. **Schanz T., Vermeer P.A., Bonnier P.G.** The hardening soil model: formulation and verification // Proceedings of the International Plaxis symposium “Beyond 2000 in computational geotechnics”. Rotterdam: Balkema, 1999 P. 281–296.

Rashid A. Mangushev. Corresponding Member of the RAACS, Professor, Doctor of Technical Sciences; Head of the Department of Geotechnics, St. Petersburg State University of Architecture and Civil Engineering (SPbGASU), Director of the Scientific and Production Consulting Center for Geotechnology, SPbGASU. Russia, St. Petersburg, 2nd Krasnoarmeiskaya 4; email: ramangushev@yandex.ru.

Nadezhda S. Nikitina. Candidate of Technical Sciences, Professor of the Department of Soil Mechanics and Geotechnics; National Research Moscow State University of Civil Engineering (NRU MSUCE); Moscow, Russia, 129337, Yaroslavskoe shosse, 26; tel./fax: +7 (495) 287-49-14; e-mail: nsnikitina@mail.ru;

Le Van Chong – Candidate of Technical Sciences, lecturer of the Department of Civil Engineering, Da Nang University of Architecture. 566 Nui Thanh Street, Hoa Cuong Nam Ward, Hai Chau District, Da Nang City. Tel.: +84(931)946-710. E-mail: tronglv@dau.edu.vn

Ivan Yu. Tereshchenko – Chief Specialist of GIPROATOM LLC; Moscow, Nauchny proezd, house 8, building 1; e-mail: i.tereshchenko@giproatom.com.

Мангушев Рашид Абдуллович – член-корреспондент РААСН, профессор, доктор технических наук; заведующий кафедрой геотехники Санкт-Петербургского государственного архитектурно-строительного университета (СПбГАСУ), директор научно производственного консалтингового центра геотехнологий СПбГАСУ. Россия, Санкт-Петербург, 2-я Красноармейская 4; email: ramangushev@yandex.ru.

Никитина Надежда Сергеевна – к.т.н., профессор кафедры «Механики грунтов и геотехники»; Национальный исследовательский Московский государственный строительный университет (НИУ МГСУ); г. Москва, Россия, 129337, Ярославское шоссе, д.26; тел./факс: +7(495) 287-49-14; e-mail: nsnikitina@mail.ru;

Ле Ван Чонг – к.т.н., преподаватель кафедры гражданского строительства, архитектурный университет Дананга. Дананг, ул. Нуй Тхань, район Хай Чау, д. 566. Моб.: +84(931) 946-710. E-mail: tronglv@dau.edu.vn

Терещенко Иван Юрьевич – главный специалист ООО "ГИПРОАТОМ"; г. Москва, Научный проезд, дом 8, строение 1; e-mail: i.tereshchenko@giproatom.com.

International Journal for Computational Civil and Structural Engineering, 18(1) 129–140 (2022)

DOI:10.22337/2587-9618-2022-18-1-129-140

FILTRATION PROBLEM WITH NONLINEAR FILTRATION AND CONCENTRATION FUNCTIONS

Galina L. Safina

Moscow State University of Civil Engineering, Moscow, RUSSIA

Abstract: Ancient architectural buildings are of great value for all modern humanity. Over time, under the influence of vibrations, water and other man-made and natural factors, the foundations of such buildings are destroyed, the soil structure changes. Currently, one of the most popular methods of strengthening soils and strengthening foundations is the jet grouting technology. When the liquid grout passes through the porous rock, the suspended particles of the grout form a deposit. In this paper, we study a one-dimensional model of suspension deep bed filtration in a porous medium with different particle capture mechanisms. The considered filtration model consists of the balance equation for the masses of suspended and retained particles and the kinetic equation for deposit growth. In this case, the deposit growth rate is determined by the concentration function of suspended particles, which, in turn, depends on the properties of the suspension and the geometry of the porous medium. The solution to the problem is obtained for linear and non-linear concentration functions. An asymptotic solution of the problem is constructed for both types of functions near the concentration front of suspended and retained particles. It is shown that the asymptotic and numerical solutions are close over a long time interval.

Keywords: deep bed filtration, suspended and retained particles, suspension, porous medium, concentration function, asymptotic solution.

ЗАДАЧА ФИЛЬТРАЦИИ С НЕЛИНЕЙНЫМИ ФУНКЦИЯМИ ФИЛЬТРАЦИИ И КОНЦЕНТРАЦИИ

Г.Л. Сафина

Национальный исследовательский Московский государственный строительный университет, г. Москва, РОССИЯ

Аннотация: Старинные архитектурные здания представляют собой огромную ценность для всего современного человечества. Со временем под воздействием вибраций, воды и других техногенных и природных факторов происходит разрушение фундаментов таких зданий, изменение структуры грунтов. В настоящее время одним из наиболее популярных методов усиления грунтов и укрепления фундаментов является технология струйной цементации. При прохождении жидкого раствора через пористую породу взвешенные частицы укрепителя образуют осадок. В работе исследуется одномерная модель долговременной глубинной фильтрации суспензии в пористой среде с различными механизмами захвата частиц. Рассматриваемая модель фильтрации состоит из уравнения баланса масс взвешенных и задержанных частиц и кинетического уравнение роста осадка. При этом скорость роста осадка определяется функцией концентрации осажденных частиц, которая в свою очередь зависит от свойств суспензии и геометрии пористой среды. Решение задачи получено для линейной и нелинейной функций концентрации. Построено асимптотическое решение задачи для обоих видов функций вблизи фронта концентрации взвешенных и осажденных частиц. Показано, что асимптотические и численные решения близки в большом временном интервале.

Ключевые слова: фильтрация, взвешенные и осажденные частицы, суспензия, пористая среда, функция концентрации, асимптотическое решение.

INTRODUCTION

Historical buildings are an integral part of the world cultural heritage. They reflect the historical trajectory of the country's development and are the product of the development of ancient history, culture, art and religion. Humanity needs history and culture, and it is through historical monuments that it comes into contact with both. Thanks to the protection and restoration of historical buildings, a person can complement the cultural heritage of his country, record history, and ensure his identity [1].

In most cases, the age of buildings with architectural value exceeds 100 years. Over a long service life, the foundations of monuments are under threat of destruction due to increased loads and vibrations, and the structure of soils changes over time. Water penetrating into the soil in various ways has a special effect (a sewer breakthrough, an increase in the groundwater level). To prevent the loss of historical values and cultural monuments, it is necessary to strengthen the soils under them, which will reduce the risk of deformations and destruction.

There are many examples of strengthening the soils of historical buildings in the world practice. For example, this is the Angel's Stradome in Krakow, the Branicki Palace and the historic Foxal 13 and 15 building in Warsaw, the Kutb Miner in Delhi (fig. 1), the Tsaritsyno State Museum-Reserve in Moscow (fig. 2), etc. [2-6].

Figure 1. The Qutb Miner

Figure 2. Tsaritsyno State Museum-Reserve

Since the 1970s, jet grouting technology has been used in the work on effective soil strengthening and foundation strengthening [7-9], which is currently one of the most popular in this field. Grout (fluid system), or grout with air (double fluid system), or grout with air and water (triple fluid system) is injected into the ground through nozzles of small diameter placed in a pipe for the grout lowered into the well. The tube rotates continuously at a constant speed and slowly rises to the surface of the earth. The jet propagates radially from the axis of the well, and after a while the injected solution solidifies, forming a body of cemented soil of a quasi-cylindrical shape [10].

Filtration of a suspension transporting through a porous medium, taking into account the retention of solid particles on a porous frame and a gradual decrease in the porosity and permeability of the medium, is of great interest in jet grouting. Suspension filtration is divided into two groups: cake filtration and deep bed filtration [11]. The first type of filtration consists in the retention of particles at the porous medium inlet, it is characteristic of suspensions with large particles and a high concentration, the second is associated with the deposit formation in the entire porous medium, if small suspended particles of a suspension with a low concentration can be freely transported through the pores [12]. In the case when the suspension has particles of different sizes, these two types of filtration are used

simultaneously [13]. We will consider the deep bed filtration model.

There are various mechanisms for capturing particles in a porous medium: size exclusion, electric forces (London-Van der Waals, double electric layer, etc.), gravitational segregation, multi particle bridging [14]. In this paper, size exclusion mechanism is considered, when large particles are captured by small pores, clog them, and pass unhindered through large pores [15-17], and a mixed mechanism that includes size exclusion mechanism and multi particle bridging mechanism [fig. 3]. In the case of multi particle bridging, suspension particles form arched bridges at the pores, thereby block them.

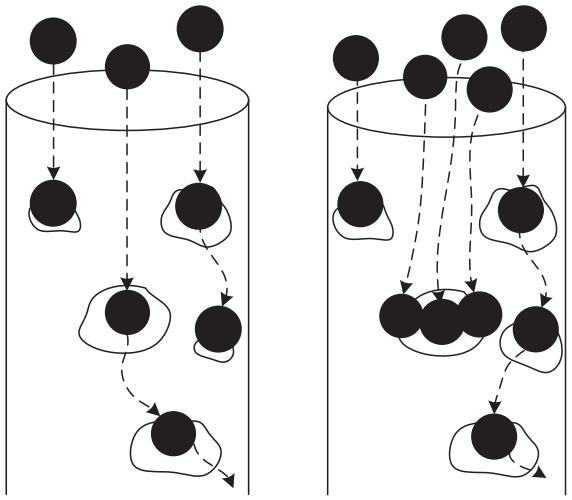

a) *b)*

Figure 3. Particle capture mechanisms in the porous medium a) size exclusion b) size exclusion together with multi particle bridging

In the classical model of deep bed filtration, the system of partial differential equations consists of mass balance equation end kinetic equation of deposition. Exact solutions have been found for some classes of one-dimensional problems [18-20], for others it is possible to obtain only an asymptotic solution [21-23]. For a wide class of models, a solution is obtained by numerical methods [24-26].

MATHEMATICAL MODEL

Consider the classical model of deep bed filtration in the domain $\Omega = \{0 \le x \le 1,\ t \ge 0\}$

$$\frac{\partial C(x,t)}{\partial t} + \frac{\partial C(x,t)}{\partial x} + \frac{\partial S(x,t)}{\partial t} = 0, \quad (1)$$

$$\frac{\partial S(x,t)}{\partial t} = \Lambda\left(S(x,t)\right) F\left(C(x,t)\right) \quad (2)$$

with a boundary condition

$$x = 0: \quad C(0,t) = 1 \quad (3)$$

and initial conditions

$$t = 0: \quad C(x,0) = 0; \quad S(x,0) = 0. \quad (4)$$

Here $C(x,t)$ is the concentration of suspended particles, $S(x,t)$ is the concentration of retained particles, $\Lambda\left(S(x,t)\right)$ is the filtration function, $F\left(C(x,t)\right)$ is the concentration function.

The line $t = x$ determines the concentration front of suspended and retained particles. In the domain $\Omega^{(1)} = \{0 < x < 1,\ 0 < t < x\}$, located below this line, concentrations $C(x,t)$ and $S(x,t)$ are equal to zero. In the domain $\Omega^{(2)} = \{0 < x < 1,\ t > x\}$ concentrations $C(x,t)$ and $S(x,t)$ are positive. The solution $C(x,t)$ has a break along the front, the solution $S(x,t)$ is continuous everywhere and is zero at the concentration front.

In this paper, we will consider a cubic function of the general form as a filtration function

$$\Lambda\left(S\right) = \lambda_0 + \lambda_1 S + \lambda_2 S^2 + \lambda_3 S^3,$$

which is decreasing to zero, i.e. there is a value $\tilde{S}$ such that $\lambda_0 + \lambda_1 \tilde{S} + \lambda_2 \tilde{S}^2 + \lambda_3 \tilde{S}^3 \equiv 0$. The specific type of filtration function used in our calculations has been determined experimentally [27].

The system (1)-(2) takes the form

$$\frac{\partial C}{\partial t}+\frac{\partial C}{\partial x}+\left(\lambda_0+\lambda_1 S+\lambda_2 S^2+\lambda_3 S^3\right)F(C)=0\,, \quad (5)$$

$$\frac{\partial S}{\partial t}=\left(\lambda_0+\lambda_1 S+\lambda_2 S^2+\lambda_3 S^3\right)F(C) \quad (6)$$

with boundary and initial conditions (3)-(4).
Turning in equation (5) to the characteristic variables $\tau=t-x,\ x=x$, we obtain the equation

$$\frac{\partial C}{\partial x}+\left(\lambda_0+\lambda_1 S+\lambda_2 S^2+\lambda_3 S^3\right)F(C)=0\,.$$

Let us find a solution $C(x,\tau)$ at $\tau=0$, which corresponds to the concentration front line $t=x$. Given that the solution $S(x,\tau)$ is zero at $\tau=0$, we get

$$\frac{\partial C}{\partial x}+\lambda_0 F(C)=0\,.$$

Consider concentration functions of the form $F\left(C\right)=C$ and $F\left(C\right)=(1-\alpha)C+\alpha C^3$, which correspond to the size-exclusion and mixed mechanisms of particle capture. For a linear function $F\left(C\right)=C$ we get

$$\frac{\partial C}{\partial x}=-\lambda_0 C\,.$$

Taking into account (3), we have

$$\int\limits_{C_0(x)}^{1}\frac{dc}{C}=\lambda_0 x\,,$$

the solution $C_0(x)$ is determined with formula

$$C_0(x)=e^{-\lambda_0 x}\,. \quad (7)$$

For a nonlinear function $F\left(C\right)=(1-\alpha)C+\alpha C^3$ we get

$$\int\limits_{C_0(x)}^{1}\frac{dc}{(1-\alpha)C+\alpha C^3}=\lambda_0 x\,,$$

then

$$C_0(x)=\frac{\sqrt{1-\alpha}e^{-(1-\alpha)\lambda_0 x}}{\sqrt{1-\alpha e^{-2(1-\alpha)\lambda_0 x}}}\,. \quad (8)$$

At the filter inlet $x=0$ taking into account the boundary condition (3), the solution $S_0(0,t)$ is determined by equation (6):

$$\frac{\partial S}{\partial t}=\left(\lambda_0+\lambda_1 S+\lambda_2 S^2+\lambda_3 S^3\right),$$

Then

$$\int\limits_{0}^{S(0,t)}\frac{dS}{\lambda_0+\lambda_1 S+\lambda_2 S^2+\lambda_3 S^3}=t\,. \quad (9)$$

ASYMPTOTIC SOLUTION NEAR THE CONCENTRATION FRONT

Linear concentration function

For linear concentration function $F\left(C\right)=C$ let us find asymptotic solutions near the concentration front $t=x$ in the form:

$$C(x,t)=C_0(x)+C_1(x)(t-x)+\\+\frac{1}{2}C_2(x)(t-x)^2+...,\quad (10)$$

$$S(x,t)=S_1(x)(t-x)+\frac{1}{2}S_2(x)(t-x)^2+...\\+\frac{1}{6}S_3(x)(t-x)^3...,\quad (11)$$

limiting in both solutions to the first three terms due to cumbersome calculations. The first term of the suspended particle asymptotic $C_0(x)$ is determined by the formula (7), $S_0(x)=0$ since

the concentration of deposited particles is zero at the concentration front.

Differentiate the expansion (10) by x and t, the expansion (11) by t and substitute these expressions into the system of equations (5)-(6). Grouping the terms at the same degrees of $(t-x)$, equate them to zero and get a system of equations:

$$(t-x)^0: \quad C_0'(x) = -\lambda_0 C_0(x),\ S_1(x) = \lambda_0 C_0(x);$$

$$(t-x)^1: \quad C_1'(x) = -\lambda_0 C_1(x) - \lambda_1 S_1(x) C_0(x),\ S_2(x) = \lambda_0 C_1(x) + \lambda_1 C_0(x) S_1(x);$$

$$(t-x)^2: \quad \frac{1}{2} C_2'(x) = -\frac{1}{2}\lambda_0 C_2(x) - \lambda_1 C_1(x) S_1(x) - \frac{1}{2}\lambda_1 C_0(x) S_2(x) - \lambda_2 C_0(x) S_1^2(x)$$

$$\frac{1}{2} S_3(x) = \frac{1}{2}\lambda_0 C_2(x) + \lambda_1 C_1(x) S_1(x) + \frac{1}{2}\lambda_1 C_0(x) S_2(x) + \lambda_2 C_0(x) S_1^2(x)$$

Solving this system of equations, we obtain:

$$C_0(x) = e^{-\lambda_0 x},\ S_1(x) = \lambda_0 e^{-\lambda_0 x};$$

$$C_1(x) = \lambda_1 e^{-\lambda_0 x}\left(e^{-\lambda_0 x} - 1\right),\ S_2(x) = \lambda_0\lambda_1 e^{-\lambda_0 x}\left(2e^{-\lambda_0 x} - 1\right);$$

$$C_2 = e^{-\lambda_0 x}\left(\left(2\lambda_1^2 + \lambda_0\lambda_2\right)e^{-2\lambda_0 x} - 3\lambda_1^2 e^{-\lambda_0 x} + \left(\lambda_1^2 - 2\lambda_0\lambda_2\right)\right),$$

$$S_3(x) = \lambda_0 e^{-\lambda_0 x}\left(3(2\lambda_1^2 + \lambda_0\lambda_2)e^{-2\lambda_0 x} - 6\lambda_1^2 e^{-\lambda_0 x} + \lambda_1^2 - 2\lambda_0\lambda_2\right).$$

Note that the first solution of the obtained system coincides with solution (7).

Substituting the obtained solutions in (10)-(11), we obtain asymptotic expansions:

$$C(x,t) = e^{-\lambda_0 x} + \lambda_1 e^{-\lambda_0 x}\left(e^{-\lambda_0 x} - 1\right)(t-x) +$$

$$+\frac{1}{2}e^{-\lambda_0 x}\left(\left(2\lambda_1^2 + \lambda_0\lambda_2\right)e^{-2\lambda_0 x} - 3\lambda_1^2 e^{-\lambda_0 x} + \left(\lambda_1^2 - 2\lambda_0\lambda_2\right)\right)(t-x)^2 + ...,$$

$$S(x,t) = \lambda_0 e^{-\lambda_0 x}(t-x) + \frac{1}{2}\lambda_0\lambda_1 e^{-\lambda_0 x}\left(2e^{-\lambda_0 x} - 1\right)(t-x)^2 +$$

$$+\frac{1}{6}\lambda_0 e^{-\lambda_0 x}\left(3(2\lambda_1^2 + \lambda_0\lambda_2)e^{-2\lambda_0 x} - 6\lambda_1^2 e^{-\lambda_0 x} + \lambda_1^2 - 2\lambda_0\lambda_2\right)(t-x)^3 + ...$$

Nonlinear concentration function

Consider the nonlinear concentration function $F(C) = (1-\alpha)C + \alpha C^3$. In order to avoid cumbersome calculations, we will limit ourselves in expansions (10)-(11) to the first two terms:

$$C(x,t) = C_0(x) + C_1(x)(t-x) + ..., \qquad (12)$$

$$S(x,t) = S_1(x)(t-x) + \frac{1}{2}S_2(x)(t-x)^2 + ... \qquad (13)$$

Here the main term of the asymptotic is given by formula (8).

Similarly to the case with a linear function, we obtain a system of equations:

$$(t-x)^0: \quad C_0'(x) = -(1-\alpha)\lambda_0 C_0(x) - \alpha\lambda_0 C_0^3(x),\ S_1(x) = (1-\alpha)\lambda_0 C_0(x) + \alpha\lambda_0 C_0^3(x);$$
$$(t-x)^1: \quad C_1'(x) = -(1-\alpha)\lambda_0 C_1(x) - (1-\alpha)\lambda_1 C_0(x) S_1(x) - 3\alpha\lambda_0 C_0^2(x) C_1(x) - \alpha\lambda_1 C_0^3(x) S_1(x),$$
$$S_2(x) = (1-\alpha)\lambda_0 C_1(x) + (1-\alpha)\lambda_1 C_0(x) S_1(x) + 3\alpha\lambda_0 C_0^2(x) C_1(x) + \alpha\lambda_1 C_0^3(x) S_1(x).$$

Solving the recurrent system, we obtain:

$$C_0 = \frac{\sqrt{1-\alpha}e^{-(1-\alpha)\lambda_0 x}}{\sqrt{1-\alpha e^{-2(1-\alpha)\lambda_0 x}}},\ S_1(x) = \frac{\sqrt{(1-\alpha)^3}\lambda_0 e^{-(1-\alpha)\lambda_0 x}}{\sqrt{1-\alpha e^{-2(1-\alpha)\lambda_0 x}}} + \frac{\alpha\sqrt{(1-\alpha)^3}\lambda_0 e^{-3(1-\alpha)\lambda_0 x}}{\sqrt{(1-\alpha e^{-2(1-\alpha)\lambda_0 x})^3}};$$
$$C_1(x) = \lambda_1 C_0(x)\left(C_0(x)-1\right)\left(1-\alpha+\alpha C_0^2(x)\right),$$
$$S_2(x) = 4\alpha^2\lambda_0\lambda_1 C_0^6(x) - 3\alpha^2\lambda_0\lambda_1 C_0^5(x) + 6\alpha\lambda_0\lambda_1 C_0^4(x)(1-\alpha) - 4\alpha\lambda_0\lambda_1 C_0^3(x)(1-\alpha) +$$
$$+2\lambda_0\lambda_1 C_0^2(x)(1-\alpha)^2 - \lambda_0\lambda_1 C_0(x)(1-\alpha)^2.$$

Substituting the obtained expressions into decompositions (12), (13), we obtain asymptotic solutions

$$C(x,t) = \frac{\sqrt{1-\alpha}e^{-(1-\alpha)\lambda_0 x}}{\sqrt{1-\alpha e^{-2(1-\alpha)\lambda_0 x}}} + \lambda_1 C_0(x)\left(C_0(x)-1\right)\left(1-\alpha+\alpha C_0^2(x)\right)(t-x),$$
$$S(x,t) = \left(\frac{\sqrt{(1-\alpha)^3}\lambda_0 e^{-(1-\alpha)\lambda_0 x}}{\sqrt{1-\alpha e^{-2(1-\alpha)\lambda_0 x}}} + \frac{\alpha\sqrt{(1-\alpha)^3}\lambda_0 e^{-3(1-\alpha)\lambda_0 x}}{\sqrt{(1-\alpha e^{-2(1-\alpha)\lambda_0 x})^3}}\right)(t-x) +$$
$$+\frac{1}{2}\left(4\alpha^2\lambda_0\lambda_1 C_0^6(x) - 3\alpha^2\lambda_0\lambda_1 C_0^5(x) + 6\alpha\lambda_0\lambda_1 C_0^4(x)(1-\alpha) - 4\alpha\lambda_0\lambda_1 C_0^3(x)(1-\alpha) +\right.$$
$$\left.+2\lambda_0\lambda_1 C_0^2(x)(1-\alpha)^2 - \lambda_0\lambda_1 C_0(x)(1-\alpha)^2\right)(t-x)^2.$$

NUMERICAL SOLUTION OF THE PROBLEM

Let us solve the problem by the numerical method of finite differences. For the convergence of the method, the steps along the time axis t and the coordinate axis x are chosen $h_t = h_x = 0.01$, it ensures the fulfillment of the Courant condition [28]. The coefficients of the filtration function are obtained experimentally: $\lambda_0 = 1.551$, $\lambda_1 = -3.467\cdot 10^{-3}$, $\lambda_2 = -1.16\cdot 10^{-6}$, $\lambda_3 = -1.16\cdot 10^{-7}$ [29]. In this case, the solution at the filter inlet, determined by equation (9), is given implicitly

$$71.87\,\mathrm{arctg}(0.41+2S) - 59.12\ln(193.28-S) +$$
$$+29.56\ln(69177.9+203.28S+S^2) -$$
$$-71.87\,\mathrm{arctg}\,0.41 + 59.12\ln 193.28 -$$
$$-29.56\ln(69177.9) = t.$$

The graphs of suspended particle concentrations at a time $t = 100$ for linear (fig. 4a) and cubic (fig. 4b) concentration functions are shown in fig. 4: the red line corresponds to the numerical solution of the problem, the black line corresponds to the asymptotic solution. It can be seen from the figures that the asymptotics for both concentration functions gives a fairly good approximation, the greatest discrepancy is

observed at the filter inlet. The relative error of the asymptotics in the case of a linear concentration function is about 5%, in the case of a nonlinear filtration function – 3%.

Fig. 5 shows the relative errors of the asymptotic concentration of suspended particles for different times t: $t=1$ (black line), $t=10$ (blue line), $t=50$ (green line), $t=100$ (red line).

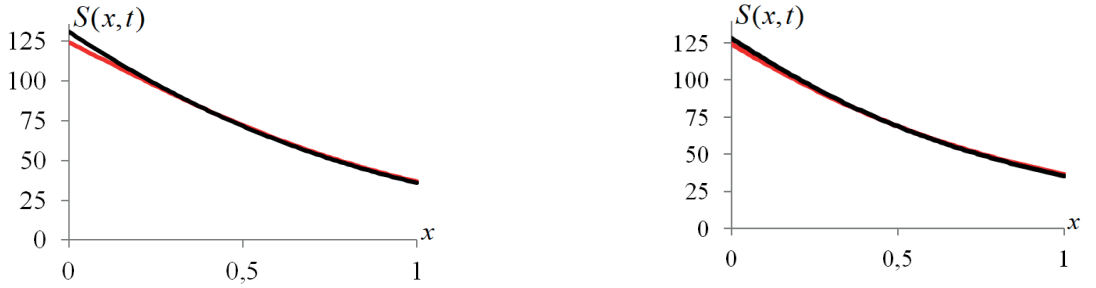

a) $F(C)=C$ *b)* $F(C)=(1-\alpha)C+\alpha C^3$

Figure 4. Numerical and asymptotic solutions of suspended particles concentrations at $t=100$

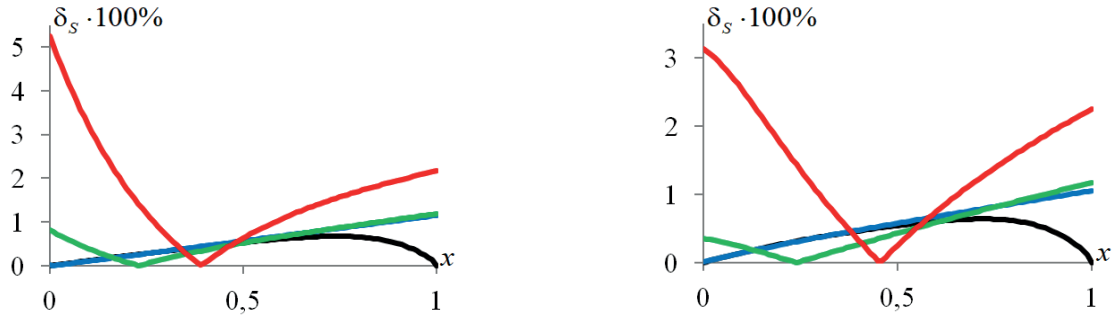

a) $F(C)=C$ *b)* $F(C)=(1-\alpha)C+\alpha C^3$

Figure 5. Relative errors of suspended particles concentration asymptotics for various t

In fig. 6 the graphs of retained particle concentrations at $x=0.5$ (fig. 6a) and at the filter outlet $x=1$ (fig. 6b) for the concentration function $F(C)=C$ are presented. The numerical solution is indicated by a red line, the asymptotic solution is indicated by a black line. Similar graphs for the case $F(C)=(1-\alpha)C+\alpha C^3$ are shown in fig. 7. The relative errors of the asymptotic concentration of retained particles for various filtration functions are shown in fig. 8. The case $x=0.5$ corresponds to the red line and the case $x=1$ corresponds to the black line.

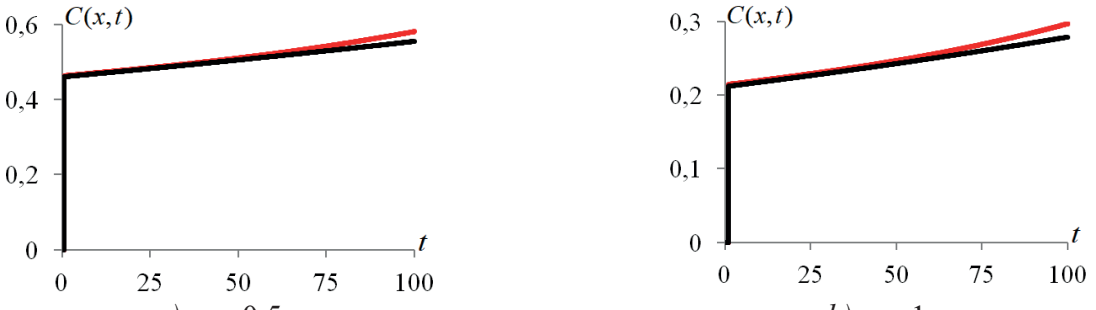

a) $x=0.5$ *b)* $x=1$

Figure 6. Numerical and asymptotic solutions of retained particle concentrations for $F(C)=C$

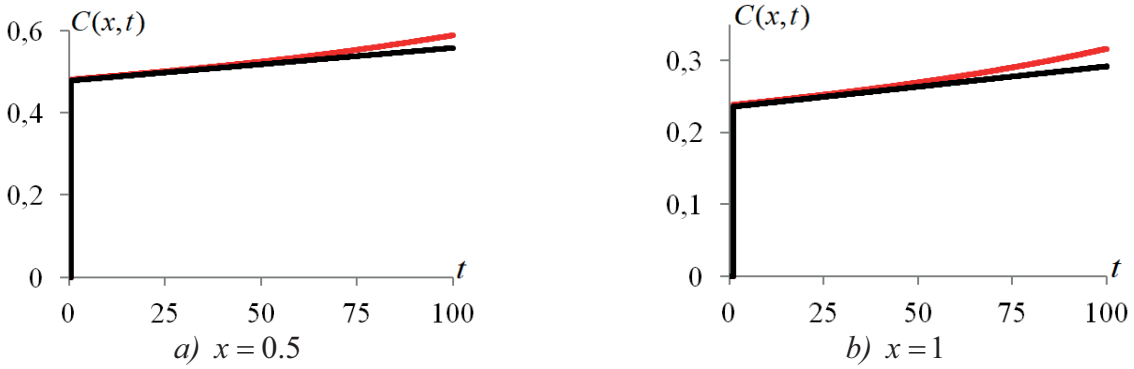

Figure 7. Numerical and asymptotic solutions of retained particle concentrations for $F(C) = (1-\alpha)C + \alpha C^3$

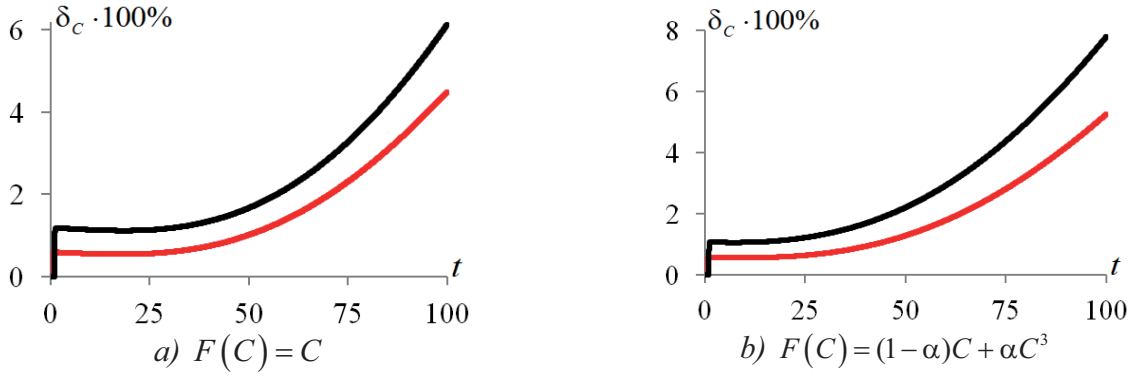

Figure 8. Relative errors of suspended particles concentration asymptotics at $x = 0.5$ *and* $x = 1$

The graphs show that the deviation of the asymptotic from the numerical solution increases with increasing time, approximately up to the time moment $t = 50$, the relative error of the asymptotic for both concentration functions is less than 2%, at the time $t = 100$ at the filter outlet, the relative error of the asymptotic in the case of a linear concentration function is slightly more than 6%, with a nonlinear function – 8%.

CONCLUSION

The mathematical model of deep filtration with a dimensional particle capture mechanism and mixed mechanism that includes size exclusion mechanism and multi particle bridging mechanism is considered in paper. With the first particle capture mechanism, solid particles freely pass through pores whose diameter is larger than the particle size and clog pores with a smaller diameter. With mixed mechanism, some solid particles freely pass through the pore necks, some get stuck in them, and others can block the pores, forming arch bridges. Several particles are connected, attached to the edges of the pore, thereby blocking it and preventing the suspended particles from entering the pore. In the considered model, the linear concentration function $F(C) = C$ describes size exclusion mechanism, the nonlinear function $F(C) = (1-\alpha)C + \alpha C^3$ describes mixed mechanism. In the filtration model, a polynomial of the third degree was used as a filtration function $\Lambda(S)$.

The constructed asymptotics of the concentrations of suspended and retained particles near the concentration front give good approximations to numerical solutions even in sufficiently large time intervals. The asymptotic solution of the suspended particle concentration of the second order, constructed for a nonlinear

concentration function, is closer to the numerical solution, the relative error at the time is about 3%, while the error of the third-order asymptotic in the case of a linear concentration function is slightly more than 5%. For retained particles, the second-order asymptotic in the case of a linear concentration function better approximates the numerical solution than the first-order asymptotic when using a nonlinear concentration function, for example, at the filter outlet at a time $t = 100$, the relative error of the second-order asymptotic is 2% less than the error of the first-order asymptotic.

It should be noted that by limiting the asymptotic of suspended particle concentration to two terms with a nonlinear concentration function, an approximate solution for the linear filtration function is actually constructed. Thus, we can determine when a solution with a nonlinear filtering function begins to deviate significantly from the asymptotic of the linear function.

In field studies of reservoir water filtration in porous rock, measurement errors are at least 10 % [30]. Therefore, the proposed asymptotic formulas adequately describe the filtration process up to time $t = 100$.

REFERENCES

1. **Li B., Han J.** Conservation and regeneration of historical buildings // IOP Conference Series: Earth and Environmental Science, 2021, vol. 787, 012179.
2. **Makowski A., Polanska B.** Application of jet grouting technology for the renovation of historic buildings // IOP Conference Series: Journal of Physics, 2020, vol. 1425, 012201.
3. **Redina T.** Reconstuction of the historical building foksal 13 and 15 in Warsaw // Acta Polytechnica CTU Proceedings, 2019, vol. 23, pp. 44-48.
4. **Sengupta R.** Grouting for strengthening the Qutb Minar, Delhi // Mortars, Cements and Grouts used in the Conservation of Historic Buildings, 1981, pp. 147-164.
5. **Wanik K.** Use of jet grouting technique to realize substructures of historic buildings: The example of an apartment building in Warsaw // Geotechnical Engineering for the Preservation of Monuments and Historic Sites, 2013, pp. 769-777.
6. **Chernyakov A.V.** Application of jet grouting during foundation reinforcement and reconstruction of historic buildings on land occupied by the state museum and reservation «Tsarutsyno» // Soil Mechanics and Foundation Engineering, 2011, vol. 48(5), pp. 769-777.
7. **Hofmann H.** Unterfangungen mit einpressung von zementsuspension unter hohem Druck // Beton- und Stahlbetonbau, 1989, vol. 84(8), pp. 199-202.
8. **Morey J.J.** Les domaines d'application du jet-grouting // Revue Francaise de Geotechnique, 1992, vol. 61, 17-30.
9. **Drooff E.R., Furth A.J., Scarborough J. A.** Jet grouting to support historic buildings // Geotechnical Special Publication, 1995, vol. 50, pp. 42-55.
10. **Modoni G., Croce P., Mongiovi L.** Theoretical modelling of jet grouting // Geotechnique, 2006, vol. 56(5), pp. 335-347.
11. **Tien C.** Principles of filtration // Elsevier: Amsterdam, 2012.
12. **Tien C.** Introduction to cake filtration // Elsevier: Amsterdam, 2006.
13. **Sacramento R.N., Yang Y., You Z., Waldmann A., Martins A.L., Vaz A.S.L., Zitha P.L.J., Bedrikovetsky P.** Deep bed and cake filtration of two-size particle suspension in porous media // Journal of Petroleum Science and Engineering, 2015, vol. 126, pp. 201-210.
14. **Fallah H., Barzegar Fathi H., Mohammadi H.** The mathematical model for particle suspension flow through porous medium // Geomaterials, 2012, vol. 2, pp. 57-62.

15. **Fallah H., Fallah A., Rahmani A., Afkhami M., Ahmadi A.** Size exclusion mechanism, suspension flow through porous medium // International Journal of Modern Nonlinear Theory and Application, 2012, vol. 1, pp. 113-117.
16. **Santos A., Bedrikovetsky P.** Size exclusion during particle suspension transport in porous media: stochastic and averaged equations // Computational and Applied Mathematics, 2004, vol. 23(2-3), pp. 259-284.
17. **You Z., Bedrikovetsky P., Kuzmina L.** Exact solution for long-term size exclusion suspension-colloidal transport in porous media // Hindawi Publishing Corporation Abstract and Applied Analysis, 2013, vol. 2013, 680693.
18. **Kuzmina L.I., Osipov Yu.V.** Exact solution for 1D deep bed filtration with particle capture by advection and dispersion // International Journal of Non-Linear Mechanics, 2021, vol. 137, 103830.
19. **Nazaikinskii V.E., Bedrikovetsky P.G., Kuzmina L.I., Osipov Y.V.** Exact solution for deep bed filtration with finite blocking time // SIAM Journal on Applied Mathematics, 2020, vol. 80 (5), pp. 2120-2143.
20. **Kuzmina L.I., Osipov Y.V. and Zheglova Y.G.** Analytical model for deep bed filtration with multiple mechanisms of particle capture // International Journal of Non-linear Mechanics, 2018, vol. 105, pp. 242-248.
21. **Kuzmina L.I., Osipov Y.V., Gorbunova T.N.** Asymptotics for filtration of polydisperse suspension with small impurities // Applied Mathematics and Mechanics (English Edition), 2021, vol. 42(1), pp. 109-126.
22. **Osipov Y.V.** Calculation of filtration of polydisperse suspension in a porous medium // MATEC Web of Conferences, 2017, vol. 117, 00131.
23. **Kuzmina L.I., Osipov Yu.V.** Deep bed filtration asymptotics at the filter inlet // Procedia Engineering, 2016, vol. 153, pp. 366-370.
24. **Safina G.L.** Calculation of retention profiles in porous medium // Lecture Notes in Civil Engineering, 2021, vol. 170, pp. 21-28.
25. **Safina G.L.** Numerical solution of filtration in porous rock // E3S Web of Conferences, 2019, vol. 97, 05016.
26. **Osipov Yu., Safina G., Galaguz Yu.** Filtration model with multiple particle capture // Journal of Physics Conference Series, 2019, vol. 1425(1), 012110.
27. **Yang S., Russell T., Badalyan A., Schacht U., Woolley M., Bedrikovetsky P.** Characterisation of fines migration system using laboratory pressure measurements // Journal of Natural Gas Science and Engineering, 2019, vol. 65, pp. 108-124.
28. **Osipov Yu., Safina G., Galaguz Yu.** Calculation of the filtration problem by finite differences methods // MATEC Web of Conferences, 2018, vol. 251, 04021.
29. **You Z., Osipov Y., Bedrikovetsky P., Kuzmina L**. Asymptotic model for deep bed filtration // Chemical Engineering Journal, 2014, vol. 258, pp. 374-385.
30. **Dev Burman G.K., Das P.K.** Groundwater exploration in hard rock terrain: An experience from eastern India // The Hydrological Basis for Water Resources Management, 1990, vol. 197, pp. 19-30.

СПИСОК ЛИТЕРАТУРЫ

1. **Li B., Han J.** Conservation and regeneration of historical buildings // IOP Conference Series: Earth and Environmental Science, 2021, vol. 787, 012179.
2. **Makowski A., Polanska B.** Application of jet grouting technology for the renovation of historic buildings // IOP Conference Series: Journal of Physics, 2020, vol. 1425, 012201.

3. **Redina T.** Reconstuction of the historical building foksal 13 and 15 in Warsaw // Acta Polytechnica CTU Proceedings, 2019, vol. 23, pp. 44-48.
4. **Sengupta R.** Grouting for strengthening the Qutb Minar, Delhi // Mortars, Cements and Grouts used in the Conservation of Historic Buildings, 1981, pp. 147-164.
5. **Wanik K.** Use of jet grouting technique to realize substructures of historic buildings: The example of an apartment building in Warsaw // Geotechnical Engineering for the Preservation of Monuments and Historic Sites, 2013, pp. 769-777.
6. **Chernyakov A.V.** Application of jet grouting during foundation reinforcement and reconstruction of historic buildings on land occupied by the state museum and reservation «Tsarutsyno» // Soil Mechanics and Foundation Engineering, 2011, vol. 48(5), pp. 769-777.
7. **Hofmann H.** Unterfangungen mit einpressung von zementsuspension unter hohem Druck // Beton- und Stahlbetonbau, 1989, vol. 84(8), pp. 199-202.
8. **Morey J.J.** Les domaines d'application du jet-grouting // Revue Francaise de Geotechnique, 1992, vol. 61, 17-30.
9. **Drooff E.R., Furth A.J., Scarborough J. A.** Jet grouting to support historic buildings // Geotechnical Special Publication, 1995, vol. 50, pp. 42-55.
10. **Modoni G., Croce P., Mongiovi L.** Theoretical modelling of jet grouting // Geotechnique, 2006, vol. 56(5), pp. 335-347.
11. **Tien C.** Principles of filtration // Elsevier: Amsterdam, 2012.
12. **Tien C.** Introduction to cake filtration // Elsevier: Amsterdam, 2006.
13. **Sacramento R.N., Yang Y., You Z., Waldmann A., Martins A.L., Vaz A.S.L., Zitha P.L.J., Bedrikovetsky P.** Deep bed and cake filtration of two-size particle suspension in porous media // Journal of Petroleum Science and Engineering, 2015, vol. 126, pp. 201-210.
14. **Fallah H., Barzegar Fathi H., Mohammadi H.** The mathematical model for particle suspension flow through porous medium // Geomaterials, 2012, vol. 2, pp. 57-62.
15. **Fallah H., Fallah A., Rahmani A., Afkhami M., Ahmadi A.** Size exclusion mechanism, suspension flow through porous medium // International Journal of Modern Nonlinear Theory and Application, 2012, vol. 1, pp. 113-117.
16. **Santos A., Bedrikovetsky P.** Size exclusion during particle suspension transport in porous media: stochastic and averaged equations // Computational and Applied Mathematics, 2004, vol. 23(2-3), pp. 259-284.
17. **You Z., Bedrikovetsky P., Kuzmina L.** Exact solution for long-term size exclusion suspension-colloidal transport in porous media // Hindawi Publishing Corporation Abstract and Applied Analysis, 2013, vol. 2013, 680693.
18. **Kuzmina L.I., Osipov Yu.V.** Exact solution for 1D deep bed filtration with particle capture by advection and dispersion // International Journal of Non-Linear Mechanics, 2021, vol. 137, 103830.
19. **Nazaikinskii V.E., Bedrikovetsky P.G., Kuzmina L.I., Osipov Y.V.** Exact solution for deep bed filtration with finite blocking time // SIAM Journal on Applied Mathematics, 2020, vol. 80 (5), pp. 2120-2143.
20. **Kuzmina L.I., Osipov Y.V. and Zheglova Y.G.** Analytical model for deep bed filtration with multiple mechanisms of particle capture // International Journal of Non-linear Mechanics, 2018, vol. 105, pp. 242-248.
21. **Kuzmina L.I., Osipov Y.V., Gorbunova T.N.** Asymptotics for filtration of polydisperse suspension with small impurities // Applied Mathematics and Mechanics (English Edition), 2021, vol. 42(1), pp. 109-126.

22. **Osipov Y.V.** Calculation of filtration of polydisperse suspension in a porous medium // MATEC Web of Conferences, 2017, vol. 117, 00131.
23. **Kuzmina L.I., Osipov Yu.V.** Deep bed filtration asymptotics at the filter inlet // Procedia Engineering, 2016, vol. 153, pp. 366-370.
24. **Safina G.L.** Calculation of retention profiles in porous medium // Lecture Notes in Civil Engineering, 2021, vol. 170, pp. 21-28.
25. **Safina G.L.** Numerical solution of filtration in porous rock // E3S Web of Conferences, 2019, vol. 97, 05016.
26. **Osipov Yu., Safina G., Galaguz Yu.** Filtration model with multiple particle capture // Journal of Physics Conference Series, 2019, vol. 1425(1), 012110.
27. **Yang S., Russell T., Badalyan A., Schacht U., Woolley M., Bedrikovetsky P.** Characterisation of fines migration system using laboratory pressure measurements // Journal of Natural Gas Science and Engineering, 2019, vol. 65, pp. 108-124.
28. **Osipov Yu., Safina G., Galaguz Yu.** Calculation of the filtration problem by finite differences methods // MATEC Web of Conferences, 2018, vol. 251, 04021.
29. **You Z., Osipov Y., Bedrikovetsky P., Kuzmina L**. Asymptotic model for deep bed filtration // Chemical Engineering Journal, 2014, vol. 258, pp. 374-385.
30. **Dev Burman G.K., Das P.K.** Groundwater exploration in hard rock terrain: An experience from eastern India // The Hydrological Basis for Water Resources Management, 1990, vol. 197, pp. 19-30.

Galina L. Safina, Ph. D, Head of the Department of Fundamental Education, branch of Moscow State University of Civil Engineering in Mytishchi, Associate Professor of the Department of Computer Science and Applied Mathematics, Moscow State University of Civil Engineering; 129337, Russia, Moscow, Yaroslavskoe Shosse, 26, tel. +7(499)1835994, e-mail: minkinag@mail.ru.

Сафина Галина Леонидовна, кандидат технических наук, заведующий кафедрой Фундаментального образования филиала НИУ МГСУ в г. Мытищи, доцент кафедры информатики и прикладной математики Национального исследовательского Московского государственного строительного университета; 129337, Россия, г. Москва, Ярославское шоссе, д. 26, тел. +7(499)1835994, e-mail: minkinag@mail.ru.

International Journal for Computational Civil and Structural Engineering, 18(1) 141–150 (2022)

DOI:10.22337/2587-9618-2022-18-1-141-150

FORECAST OF THE SOIL DEFORMATIONS AND DECREASE OF THE BEARING CAPACITY OF PILE FOUNDATIONS OPERATING IN THE CRYOLITHOZONE

Nadezhda S. Nikiforova [1], Artem V. Konnov [2]

[1] National Research Moscow State University of Civil Engineering, Moscow, RUSSIA
[2] Research Institute of Building Physics of Russian Academy of Architecture and Construction Sciences, Moscow, RUSSIA

Abstract: Currently, permafrost is degrading due to global warming. The destructive impact of cryogenic processes on buildings and structures in the permafrost zone is increasing. The purpose of this study was to predict the decrease in the bearing capacity of pile foundations of existing buildings and the resulting deformations of the permafrost soils due to climate change. Numerical studies of the bearing capacity of pile foundations and deformations of the base of a building erected in the 1980s in Norilsk according to the first principle of construction on permafrost soils were carried out. Modeling showed a decrease in the bearing capacity of the piles of the building up to 50% over 60 years (mesured since 2000). The period after which the building will come into an emergency condition is determined. Article provides an assessment of the effectiveness of the use of seasonally operating cooling devices to ensure its operational reliability.

Keywords: permafrost soils, cryolithozone, pile foundations, thermal stabilizers, bearing capacity of piles, building maintenance.

ПРОГНОЗ ДЕФОРМАЦИЙ ОСНОВАНИЯ И СНИЖЕНИЯ НЕСУЩЕЙ СПОСОБНОСТИ СВАЙНЫХ ФУНДАМЕНТОВ В КРИОЛИТОЗОНЕ

Н.С. Никифорова [1], А.В. Коннов [2]

[1] Национальный исследовательский Московский государственный строительный университет (НИУ МГСУ), Москва, РОССИЯ
[2] Научно-исследовательский институт строительной физики Российской академии архитектуры и строительных наук (НИИСФ РААСН), Москва, РОССИЯ

Аннотация: В настоящее время по причине глобального потепления климата происходит деградация вечной мерзлоты. Усиливается деструктивное воздействие криогенных процессов на здания и сооружения в криолитозоне. Целью данной работы являлось прогнозирование в связи с изменением климата снижения несущей способности свайных фундаментов существующих зданий и вызванных этим деформаций основания из многолетнемерзлых грунтов. Были проведены численные исследования несущей способности свайных фундаментов и деформаций основания здания, возведенного в 80-х годах прошлого века в Норильске по I принципу строительства на многолетнемерзлых грунтах. Моделирование показало снижение несущей способности свай здания до 50% за 60 лет (начиная с 2000 г.). Определен срок, по истечении которого здание придет в аварийное состояние. Дана оценка эффективности применения сезонно-действующих охлаждающих устройств для обеспечения его эксплуатационной надежности.

Ключевые слова: многолетнемерзлые грунты, криолитозона, свайные фундаменты, термостабилизаторы, несущая способность свай, эксплуатация зданий.

INTRODUCTION

The Earth's climate has changed throughout the humanity's existence. The modern warming period began from the mid-70s of the twentieth century and continues up to the present time [1] It is worth noting that in the 30s–40s there was also warming, which was especially evident in the Arctic. This led to its rapid development at that time [2]. The Earth's climate has changed throughout the existence of mankind. The modern period of warming began in the period from the mid-70s of the twentieth century and continues up to the present time [1] It is worth noting that in the 30s–40s there was also warming, which was especially evident in the Arctic, which led to its rapid development at that time [2]. An analysis of modern research allows us to identify five scenarios of climate change, for which the positions of the boundaries of the distribution of permafrost soils (PS) and the depths of seasonal thawing are calculated. The most popular is the scenario in which global warming will occur relatively quickly. By the end of the 21st century, the average temperature of the Earth's surface may increase from 1.1 to 6.4 °C in comparison with 1990. In the northern hemisphere, where the most rapid and significant warming will be observed, the area of distribution of PS will decrease to 40% by 2050 [3].

The degradation of permafrost has a direct impact on the construction sites located there [4]. The destructive impact of cryogenic processes on infrastructure facilities in the area of permafrost has increased as follows: by 61% in Yakutsk, 90% in Amderma, 42% in Norilsk [5]. In the Norilsk region, climate warming should be considered as a significant factor in the occurrence of accidents, which must be taken into account when calculating the bases in the permafrost zone for the entire period of construction and operation of facilities [6].

The observed upward redistribution of permafrost temperatures at the depth of annual zero amplitudes is especially dangerous for existing buildings and structures.

More than 75% of all buildings and structures in the permafrost zone of Russia are built and operated according to the principle of maintaining the frozen state of foundation soils. That is the foundations are frozen into the soil, and this ensures the required bearing capacity [7]. Most urban buildings are typical panel or brick five-nine-story buildings on pile foundations [8].

Thus, the relevant problem is the prediction of deformations of the PS base and the decrease in the bearing capacity of pile foundations due to climate warming.

Analytical forecast of reducing the bearing capacity of pile foundations by the middle of the 21st century [9,10 showed that at the moment for buildings built in the 60-80s (I principle of construction on PS), the reduction in the bearing capacity of the pile foundation reaches 25% (North European parts of Russia). However, it remains at an average level (10-20%) for most regions. By 2050, it's a high (>30%) decrease will be observed.

Khrustalev L.N. determined an increase in the required depth of pile driving to ensure the stability of buildings for the period from 1950 to 2010 for Vorkuta and to 2030 for Yakutsk due to an increase in the temperature of the permafrost caused by climate warming [11].

Kudryavtsev S.A. et al., propose a conceptual basis for the model for determining the bearing capacity of pile foundations based on studies conducted over the past 45 years of observations for the infrastructure facilities of the Eastern Range of the Far Eastern Railway located on the PS. According to this, the bearing capacity of piles decreased by 3 times from 1990 to 2020. [12,13].

The purpose of this article is to predict the decrease in the bearing capacity of pile foundations of existing buildings in the conditions of Norilsk and the resulting deformations of the PS base in relation with climate warming.

RESEARCH METHOD

The determination of the reduction in the bearing capacity of pile foundations and the calculation of deformations of the PS base were

carried out by a numerical method in the Settlement Calculator, which is part of the Frost 3D software package.

In the Frost 3D Settlement Calculator, the calculation of soil settlement and bearing capacity of piles is carried out in accordance with Chapter 7 of Building Code of Russian Federation SP 25.13330.2012 " Soil bases and foundations on permafrost soils". The calculations used the modified method SP 25.13330.2012 embedded in the Calculator, which allows performing calculations on a three-dimensional finite-difference computational grid and taking into account the proportion of unfrozen water in the ground.

Determination of the deformation of the base of the foundations performed using the numerical solution of a stationary differential equation in partial derivatives, which describes small transverse deflections of a thin plate, considering the elastic forces under perpendicular effects of external forces.

The pile foundation of a multi-storey building with dimensions of 12x24 m, built according to the I principle of construction on the PS, was modeled. There was a ventilated underground under the entire volume of the building. The foundation consists of reinforced concrete piles d = 0.35 m, buried in the ground to a depth of 13 m (piles of the extreme row) and 15 m (piles under the middle of the building) and united by a tape or slab grillage. The pressure from the building to the foundation was set in the case of a strip grillage of 204 kPa for a row of piles under the wall in the middle of the building and 149 kPa in the case of an extreme row of piles, for a slab grillage it was 120 kPa.

When calculating the bearing capacity and deformations, the temperature distribution obtained by the authors in the course of previous studies [9,6] at the base of the building in Norilsk, which was erected according to the I principle of construction on PS with a ventilated underground, was used, taking into account climate warming (Figure 1). The bearing capacity of pile foundations was determined by 2000 using the temperature distribution obtained from meteorological data. By 2021 and 2059, it was determined considering the trend of climate warming.

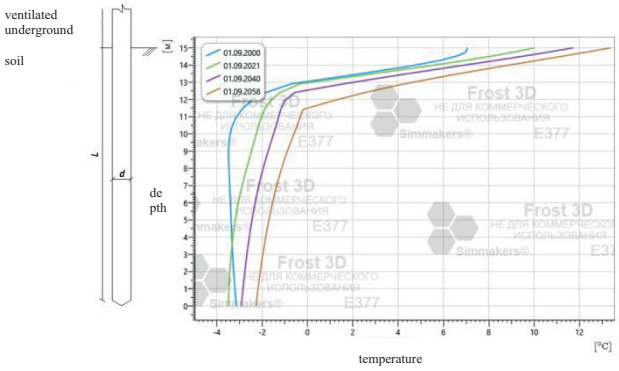

Figure 1. Soil temperature distribution along a pile with a length L = 16 m, d = 0.35 m, located under the middle of the building

RESULTS

By 2021, the calculation condition for the first limit state (ultimate state) is met. The bearing capacity of piles exceeds the calculated load applied to them (Figure 2), despite the decrease by 2021 compared to 2000 of the bearing capacity of piles of the extreme row by 13%, piles under the middle of the building by 11%.

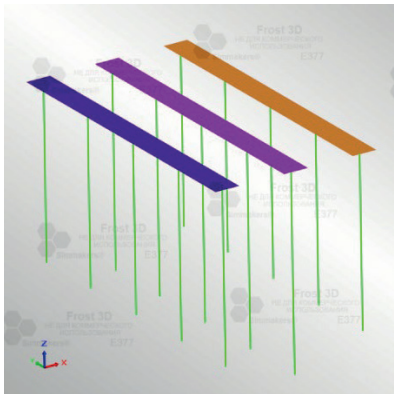

Figure 2. Calculation of the bearing capacity of piles by 2021. Piles are highlighted in green in the model. The calculation condition for the first limit state is met

By 2040, part of the piles is predicted to lose stability due to a decrease in their bearing capacity caused by the predicted increase in the

temperature of permafrost with climate warming (Figure 3a). In comparison with 2000, a decrease in bearing capacity was obtained by 30% and 28% for the piles of the extreme row and piles under the middle of the building, respectively. The calculation of deformations of the building base was made. A settlement of 30 cm was obtained and the relative difference in settlements was 0.047 in the transverse and 0.016 in the longitudinal directions (Figure 3b) due to the loss of bearing capacity by some of the piles for the strip grillage.

By the end of the simulated time period (2059), the bearing capacity is predicted to decrease by 52% for the piles of the outermost row, by 49% for those located under the middle of the building, and, in the case of a strip grillage, the latter will lose stability.

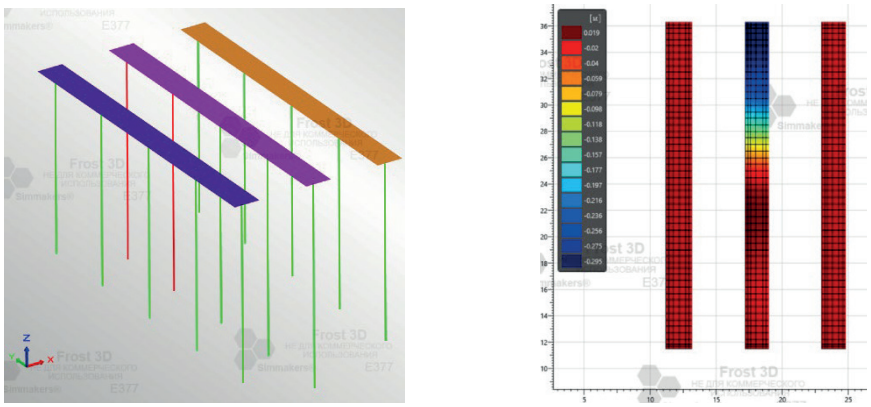

a) *b)*

Figure 3. Loss of stability by part of the piles, caused by a decrease in their bearing capacity due to the predicted increase in the temperature of the permafrost by 2040: a) calculation model of piles and strip grillage, in red - piles that have lost stability; b) additional sediment received

For a slab grillage, the piles' loss of stability is shown in Figure 4a. Figure 4b presents the results of the settlement calculation. The following values of deformations were obtained: draft 62 cm, relative difference of draft 0.035 in transverse and 0.033 in longitudinal directions. Figure 5 shows the general diagram of the decrease in the bearing capacity of piles by 2059 in relation to 2000 due to an increase in the temperature of the permafrost with a warming climate.

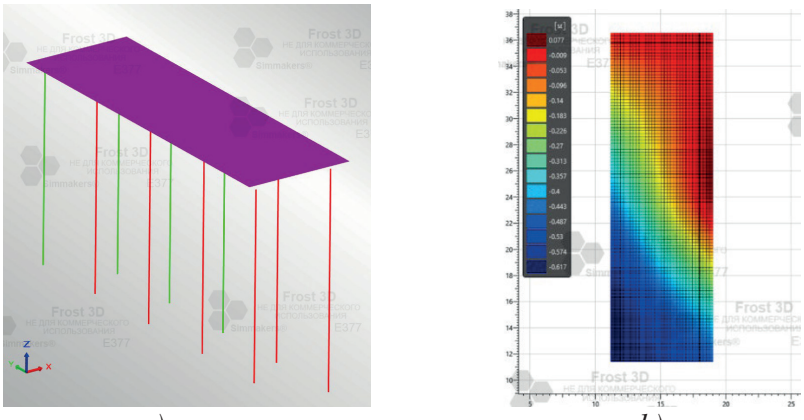

a) *b)*

Figure 4. Loss of stability by part of the piles (red) caused by a decrease in their bearing capacity due to the predicted increase in the temperature of the permafrost by 2059: a) calculation model of piles and slab grillage; b) additional sediment received

As a result, it was found decrease of bearing capacity of the piles of the facilities built in 1981 according to principle I in Norilsk. And by 2040, the building will come into an emergency condition. It is necessary to plan structural and technological measures to ensure operational reliability, as well as the organization of geocryological and geotechnical monitoring of such buildings.

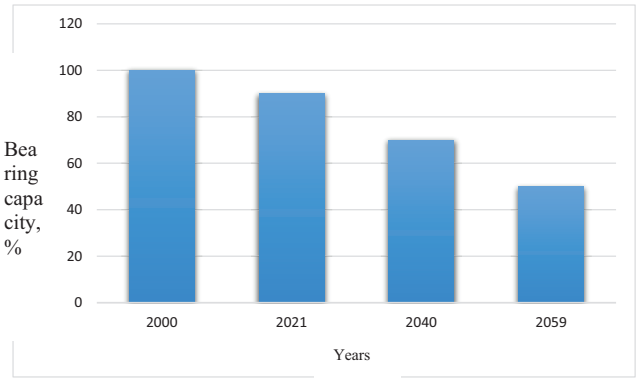

Figure 5. Diagram of the decrease in the bearing capacity of piles by 2059 relative to 2000 due to climate warming

USE OF SEASONAL COOLING DEVICES

The main existing types of structures and technologies used to prevent the degradation of permafrost soils at the base of buildings and structures were identified: ventilated undergrounds (including adjustable ones) [14], enclosing clips arranged in the base using various technologies along the contour of the building [15]; thermal stabilization of soils with the help of seasonally operating cooling devices (SOCD).

Soil thermal stabilizers, otherwise called thermosiphons or seasonal cooling devices, have been successfully used since the 1960s [16, 17, 18]. The operation of such an installation is based on a physical phenomenon - convection. Provided that the outdoor air temperature is lower than the ground temperature, heat exchange takes place with the help of a condenser and a refrigerant.

On the example of the considered model of a building in Norilsk, the problem was solved to assess the effectiveness of the use of the SOCD to prevent a decrease in the bearing capacity of foundation piles and extend the life of the building.

In the Frost 3D software, the use of the SDA with the following characteristics was simulated: the length of the above-ground part is 2 m, the underground isolated section is 3 m, the length of the evaporator part is 10 m, the radius of the evaporator pipe is 16.85 mm, the area of the condenser part is 2.43 m2, the evaporator part - 1.06 m2.

Using the Frost 3D Heat Transfer Conditions Calculator, based on long-term meteorological data on wind speed (Scientific and Applied Handbook on Climate of the USSR, 1990) and the design parameters of the condenser, the heat exchange coefficients of the heat exchanger finned tube with air were calculated for the entire forecast period: 2021-2059. The decrease in wind speed for the SDA located in the ventilated underground was taken into account.

The layout of the JCS is shown in Figure 6. In Frost 3D, only the evaporative part of the condenser is graphically specified in the model.

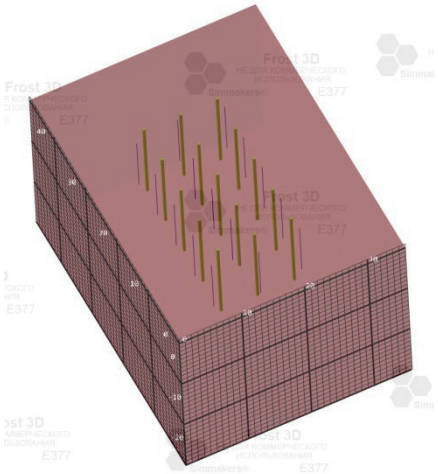

Figure 6. Model of a soil mass containing piles and SOCD

The technique for conducting a numerical study was similar to that given for modeling without a SOCD.

In the Frost 3D program, the temperature distribution in the soil mass was obtained with an interval of one month for the time interval 1981-2059. It was assumed that the SOCD were installed in 2021. Figure 7 shows the base temperature isofields at the end of the simulated time period (on February 2059).

Forecasting the change in the bearing capacity of pile foundations and deformations of the foundation from PS during the construction of the SOCD in connection with climate warming was carried out by a numerical method in the Settlement Calculator of the PC Frost 3D.

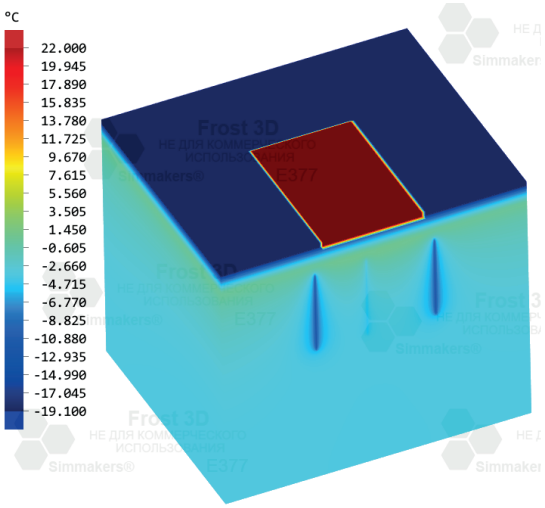

Figure 7. Temperature distribution in the soil mass in February 2059

The bearing capacity of pile foundations was determined after the installation of the SOCD (2021) by 2040 and 2059 using the obtained temperature distribution, considering the trend of climate warming.

By 2040, the bearing capacity of the piles of the extreme row increases by 12%, the piles under the middle of the building - by 14% in relation to 2000 due to the installation of the SOCD. The calculation condition for the first limit state is fulfilled: the bearing capacity of the piles exceeds that applied to them calculated load.

In the period from 2041 to 2059, a decrease in the bearing capacity of piles is again predicted due to an increase in the temperature of the permafrost due to climate warming. By 2059, a decrease in bearing capacity relative to 2000 was obtained by 7% and 5% for the piles of the outer row and under the middle of the building, respectively. The calculation condition for the first limit state is met. The diagram of changes in the bearing capacity of piles in relation to 2000 before and after the installation of the SOCD is shown in Figure 8.

The use of SOCD guarantees the operational suitability of buildings until the middle of the 21st in the conditions of a predicted increase in air temperature. However, it is necessary to consider the economic costs associated with the limited period of their operation and the need for replacement when making a decision on the construction of the SOCD.

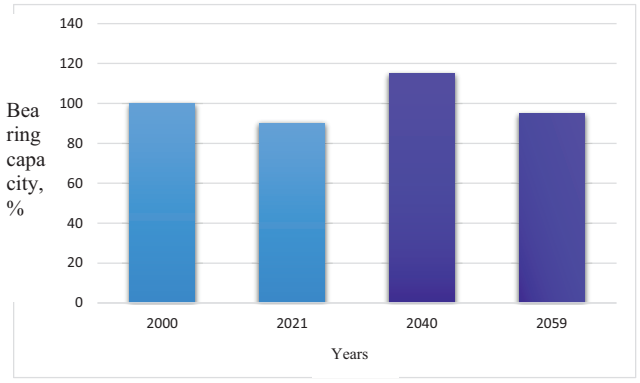

a)

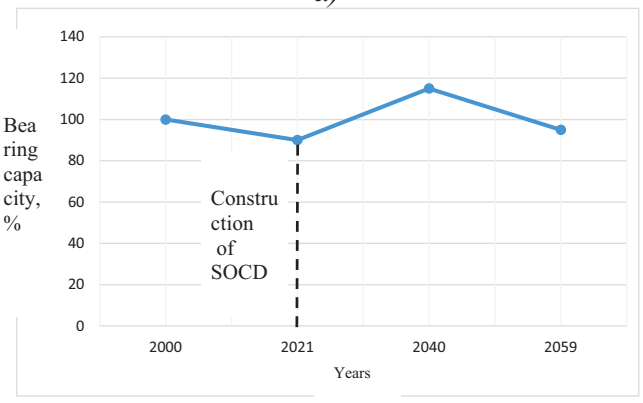

b)

Figure 8. Change in the bearing capacity of piles by 2059 relative to 2000 when installing a SDA in 2021 to prevent the degradation of permafrost due to climate warming: a) diagram; b) schedule

CONCLUSION

1. Numerical modeling in the Frost 3D program showed a decrease in the bearing capacity of piles of a building built in Norilsk in 1981 according to the first principle by 10% by 2021, by 30% by 2040, by 50% by 2059 compared to 2000. The operational suitability of the building in 2021 is ensured (the maximum settlement did not exceed 5 mm), by 2040 the building will be in an emergency condition (the projected settlement will be 30 cm, the relative difference of the settlement is 0.033-0.035).
2. Modeling the use of SOCD to prevent the reduction in the bearing capacity of foundation piles and extend the life of a building with a ventilated underground showed that the bearing capacity of piles first increases by 15% by 2040 compared to 2000, and then there is a slight decrease (5-7%). Thus, the use of SOCD guarantees the operational suitability of buildings until the middle of the 21st in the conditions of a predicted increase in air temperature.
3. It is necessary to continue research aimed at developing scientific foundations for the preservation of soils in the permafrost zone in the permafrost state at the base of existing buildings, communications and highways by controlling the temperature regime of soils using new technologies and constructive measures.

REFERENCES

1. IPCC: Climate Change 2014: Synthesis Report. Contribution of Working Groups I, II and III to the Fifth Assessment Report of the Intergovernmental Panel on Climate Change [Core Writing Team, R.K. Pachauri and L.A. Meyer (eds.)]. IPCC, Geneva, Switzerland, 2014, 151 p.
2. **Shats M.M.** Sovremennoye izmeneniye klimata severa RF. Tendentsii i posledstviya [Modern climate change in the north of the Russian Federation. Trends and consequences] // GeoInfo: nezavisimyy elektronnyy zhurnal – 2017. https://www.geoinfo.ru/product/shac-mark-mihajlovich/sovremennoe-izmenenie-klimata-severa-rf-tendencii-i-posledstviya-35141.shtml (data obrashcheniya 28.01.2022)
3. **Belolutskaya. M. A.** Vliyaniye izmeneniya klimata na vechnuyu merzlotu i inzhenernuyu infrastrukturu Kraynego Severa [Influence of climate change on permafrost and engineering infrastructure of the Far North]: Abstract of the thesis. ... candidate of physical and mathematical sciences: 25.00.30 St. Petersburg, 2004. - 24 p.
4. **Il'ichev V.A. et al.** Perspektivy razvitiya poseleniy Severa v sovremennykh usloviyakh [Prospects for the development of the settlements of the North in modern conditions]. – Moscow: RAACS, 2003. – 151 p.
5. **Anisimov O., Lavrov S.** Global'noye potepleniye i tayaniye vechnoy merzloty: otsenka riskov dlya proizvodstvennykh ob"yektov TEK RF [Global warming and thawing of permafrost: risk assessment for production facilities of the RF fuel and energy complex] // Tekhnologii TEK. 2004. No 3. P. 78–83.
6. **Il'ichev V.A., Nikiforova N.S. Konnov A.V.** Prognoz izmeneniya temperaturnogo sostoyaniya osnovaniya zdaniya v usloviyakh potepleniya klimata [Forecast of changes in the temperature state of the base of the building in the conditions of climate warming] // Zhilishchnoye stroitel'stvo. – 2021. – No 6. – P. 18-24. DOI: https://doi.org/10.31659/0044-4472-2021-6-18-24
7. Vtoroy otsenochnyy doklad Rosgidrometa ob izmeneniyakh klimata i ikh posledstviyakh na territorii Rossiyskoy Federatsii [The second assessment report of Roshydromet on climate change and its consequences on the territory of the

Russian Federation] / Rosgidromet. – Moscow, 2014. – 1007 p.
8. **Shur Y. and Goering D.** Climate change and foundations of buildings in permafrost regions. In: Margesin R. (eds) Permafrost Soils. Soil Biology. Berlin: Springer, 2008. vol. 16, – pp. 251-260. DOI: 10.1007/978-3-540-69371-0_17
9. **Nikiforova N.S., Konnov A.V**. Nesushchaya sposobnost' svay v mnogoletnemerzlykh gruntakh pri izmenenii klimata [Bearing capacity of piles in permafrost soils under climate change] // Construction and Geotechnics, – t. 12, – No 3 (2021), – P. 14–24
10. **Nikiforova N.S., Konnov A.V.** Influence of permafrost degradation on piles bearing capacity // Journal of Physics: Conference Series. – 2021. – Vol. 1928. – No 012046. DOI: 10.1088/1742-6596/1928/1/012046.
11. **Khrustalev L.N., Pustovoyt G.P., Yemel'yanova L.V.** Nadezhnost' i dolgovechnost' osnovaniy inzhenernykh sooruzheniy na vechnomerzlykh gruntakh v usloviyakh global'nogo potepleniya klimata [Reliability and durability of the bases of engineering structures on permafrost soils in the conditions of global climate warming] // Osnovaniya i fundamenty – No3. – 1993. – P.10-13.
12. **Kudryavtsev S.** Numerical Simulation of the Work of a Low-Settlement Embankment on a Pile Foundation in the Process of Permafrost Soil Thawing / Kudryavtsev S., Valtseva T., Bugunov S., Kotenko Z., Paramonov V., Igor Saharov I., Sokolova N. // Transportation Soil Engineering in Cold Regions, –Vol. 2, Proceedings of TRANSOILCOLD 2019, pp.73-81.
13. **Kudryavtsev S.A.** Geotechnical monitoring bearing capacity boring pile foundations of bridge during permafrost degradation / S A Kudryavtsev, T Y Valtseva, I I Gavrilov, Zh I Kotenko and N Sokolova // Journal of Physics: Conference Series. - 2021. - Vol. 1928. - No 012057. DOI: 10.1088/1742-6596/1928/1/012057
14. **Khrustalev L.N.** Osnovy geotekhniki v kriolitozone [Fundamentals of geotechnics in permafrost zone]. -Moscow: Publishing of Moskowy university, 2005. – 544 p.
15. **Nuzhdin L.V.** Research of effective parameters to strengthen soil foundations by cement-sand mixture injection method / L.V. Nuzhdin, M.L. Nuzhdin // Geotechnical Engineering for Infrastructure and Development: Proc. of the XVI European Conf. on Soil Mech. – London, ICE Publishing Ltd, 2015. – P. 3273-3278.
16. **Vyalov, S.S.** Termosvai v stroitel'stve na severe [Thermal piles in construction in the north] / S.S. Vyalov, S.E. Gorodetskiy, YU.A. Aleksandrov et al. – Leningrad: Stroyizdat, 1984. –149 p.
17. **Ibragimov, E.V.** Prognoz napryazhenno-deformirovannogo sostoyaniya termostabi-lizirovannogo osnovaniya [Forecast of the stress-strain state of a thermally stabilized foundation] / E.V. Ibragimov, YA.A. Kronik, V.N. Paramonov // Osnovaniya, fundamenty i mekhanika gruntov. – 2018. – No 6. – P. 36-40.
18. Means for Maintaining Permafrost Foundations. Pat. USA. N 3, 217, 791, Cl 165-45 / Long E.L. – 1964.

СПИСОК ЛИТЕРАТУРЫ

1. IPCC: Climate Change 2014: Synthesis Report. Contribution of Working Groups I, II and III to the Fifth Assessment Report of the Intergovernmental Panel on Climate Change [Core Writing Team, R.K. Pachauri and L.A. Meyer (eds.)]. IPCC, Geneva, Switzerland, 2014, 151 p.
2. **Шац М.М.** Современное изменение климата севера РФ. Тенденции и последствия // ГеоИнфо: независимый электронный журнал – 2017. https://www.geoinfo.ru/product/shac-

mark-mihajlovich/sovremennoe-izmenenie-klimata-severa-rf-tendencii-i-posledstviya-35141.shtml (дата обращения 28.01.2022)
3. **Белолуцкая. М. А.** Влияние изменения климата на вечную мерзлоту и инженерную инфраструктуру Крайнего Севера: автореферат дис. ... кандидата физико-математических наук: 25.00.30 Санкт-Петербург, 2004. - 24 с.
4. **Ильичев В.А. и др.** Перспективы развития поселений Севера в современных условиях. – М.: Российская академия архитектуры и строительных наук, 2003. – 151 с.
5. **Анисимов О., Лавров С.** Глобальное потепление и таяние вечной мерзлоты: оценка рисков для производственных объектов ТЭК РФ // Технологии ТЭК. 2004. No 3. С. 78–83.
6. **Ильичев В.А., Никифорова Н.С. Коннов А.В.** Прогноз изменения температурного состояния основания здания в условиях потепления климата // Жилищное строительство. – 2021. – No 6. – С. 18-24. DOI: https://doi.org/10.31659/0044-4472-2021-6-18-24
7. Второй оценочный доклад Росгидромета об изменениях климата и их последствиях на территории Российской Федерации / Росгидромет. – М., 2014. – 1007 с.
8. **Shur Y. and Goering D.** Climate change and foundations of buildings in permafrost regions. In: Margesin R. (eds) Permafrost Soils. Soil Biology. Berlin: Springer, 2008. vol. 16, – pp. 251-260. DOI: 10.1007/978-3-540-69371-0_17
9. **Никифорова Н.С., Коннов А.В.** Несущая способность свай в многолетнемерзлых грунтах при изменении климата. // Construction and Geotechnics, – т. 12, – No 3 (2021), – С. 14–24
10. **Nikiforova N.S., Konnov A.V.** Influence of permafrost degradation on piles bearing capacity // Journal of Physics: Conference Series. – 2021. – Vol. 1928. – No 012046. DOI: 10.1088/1742-6596/1928/1/012046.
11. **Хрусталев Л.Н., Пустовойт Г.П., Емельянова Л.В.** Надежность и долговечность оснований инженерных сооружений на вечномерзлых грунтах в условиях глобального потепления климата // Основания и фундаменты – No3. – 1993. – С.10-13.
12. **Kudryavtsev S.** Numerical Simulation of the Work of a Low-Settlement Embankment on a Pile Foundation in the Process of Permafrost Soil Thawing / Kudryavtsev S., Valtseva T., Bugunov S., Kotenko Z., Paramonov V., Igor Saharov I., Sokolova N. // Transportation Soil Engineering in Cold Regions, –Vol. 2, Proceedings of TRANSOILCOLD 2019, pp.73-81.
13. **Kudryavtsev S.A.** Geotechnical monitoring bearing capacity boring pile foundations of bridge during permafrost degradation / S A Kudryavtsev, T Y Valtseva, I I Gavrilov, Zh I Kotenko and N Sokolova // Journal of Physics: Conference Series. - 2021. - Vol. 1928. - No 012057. DOI: 10.1088/1742-6596/1928/1/012057
14. **Хрусталев Л.Н.** Основы геотехники в криолитозоне. -М.:Изд-во Московский университет, 2005. – 544 с.
15. **Nuzhdin L.V.** Research of effective parameters to strengthen soil foundations by cement-sand mixture injection method / L.V. Nuzhdin, M.L. Nuzhdin // Geotechnical Engineering for Infrastructure and Development: Proc. of the XVI European Conf. on Soil Mech. – London, ICE Publishing Ltd, 2015. – P. 3273-3278.
16. **Вялов, С.С.** Термосваи в строительстве на севере [Текст] / С.С. Вялов, С.Э. Городецкий, Ю.А. Александров и др. – Л.: Стройиздат, 1984. –149 с.
17. **Ибрагимов, Э.В.** Прогноз напряженно-деформированного состояния термостабилизированного основания / Э.В.

Ибрагимов, Я.А. Кроник, В.Н. Парамонов // Основания, фундаменты и механика грунтов. – 2018. – No 6. – С. 36-40.

18. Means for Maintaining Permafrost Foundations. Pat. USA. N 3, 217, 791, Cl 165-45 / Long E.L. – 1964.

Nikiforova S. Nadezhda – RAACS adviser, senior researcher, doctor of technical sciences, professor of "Soil mechanics and geotechnics" department in Federal state budget educational institution of higher education "Moscow State University of Civil Engineering (National Research University)"; 129337, Moscow, Yaroslavskoye Shosse, 26, phone: +7 (495) 287-49-14 * 1425, e-mail: n.s.nikiforova@mail.ru

Konnov V. Artem – candidate of technical sciences, researcher at Bases, foundations and underground structures laboratory of the Scientific-Research Institute of Building Physics of the Russian Academy of Architecture and Construction Sciences (NIISF RAACS); 127238, Moscow, Lokomotivnyj proezd, 21, phone:+7 495 482 4076, e-mail: artem.konnov@gmail.com

Никифорова Надежда Сергеевна, советник РААСН, старший научный сотрудник, доктор технических наук, профессор кафедры «Механика грунтов и геотехника» ФГБОУ ВО НИУ МГСУ Национальный исследовательский Московский государственный строительный университет; 129337, г. Москва, Ярославское шоссе, д. 26, телефон: +7 (495) 287-49-14, доб.1425, e-mail: n.s.nikiforova@mail.ru

Коннов Артем Владимирович, кандидат технических наук, научный сотрудник лаборатории «Основания, фундаменты и подземные сооружения» Научно-исследовательского института строительной физики Российской академии архитектуры и строительных наук (НИИСФ РААСН); 127238, г. Москва, Локомотивный проезд, д. 21, телефон +7 495 482 4076, e-mail: artem.konnov@gmail.com

International Journal for Computational Civil and Structural Engineering, 18(1) 151–155 (2022)

DOI:10.22337/2587-9618-2022-18-1-151-155

ABOUT THE NATIONAL SOFTWARE SYSTEM FOR STRUCTURAL ANALYSIS

Pavel A. Akimov, Alexander M. Belostotsky, Oleg V. Kabantsev, Vladimir N. Sidorov, Alexander R. Tusnin

National Research Moscow State University of Civil Engineering, Moscow, RUSSIA

Abstract: As is known, design solutions for the load-bearing systems of buildings and structures, as well as individual structural elements, are based on the results of a design analysis, which is usually performed by numerical methods using software systems. The same is true for structural analysis of construction objects at the stages of construction, operation, reconstruction. The distinctive paper is devoted to the current task of developing the Russian national software system for adequate determination of loads and impacts, stress-strain state, strength, stability, reliability and safety of buildings, structures and complexes at significant stages of their life cycle.

Keywords: national software system, structural analysis, finite element analysis, buildings and structures, stress-strain state, strength, stability

О НАЦИОНАЛЬНОМ ВЫЧИСЛИТЕЛЬНОМ КОМПЛЕКСЕ ДЛЯ СТРОИТЕЛЬНОЙ ОТРАСЛИ

П.А. Акимов, А.М. Белостоцкий, О.В. Кабанцев, В.Н. Сидоров, А.Р. Туснин

Национальный исследовательский Московский государственный строительный университет, г. Москва, РОССИЯ

Аннотация: Проектные решения несущих систем зданий и сооружений, а также отдельных конструктивных элементов базируются на результатах проектного анализа, который выполняется, как правило, численными методами с применением вычислительных комплексов. То же справедливо и для расчетного обоснования объектов строительства на стадиях строительства, эксплуатации, реконструкции. Настоящая статья посвящена актуальнейшей задаче разработки российского национального вычислительного комплекса (НВК) для адекватного определения нагрузок и воздействий, напряженно-деформированного состояния, оценки прочности, устойчивости, надежности и безопасности зданий, сооружений и комплексов на значимых этапах их жизненного цикла.

Ключевые слова: национальный вычислительный комплекс, расчеты строительных конструкций, здания и сооружения, напряженно-деформированное состояние, прочность, устойчивость

Currently, the following specialized (problem-oriented) software systems are used in the Russian Federation for analysis the strength, stability and deformability of building systems and foundations, which to some extent implement the requirements of the current Russian design codes: LIRA-SAPR, LIRA-SOFT, SCAD-SOFT, MICRO-FE, Stark ES, PLAXIS [1-3].

In some cases, more powerful software systems are also used (ANSYS, NASTRAN, SIMULIA Abaqus, etc.). These software systems, as a rule, are not used in the practice of mass design, but are used for the purposes of scientific research, for example, within the framework of scientific and technical support for the design and construction of unique and especially critical facilities (buildings, structures, complexes).

All the main modules of these software systems (first of all – solvers) are developed outside the Russian Federation. At the same time, formally

majority of above mentioned software systems (LIRA-SAPR, LIRA-SOFT, SCAD-SOFT, MICRO-FE, Stark ES) are distributed (with copyright) by legal entities registered in the Russian Federation. However, due to historical reasons, the actual developers of LIRA-SAPR, LIRA-SOFT and SCAD-SOFT are deployed in Kyiv (Ukraine). Besides, MICRO-FE and Stark ES are based on solvers developed by Germany. The PLAXIS geotechnical software system was developed at the Delft University of Technology (Netherlands).

The most important (from the point of view of the functioning of the construction industry) foreign software systems are discussed below.

SIMULIA Abaqus software system is widely used for computational justification of complex load-bearing systems, assemblies and structures. It is the main one in the line of the International Atomic Energy Agency (IAEA), where the calculation justifications of structures of nuclear power plants (NPP) made using this software system are accepted. Within the framework of sanctions analysis performed in the updated version of the software system, which will be banned, can be required.

PLAXIS is the main software system for computational research and computational justification in the direction of geotechnics. It is widely used in the design of civil and industrial facilities, transport infrastructure facilities. The IAEA also requires the use of this software system to justify design solutions for bases and foundations for nuclear power plants. This software system can be used without upgrade option. Within the framework of sanctions analysis performed in the updated version of the software system, which will be banned, can be required.

Tekla is the main software system the computational justification of steel structures and load-bearing systems. It is widely used in the design of industrial buildings and technological complexes (petrochemistry). This software system can be used without upgrade option. For individual objects, requirements for computational justification may be established in the updated version of the complex, which will be banned.

LIRA-SAPR, *LIRA-SOFT*, *SCAD-SOFT* and *MICRO-FE* are the main professionally oriented software systems with advanced post-processors that take into account the provisions of design codes of the Russian Federation. These software systems can be used without the possibility of updating.

ANSYS is the main software system for analysis of construction (building) aerodynamics. This software system can be used without upgrade option.

NASTRAN software system is normally used for research purposes with minimal use in industrial purposes. This software system can also be used without upgrade option.

Practice shows that in recent years sanctions instruments have been actively used in international relations, which in some cases can lead to significant delays in industrial processes, and in some cases, to the inability to perform certain procedures. Thus, several years ago, in the sanctions regime, access to updates of the PLAXIS software system was closed for some time, which led to delays in the performance of computational studies and the impossibility of performing individual computational procedures.

Due to the fact that the most important modules (solvers) of problem-oriented software systems are de facto developed outside the Russian Federation, there is a risk that they will fall under sanctions. The situation with the denial of access (in the case of sanctions) to a single or several simultaneously problem-oriented software systems for analysis of building systems and foundations can lead to blocking of the most important component of the construction process – the analysis of design solutions for construction objects.

In addition, the mentioned building-oriented software systems have a number of limitations that can be explained 10-20 years ago, but which constrain the construction industry today: a relatively poor set of finite element types, a selective and small set of types of nonlinearities (physical, geometric, structural, geometric), weak implementation of modern dynamic algorithms, etc.

We believe it is expedient to consider in a short time the issue of developing a national problem-oriented software system for adequate determination of loads and impacts, stress-strain state, strength, stability, reliability and safety of buildings, structures and complexes at significant

stages of their life cycle. It will be vital to ensure state ownership of such national problem-oriented software system.

The development of a national software system can be carried out on the basis of the National Research Moscow State University of Civil Engineering (MGSU) in collaboration with Universities that are members of the Industry Consortium "Construction and Architecture" (established in 2021) and partner companies with successful experience in development and verification in related industries (organizations with all the necessary competencies and highly professional specialists). The international practice of developing problem-oriented software systems shows the validity and effectiveness of using the potential of leading universities for such work.

Stages of development of the national software system are described below.

The first stage includes development and approval of the concept and architecture of the national software system, development of Terms of Reference. In particular it includes the following items:

– analysis of the problem-oriented software systems of the construction profile; formation of goals and objectives for the development of the national software system;

– development and approval of the concept and architecture of the national software system;

– development and approval of the Terms of Reference for the development of the national software system.

The second stage includes the development of the basic version of the national software system for the analysis of construction objects (so-called, "Engineering level"). In particular it includes the following items:

– development of a basic library of finite elements;

– development of basic models of physical, geometric, structural and genetic non-linearities;

– development of basic effective (direct sparse and iterative with preconditioners) "solvers" of systems of linear algebraic equations (SLAE);

– development of "solvers" of the partial eigenvalue problem;

– development of methods for solving problems of explicit and implicit schemes for direct integration of dynamic equations, including seismic analysis (for earthquake accelerograms) and progressive collapse analysis;

– development of methods for tasks of the linear-spectral approach for seismic analysis;

– development of a preprocessor (the first ("basic") level);

– development of a post-processor (the first ("basic") level);

– development of two-way communication with information modeling systems (CAD, BIM, information (digital) twins) (the first ("basic") level);

– development of user documentation for the second stage of development of the national software system;

– verification/validation of the national software system (the first ("basic") level) according to the rules and in the system of the Russian Academy of Architecture and Construction Sciences (RAACS).

The third stage includes advanced development of the national software system (so-called "Research level"). In particular it includes the following items:

– development of an extended library of finite elements (the second ("advanced") level);

– development of advanced models of non-linearities (the second ("advanced") level);

– development of advanced non-linear static and dynamic "solvers" (the second ("advanced") level);

– development of effective superelement schemes, including methods for dynamic synthesis of substructures;

– implementation of parallel procedures on systems with distributed computing for high-dimensional problems;

– implementation of quantum algorithms for particular problems of computational mechanics and data processing;

– development of a preprocessor (the second ("advanced") level);

– development of a post-processor (the second ("advanced") level);

– development of user documentation for the third stage of development of the national software system;

– verification/validation of the national software system (the second ("advanced") level) according to the rules and in the RAASN system.

Implementation of parallel development of separate stages is planned as well.

We invite all interested persons and organizations to collaboration in development of the Russian national software system for adequate determination of loads and impacts, stress-strain state, strength, stability, reliability and safety of buildings, structures and complexes at significant stages of their life cycle.

REFERENCES

1. **Belostotsky A.M., Akimov P.A., Afanasyeva I.N., Kaytukov T.B.** Contemporary problems of numerical modelling of unique structures and buildings. // International Journal for Computational Civil and Structural Engineering, 2017, Volume 13, Issue 2, pp. 9-34.
2. **Belostotsky A.M., Aul A.A., Dmitriev D.S., Dyadchenko Y.N., Nagibovich A.I., Ostrovsky K.I., Pavlov A.S., Akimov P.A., Sidorov V.N.** Computer-Aided Analysis of Mechanical Safety of Stadiums for the World Cup 2018 in Russia. Part 1: Introduction, Creation of Finite Element Models, Structural Analysis at Basic Combinations of Loads and Impacts. // Proceedings of the International Conference on Information and Digital Technologies 2019, IDT 2019, pp. 21-29.
3. **Belostotsky A.M., Aul A.A., Dmitriev D.S., Dyadchenko Y.N., Nagibovich A.I., Ostrovsky K.I., Pavlov A.S., Akimov P.A., Sidorov V.N.** Computer-Aided Analysis of Mechanical Safety of Stadiums for the World Cup 2018 in Russia. Part 2: Structural Analysis at Special Combinations of Loads and Impacts, Structural Health Monitoring. // Proceedings of the International Conference on Information and Digital Technologies 2019, IDT 2019, pp. 30-37.

СПИСОК ЛИТЕРАТУРЫ

1. **Belostotsky A.M., Akimov P.A., Afanasyeva I.N., Kaytukov T.B.** Contemporary problems of numerical modelling of unique structures and buildings. // International Journal for Computational Civil and Structural Engineering, 2017, Volume 13, Issue 2, pp. 9-34.
2. **Belostotsky A.M., Aul A.A., Dmitriev D.S., Dyadchenko Y.N., Nagibovich A.I., Ostrovsky K.I., Pavlov A.S., Akimov P.A., Sidorov V.N.** Computer-Aided Analysis of Mechanical Safety of Stadiums for the World Cup 2018 in Russia. Part 1: Introduction, Creation of Finite Element Models, Structural Analysis at Basic Combinations of Loads and Impacts. // Proceedings of the International Conference on Information and Digital Technologies 2019, IDT 2019, pp. 21-29.
3. **Belostotsky A.M., Aul A.A., Dmitriev D.S., Dyadchenko Y.N., Nagibovich A.I., Ostrovsky K.I., Pavlov A.S., Akimov P.A., Sidorov V.N.** Computer-Aided Analysis of Mechanical Safety of Stadiums for the World Cup 2018 in Russia. Part 2: Structural Analysis at Special Combinations of Loads and Impacts, Structural Health Monitoring. // Proceedings of the International Conference on Information and Digital Technologies 2019, IDT 2019, pp. 30-37.

Pavel A. Akimov, Full Member of the Russian Academy of Architecture and Construction Sciences, Professor, Dr.Sc.; Rector of the National Research Moscow State University of Civil Engineering; Professor of the Department of Architecture and Construction of the Peoples' Friendship University of Russia; Professor of the Department of Structural Mechanics of Tomsk State University of Architecture and Building; Acting Vice-President of the Russian Academy of Architecture and Construction Sciences; 26, Yaroslavskoe Shosse, Moscow, 129337, Russia; phone: +7(495) 651-81-85; Fax: +7(499) 183-44-38; e-mail: AkimovPA@mgsu.ru, rector@mgsu.ru, pavel.akimov@gmail.com.

Alexander M. Belostotsky, Full Member of the Russian Academy of Architecture and Construction Sciences, Professor, Dr.Sc.; General Director of the Scientific Research Center StaDyO; Professor of the Department of Informat-

ics and Applied Mathematics of the National Research Moscow State University of Civil Engineering; Scientific director of the Research & Educational Center of Computer Simulation of Unique buildings, constructions and complexes named after A.B. Zolotov of the National Research Moscow State University of Civil Engineering; Professor of the Department of Building Structures, Buildings and Structures of the Russian University of Transport (MIIT); 125040, Russia, Moscow, 3rd Yamsky Pole, 18, office 810; Tel. +7 (499) 706-88-10. E-mail: amb@stadyo.ru.

Oleg V. Kabantsev, Associate Professor, Dr.Sc; Director of scientific and technical projects of the National Research Moscow State University of Civil Engineering; Professor of the Department of Reinforced Concrete and Stone Structures of the National Research Moscow State University of Civil Engineering; 129337, Russia, Moscow, Yaroslavl highway, 26; phone: +7(495)739-03-14, 768-14-07; email: KabantsevOV@mgsu.ru.

Vladimir N. Sidorov, Corresponding Member of Russian Academy of Architecture and Construction Science, Professor, Dr.Sc, Professor of «Building Structures, Buildings and Facilities» Department, Institute of Railway Track, Construction and Structures, Russian University of Transport (MIIT), Rectorate Counselor, Professor of National Research University Moscow State University of Civil Engineering, Professor of Department «Engineering Structures and Numerical Mechanics», Perm National Research Polytechnic University; 127994, Russia, Moscow, Obraztsova st., 9, b. 9, phone: +74956814381; E-mail: sidorov.vladimir@gmail.com.

Alexander R. Tusnin, Professor, Dr.Sc; Vice-Rector of the National Research Moscow State University of Civil Engineering; Professor of the Department of Steel and Timber Structures of the National Research Moscow State University of Civil Engineering; 129337, Russia, Moscow, Yaroslavl highway, 26; phone: +7(495)025-28-65; Email: TusninAR@mgsu.ru.

Акимов Павел Алексеевич, академик РААСН, профессор, доктор технических наук; ректор Национального исследовательского Московского государственного строительного университета; профессор Департамента архитектуры и строительства Российского университета дружбы народов; профессор кафедры строительной механики Томского государственного архитектурно-строительного университета; исполняющий обязанности вице-президента Российской академии архитектуры и строительных наук; 129337, Россия, г. Москва, Ярославское шоссе, дом 26; телефон: +7(495) 651-81-85; факс: +7(499) 183-44-38; Email: AkimovPA@mgsu.ru, rector@mgsu.ru, pavel.akimov@gmail.com.

Белостоцкий Александр Михайлович, академик РААСН, профессор, доктор технических наук; генеральный директор ЗАО «Научно-исследовательский центр СтаДиО»; профессор кафедры информатики и прикладной математики Национального исследовательского Московского государственного строительного университета (НИУ МГСУ); научный руководитель Научно-образовательного центра компьютерного моделирования уникальных зданий, сооружений и комплексов им. А.Б. Золотова (НОЦ КМ) Национального исследовательского Московского государственного строительного университета (НИУ МГСУ); профессор кафедры «Строительные конструкции, здания и сооружения» Российского университета транспорта (МИИТ); 125040, Россия, Москва, ул. 3-я Ямского Поля, д.18, офис 810; тел. +7 (499) 706-88-10; E-mail: amb@stadyo.ru.

Кабанцев Олег Васильевич, доцент, доктор технических наук, директор научно-технических проектов Национального исследовательского Московского государственного строительного университета (НИУ МГСУ); профессор кафедры железобетонных и каменных конструкций Национального исследовательского Московского государственного строительного университета (НИУ МГСУ); 129337, Россия, г. Москва, Ярославское шоссе, дом 26; телефон: +7(495)739-03-14, 768-14-07; Email: KabantsevOV@mgsu.ru.

Сидоров Владимир Николаевич, член-корреспондент РААСН, профессор, доктор технических наук, профессор кафедры «Строительные конструкции, здания и сооружения» Института пути, строительства и сооружений Российского университета транспорта (МИИТа), советник при ректорате, профессор Национального исследовательского Московского государственного строительного университета, профессор кафедры «Строительные конструкции и вычислительная механика» Пермского национального исследовательского политехнического университета; 127994, Россия, г. Москва, ул. Образцова, д.9, стр. 9, телефон: +74956814381, E-mail: sidorov.vladimir@gmail.com.

Туснин Александр Романович, профессор, доктор технических наук; проректор Национального исследовательского Московского государственного строительного университета (НИУ МГСУ); профессор кафедры металлических и деревянных конструкций Национального исследовательского Московского государственного строительного университета (НИУ МГСУ); 129337, Россия, г. Москва, Ярославское шоссе, дом 26; телефон: +7(495)025-28-65; Email: TusninAR@mgsu.ru.

REVIEW

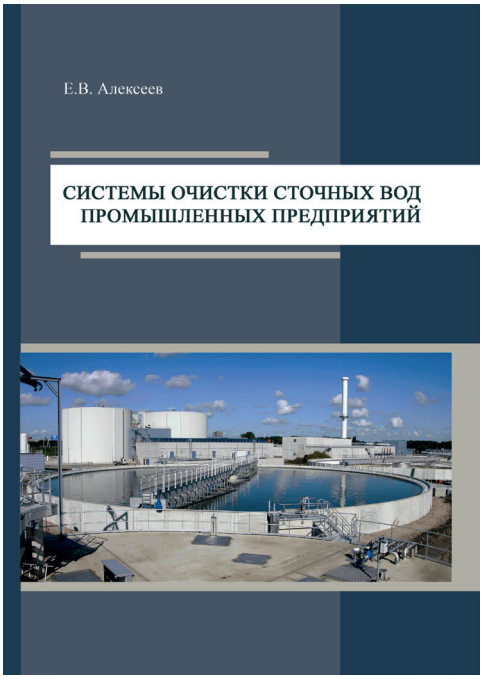

Alekseev E.V. Wastewater treatment systems for industrial enterprises: Textbook. – M. : ASV Publishing House, 2019. – 260 p.

The increasing use of chemicals in all spheres of production and household activities of the population has led to the fact that the trend of the spread and accumulation of biologically resistant organic substances in the environment, including in natural reservoirs, has become obvious.
The problem is that biological treatment facilities used in the municipal sphere cannot provide deep removal of organic substances of technogenic origin and biologically resistant organic pollutants.
Developed in the textbook, the direction of combining wastewater treatment processes that differ in their effect on pollutants is certainly promising. The book provides a technological description and basic calculations of hydromechanical, physicochemical, chemical, thermochemical and biological wastewater treatment processes. The principles of formation and examples of industrial wastewater treatment systems are given. The direction of development of industrial wastewater treatment systems proposed by the author is of both scientific and practical interest.
The compositional solution of the textbook allowed the author to optimally combine the tasks of the educational process with the presentation of useful information for practical use.
The material presented in the book is based on modern achievements in wastewater treatment technology, including the results of work performed at the Department of Water Supply and Water Disposal NRU MGSU with the participation of the author.
The textbook methodically correctly leads the reader from the conditions of wastewater formation and the properties of pollutants to the methods of their extraction, technological and engineering design of water purification processes.

DSc, Professor V. I. Bazhenov

РЕЦЕНЗИЯ

Алексеев Е.В. Системы очистки сточных вод промышленных предприятий: Учебное пособие. – М. : Издательство АСВ, 2019. – 260 с., ил.

Возрастающее применение химических препаратов во всех сферах производства и бытовой деятельности населения, привело к тому, что тенденция распространения и накопления биорезистентных органических веществ в окружающей среде, в том числе в природных водоемах, стала очевидной. Проблема состоит в том, что применяемые в коммунальной сфере биологические очистные сооружения, не могут обеспечить глубокое изъятие органических веществ техногенного происхождения и биорезистентных органических загрязнителей. Развиваемое в учебном пособии, направление сочетания процессов очистки сточных вод, отличающихся по действию на загрязняющие вещества, безусловно, перспективно. В книге приведено технологическое описание и основы расчетов гидромеханических, физико-химических, химических, термохимических и биологических процессов очистки сточных вод. Приведены принципы формирования и примеры систем очистки производственных сточных вод. Предлагаемое автором направление развития систем очистки промышленных сточных вод представляет как научный, так и практический интерес.

Композиционное решение учебного пособия позволило автору оптимально сочетать задачи учебного процесса с представлением полезных сведений для практического применения.

Приведенный в книге материал основан на современных достижениях в технологии очистки сточных вод, включая результаты работ, выполненных на кафедре водоснабжения и водоотведения НИ МГСУ с участием автора.

Учебное пособие методически верно ведет читателя от условий формирования сточных вод и свойств загрязняющих веществ к методам их извлечения, технологическому и инженерному оформлению процессов очистки воды.

Доктор техн. наук, профессор В.И. Баженов